



**US Army Corps
of Engineers**
Waterways Experiment
Station

Technical Report SL-94-24
November 1994

Shear Reinforcement in Deep Slabs

by Stanley C. Woodson

DTIC
ELECTE
JAN 11 1995
S G D

DTIC QUALITY INSPECTED 1

Approved For Public Release; Distribution Is Unlimited

19950109 005

DTIC QUALITY INSPECTED 1

Prepared for Headquarters, U.S. Army Corps of Engineers

The contents of this report are not to be used for advertising, publication, or promotional purposes. Citation of trade names does not constitute an official endorsement or approval of the use of such commercial products.



PRINTED ON RECYCLED PAPER

Technical Report SL-94-24
November 1994

Shear Reinforcement in Deep Slabs

by Stanley C. Woodson

U.S. Army Corps of Engineers
Waterways Experiment Station
3909 Halls Ferry Road
Vicksburg, MS 39180-6199

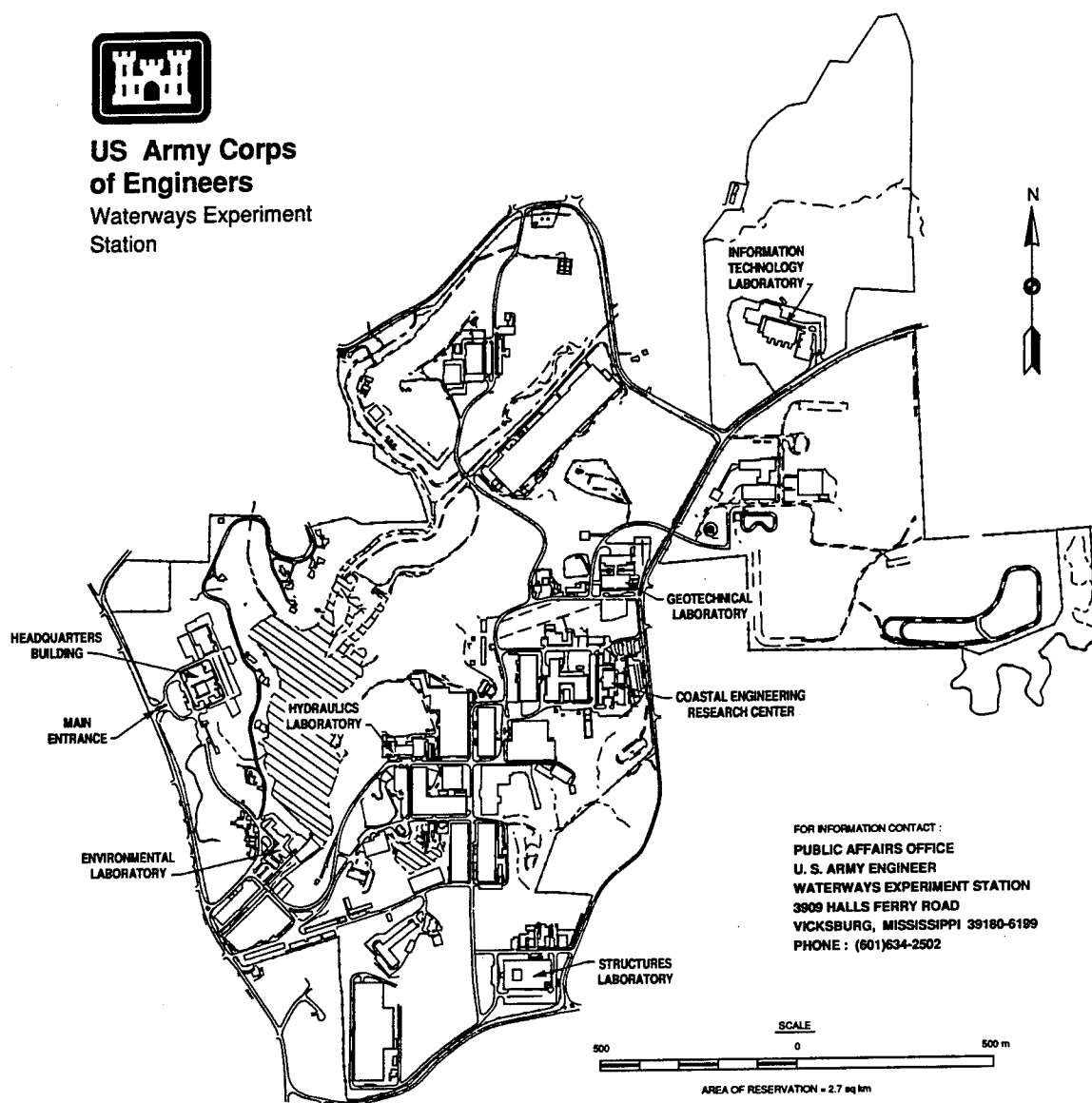
Final report

Approved for public release; distribution is unlimited

Prepared for U.S. Army Corps of Engineers
Washington, DC 20314-1000



**US Army Corps
of Engineers**
Waterways Experiment
Station



Waterways Experiment Station Cataloging-in-Publication Data

Woodson, Stanley C.

Shear reinforcement in deep slabs / by Stanley C. Woodson ; prepared for
U.S. Army Corps of Engineers.

136 p. : ill. ; 28 cm. — (Technical report ; SL-94-24)

Includes bibliographic references.

1. Concrete slabs — Design and construction. 2. Reinforced concrete —
Design and construction. 3. Shear (Mechanics) I. United States. Army. Corps of
Engineers. II. U.S. Army Engineer Waterways Experiment Station. III. Struc-
tures Laboratory (U.S.) IV. Title. V. Series: Technical report (U.S. Army Engi-
neer Waterways Experiment Station) ; SL-94-24.

TA7 W34 no.SL-94-24

Contents

Preface	iv
Conversion Factors, Non-SI to SI Units of Measurement	v
1: Introduction	1
Background	1
Objective	2
Approach	2
2: Experimental Description	3
General	3
Construction Details	3
Instrumentation	5
Experimental Procedure	6
3: Results and Discussion	7
General	7
Instrumentation Data	7
Discussion	7
Structural Damage and General Response	7
Ultimate Resistance and Response Limits	10
4: Conclusions	14
References	15
Appendix A: Recorded Data	A1

Accession For	
NTIS CRA&I	<input checked="" type="checkbox"/>
DTIC TAB	<input type="checkbox"/>
Unannounced	<input type="checkbox"/>
Justification	
By	
Distribution /	
Availability Codes	
Dist	Avail and/or Special
A-1	

Preface

The research reported herein was sponsored by Headquarters, U.S. Army Corps of Engineers, under Project Work Unit AT40-HS-008, entitled "Mechanics of Structural Elements Used in Hardened Construction."

The work was conducted at the U.S. Army Engineer Waterways Experiment Station (WES) under the general supervision of Messrs. Bryant Mather, Director, Structures Laboratory (SL), James T. Ballard, Assistant Director, SL, and Dr. Reed L. Mosher, Chief, Structural Mechanics Division (SMD), SL. Dr. Stanley C. Woodson, SMD, performed the study and prepared this report.

During publication of this report, the Director of WES was Dr. Robert W. Whalin. Commander was COL Bruce K. Howard, EN.

The contents of this report are not to be used for advertising, publication or promotional purposes. Citation of trade names does not constitute an official endorsement or approval of the use of such commercial products.

Conversion Factors, Non-SI to SI Units of Measurement

Non-SI units of measurement used in this report can be converted to SI units as follows:

Multiply	By	To Obtain
degrees (angle)	0.01745	radians
feet	0.3048	metres
inches	25.4	millimetres
kips (force) per square inch	6.894757	megapascals
pounds (force)	4.448222	newtons
pounds (force) per square inch	0.006894757	megapascals

1: Introduction

Background

A considerable amount of data is available in the literature regarding the behavior of normally-proportional slabs, those with span-to-effective-depth (L/d) ratios greater than approximately 8 and perhaps as low as 5 or 6. Woodson (1993) presented one of the most comprehensive collections of data on statically- and dynamically-tested slabs. The data base was used in the development of the Engineer Technical Letter (ETL) 1110-9-7 (Department of the Army, 1990), "Response Limits and Shear Design for Conventional Weapons Resistant Slabs,". In brief, the criteria given in the ETL for restrained slabs allow design support rotations of 12 and 20 degrees for anticipated damage levels categorized as "moderate" and "heavy", respectively. The moderate damage level is described as that recommended for the protection of personnel and sensitive equipment. Significant concrete scabbing and reinforcement rupture have not occurred at this level. The dust and debris environment on the protected side of the slab is moderate; however, the allowable slab motions are large. Heavy damage means that the slab is at incipient failure. Under this damage level, significant reinforcement rupture has occurred, and only concrete rubble remains suspended over much of the slab. The heavy damage level is recommended for cases in which significant concrete scabbing can be tolerated, such as for the protection of water tanks and stored goods and other insensitive equipment.

The ETL sets forth some design conditions that must be satisfied in conjunction with applying its response limits. These limitations reflect an aggressive approach, yet maintain appropriate conservatism based on available data. The scaled range must exceed $0.5 \text{ ft/lb}^{1/3}$ and the span-to-effective-depth (L/d) ratio of the slab must exceed 5. Principal reinforcement spacing is to be minimized and shall never exceed the effective depth (d) of the slab. Stirrup reinforcement is required, regardless of computed shear stress, to provide adequate concrete confinement and principal steel restraint in the large-deflection region. Stirrups are required along each principal bar at maximum spacing of one-half the effective depth ($d/2$) when the scaled range is less than $2.0 \text{ ft/lb}^{1/3}$ and at a maximum spacing equal to the effective depth at larger scaled ranges. All stirrup reinforcement is to provide a minimum of 50 psi shear stress capacity.

The ETL, developed to supplement Technical Manual (TM) 5-855-1 (Department of the Army, 1986), is the most recently published design document on the subject. It claims no applicability to slabs having span-to-effective-depth (L/d) ratios less than 5. In addition, due to a lack of data and understanding, the ETL sets forth strict shear reinforcement requirements for laterally-restrained slabs with L/d values less than 8, a value on the low end of the range for normally-proportioned slabs. Thus, guidance for shear design and response

limits of deep slabs used in protective structures is lacking, particularly for structures to resist the effects of conventional weapons. Although there is a lack of guidance for designing efficient deep slabs, deep slabs are very common as roofs and walls of protective structures. There is some concern that designers might inappropriately apply normally-proportioned-slab theory to deep slabs.

Objective

The overall objective was to gain a basic understanding of the behavior of deep slabs with reinforcing details typical of protective construction. A specific objective was to compare the effects of stirrups and lacing bars on the behavior of deep slabs. The intent was to obtain data that will help fill in gaps in design guidance for slabs used in protective construction.

Approach

Thirteen one-way reinforced concrete slabs were statically loaded at the U. S. Army Engineer Waterways Experiment Station (WES) in March through April, 1993. Previous studies (Woodson, 1993) emphasized that the primary parameters that affect the large-deflection behavior of a one-way slab include: support conditions, quantity and spacing of principal reinforcement, quantity and spacing of shear reinforcement, span-to-effective-depth (L/d) ratio, and scaled range (for blast loads). The slabs in this study were designed with consideration of the role of these primary parameters.

2: Experimental Description

General

The following sections describe the slabs' construction details, instrumentation, and the experimental procedure.

Construction Details

Table 1 qualitatively presents the characteristics of each slab. Table 2 presents the same characteristics in a quantitative manner, reflecting the practical designs based on available construction materials. All slabs were designed to be loaded in a clamped (laterally and rotationally restrained) condition. Each slab had a clear span of 24 inches and a width of 24 inches. Slab thickness varied as follows: 3 slabs had an overall thickness of 5.5 inches, and 10 slabs had an overall thickness of 8.9 inches. The effective depth of each slab was either approximately 4.8 or 8.0 inches. The L/d ratio of each slab was either 3 or 5. Principal reinforcement consisted of either no. 3 or no. 5 Grade 60 rebar. Stirrups and lacing bars were fabricated from D2 and D3 deformed wire in slabs with ratios of 5 and 3, respectively. The deformed wire was annealed to a yield stress of approximately 60 ksi. At the time of the experiments, the average concrete compressive strength was approximately 5900 psi.

In general, the experimental program was designed to study the behavior of uniformly-loaded deep slabs and, in particular, to compare the effects of lacing bars and stirrups on the behavior. It was important that the ratio of principal steel spacing to slab effective depth (s/d) was held nearly constant among the slabs. Data from previous studies indicated that this ratio should be less than 1.0 in order to enhance the large-deflection behavior. The s/d ratio was maintained at a value of approximately 0.5. Three shear reinforcement spacings were used: $0.17d$, $0.31d$, and $2d$ ($d/2$ is the value typically given in design manuals for blast-resistant structures). Figures 1 through 3 are plan views showing slab proportions and the principal steel and temperature steel layouts for each of the slabs. The temperature (transverse) steel spacing was identical for all of the slabs, but one difference in the temperature steel placement occurred between the laced and nonlaced slabs. The temperature steel is typically placed exterior to the principal steel in laced slabs, but it is placed interior to the principal steel in the slabs having stirrups or no shear reinforcement.

Table 1
Slab Characteristics (Qualitative)

Slab	$\rho_{tension}$	ρ_{shear}	Lacing	Stirrups	Principal Steel Spacing	Shear Steel Spacing	L/d Ratio
1	large	none	-	-	0.5d	-	5
2	large	large	-	x	0.5d	0.31d	5
3	large	large	x	-	0.5d	0.31d	5
4	small	none	-	-	0.5d	-	3
5	large	none	-	-	0.5d	-	3
6	large	none	-	-	0.5d	-	3
7	small	large	-	x	0.5d	0.17d	3
8	large	large	-	x	0.5d	0.17d	3
9	large	large	-	x	0.5d	0.17d	3
10	large	small	-	x	0.5d	2d	3
11	small	large	x	-	0.5d	0.17d	3
12	large	small	x	-	0.5d	2d	3
13	large	large	x	-	0.5d	0.17d	3

Table 2
Slab Characteristics (Quantitative)

Slab	$\rho_{tension}$	ρ_{shear}	Lacing	Stirrups	Principal Steel Spacing (inches)	Shear Steel Spacing (inches)	L/d Ratio
1	0.0096	none	-	-	No. 3 @ 2.4	-	5
2	0.0096	0.0060	-	x	No. 3 @ 2.4	1.5	5
3	0.0096	0.0060	x	-	No. 3 @ 2.4	1.5	5
4	0.0034	none	-	-	No. 3 @ 4.0	-	3
5	0.0096	none	-	-	No. 5 @ 4.0	-	3
6	0.0096	none	-	-	No. 5 @ 4.0	-	3
7	0.0034	0.0060	-	x	No. 3 @ 4.0	1.33	3
8	0.0096	0.0060	-	x	No. 5 @ 4.0	1.33	3
9	0.0096	0.0060	-	x	No. 5 @ 4.0	1.33	3
10	0.0096	0.0013	-	x	No. 5 @ 4.0	6.00	3
11	0.0034	0.0060	x	-	No. 3 @ 4.0	1.33	3
12	0.0096	0.0013	x	-	No. 5 @ 4.0	6.00	3
13	0.0096	0.0060	x	-	No. 5 @ 4.0	1.33	3

Figures 4 through 14 are sectional views cut through the lengths of the slabs. The dashed lacing bar in each figure indicates the configuration of the lacing bar associated with the next principal steel bar. The positions of the lacing bars were alternated to encompass all temperature steel bars. However, some temperature steel bars were not encompassed by lacing bars in slab no. 12 due to the spacing of the lacing bar bends. The spacings of the lacing bar bends were controlled by the shear reinforcement quantities in corresponding slabs with stirrups. In slabs with stirrups, the stirrups were spaced along the principal steel bar at the spacings shown in Table 2, never directly encompassing the temperature steel.

The slabs were constructed in the laboratory with much care to ensure quality construction with minimal error in reinforcement placement. Figures 15 through 27 are photographs of slabs no. 1 through 13 prior to the placement of concrete. Figure 28 is a close-up view of the lacing in slab no. 3, and Figure 29 is the close-up view of the stirrups in slab no. 7.

Instrumentation

Each slab was instrumented for strain, displacement, and pressure measurements. The data were digitally recorded with a personal computer. Two displacement transducers were used in each experiment to measure vertical displacement of the slab, one at one-quarter span and one at midspan. The displacement transducers used were Celesco Model PT-101, having a working range of 10 inches. These transducers measured the displacement of the slab by means of a potentiometer which detected the extension and retraction of a cable attached to a spring inside the transducer. More specifically, a Celesco Model PT-101 transducer contains a drum that is attached to a linear rotary potentiometer. When the cable is completely retracted, the potentiometer is at one end of its range. As the cable is extended, the drum rotates (thus rotating the potentiometer) until the cable is at full extension and the potentiometer is at the other end of its range. A DC voltage is applied across the potentiometer, and the output is taken from the potentiometer's wiper. As the cable is retracted and the wiper moves along the potentiometer, the output voltage varies since the potentiometer acts as a voltage divider. The body of each transducer was mounted to the floor of the reaction structure, and the cable was attached to a hook that was glued to the slab surface. Retraction of the cables into the transducers' bodies occurred as the slab deflected and downward displacement occurred at the one-quarter span and midspan locations. Two single-axis, metal film, 0.125-inch-long, 350 ohm, strain gage pairs were installed on principal reinforcement in each slab. Each pair consisted of a strain gage on a top bar and one on a bottom bar directly below. One pair was located at midspan (ST-1, SB-1), and one was located at one-quarter span (ST-2, SB-2).

Strain gages were also installed at mid-height on shear steel in the slabs that contained shear reinforcement. Strain gages were placed on lacing bars in laced slabs at locations along the length of the slabs similar to the locations of stirrups with gages in the corresponding slabs with stirrups. The gages were

placed on the shear reinforcement associated with the center principal steel bars. Figures 30 through 35 show the locations of the strain gages on the shear reinforcement in the slabs. Two Kulite Model HKM-S375, 500-psi-range pressure gages (P1 and P2) were mounted in the bonnet of the test chamber in order to measure the water pressure applied to the slab.

Experimental Procedure

The 6-foot diameter static test chamber was used to slowly load the slabs with water pressure. Huff (1969) presented a detailed description of the test device. Preparations for the experiments began with the reaction structure being placed inside the test chamber and surrounded with compacted sand. In general, the reaction structure consisted of a steel/concrete box without a top. Bolts for clamping the slabs protruded upward from the two sides. The reaction structure had a removable door to allow access to the space beneath the slab specimen, particularly for instrumentation requirements. Placement of a 36- by 24-inch slab in the reaction structure allowed 6 inches of the slab at each end to be clamped by a steel plate that was bolted into position, thereby leaving a 24- by 24-inch one-way restrained slab to be loaded with uniform pressure. After a slab was placed on the reaction structure, the wire leads from the instrumentation gages and transducers were connected. After placing the removable door into position, the sand backfill was completed on the door side of the reaction structure. A 1/8-inch-thick fiber-reinforced neoprene rubber membrane and a 1/8-inch-thick unreinforced neoprene rubber membrane were placed over the slab as shown in Figure 36, and 1/2- by 6- by 24-inch steel plates were bolted into position at each support. Prior to the bolting of the plates, a waterproofing putty was placed between the membrane and the steel plates to seal gaps around the bolts in order to prevent a loss of water pressure during the experiment. The chamber's lid was lowered into position (Figure 37), and the chamber was rolled inside the large reaction structure. A time of approximately 18 minutes was required to fill the bonnet indicated when the bonnet had been filled. At that time, the waterline valve was again closed to allow closing of the relief plug. The waterline valve was once again opened slowly, inducing a slowly increasing load to the slab's surface as the lid of the chamber was pushed upward and against the large reaction structure (shown in the background of Figure 37). A gasoline-powered pump was connected to the waterline to facilitate water pressure loading since the commercial line pressure was not great enough to reach ultimate resistance of the slab in any of the experiments. Monitoring of the pressure gages and deflection gages indicated the behavior of the slab during the experiment and enabled this author to make decision for experiment termination by closing the waterline valve. The loading was controlled at a slowly changing rate, resulting in a load application time of several minutes. Following experiment termination, measurements and photographs of the slab were taken after removal of the neoprene membrane. Finally, the damaged slab was removed and the reaction structure was prepared for another slab.

3: Results and Discussion

General

In this chapter, the data are presented in various forms (i.e., tables and composite plots), and the results of the experiments are evaluated. Posttest photographs showing the extent of structural damage are included. The implications of the results on design criteria are discussed.

Instrumentation Data

The electronically recorded data are presented in the Appendix. All of the strain gage readings and the deflection gage readings were plotted against the readings of both of the pressure transducers (P-1 and P-2) for each experiment. For the plots presented in the Appendix, the strain and deflection measurements versus only one of the pressure gage's readings are shown. The two pressure transducers provided essentially identical values.

In general, the quality of the data was good. Data were recovered from all gages, and it appears that all gages functioned properly.

Discussion

Structural Damage and General Response

Posttest measurements and inspection provided a data check and damage assessment of each slab prior to removal from the reaction structure. Figures 38 through 50 show the posttest condition of each slab. Except for slab no. 4, Figures 38 through 50 show the slab immediately after removal of the neoprene membrane. For slab no. 4, Figure 41 shows the slab after removal from the reaction structure. Slab no. 4 was only slightly damaged and, therefore, could be safely removed from the reaction structure prior to photography. Figure 41 provides a better view of the side crack pattern than was allowed while the slab remained in the reaction structure.

Figure 51 shows the general shape of the midspan load-deflection curve. Values of load and deflection at points A through C of Figure 51 are given in Table 3 for convenience in numerical comparisons. Similarly, Table 4 presents

Table 3 Midspan Load-Deflection Summary						
Slab	P _A (psi)	δ _A	P _B (psi)	δ _B	P _C (psi)	δ _C
1	399	0.20	264	1.01	349	1.98
2	571	0.40	396	0.96	369	1.80
3	543	0.41	319	1.32	-	-
4	572	0.33	-	-	-	-
5	1169	0.24	869	1.30	1211	1.92
6	1222	0.33	824	1.43	1150	2.66
7	1860	0.40	-	-	-	-
8	1550	0.40	975	1.74	1225	2.58
9	1365	0.29	1285	0.44	1260	0.87
10	1337	0.29	-	-	-	-
11	1380	0.37	-	-	-	-
12	1210	0.27	926	1.21	1163	2.93
13	1545	0.65	1315	1.79	1445	3.48

Table 4 Quarter-span Load-Deflection Summary						
Slab	P _A (psi)	δ _A	P _B (psi)	δ _B	P _C (psi)	δ _C
1	399	0.20	264	1.03	349	1.86
2	571	0.36	396	0.96	-	-
3	543	0.31	319	0.81	-	-
4	572	0.23	-	-	-	-
5	1169	0.23	869	1.30	1211	2.66
6	1222	0.28	824	1.48	1150	2.73
7	1860	0.32	-	-	-	-
8	1550	0.37	975	1.86	1225	2.58
9	1365	0.24	1285	0.46	1260	0.87
10	1337	0.29	-	-	-	-
11	1380	0.32	-	-	-	-
12	1210	0.27	926	1.32	1163	2.93
13	1545	0.53	1330	1.62	1445	3.48

load-deflection values recorded at the quarter-span location for each slab. Comparison of Figures 51 and 52 indicates that the typical experimental load-deflection curve for the deep slabs was considerably different from the general curve for normally-proportioned slabs. Specifically, the deep slabs were stiffer up to the ultimate resistance (point A). Following the attainment of ultimate resistance, the deep slabs incurred a rather sharp transition, with the remaining response being well-characterized by straight lines to points B and C. Further discussion of maximum deflections achieved will also provide insight for a comparison of the deep-slab behavior to that of normally-proportioned slabs. Additionally, the composite graphs of the load-deflection curves presented in Figures 53 through 59 aid in the evaluation of the effects of the parameters varied in this experimental series.

For the slabs with an L/d ratio of 5, Figure 53 demonstrates the significance of shear reinforcement (see Table 1) in that slab no. 1 was not able to achieve the value of ultimate resistance attained by slabs no. 2 and 3. Lacing bars (slab no. 3) and stirrups (slab no. 2) apparently provided similar levels of contribution to the shear strength of the slabs. The experiments on slabs no. 2 and 3 were terminated due to water pressure leaks; thus, they were not loaded to extremely large deflections.

Figure 54 simply indicates the differences in strength due to the L/d values. Not only is the strength directly affected by the L/d value, but a thicker slab also requires more reinforcement in order to maintain equivalent values of the principal reinforcement ratio. Figure 55 shows that the replication associated with slabs no. 5 and 6 provided very similar results.

Figure 56 compares the effects of stirrups (slab no. 8), lacing (slab no. 13), and no shear reinforcement (slab no. 6) of the slabs with an L/d of 3. As was shown in Figure 53 for the slabs with an L/d of 5, shear reinforcement did make a significant contribution to the ultimate resistance and lacing and stirrups were of approximately equal effectiveness. Slab no. 13 did appear to maintain higher values of resistance over the full range of loading. Figure 57 indicates that the data are consistent in that the smaller amount of shear reinforcement (slab no. 10) was less effective than the larger amount. In all figures containing slab no. 10, the data shown past the ultimate resistance for slab no. 10 is not true data since the deflection transducer cable apparently broke loose from the slab shortly after the ultimate resistance was reached.

Figure 58 further supports the previous observation that the lacing bars (slab no. 12) and stirrups (slab no. 10) are similarly effective in enhancing ultimate shear resistance. However, in both Figures 53 and 58, the data indicate that stirrups may be slightly more effective. As in Figure 57, Figure 59 indicates the considerable difference in effectiveness for large (slab no. 13) and small (slab no. 12) quantities of shear reinforcement.

Figures 60 through 69 present the posttest deflection survey data. In these figures, permanent deflections measured on the top (loading) surfaces of the slabs are given at numerous locations. Additionally the locations of major

cracks are drawn. The circles shown in the figures represent the locations of the bolt holes; thus, a 24-by-36-in slab is shown in each figure. The clear span for each slab was 24 inches. Slabs no. 4 and 7 are not included in the deflection survey figures since slab no. 4 was not loaded to significant damage and slab no. 7 incurred catastrophic damage.

Figures 70 through 80 are artist sketches of the bottom and side posttest views of the slabs. Sketches are not included for slabs no. 7 and 11 since they were damaged too heavily for a meaningful drawing. Figures 60 through 80 are useful for the reader that wants to carefully evaluate the response of the slabs. In this report, the figures will not be discussed in detail, but rather are used to support the observations and conclusions drawn from the instrumentation data and damage photographs.

Examination of Figures 60 through 80 indicate that shear behavior generally dominated the response of the slabs. This observation is also evident from a comparison of the midspan and quarter-span load-deflection summaries given in Tables 3 and 4. Since the electronically-measured deflections were similar at quarter-span and midspan, it appears that shear behavior dominated the response rather than flexure which would have produced a deflection profile more representative of a 3-hinge mechanism.

Ultimate Resistance and Response Limits

Two commonly-used parameters for describing slab response are the midspan-deflection-to-thickness ratio and the equivalent support rotation (defined as the arctan of the quotient of the midspan deflection divided by one-half of the clear span). Actually, for predominantly shear response, as is generally the case for deep slabs, neither of these parameters fully describe the response. However, attempts should be made to correlate the allowable response of deep slabs with these parameters for consistency in guidance documents.

Tables 5 and 6 respectively present the midspan deflection-to-thickness ratios and the equivalent support rotations for each slab at intervals corresponding to points A, B, and C of Figure 51. Table 5 shows that the midspan deflection-to-slab-thickness ratio at ultimate (δ_A/t) is considerably small when compared to typical values for normally-proportioned slabs. It is well known that, for normally-proportioned slabs, this ratio has the general value of 0.3 to 0.5. The experiments in this series indicated that the δ_A/t value for slabs with an L/d ratio of 5 (provided shear reinforcement is included to prevent premature shear failure) can be expected to be approximately 0.07. Similarly, δ_A/t values of 0.03 to 0.05 can be expected for slabs having an L/d ratio of 3.

The values given in Table 6 are useful in that they provide information to the designer on the equivalent support rotation that should be expected at ultimate resistance. Additionally, Table 6 shows that deep slabs can achieve considerably

Table 5
Midspan Deflection/Slab Thickness

Slab	δ_A/t	δ_B/t	δ_C/t
1	0.04	0.18	0.36
2	0.07	0.17	0.33
3	0.07	0.24	-
4	0.04	-	-
5	0.03	0.15	0.35
6	0.04	0.16	0.30
7	0.05	-	-
8	0.05	0.20	0.29
9	0.03	0.05	0.16
10	0.03	-	-
11	0.04	-	-
12	0.03	0.14	0.33
13	0.04	0.20	0.39

Table 6
Equivalent Support Rotation

Slab	L/d	θ_A (degrees)	θ_B (degrees)	θ_C (degrees)
1	5	1.0	4.8	9.4
2	5	1.9	4.6	8.5
3	5	2.0	6.3	-
4	3	1.6	-	-
5	3	1.1	6.2	9.1
6	3	1.6	6.8	12.5
7	3	1.9	-	-
8	3	1.9	8.3	12.1
9	3	1.4	2.1	4.1
10	3	1.4	-	-
11	3	1.8	-	-
12	3	1.3	5.8	13.7
13	3	3.1	8.5	16.2

high values of response without collapse. Values of equivalent support rotation up to approximately 16 degrees were sustained.

Under slowly applied uniform loading, a beam or one-way slab element initially undergoes elastic deflection. As loading continues, plastic hinges first form at the supports and later at midspan. As discussed by Park and Gamble (1980), the ultimate flexural capacity is enhanced in slabs whose edges are restrained against lateral movement. This plastic theory for the load-deflection behavior of a restrained strip at and after the ultimate resistance is often referred to as "compressive-membrane theory." Full restraint against rotation and vertical translation is assumed at the supports. Partial restraint against lateral displacement is assumed at the supports as compressive membrane action is dependent of the lateral restraint. As the slab deflects, changes in geometry cause the slab's edges to tend to move outward and to react against the stiff boundary elements. The membrane forces enhance the flexural strength of the slab sections at the yield lines. For the slabs in this study, the resistance at point "A" in Figure 51 corresponds to the ultimate capacity.

Two relatively difficult-to-define parameters required in the computation of the ultimate flexural resistance due to compressive-membrane action are: (a) the stiffness of the surround supporting the slab and (b) the midspan deflection occurring at ultimate capacity (often described by the δ_A/t ratio). Park and Gamble demonstrated that the surround stiffness need not be enormous to achieve membrane action similar to that for an infinitely rigid surround. Significant membrane action occurs when the surround and the one-way slab have the same stiffness. For slabs with relatively low values of the ratio of slab length to thickness (which applies to the slabs in this study), little increase in membrane action is achieved by having a surround much stiffer than the slab. As discussed by Park and Gamble, many researchers have attempted to develop methods for determining δ_A/t . This ratio is affected by the relative stiffness of the surround and slab. It is also affected by whether the slab exhibits one-way or two-way action. A computer program, consistent with the theory as presented by Park and Gamble, was used during this study to compute the enhancement due to compressive-membrane action for the slabs. The theory is based on the equilibrium and deformations of a slab strip.

From an analytical/design viewpoint, Table 7 demonstrates the application of compression membrane theory. The W_y values in Table 7 correspond to yield-line theory, and the W_c values correspond to compression membrane theory. The W_c values were computed using the (δ_A/t) values supplied in Table 5. For most of the slabs that contained a "large" amount of shear reinforcement, the experimental values and the W_c values compare rather well. Slabs with no or little shear reinforcement incurred shear failures prior to attaining the compressive membrane resistance values.

Table 7 Compressive Membrane					
Slab	W_y (psi)	W_o (psi)	Experimental (psi)	ρ_{shear}	$\frac{\delta_A}{t}$ (experimental)
1	348	606	399	0	0.036
2	348	595	571	0.0060	0.073
3	348	594	543	0.0060	0.075
4	352	1331	572	0	0.037
5	966	1718	1169	0	0.027
6	966	1713	1222	0	0.037
7	352	1322	1860	0.0060	0.045
8	966	1705	1550	0.0060	0.045
9	966	1716	1365	0.0060	0.033
10	966	1716	1337	0.0013	0.033
11	352	1326	1380	0.0060	0.042
12	966	1717	1210	0.0013	0.030
13	966	1668	1545	0.0060	0.073

4: Conclusions

A relatively large amount of shear reinforcement is critical for achieving the potential ultimate resistance of a deep slab. The experiments indicated that the contributions from lacing bars and stirrups are similar. Since deep slabs can achieve relatively high values of resistance, it was difficult to maintain the loading water pressure at large deflections. Therefore, a through comparison of the effects of lacing bars and stirrups at extremely high deflection levels was not possible.

The post-ultimate behavior of the slabs indicates that a substantial amount of reserve capacity is available in deep slabs with large quantities of principal reinforcement. However, the series indicated that deep slabs with relatively low quantities of principal reinforcement ($\rho=0.0034$) are considerably less ductile. Based on this series, the recommended response limit (support rotation) for deep slabs having a principal steel ratio of approximately 0.01 and adequate shear reinforcement is approximately 12 degrees. For deep slabs with relatively small quantities of principal steel, the response should probably be limited to approximately 8 degrees for design purposes.

The implications of the results are significant in that relatively simple analysis techniques can be successfully employed to define the resistance of deep slabs. Compression membrane theory provides a good estimate of the potential ultimate resistance of a deep slab, provided appropriate values of δ_A/t are used in the computations. However, the typically-used δ_A/t values of 0.3 to 0.5 are inappropriate for deep slabs. The experimentally-determined δ_A/t values were approximately 0.07 and 0.03 to 0.05 for the slabs with L/d values of 5 and 3, respectively. Since, these δ_A/t values resulted in slightly high compressive membrane resistance values, δ_A/t should be increased slightly in order to decrease the W_c values and to provide conservative design values.

References

Department of the Army (1986), "Fundamentals of Protective Design for Conventional Weapons," Technical Manual 5-855-1, Washington, D.C.

Department of the Army (1990), "Response Limits and Shear Design for Conventional Weapons Resistant Slabs," Engineer Technical Letter 1110-9-7, Washington, D.C.

Huff, W. L. (1969), "Test Devices of the Blast Load Generator Facility," Miscellaneous Paper N-69-1, U.S. Army Engineer Waterways Experiment Station, Vicksburg, Mississippi.

Park, R. and Gamble, W. L. (1980), Reinforced Concrete Slabs, John Wiley and Sons, New York, pp. 562-609.

Woodson, S. C. (1993), "Effects of Shear Reinforcement on the Large-Deflection Behavior of Reinforced Concrete Slabs," thesis, University of Illinois at Urbana-Champaign.

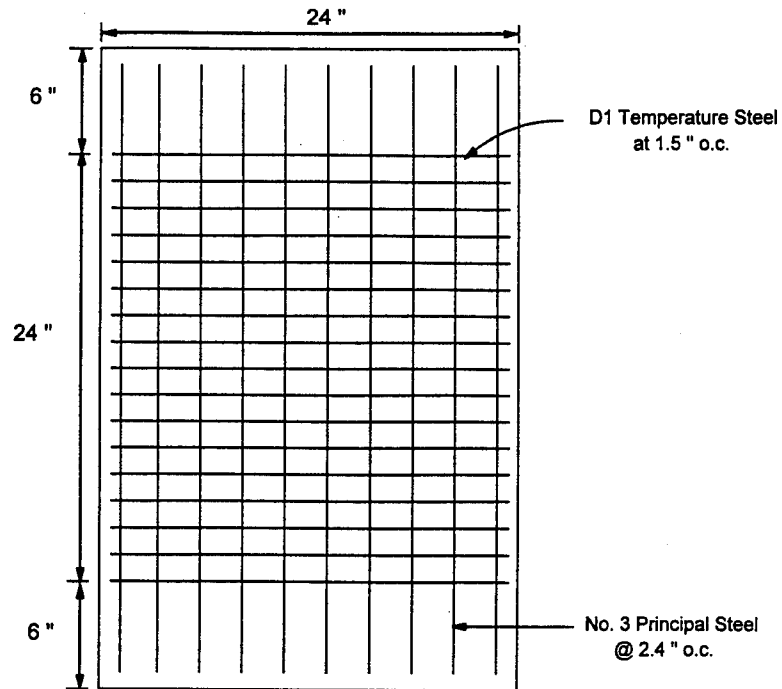


Figure 1. Plan View of Slabs No. 1, 2, and 3

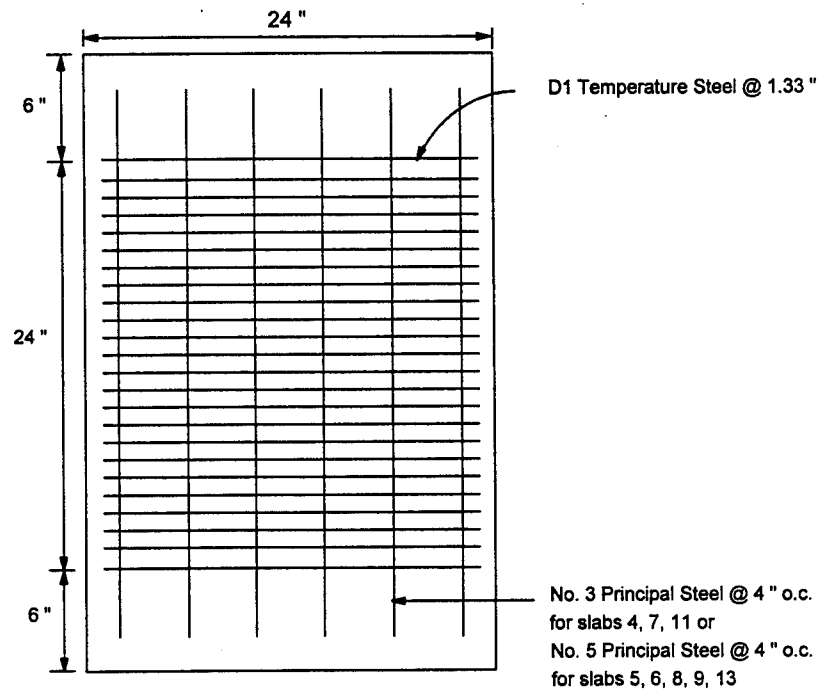


Figure 2. Plan View of Slabs No. 4, 5, 6, 7, 8, 9, 11, and 13

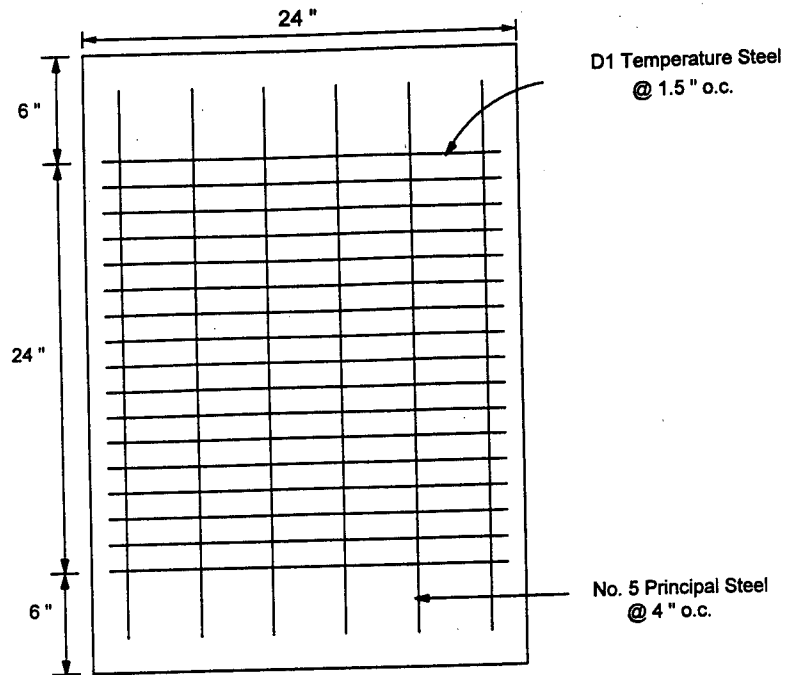


Figure 3. Plan View of Slabs No. 10 and 12

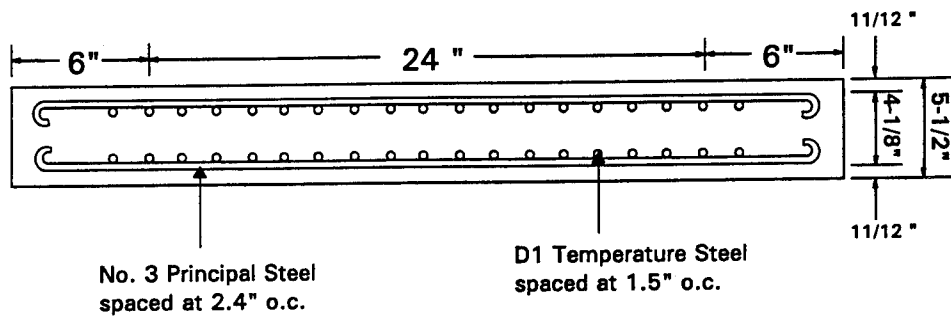


Figure 4. Sectional View Through Length of Slab No. 1

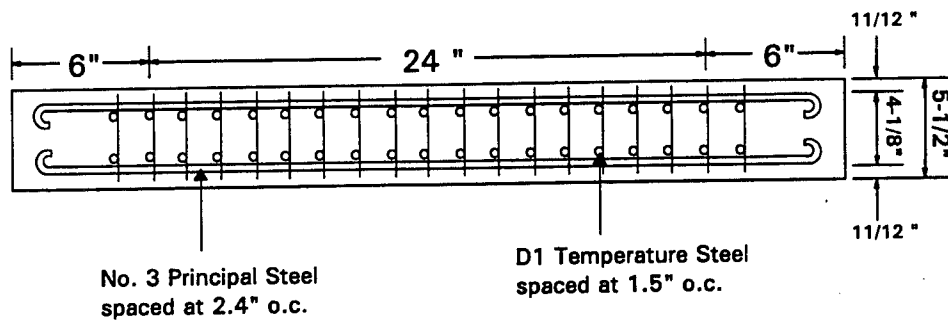


Figure 5. Sectional View Through Length of Slab No. 2

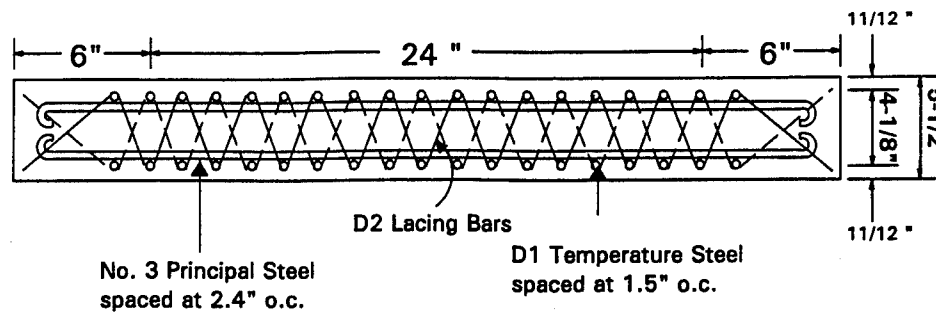


Figure 6. Sectional View Through Length of Slab No. 3

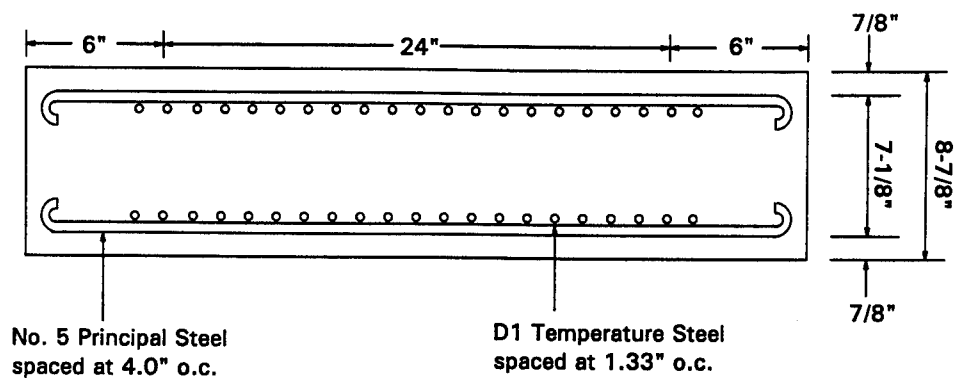


Figure 7. Sectional View Through Length of Slab No. 4

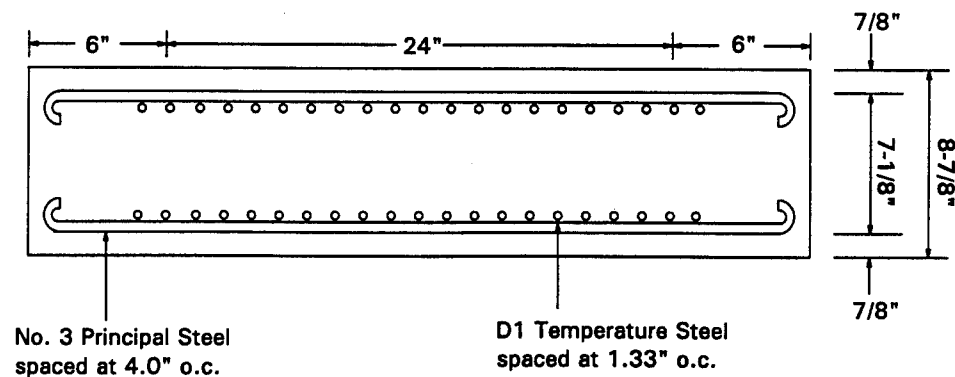


Figure 8. Sectional View Through Length of Slabs No. 5 & 6

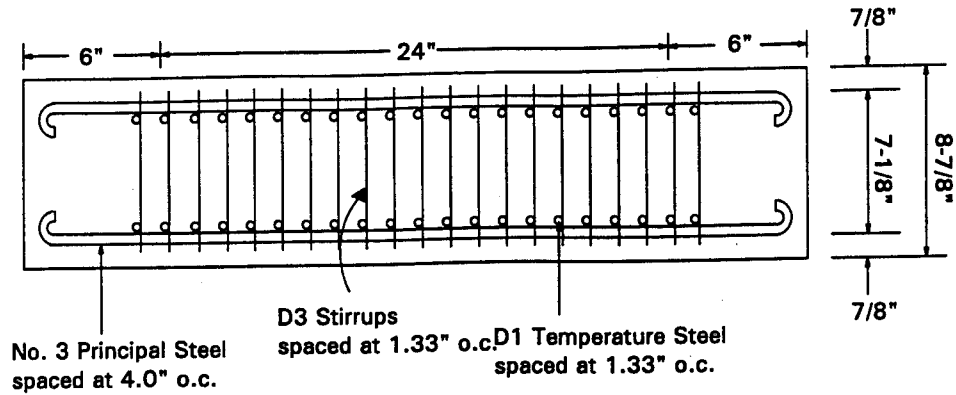


Figure 9. Sectional View Through Length of Slab No. 7

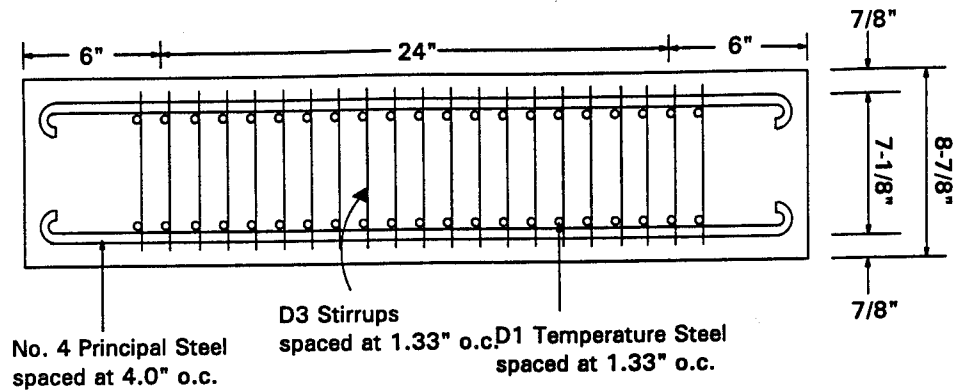


Figure 10. Sectional View Through Length of Slabs No 8 & 9

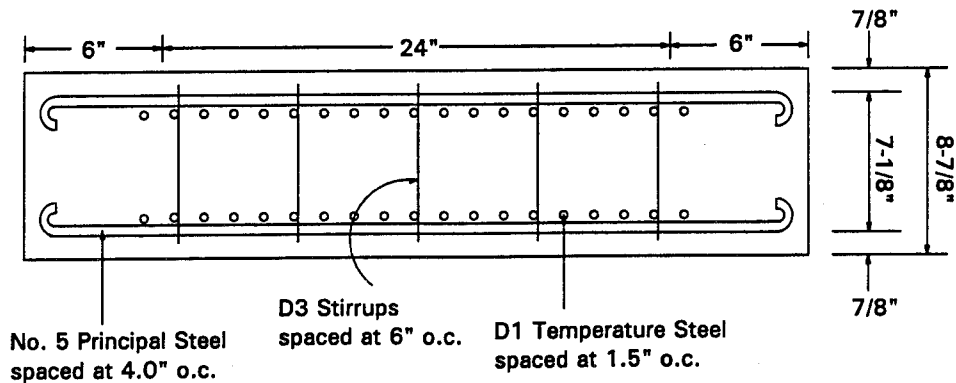


Figure 11. Sectional View Through Length of Slabs No 10

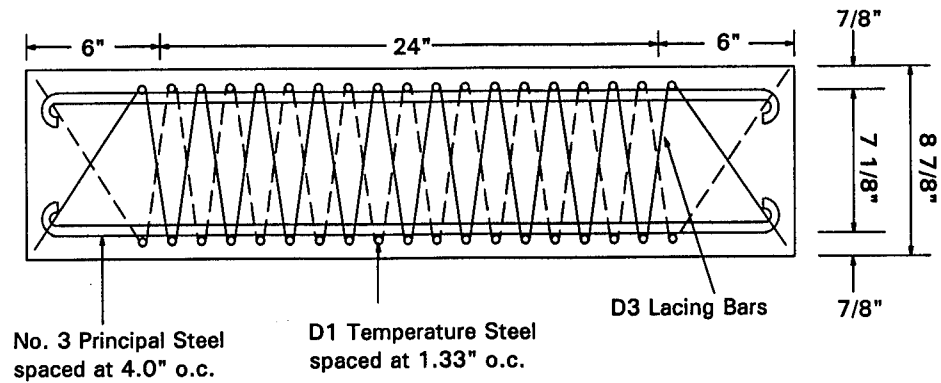


Figure 12. Sectional View Through Length of Slab No. 11

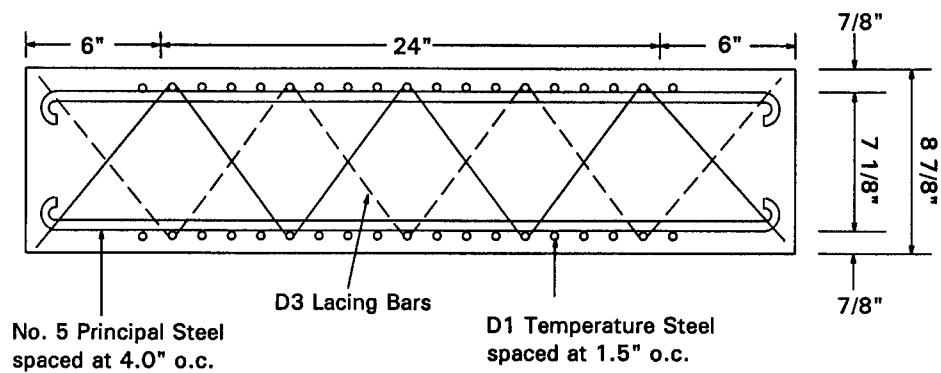


Figure 13. Sectional View Through Length of Slab No. 12

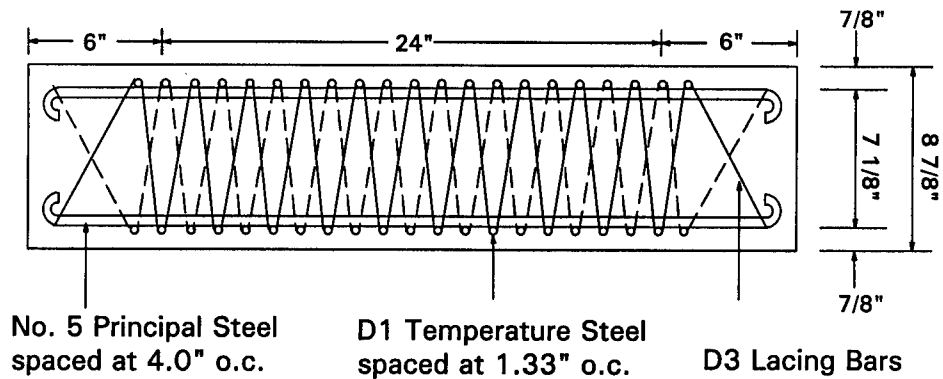


Figure 14. Sectional View Through Length of Slab No. 13

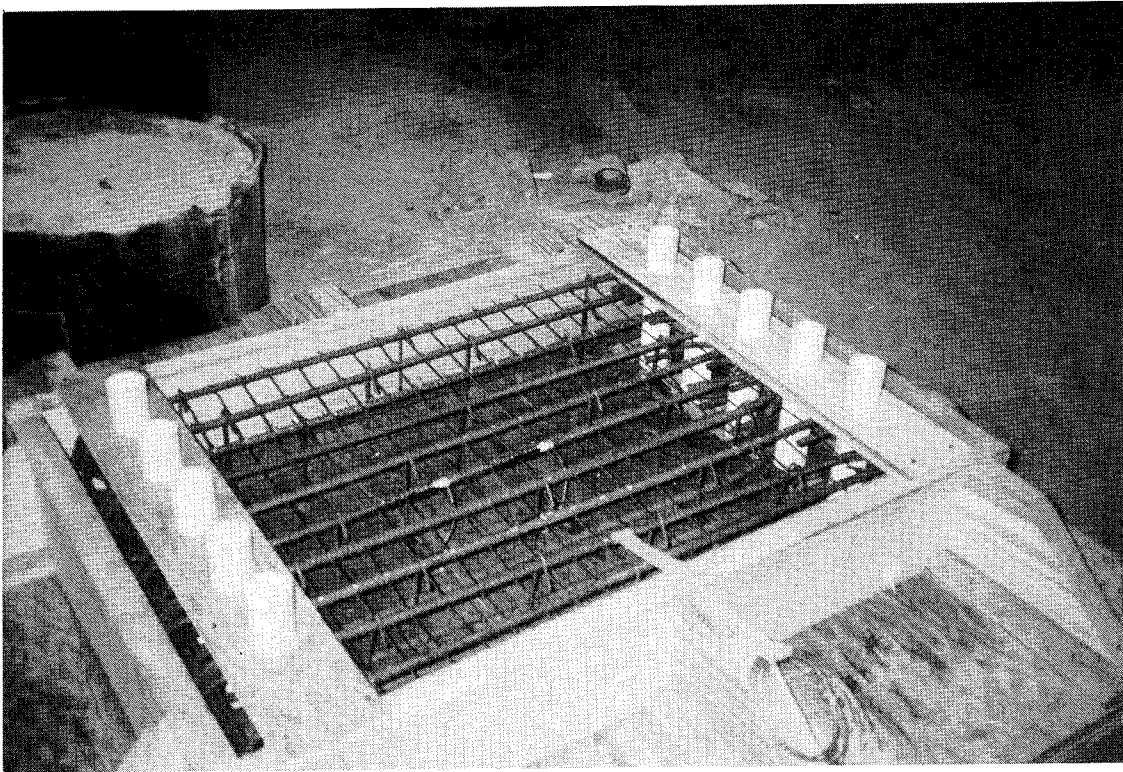


Figure 15. Slab No. 1 Prior to Concrete Placement

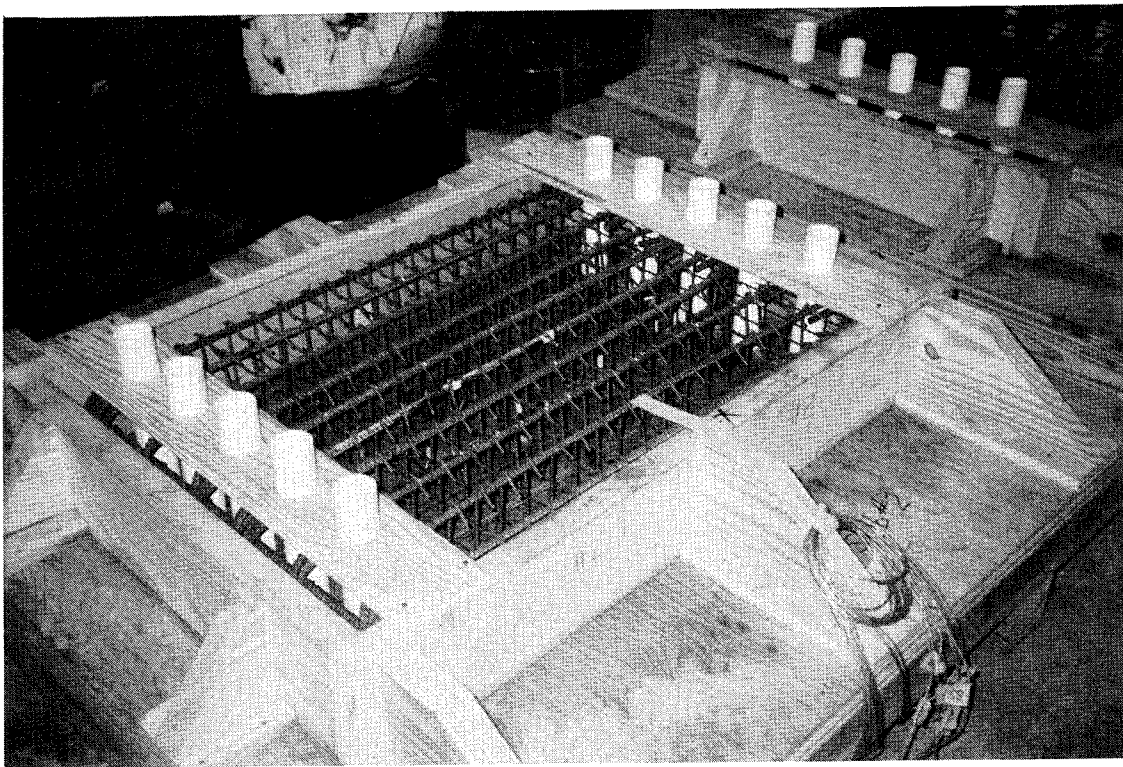


Figure 16. Slab No. 2 Prior to Concrete Placement

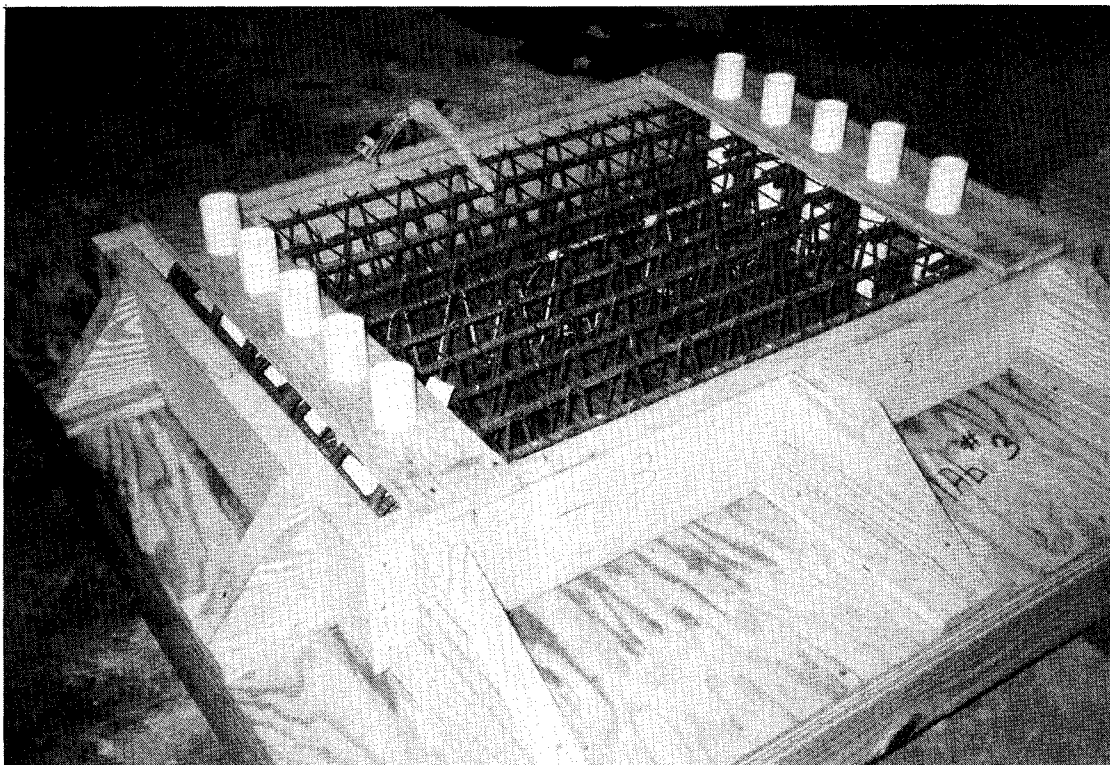


Figure 17. Slab No. 3 Prior to Concrete Placement

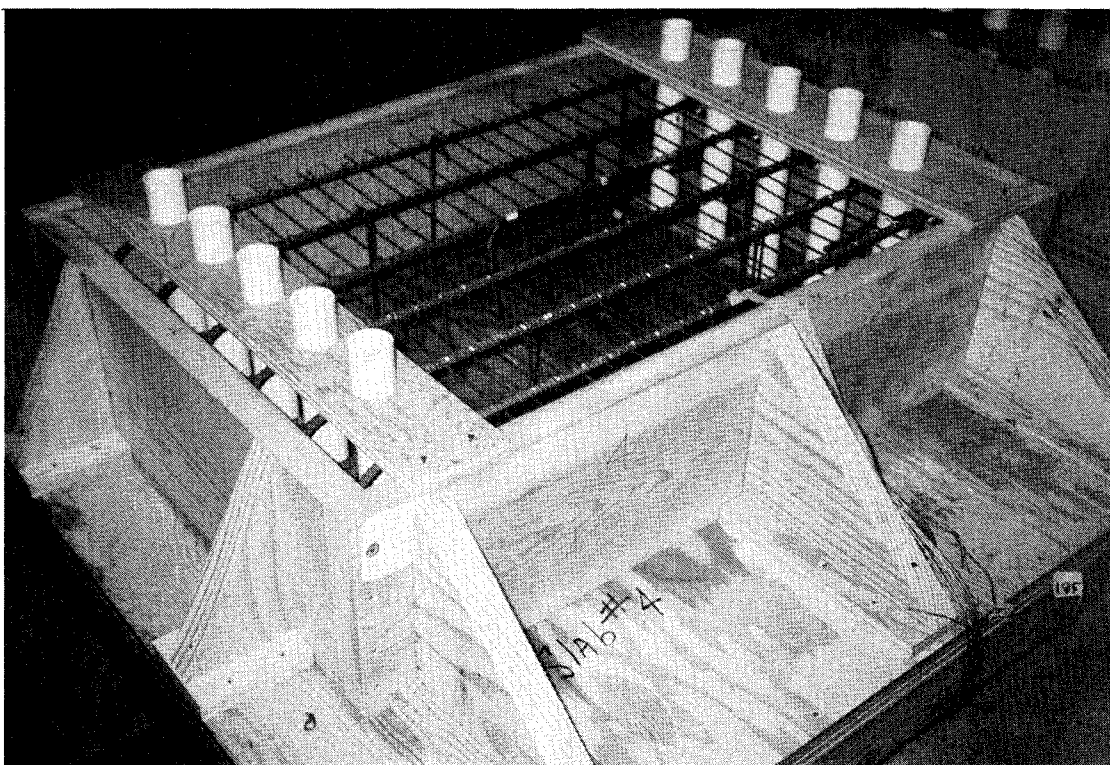


Figure 18. Slab No. 4 Prior to Concrete Placement

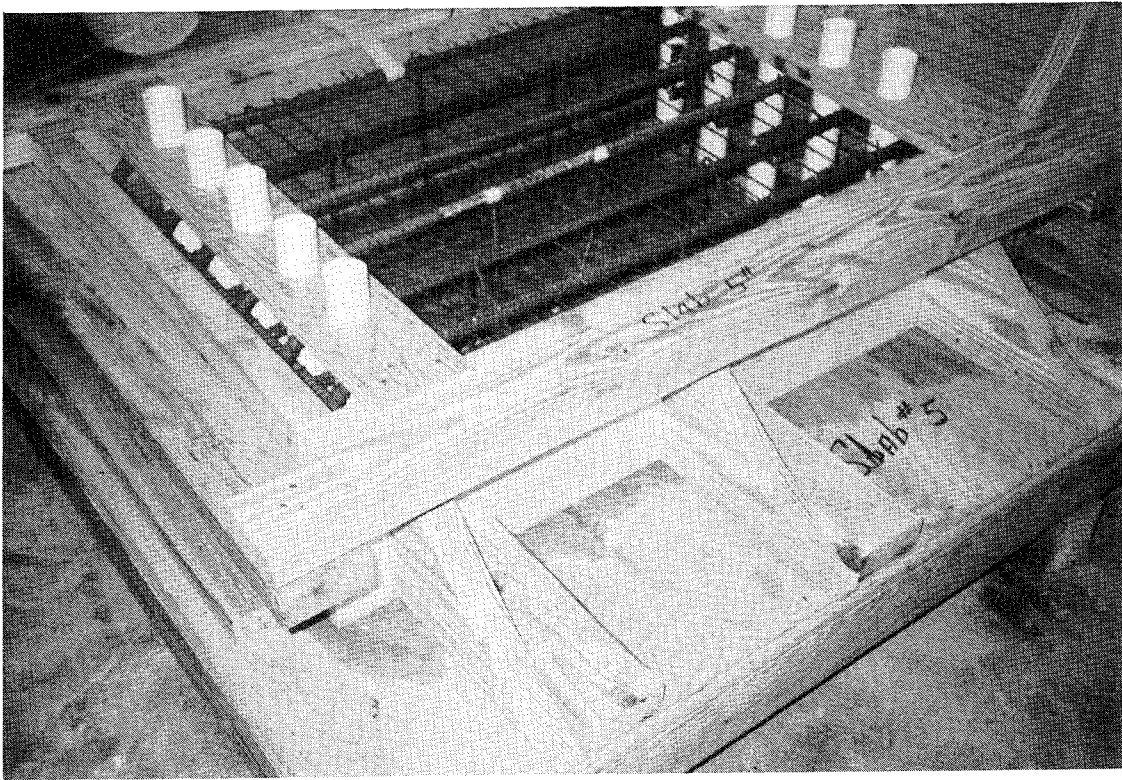


Figure 19. Slab No. 5 Prior to Concrete Placement

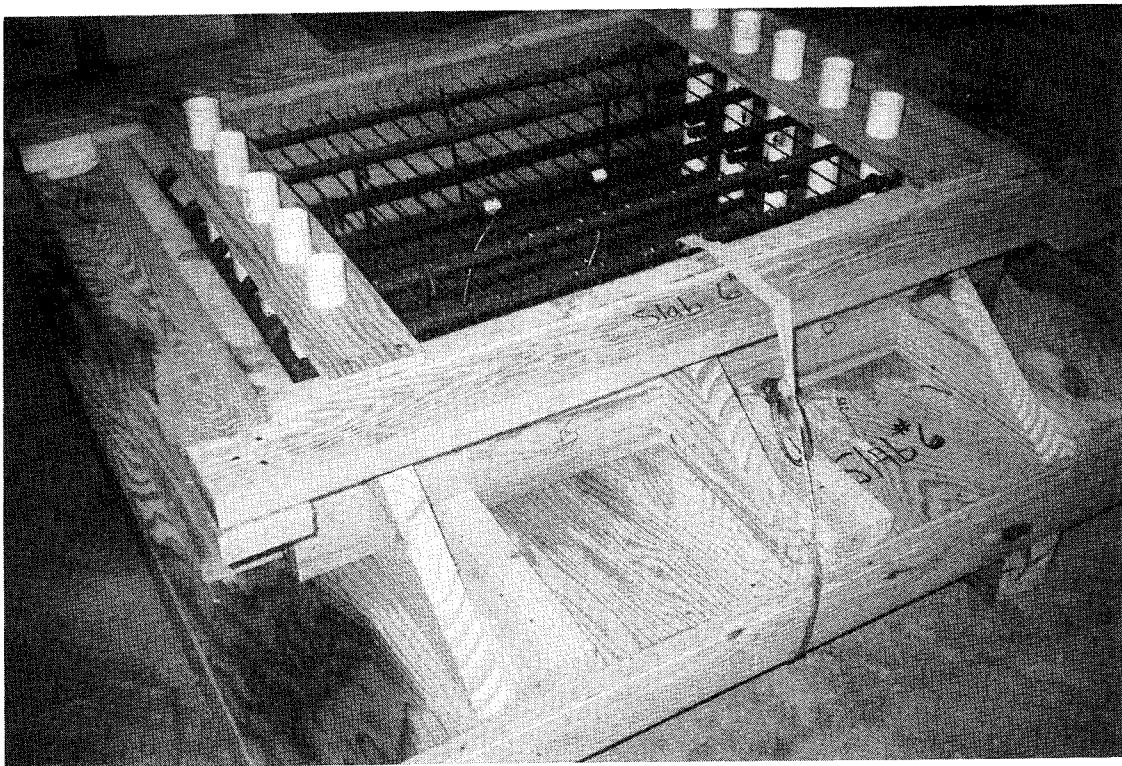


Figure 20. Slab No. 6 Prior to Concrete Placement

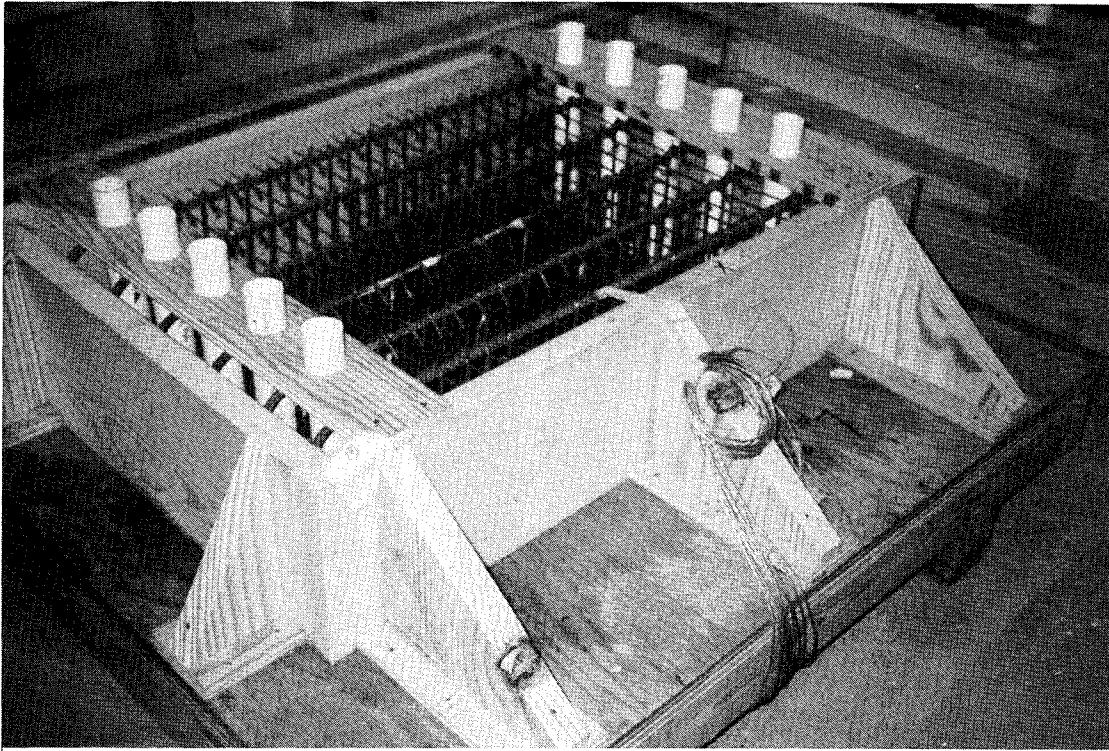


Figure 21. Slab No. 7 Prior to Concrete Placement

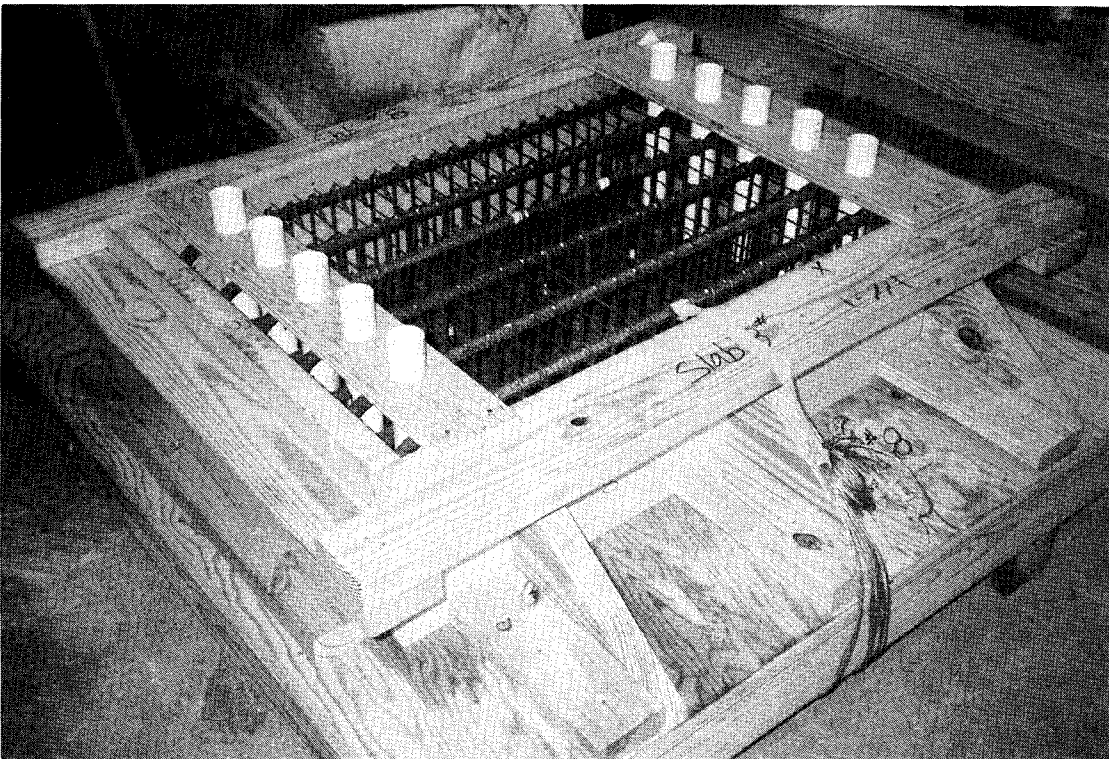


Figure 22. Slab No. 8 Prior to Concrete Placement

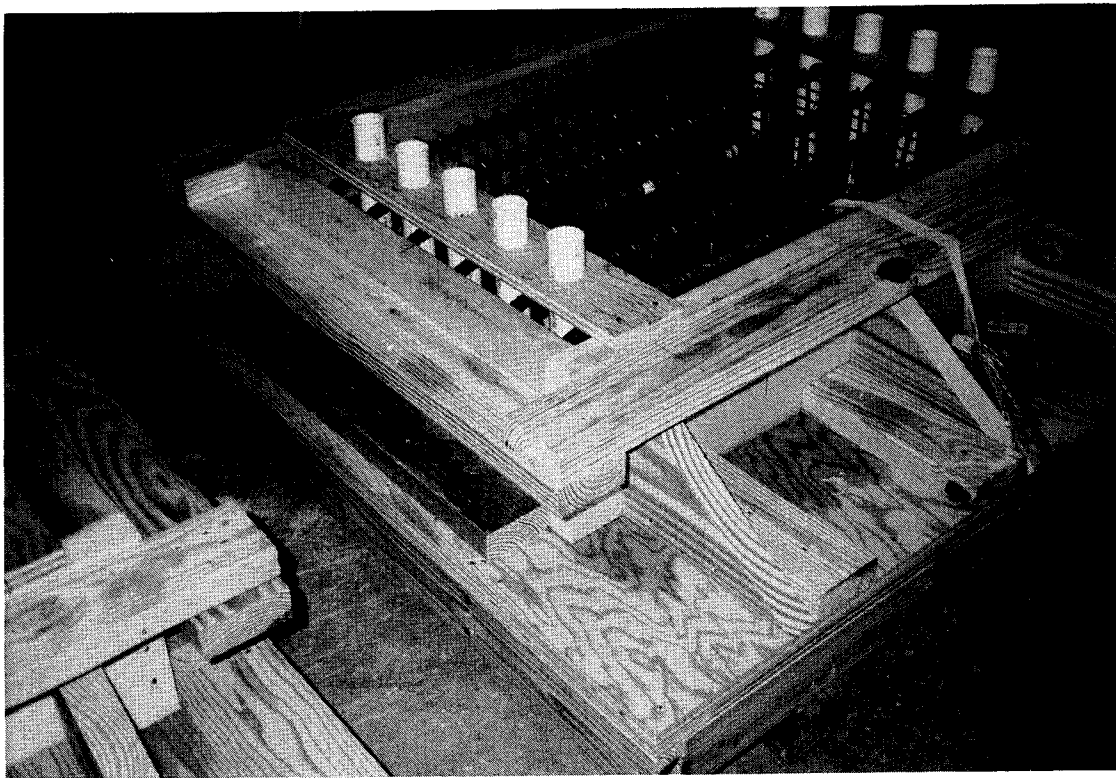


Figure 23. Slab No. 9 Prior to Concrete Placement

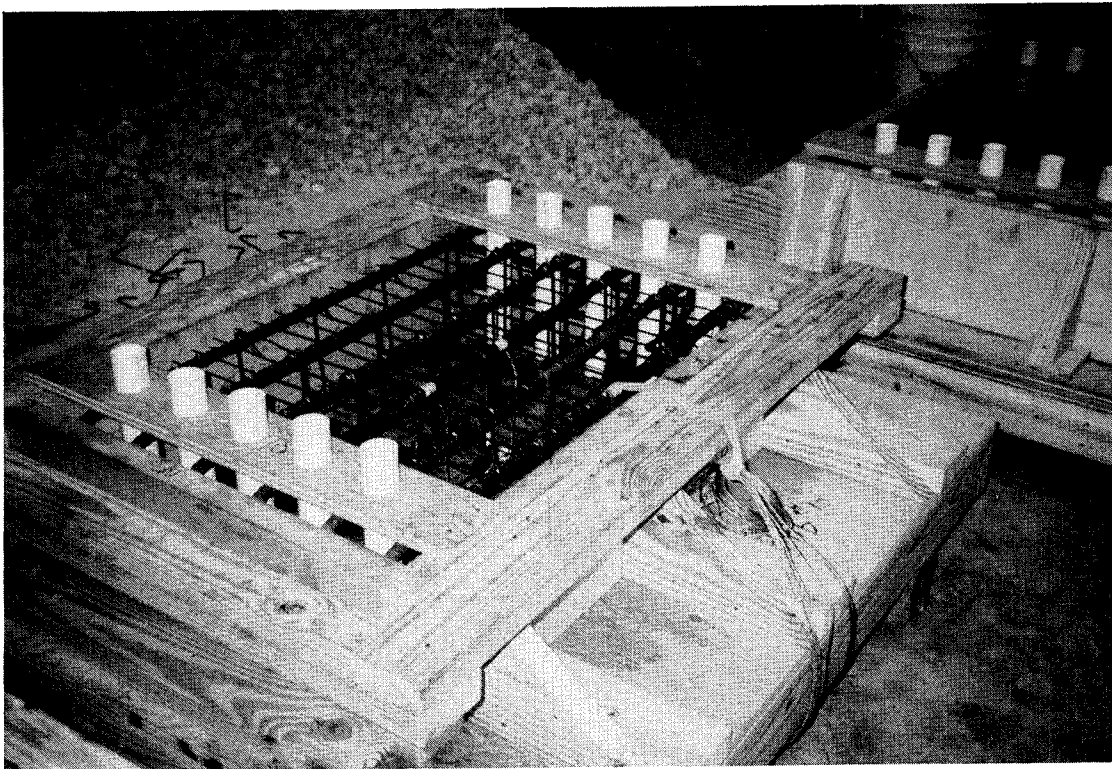


Figure 24. Slab No. 10 Prior to Concrete Placement

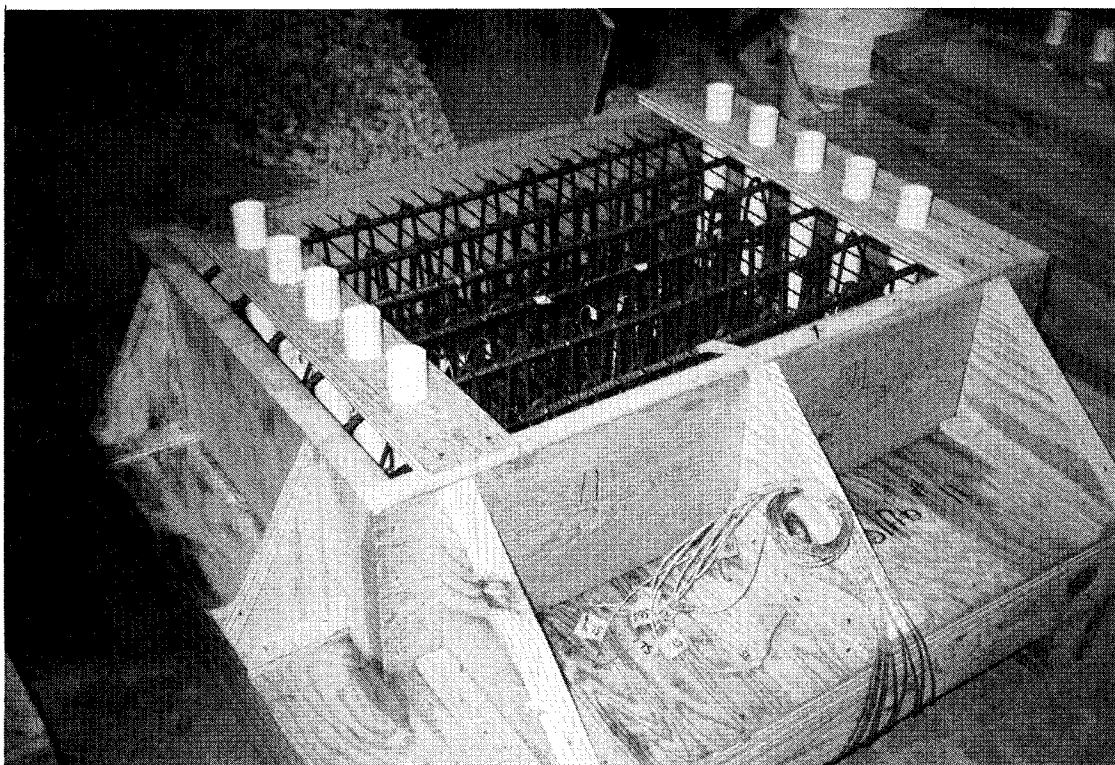


Figure 25. Slab No. 11 Prior to Concrete Placement

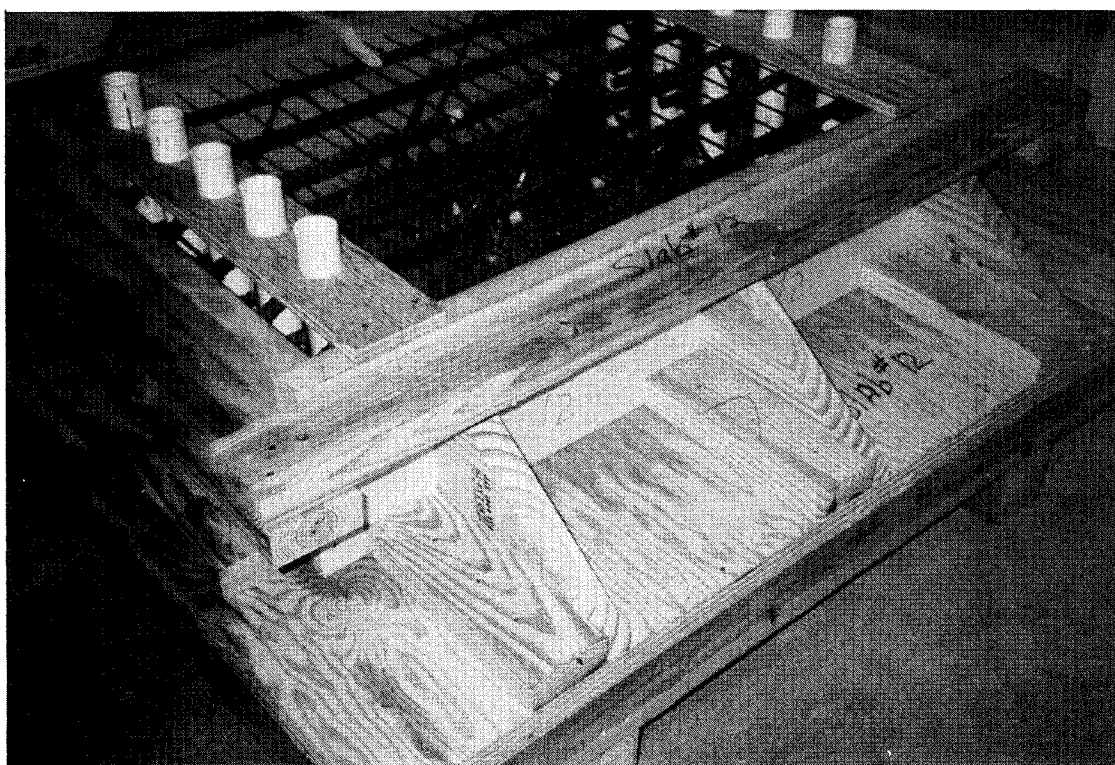


Figure 26. Slab No. 12 Prior to Concrete Placement

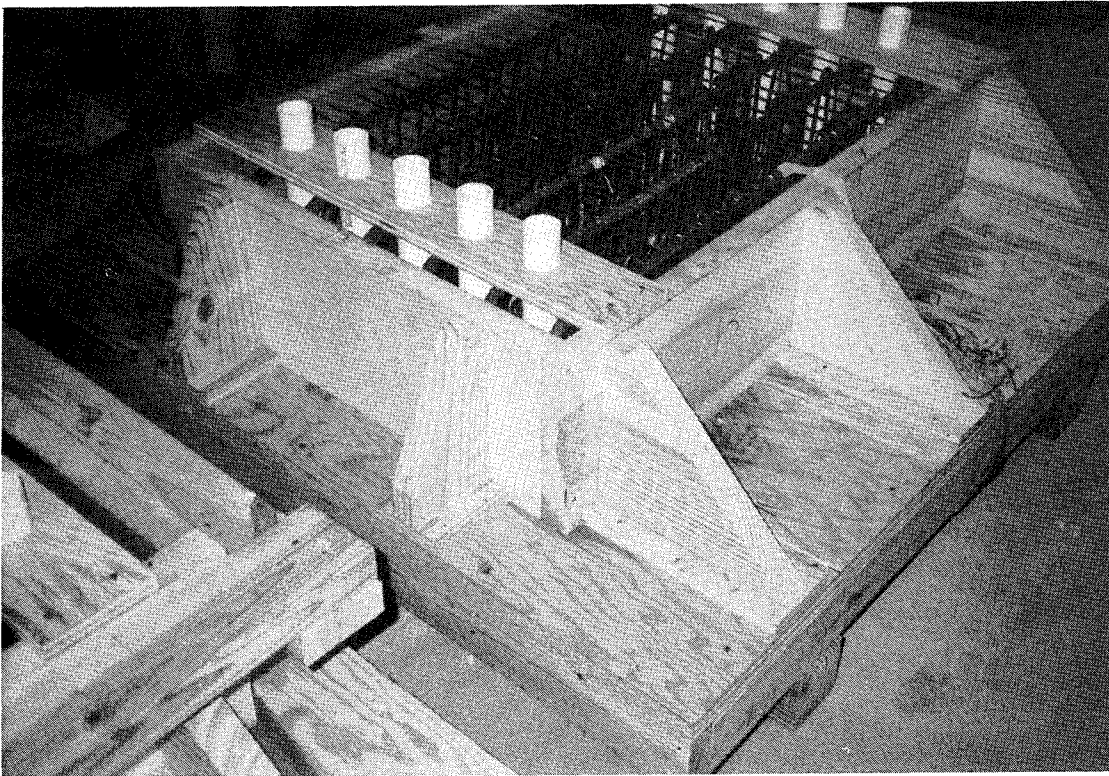


Figure 27. Slab No. 13 Prior to Concrete Placement

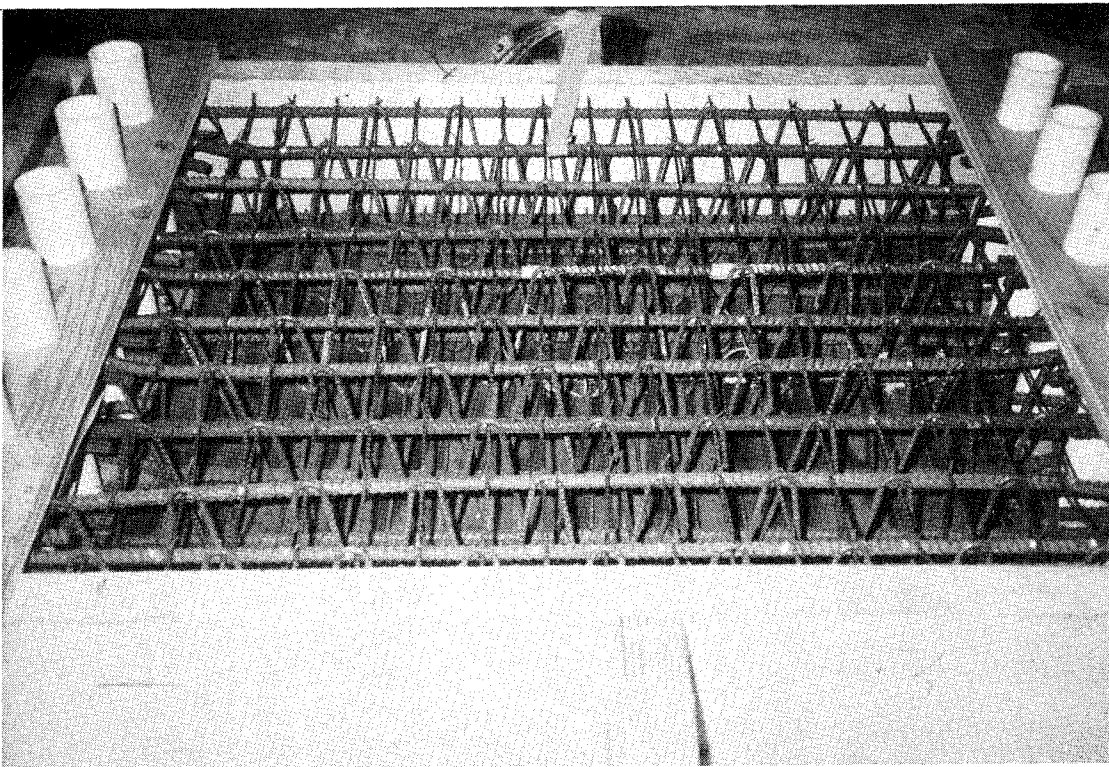


Figure 28. Close-up View of Lacing in Slab No. 3

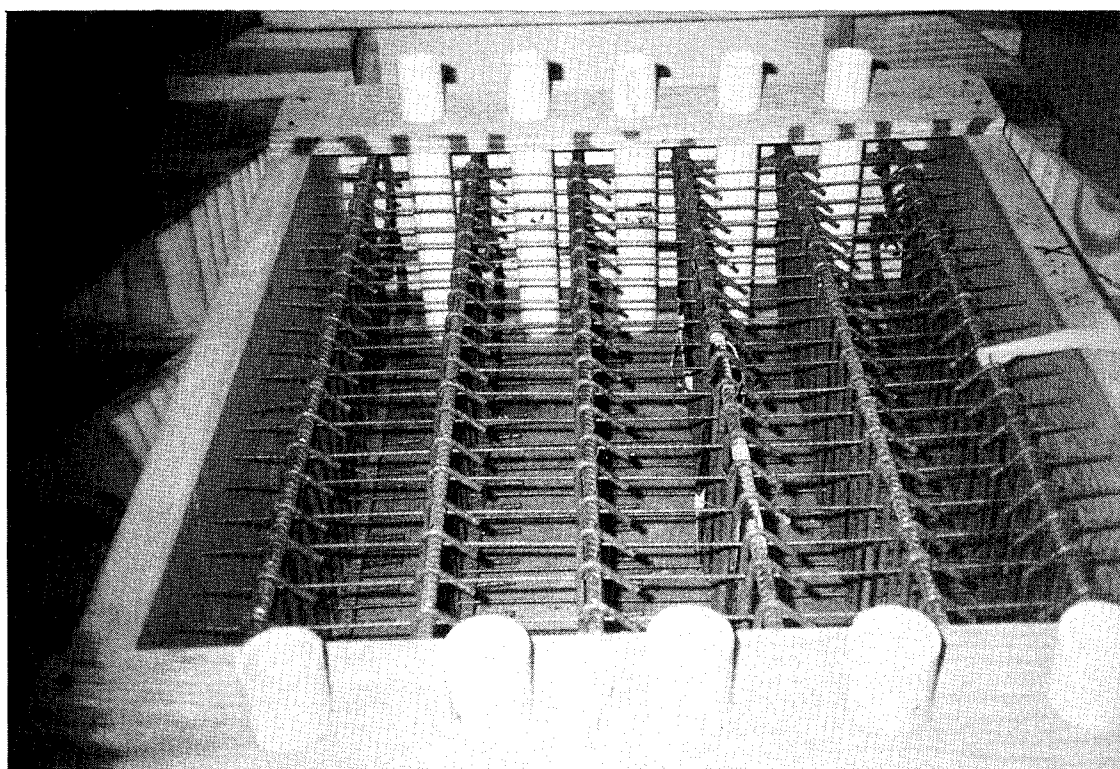


Figure 29. Close-up View of Stirrups in Slab No. 7

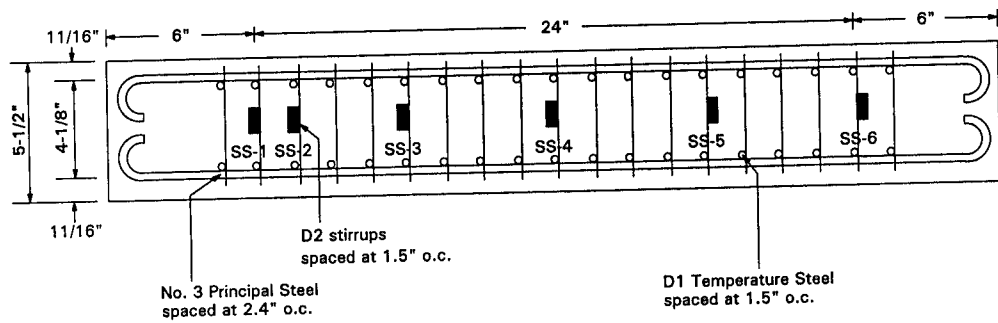


Figure 30. Strain Gage Locations on Stirrups in Slab No. 2

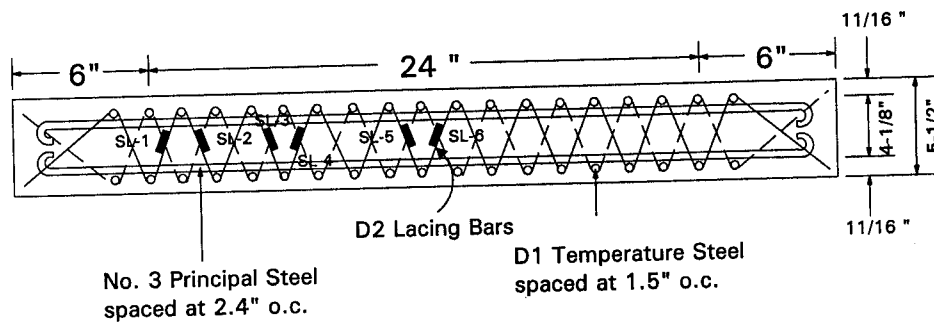


Figure 31. Strain Gage Locations on Stirrups in Slab No. 3

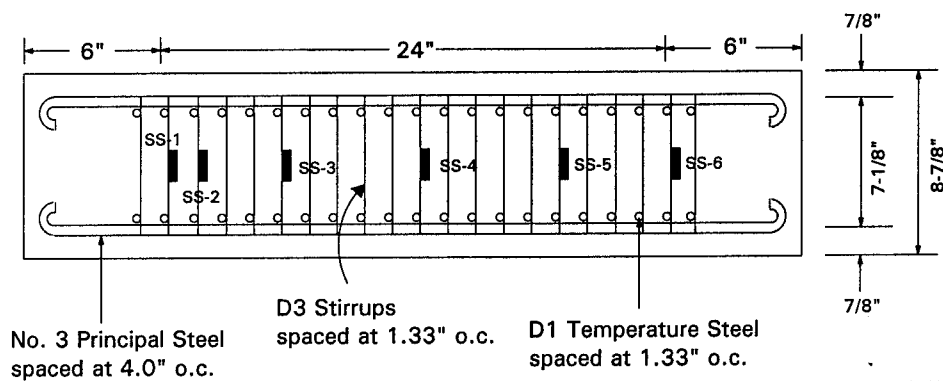


Figure 32. Strain Gage Locations on Stirrups in Slabs No. 7, 8, 9

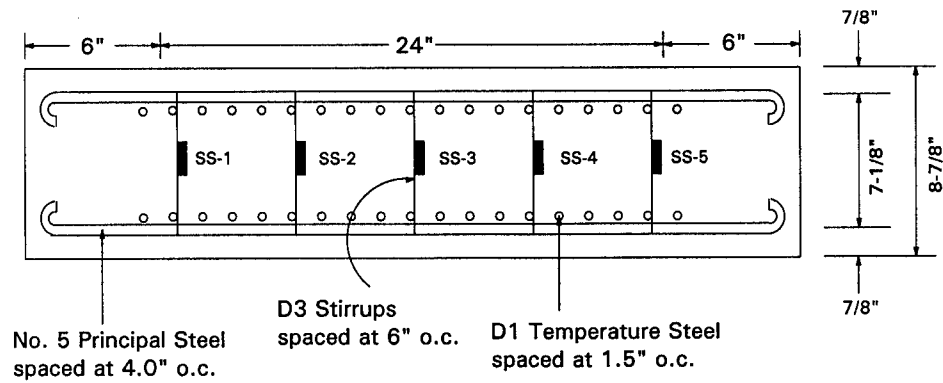


Figure 33. Strain Gage Locations on Stirrups in Slab No. 10

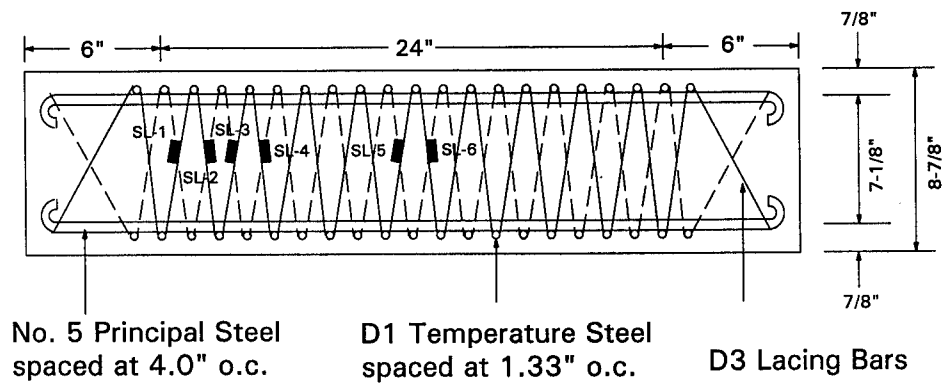


Figure 34. Strain Gage Locations on Lacing in Slabs No. 11 and 13

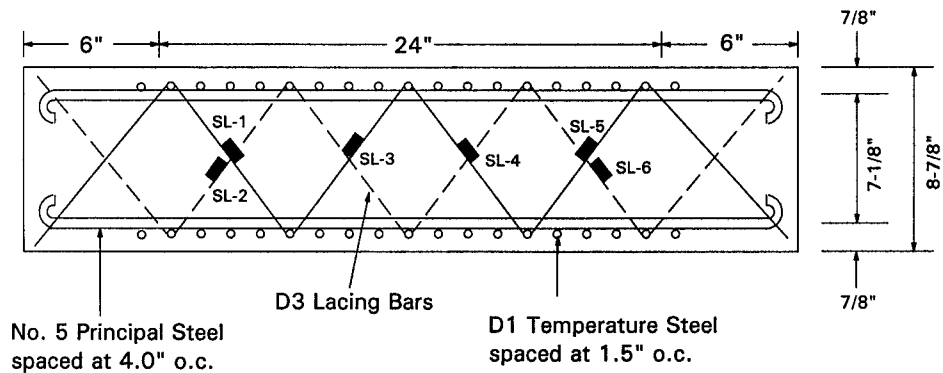


Figure 35. Strain Gage Locations on Lacing in Slab No. 12

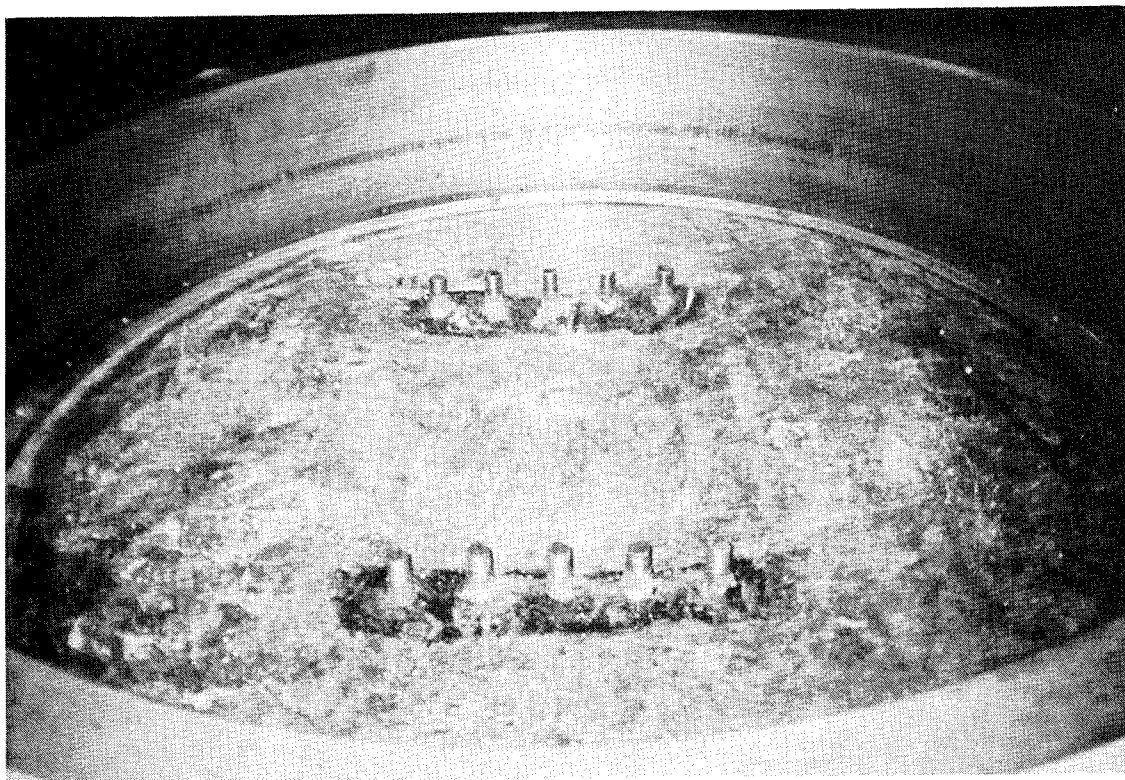


Figure 36. Membrane Covering Slab

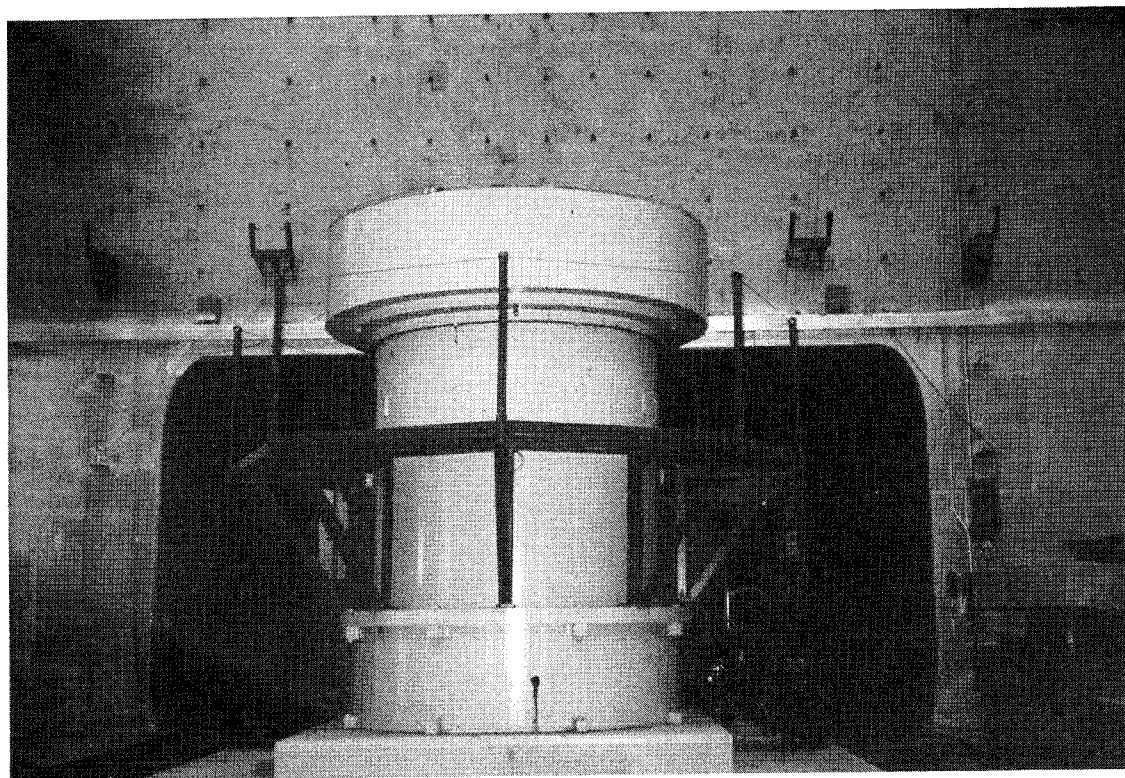


Figure 37. Test Chamber Ready to Roll Inside Large Reaction Structure



Figure 38. Posttest View of Slab No. 1

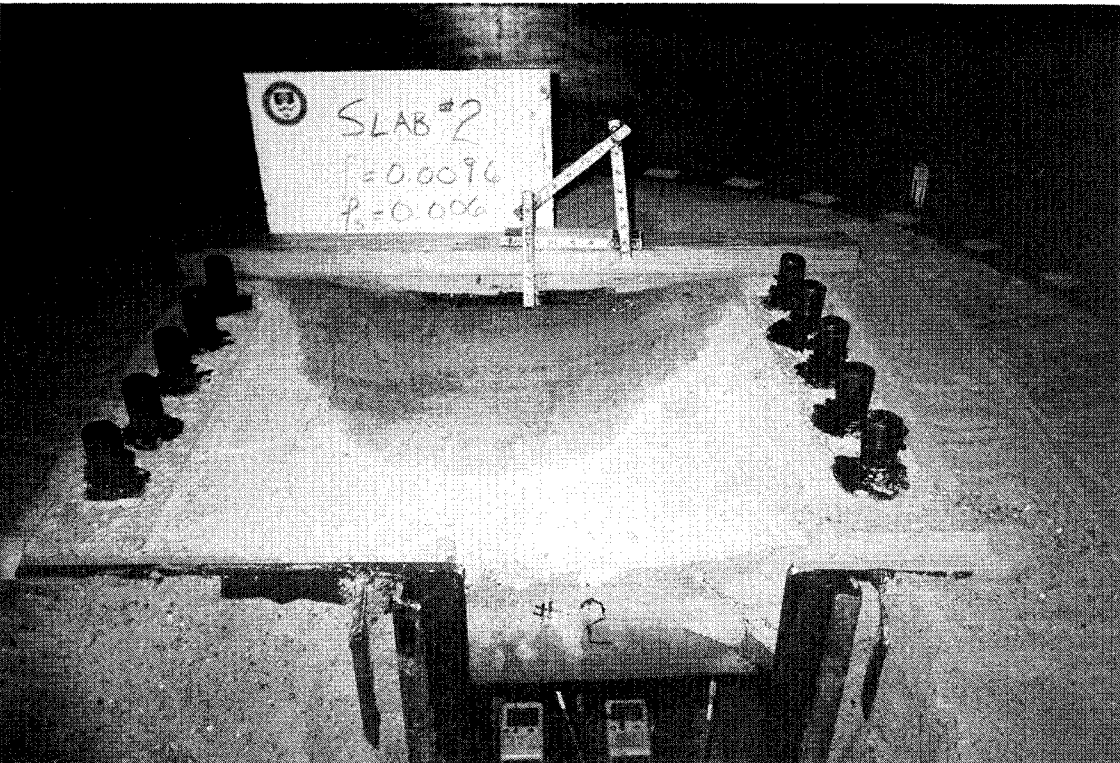


Figure 39. Posttest View of Slab No. 2

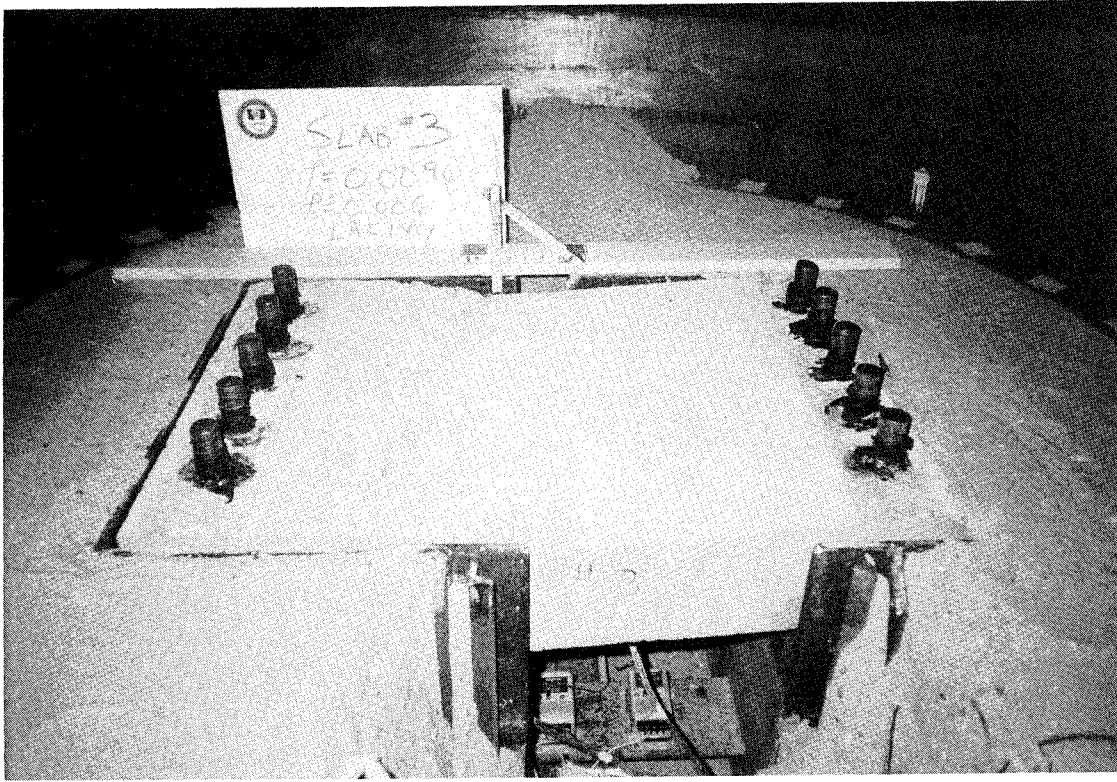


Figure 40. Posttest View of Slab No. 3

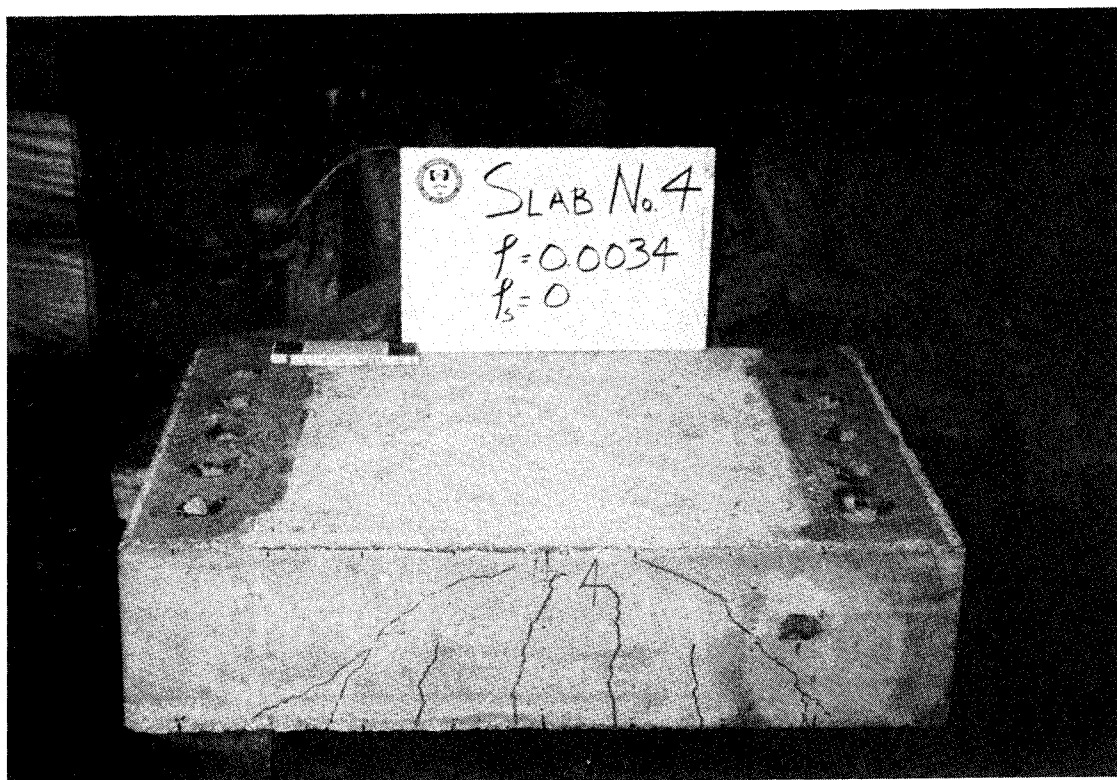


Figure 41. Posttest View of Slab No. 4

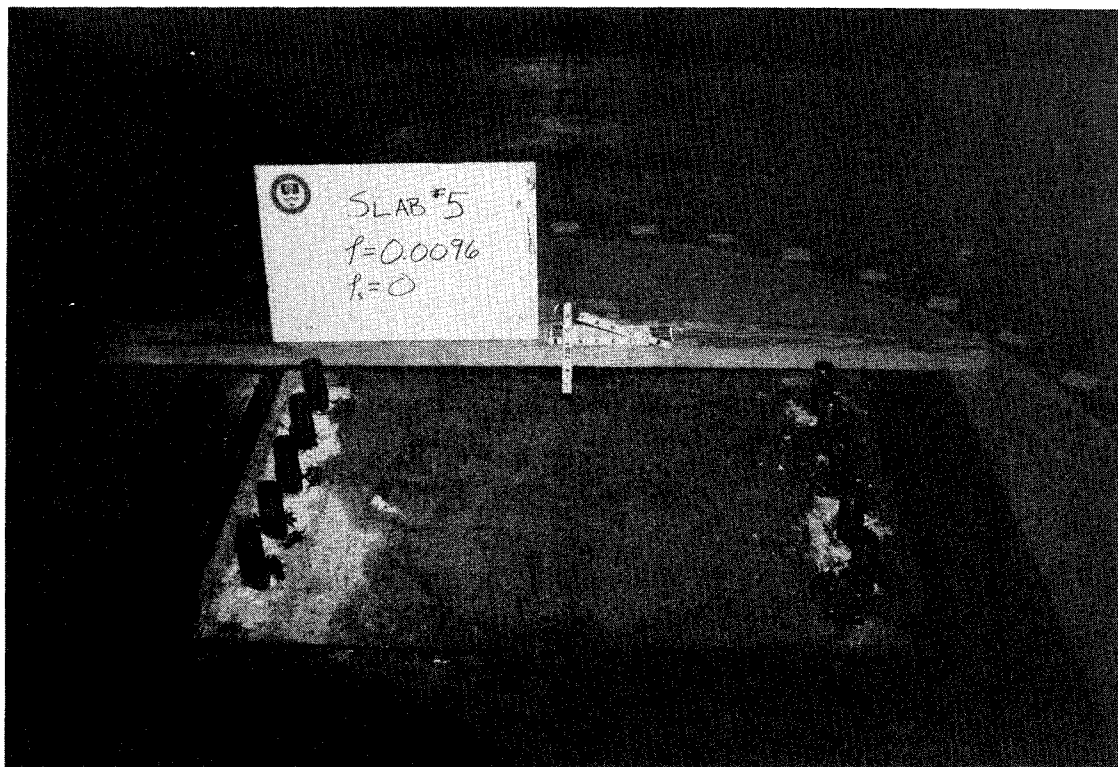


Figure 42. Posttest View of Slab No. 5

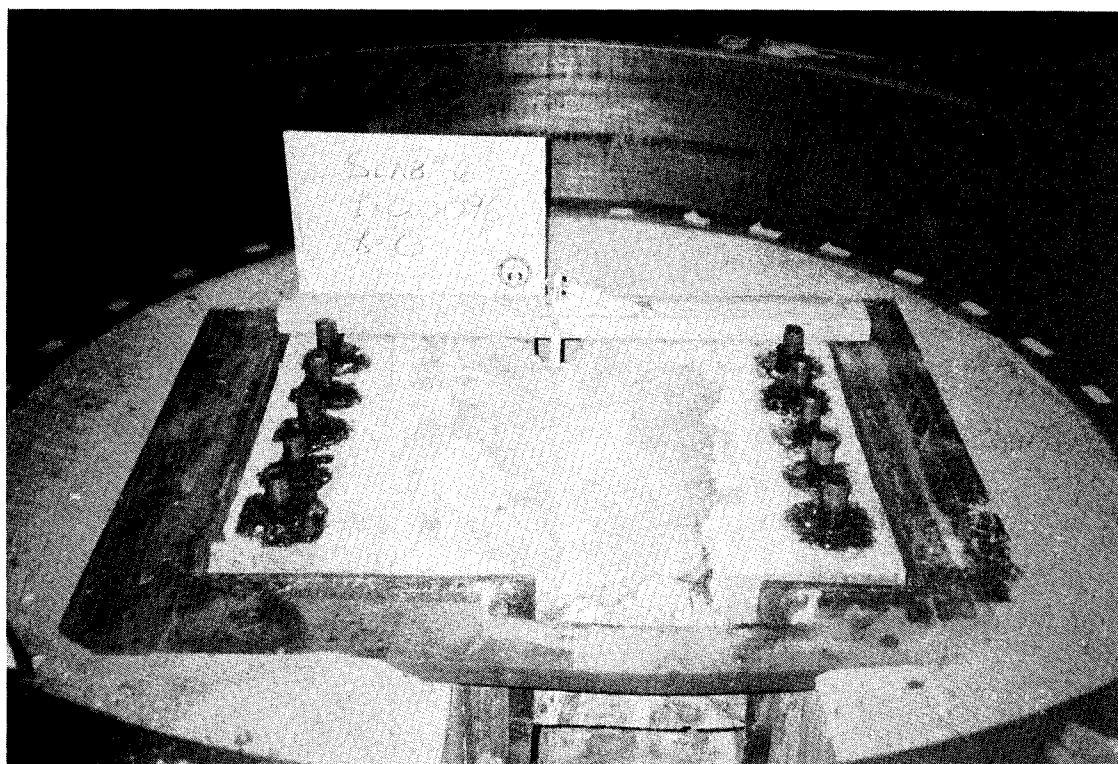


Figure 43. Posttest View of Slab No. 6

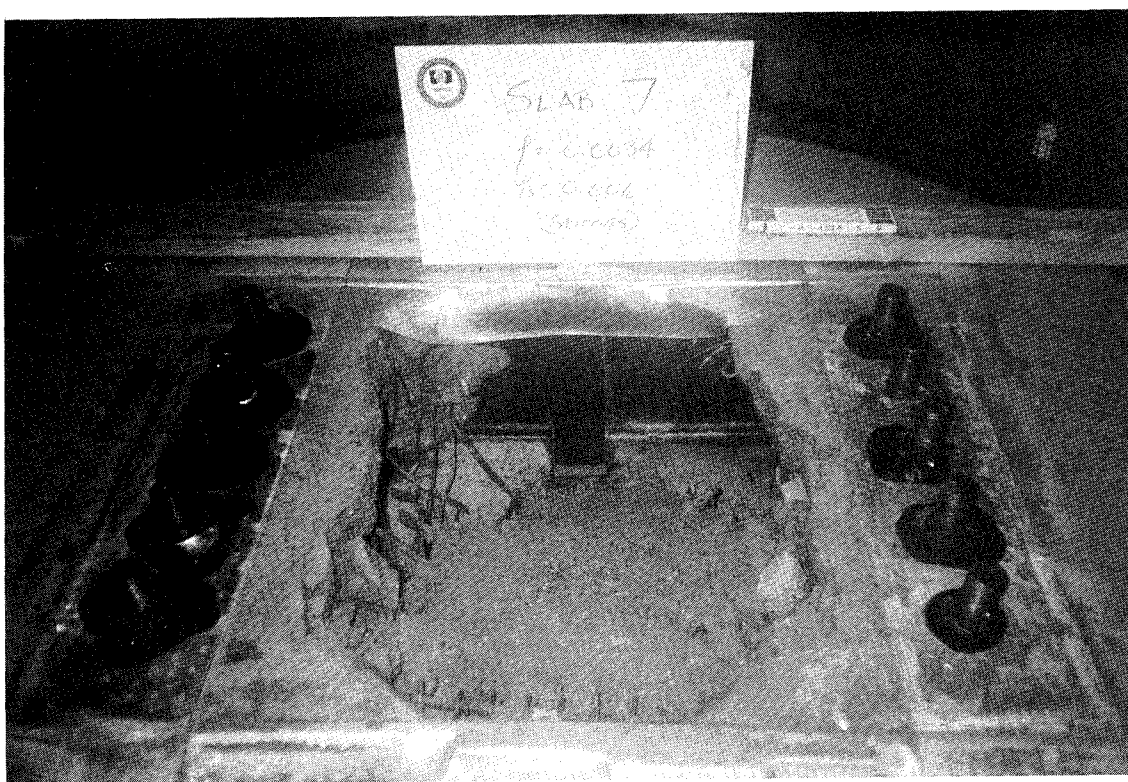


Figure 44. Posttest View of Slab No. 7

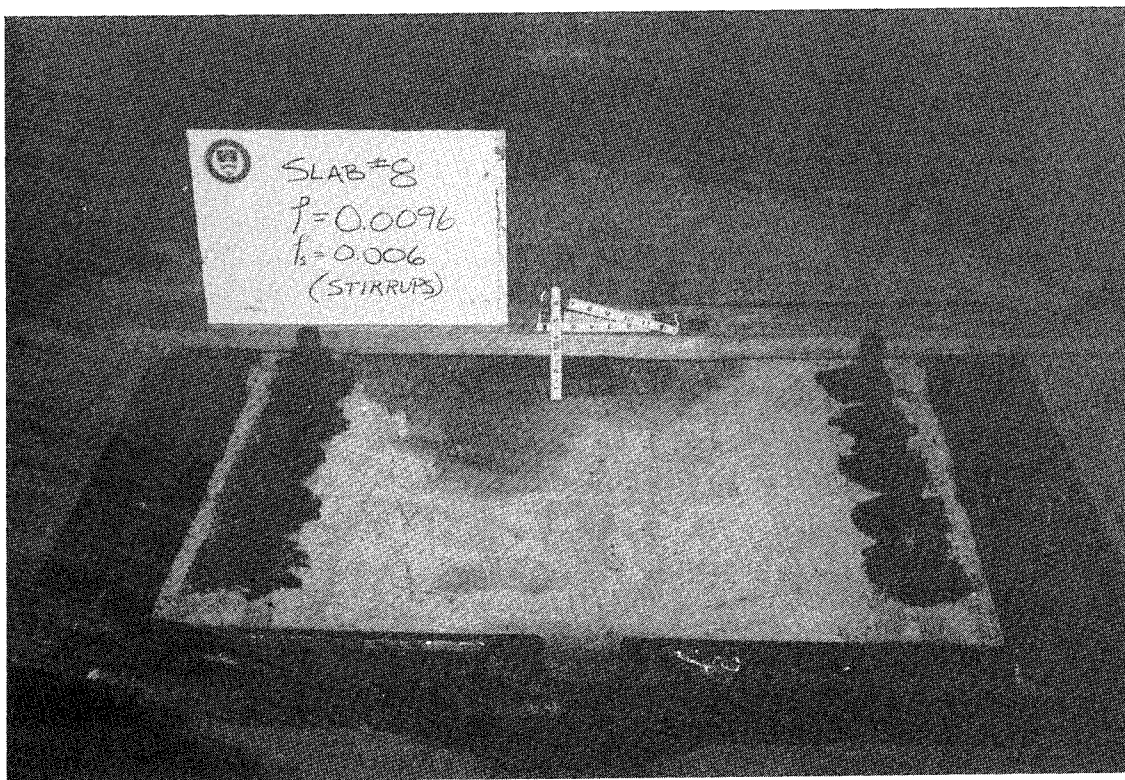


Figure 45. Posttest View of Slab No. 8



Figure 46. Posttest View of Slab No. 9

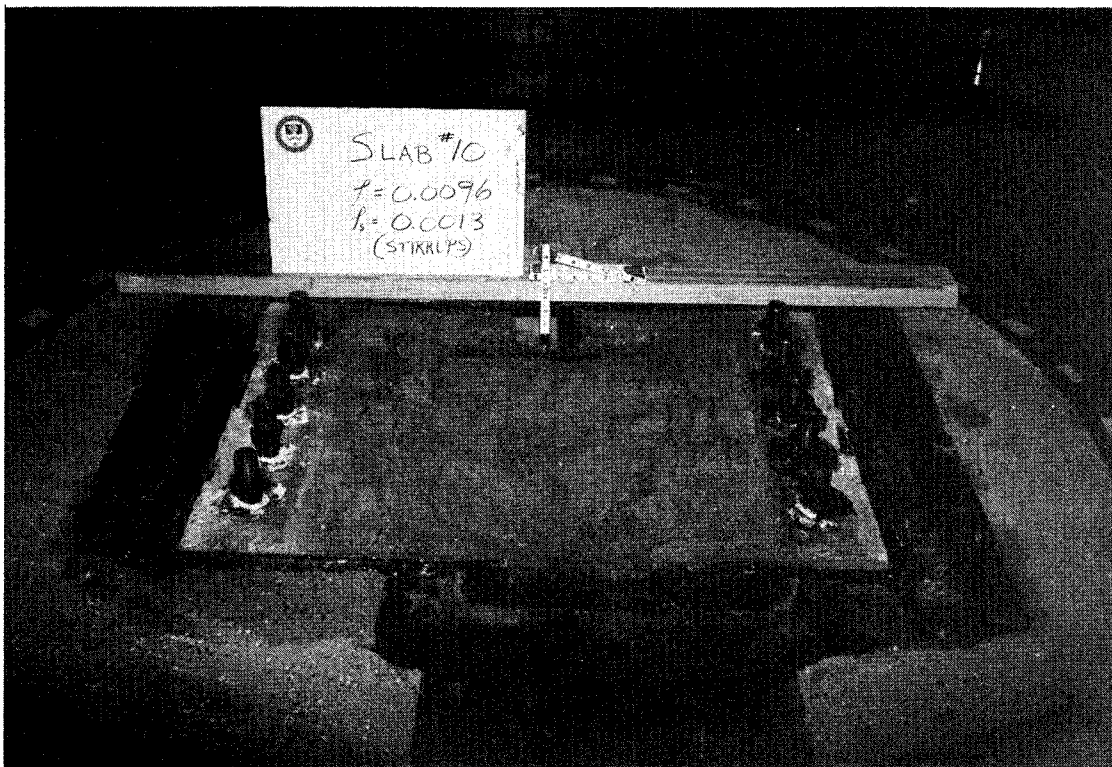


Figure 47. Posttest View of Slab No. 10

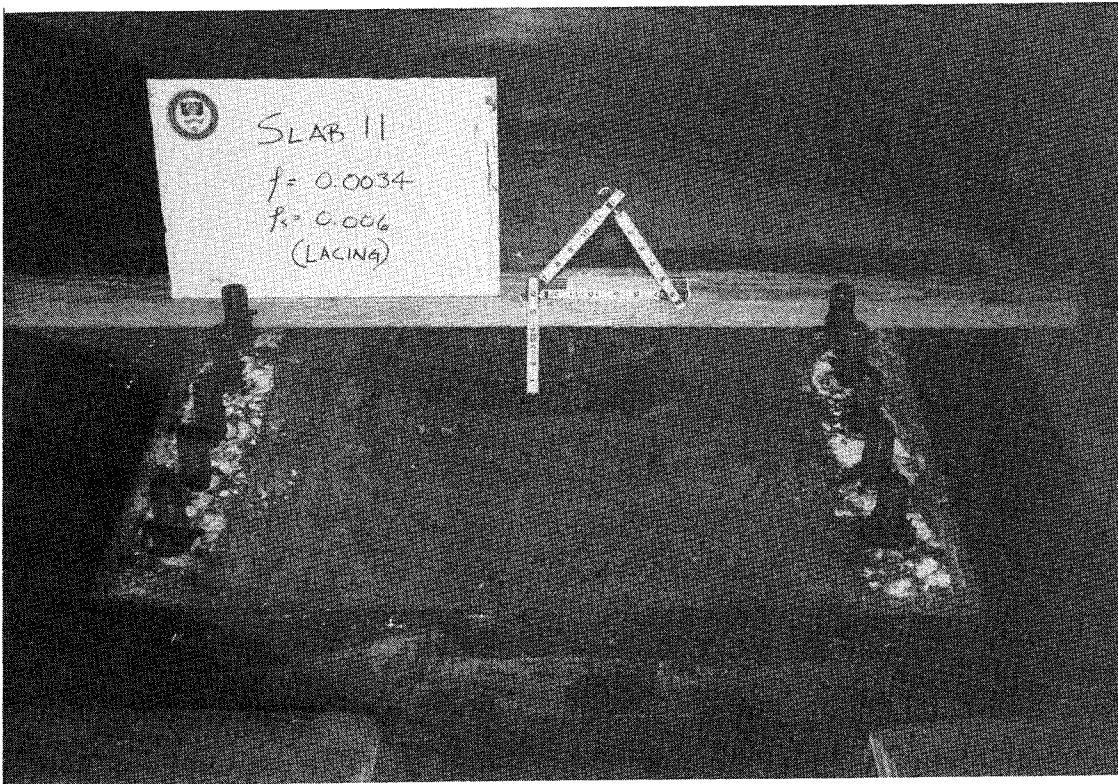


Figure 48. Posttest View of Slab No. 11

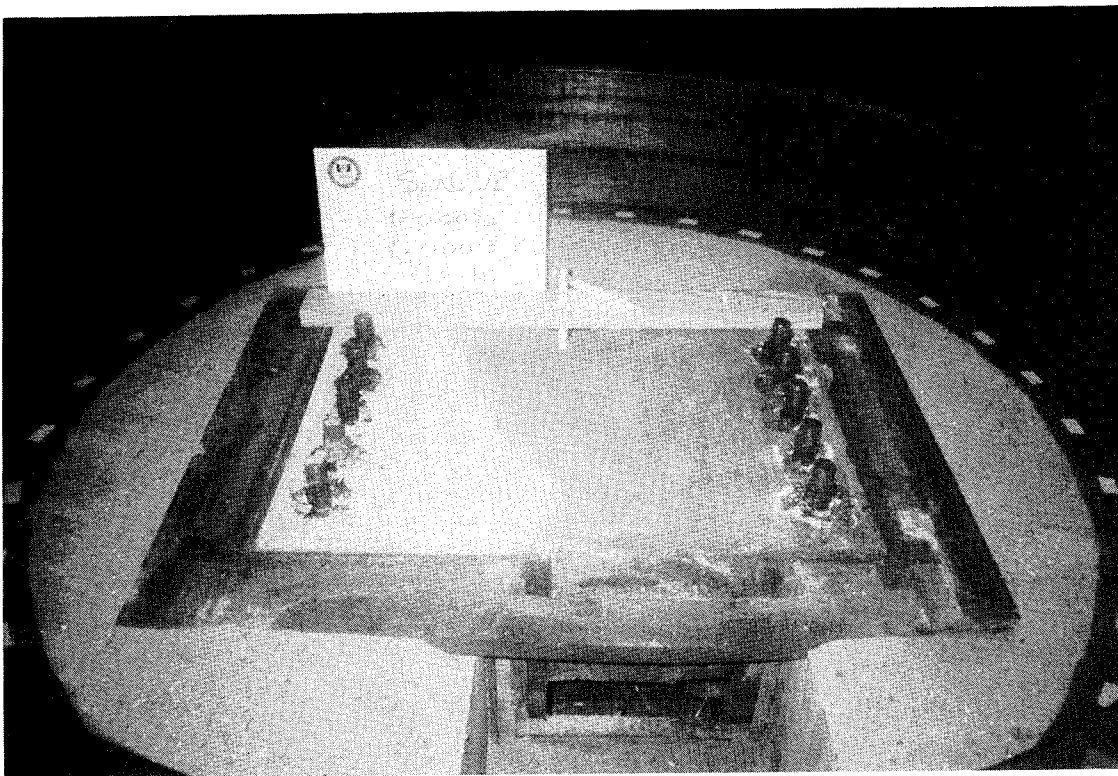


Figure 49. Posttest View of Slab No. 12

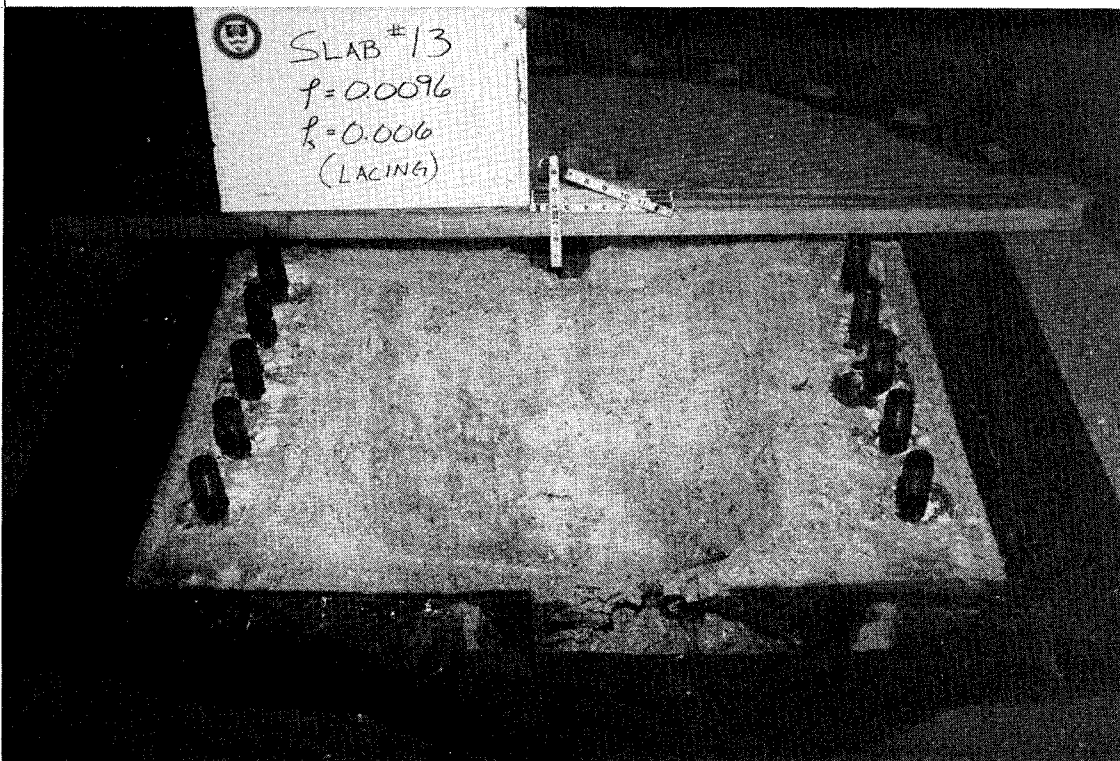


Figure 50. Posttest View of Slab No. 13

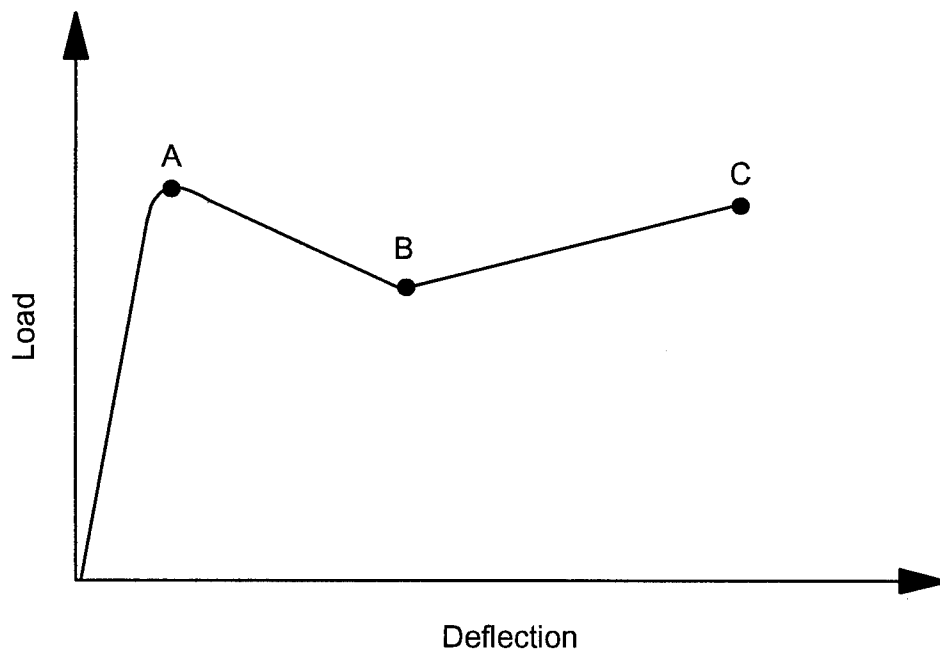


Figure 51. General Load-Deflection Curve

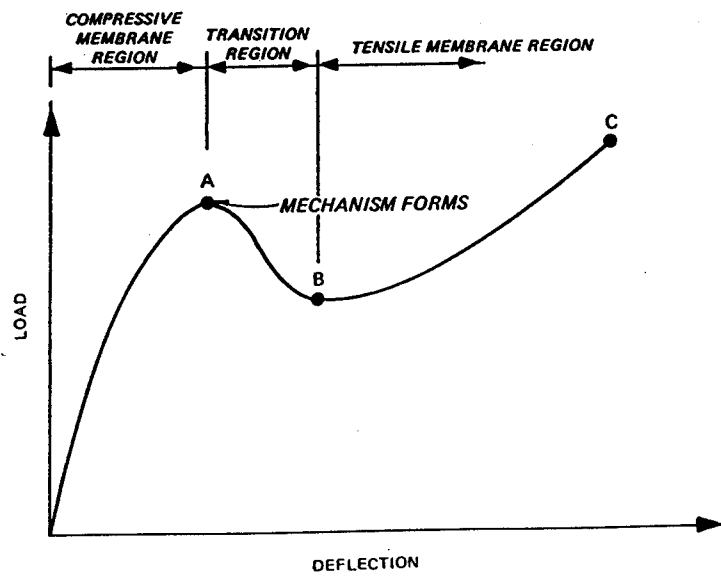


Figure 52. General Load-Deflection Curve for a Normally-Proportioned Restrained Slab

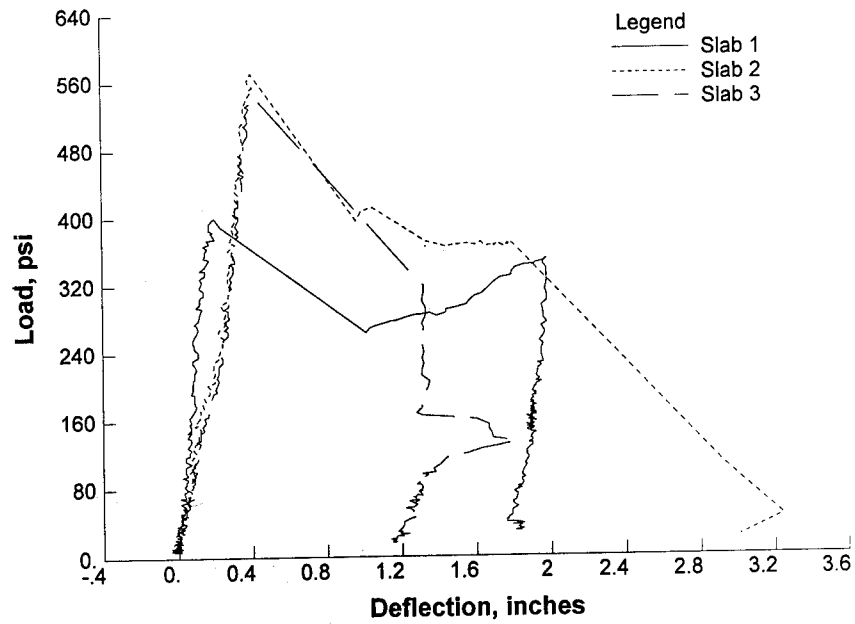


Figure 53. Composite Midspan Load-Deflection Data for Slabs No. 1, 2, and 3

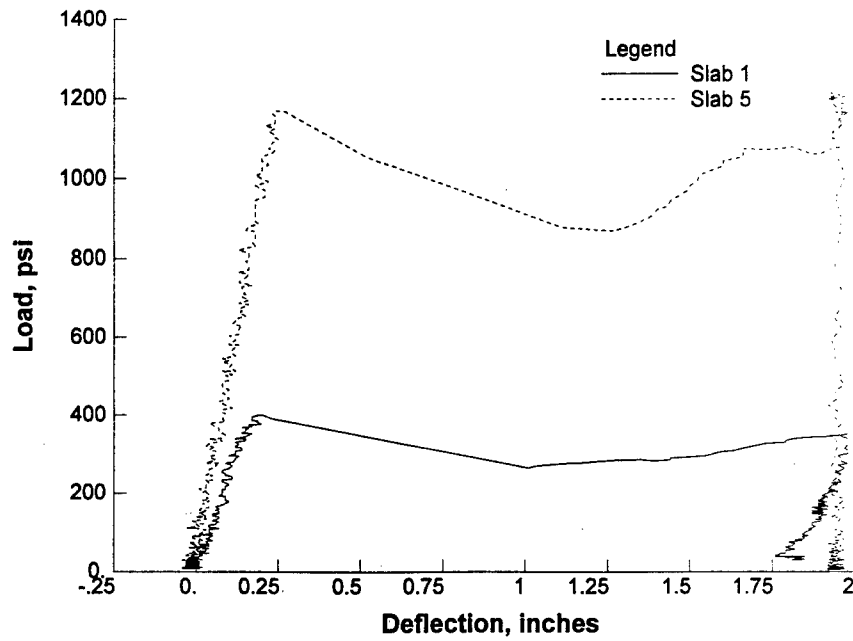


Figure 54. Composite Midspan Load-Deflection Data for Slabs No. 1 and 5

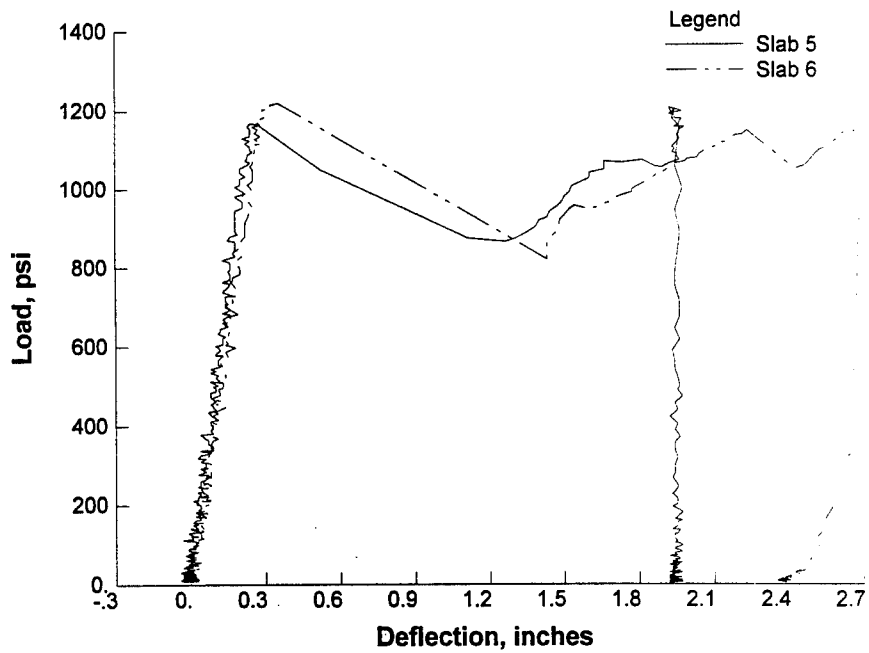


Figure 55. Composite Midspan Load-Deflection Data for Slabs No. 5 and 6

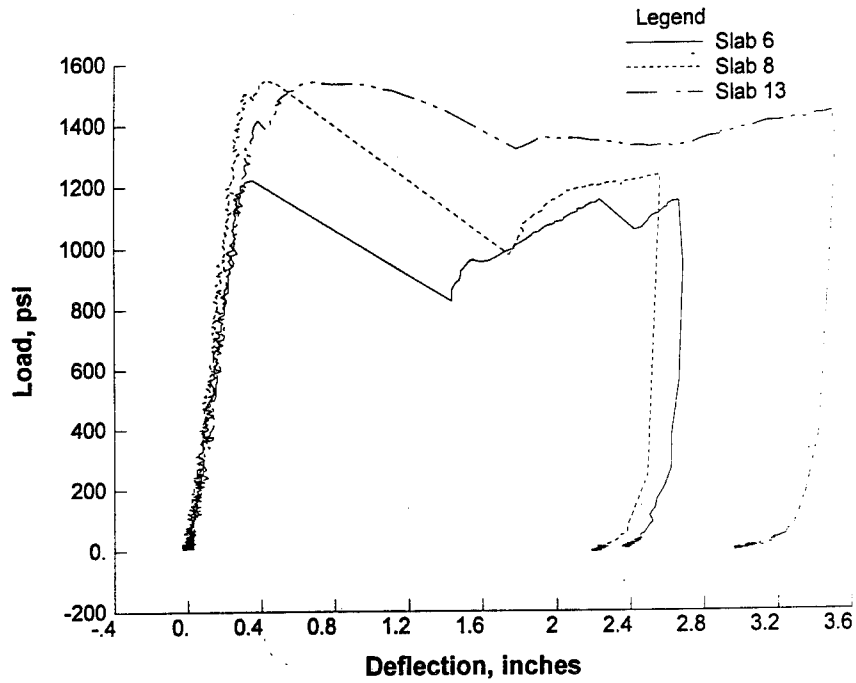


Figure 56. Composite Midspan Load-Deflection Data for Slabs No. 6, 8, and 13.

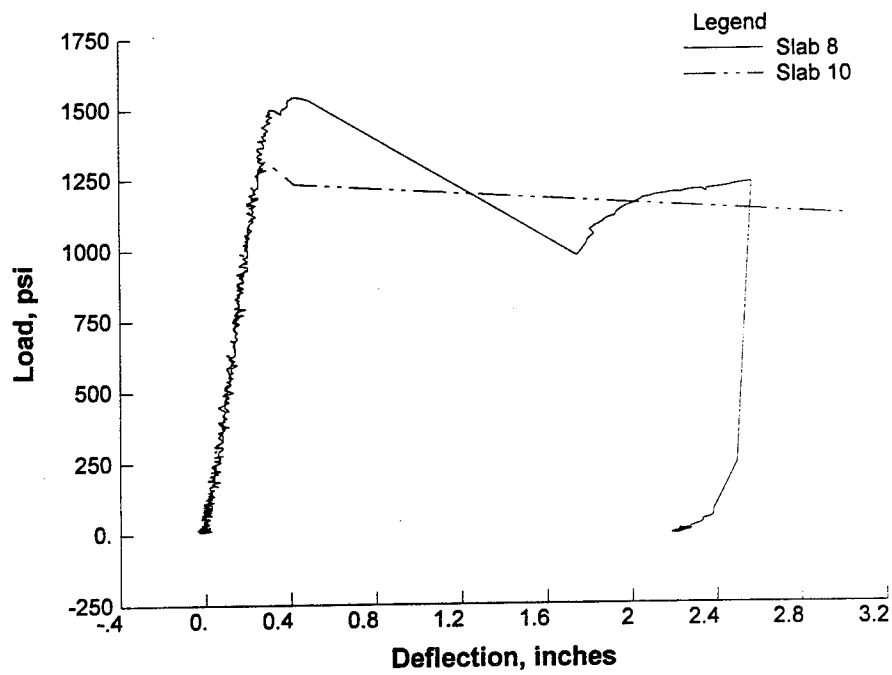


Figure 57. Composite Midspan Load-Deflection Data for Slabs No. 8 and 10

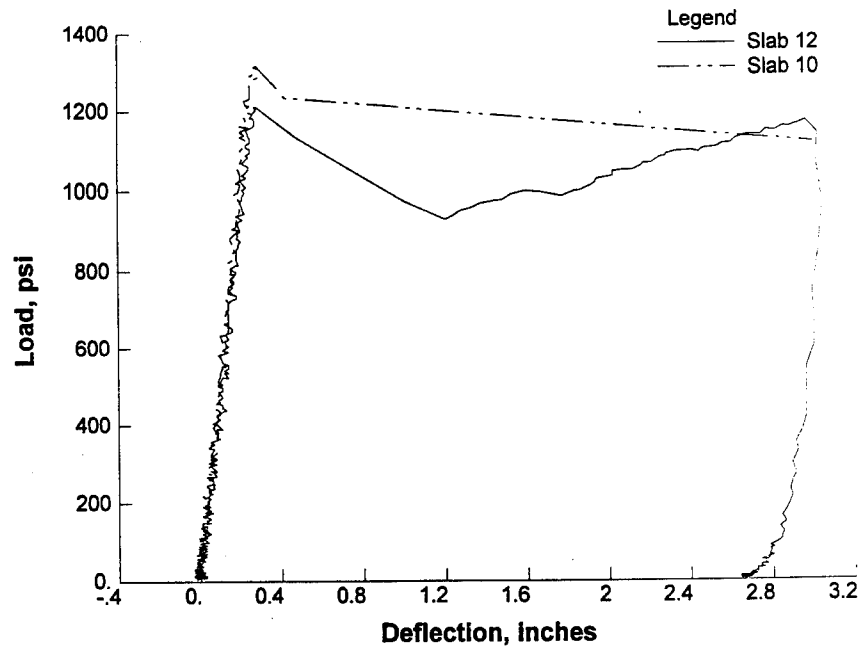


Figure 58. Composite Midspan Load-Deflection Data for Slabs No. 12 and 10

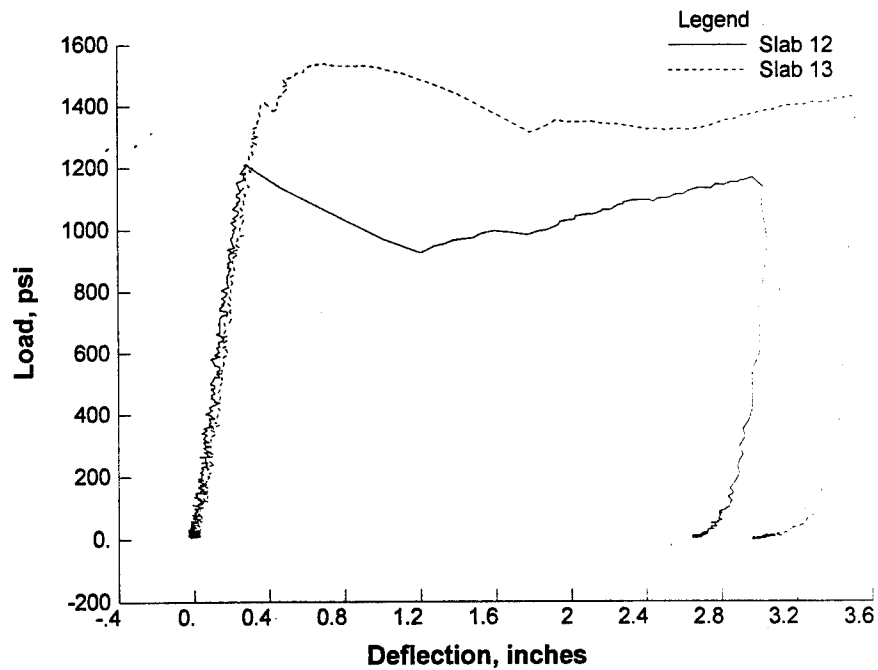


Figure 59. Composite Midspan Load-Deflection Data for Slabs No. 12 and 13

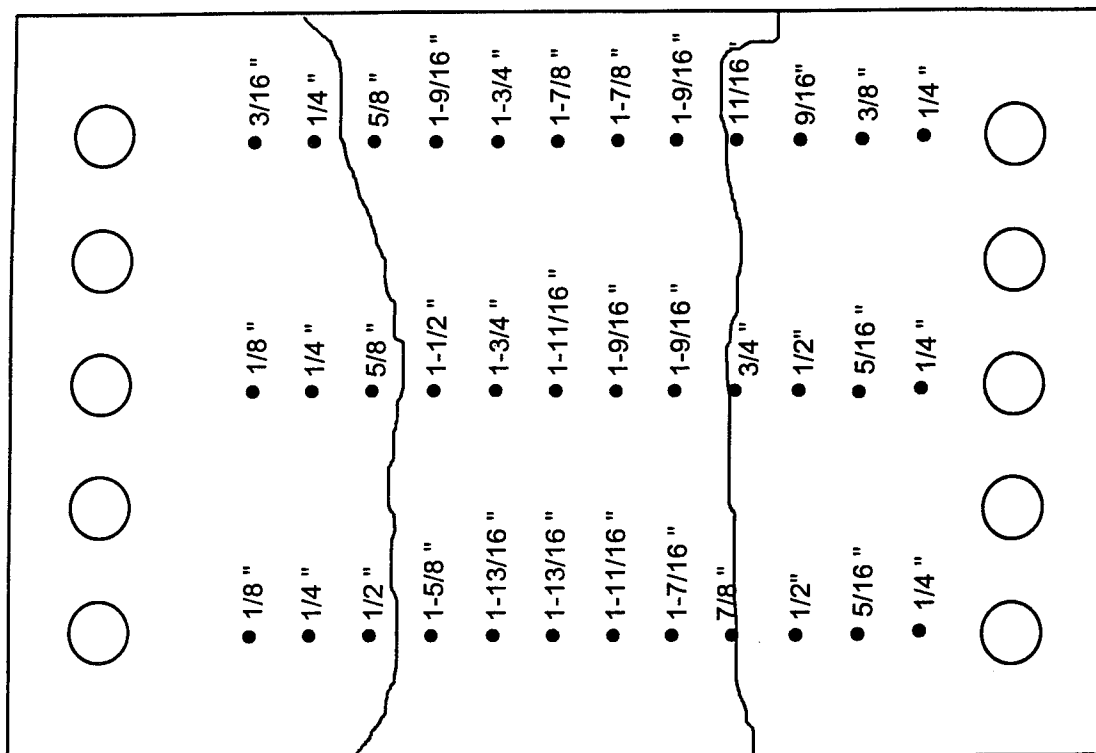


Figure 60. Posttest Deflection Survey for Slab No. 1

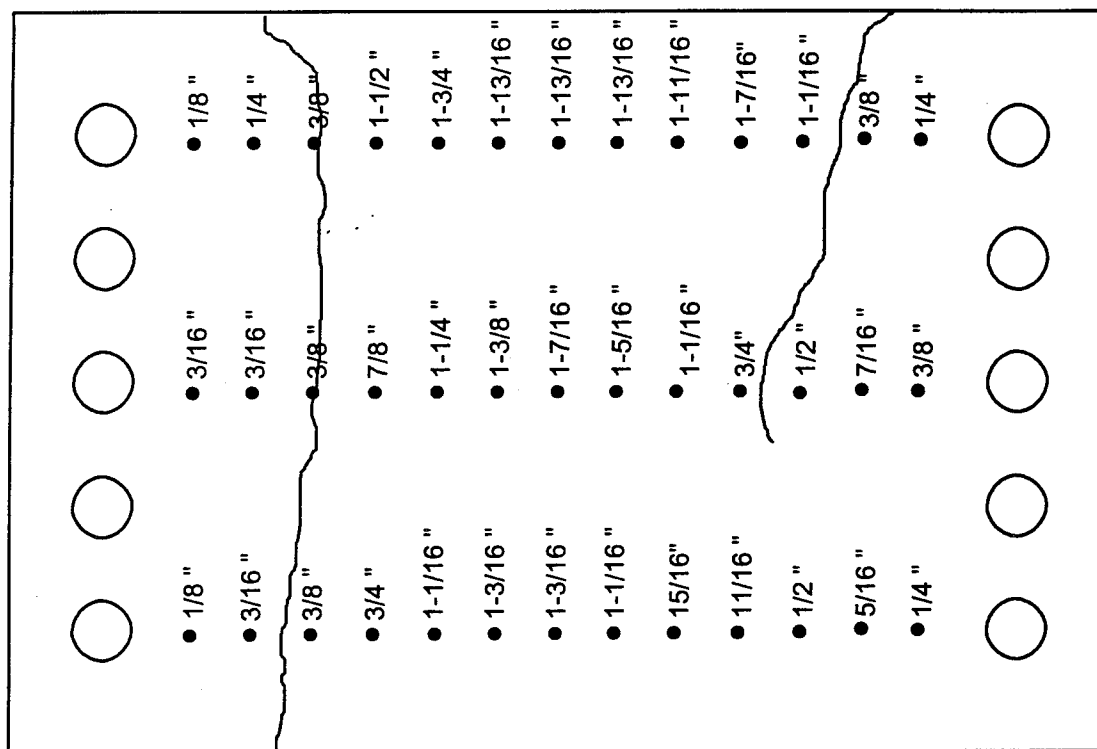


Figure 61. Posttest Deflection Survey for Slab No. 2

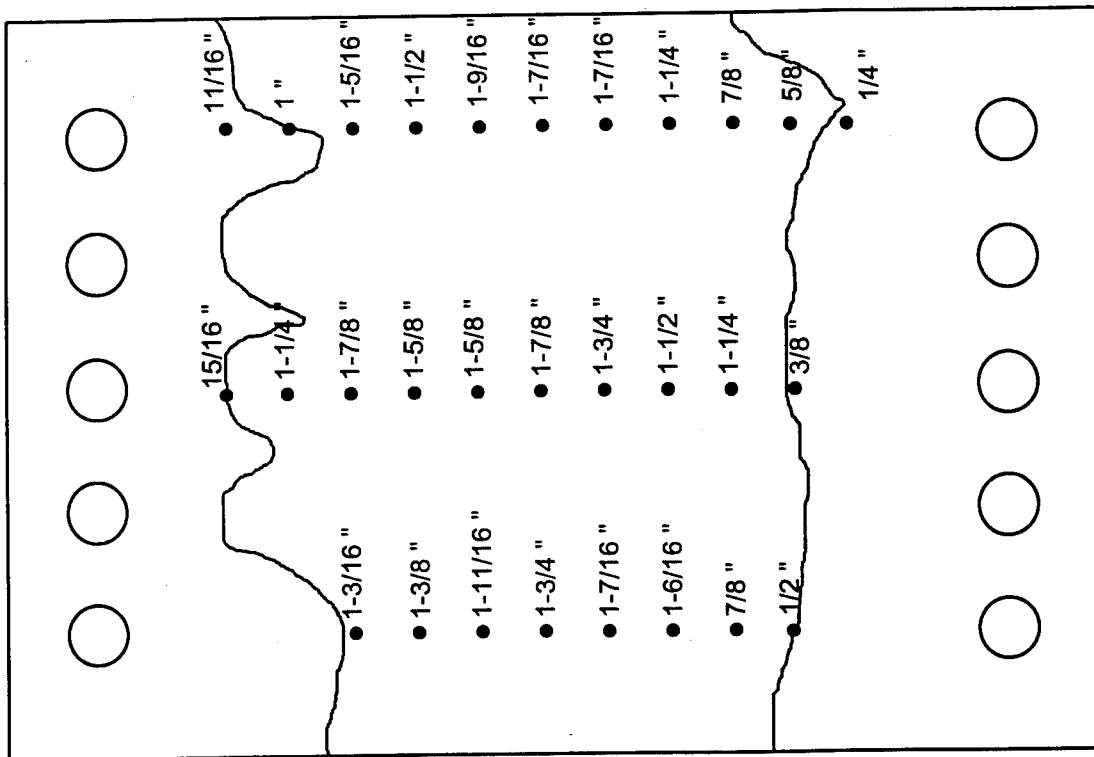


Figure 62. Posttest Deflection Survey for Slab No. 5

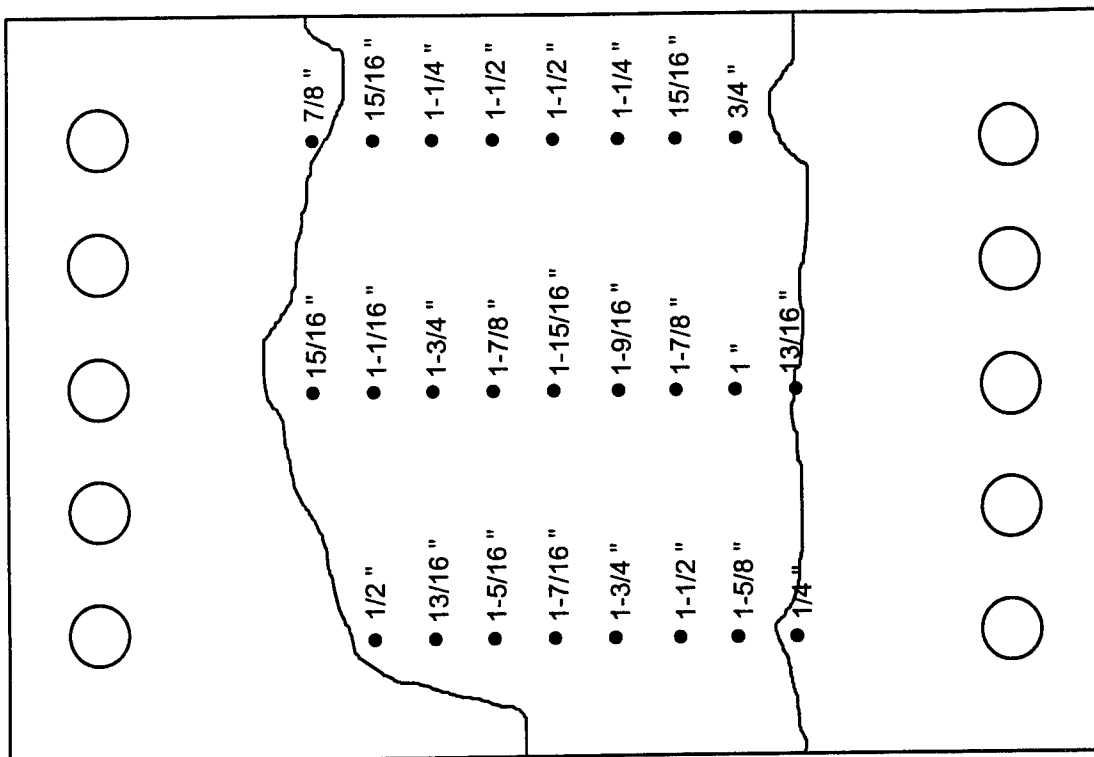


Figure 63. Posttest Deflection Survey for Slab No. 6

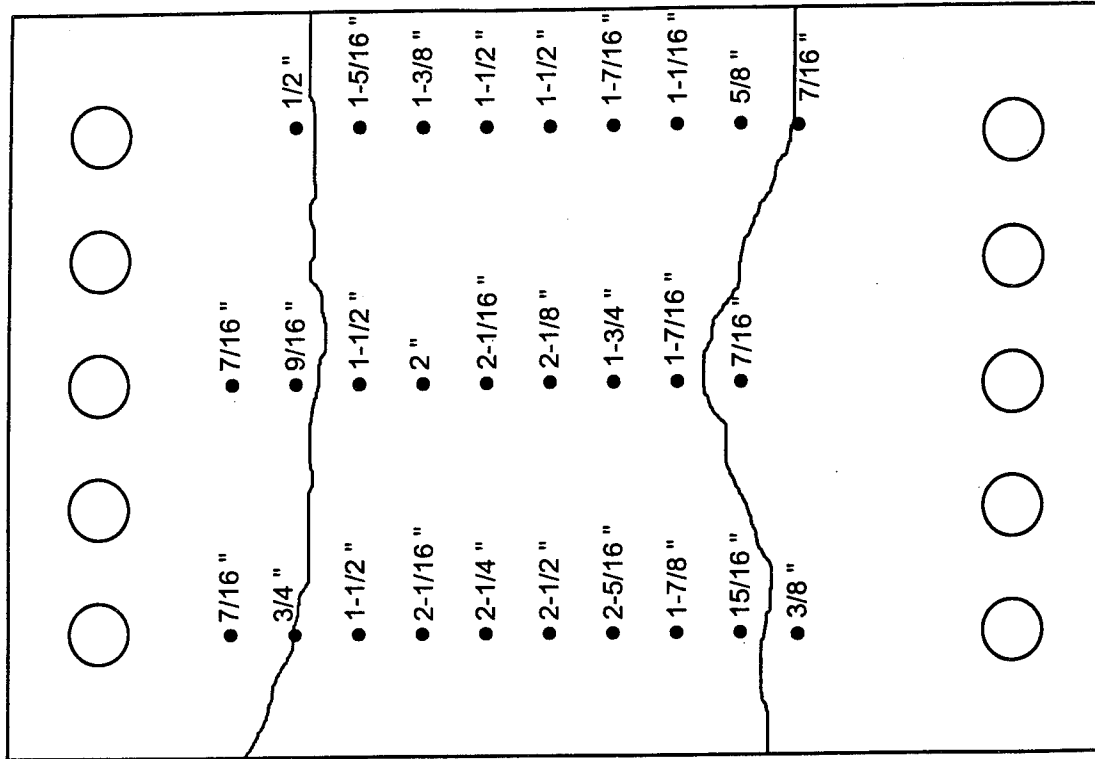


Figure 64. Posttest Deflection Survey for Slab No. 8

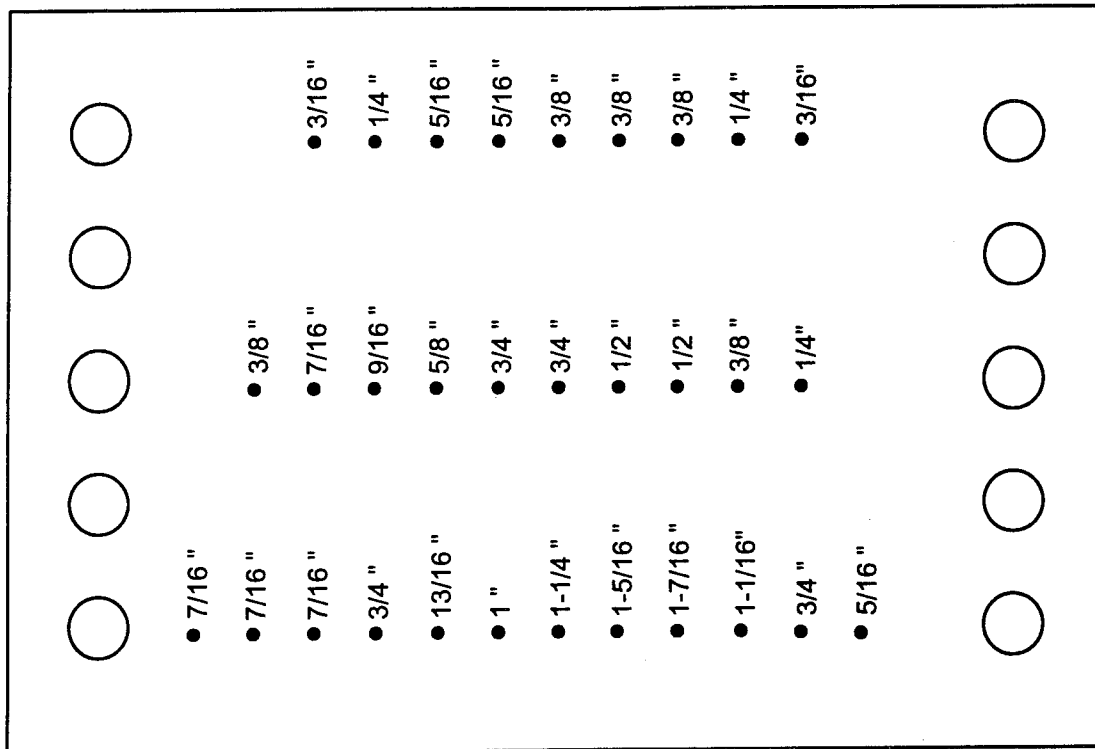


Figure 65. Posttest Deflection Survey for Slab No. 9

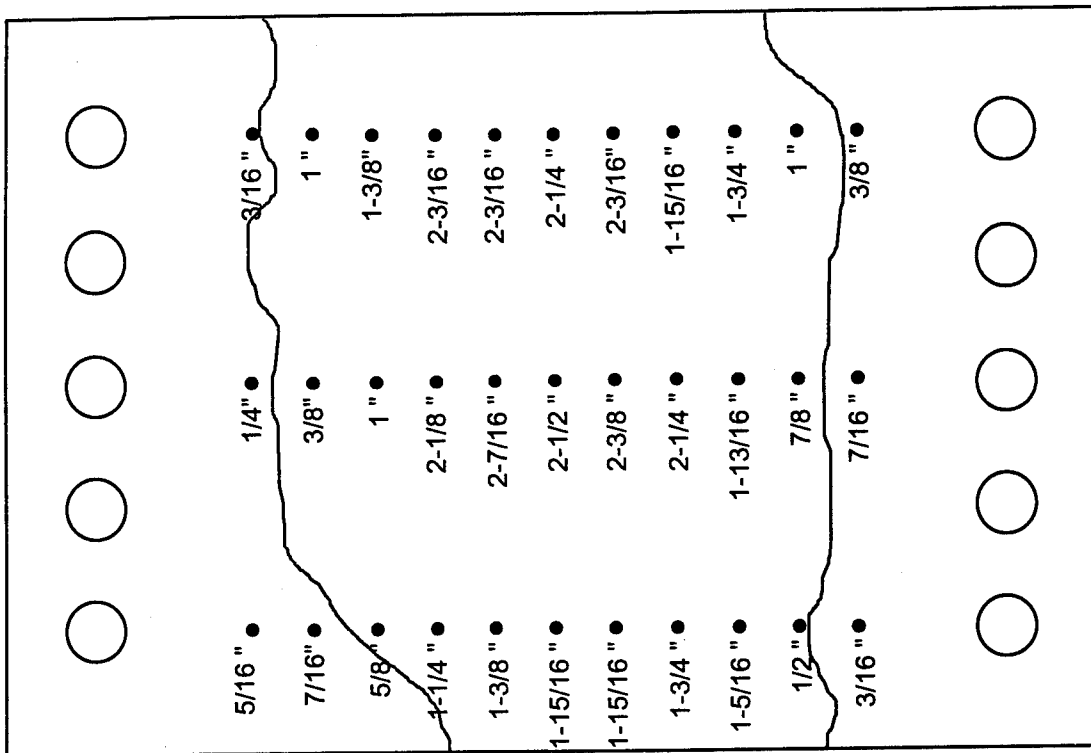


Figure 66. Posttest Deflection Survey for Slab No. 10

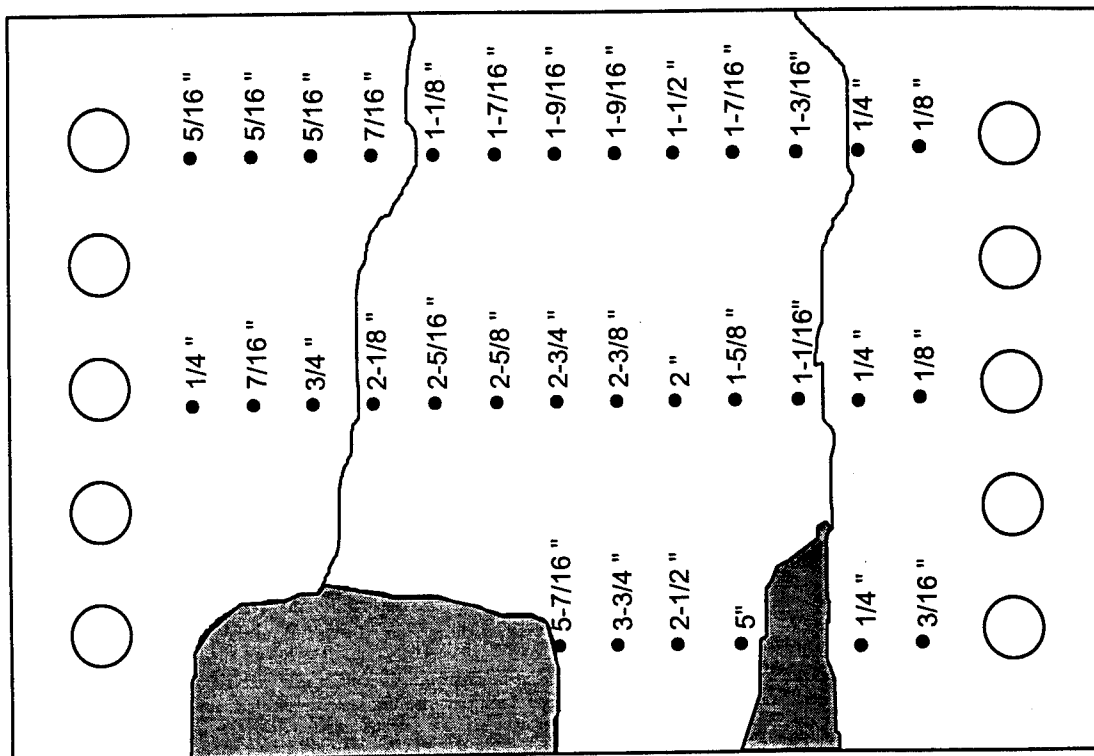


Figure 67. Posttest Deflection Survey for Slab No. 11

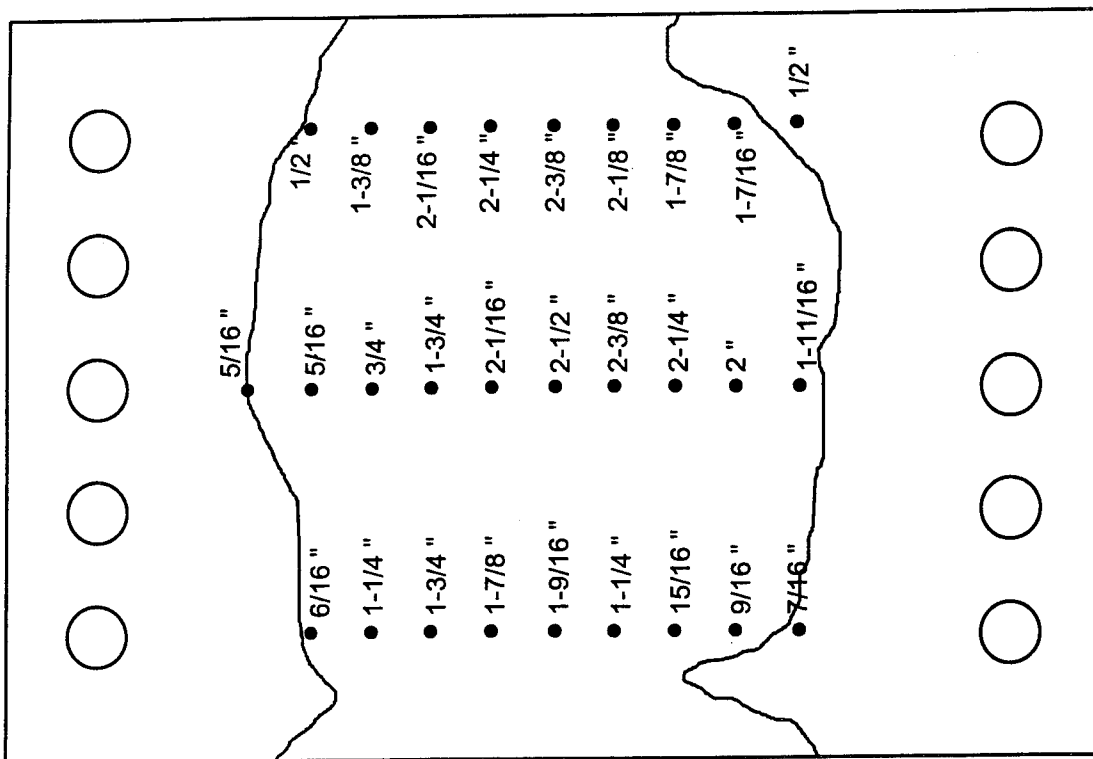


Figure 68. Posttest Deflection Survey for Slab No. 12

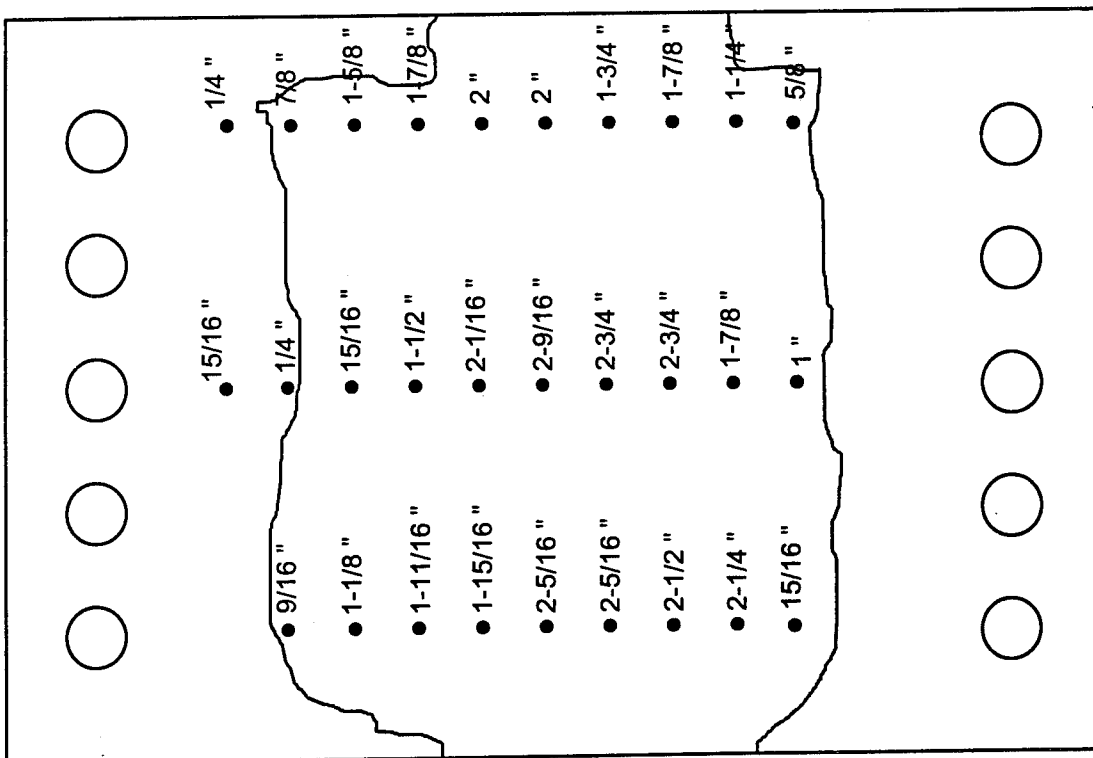
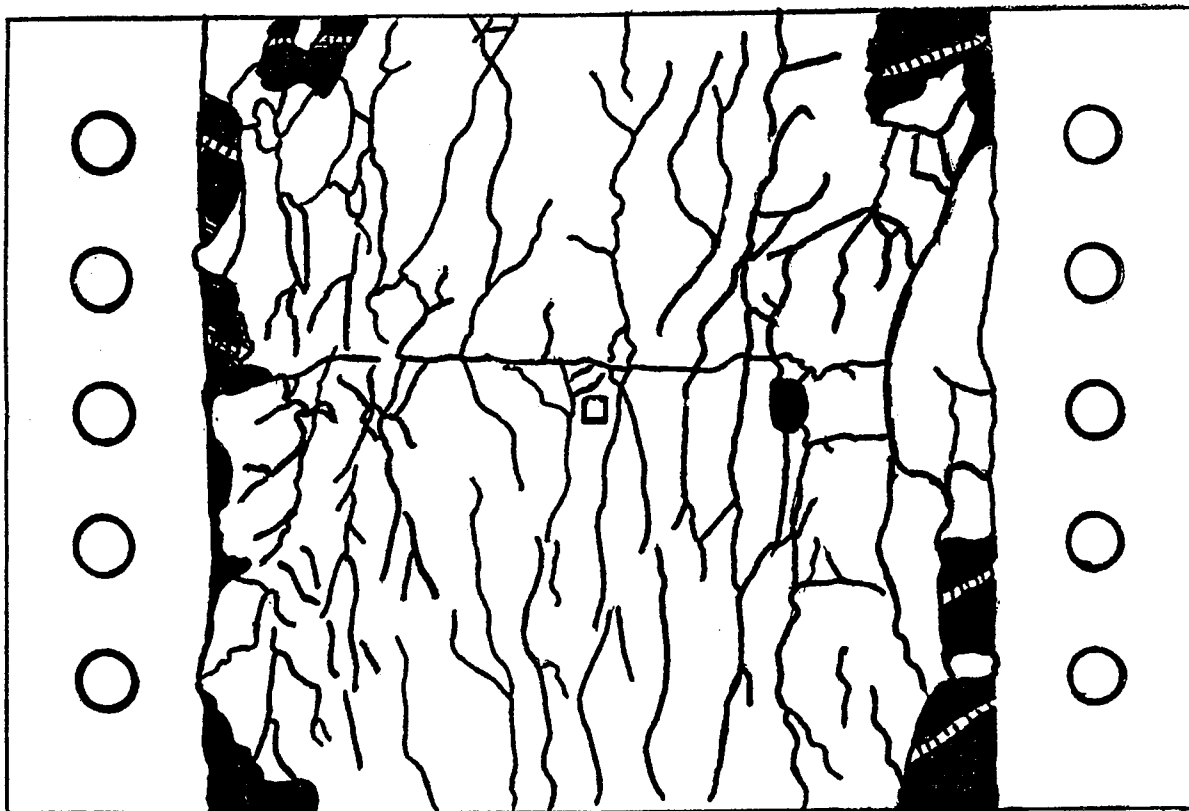
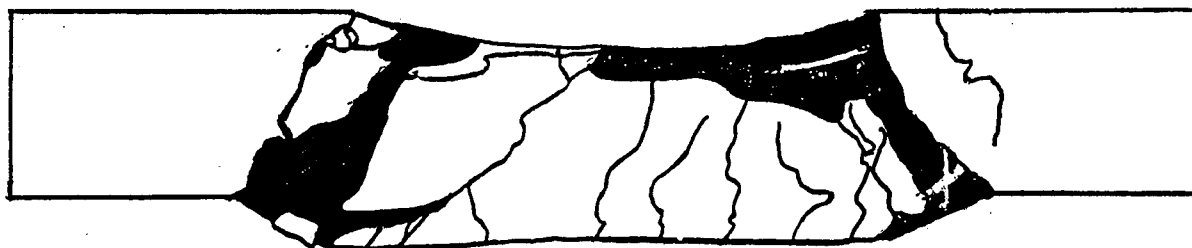


Figure 69. Posttest Deflection Survey for Slab No. 13

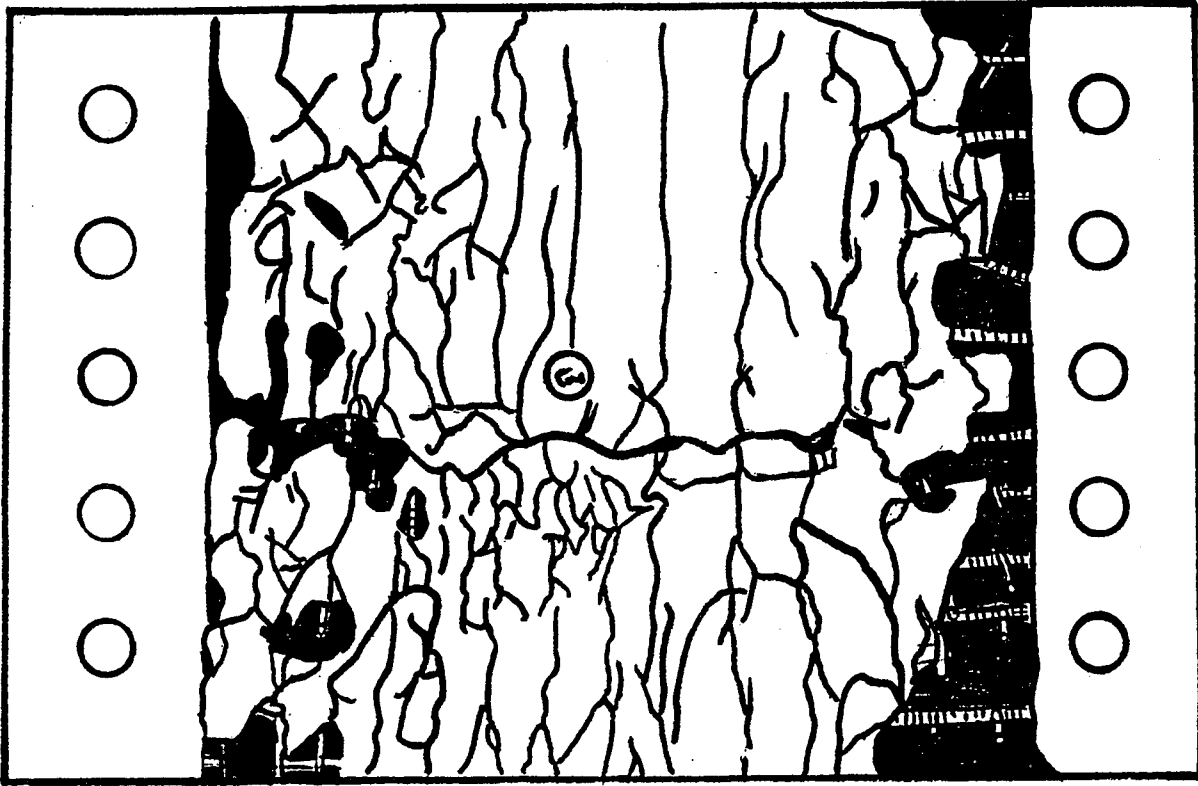


a. Bottom View

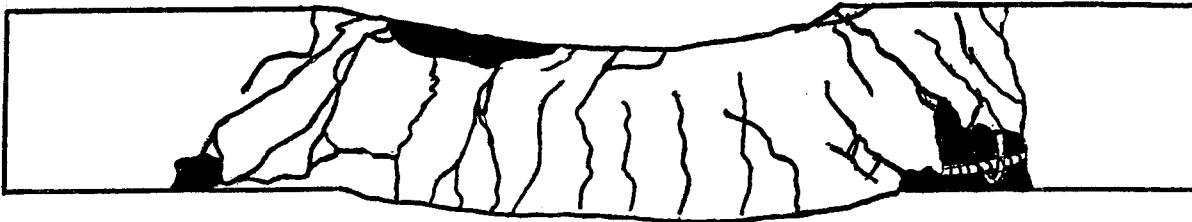


b. Side View

Figure 70. Sketch of Damage for Slab No. 1

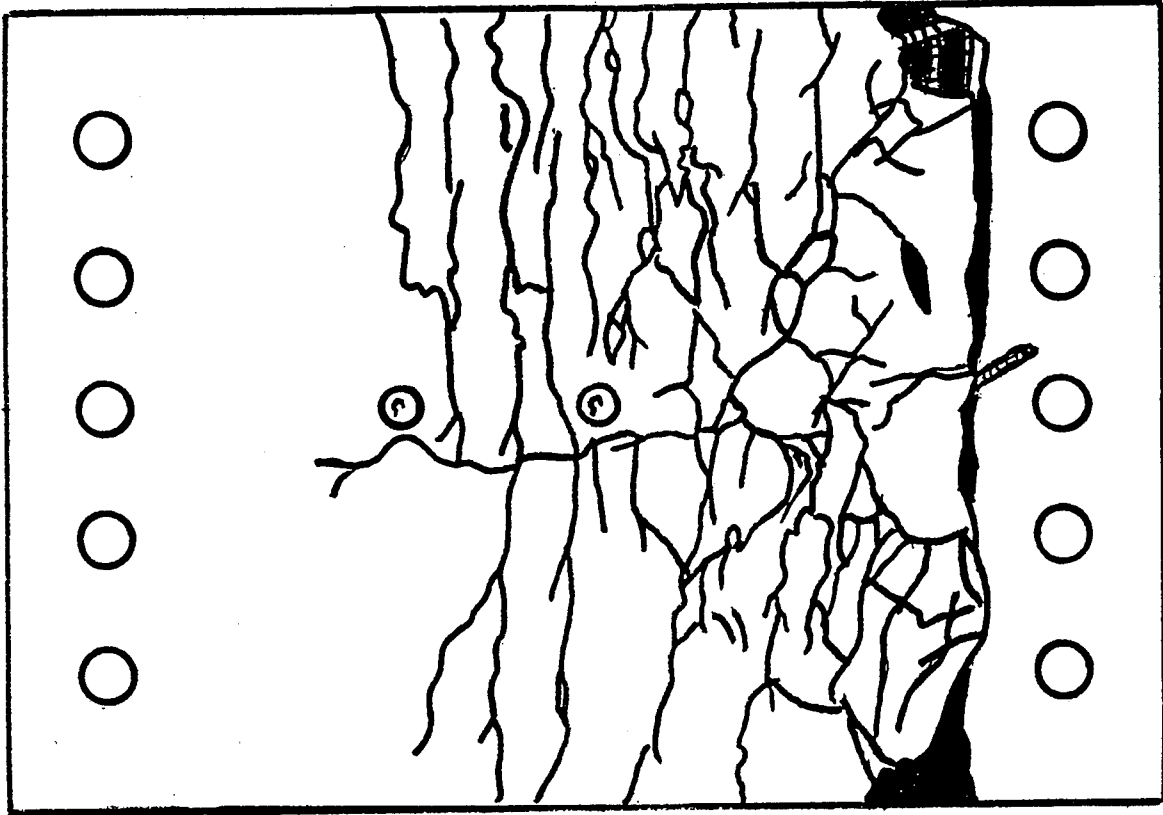


a. Bottom View

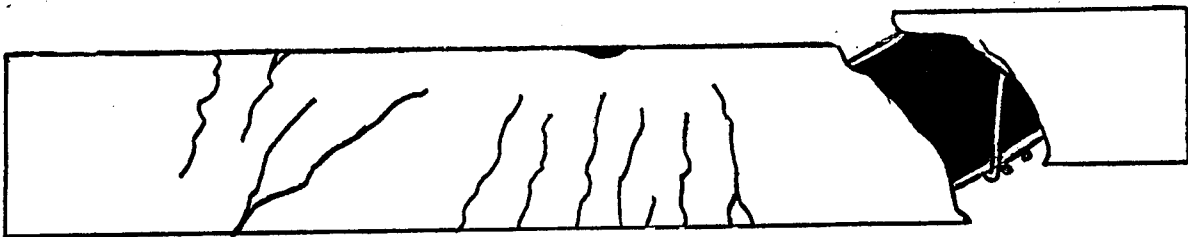


b. Side View

Figure 71. Sketch of Damage for Slab No. 2

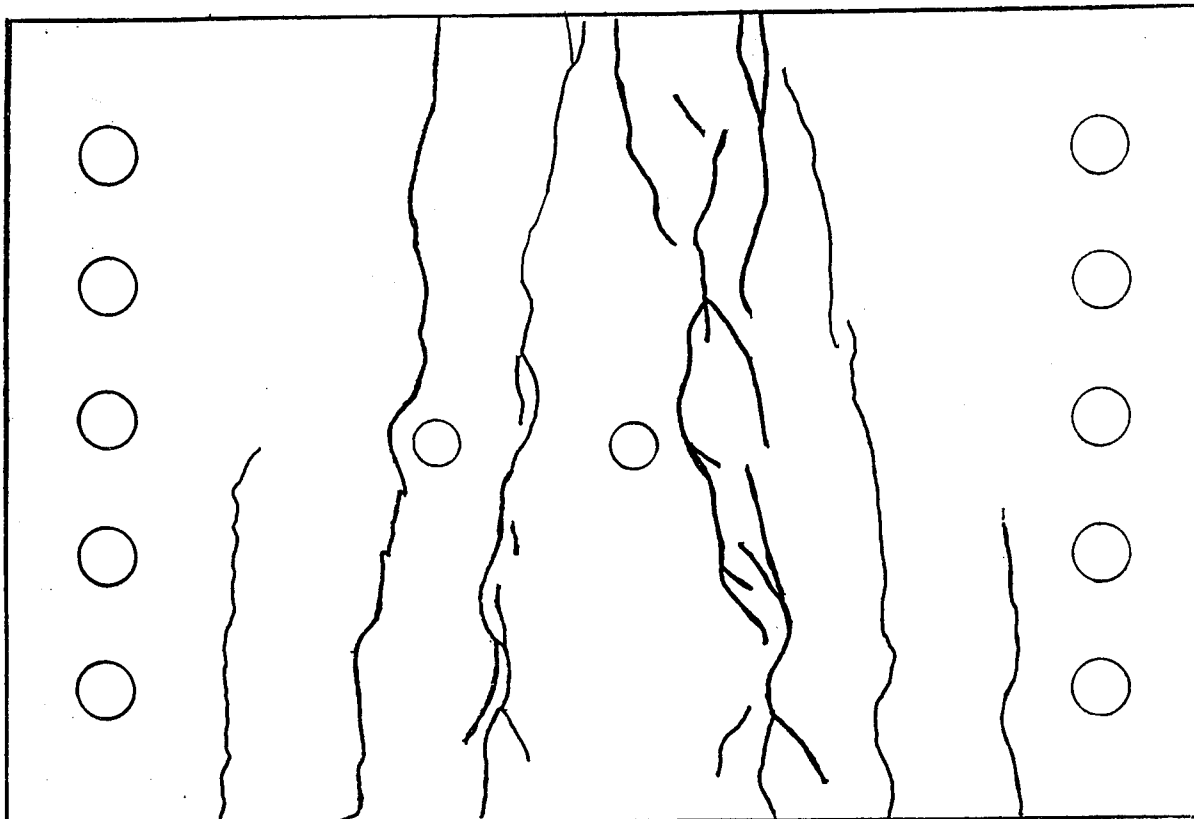


a. Bottom View

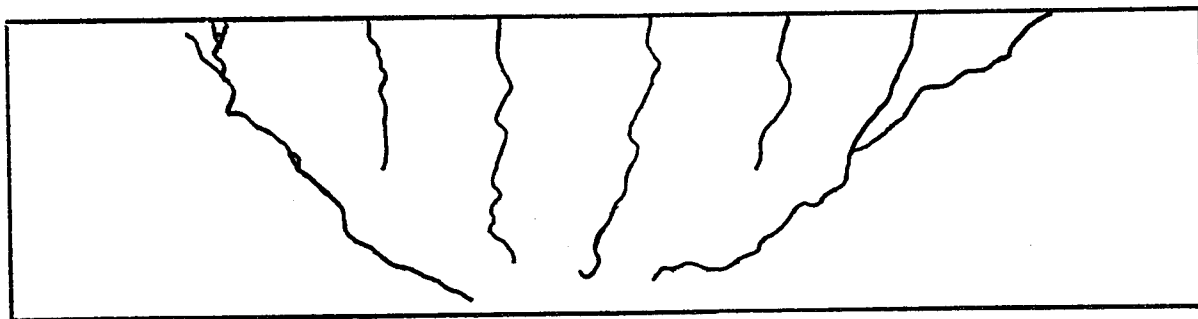


b. Side View

Figure 72. Sketch of Damage for Slab No. 3

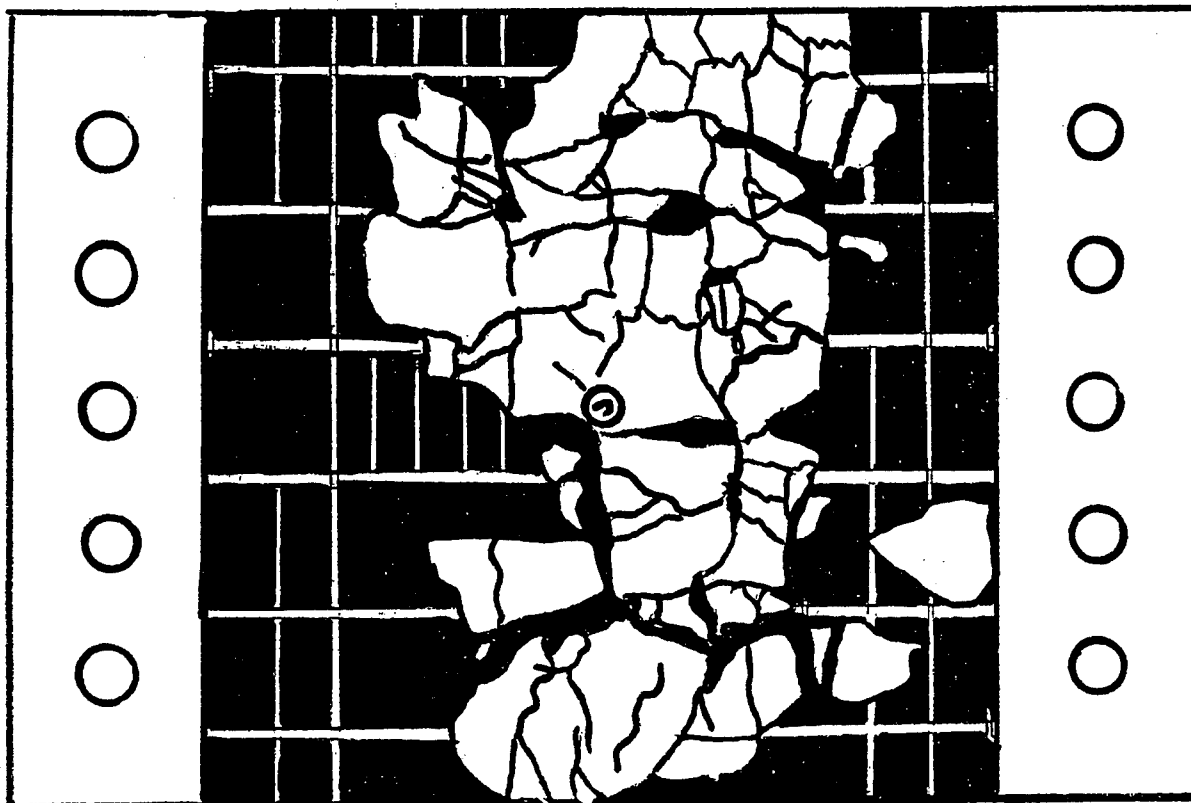


a. Bottom View

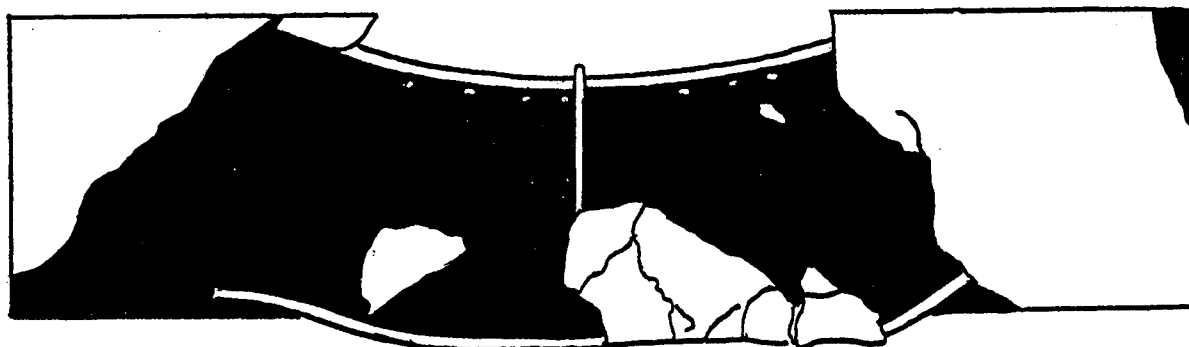


b. Side View

Figure 73. Sketch of Damage for Slab No. 4

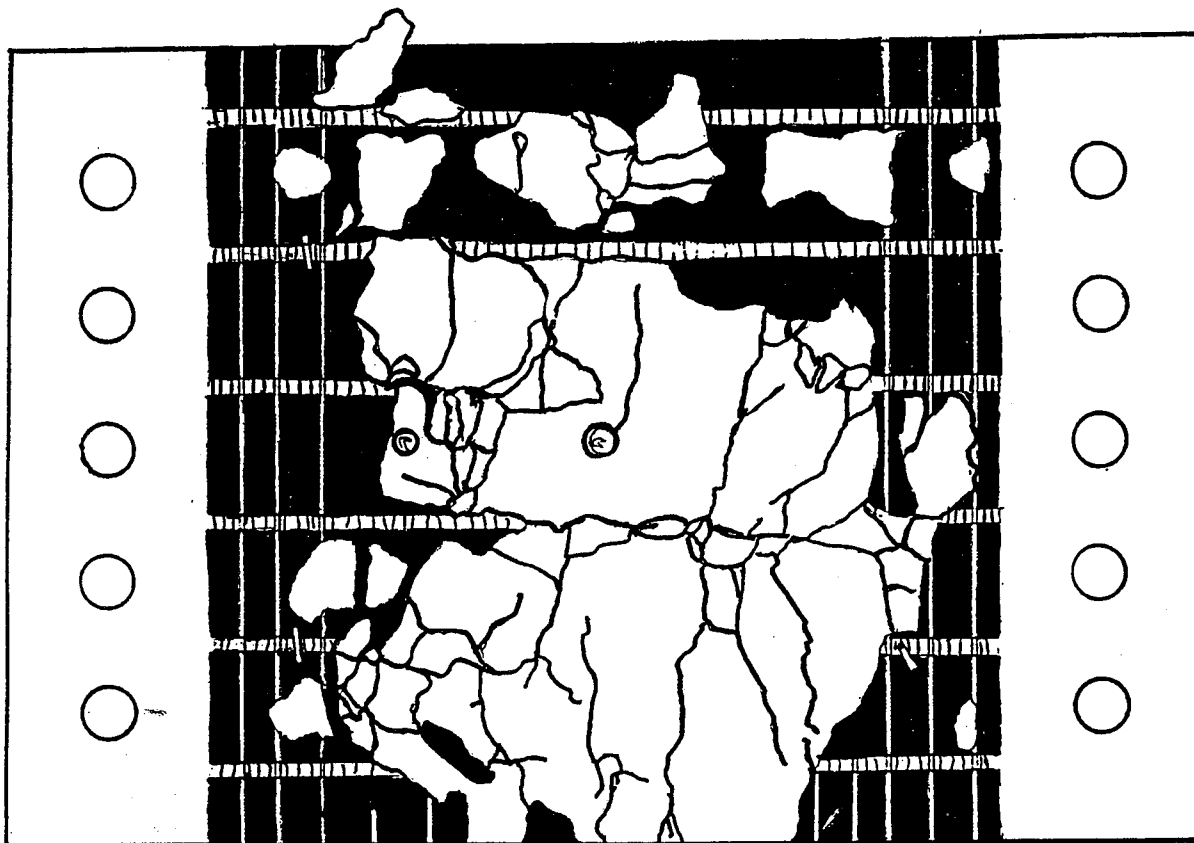


a. Bottom View

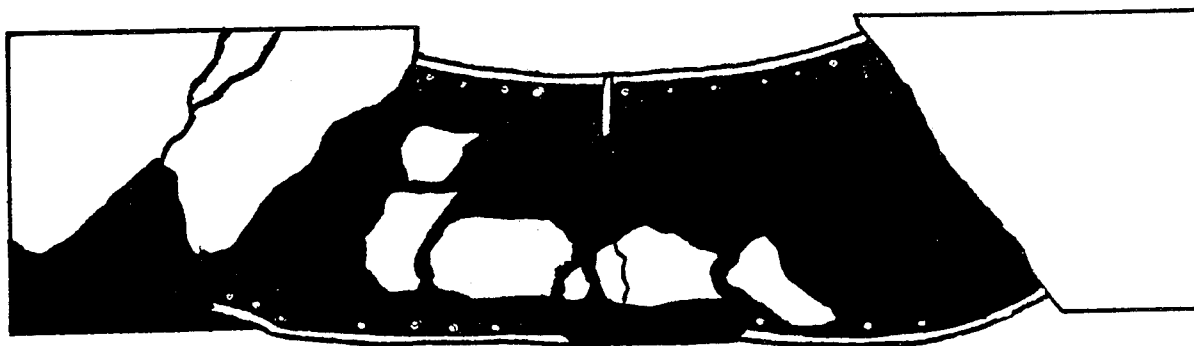


b. Side View

Figure 74. Sketch of Damage for Slab No. 5

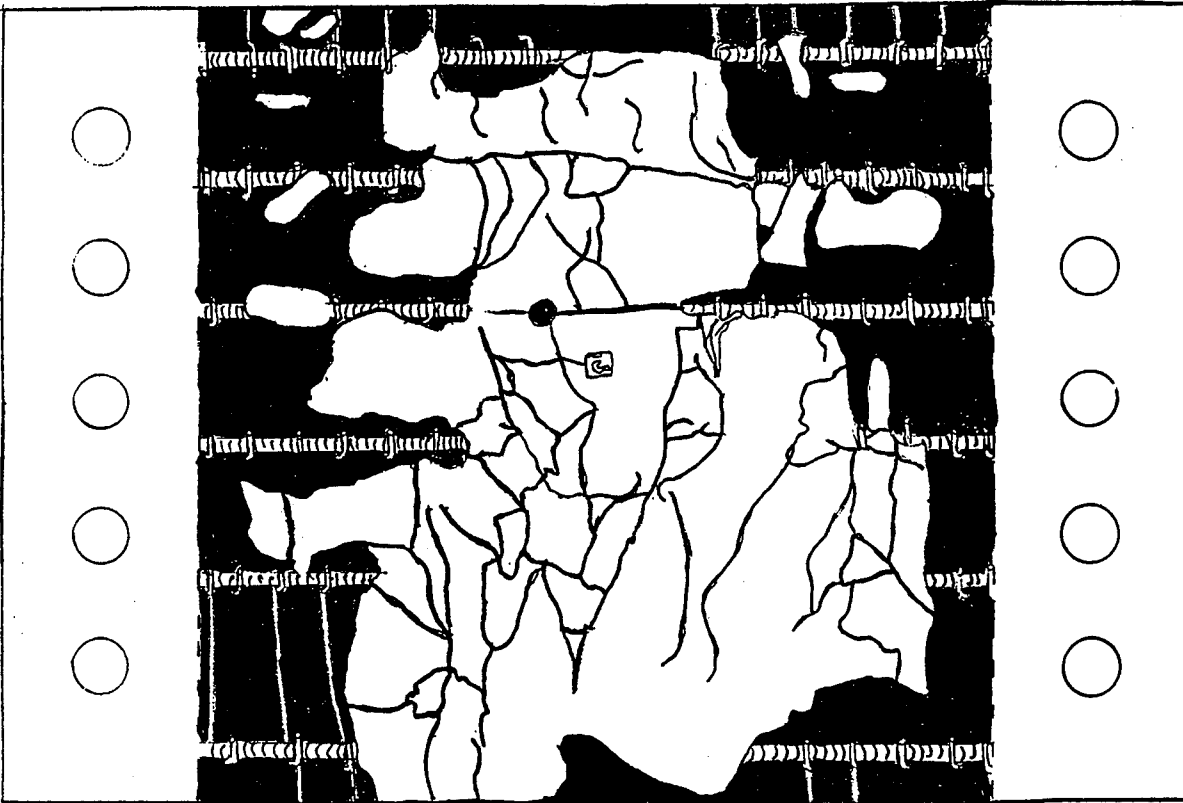


a. Bottom View

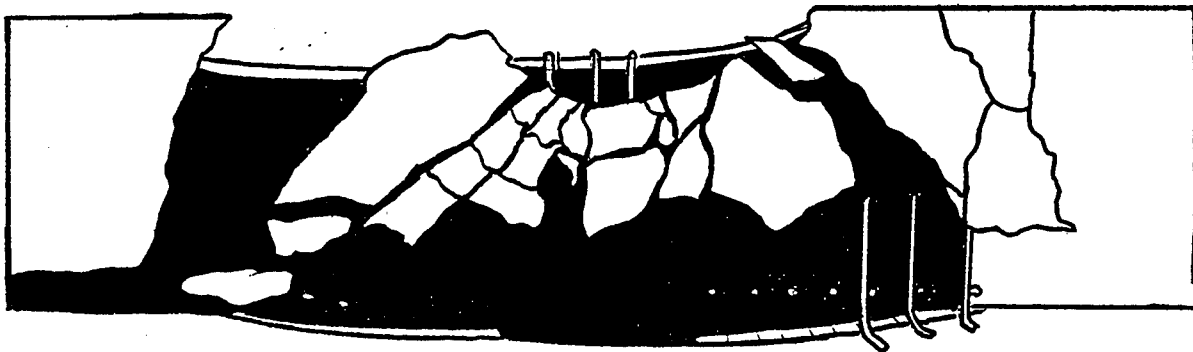


b. Side View

Figure 75. Sketch of Damage for Slab No. 6



a. Bottom View

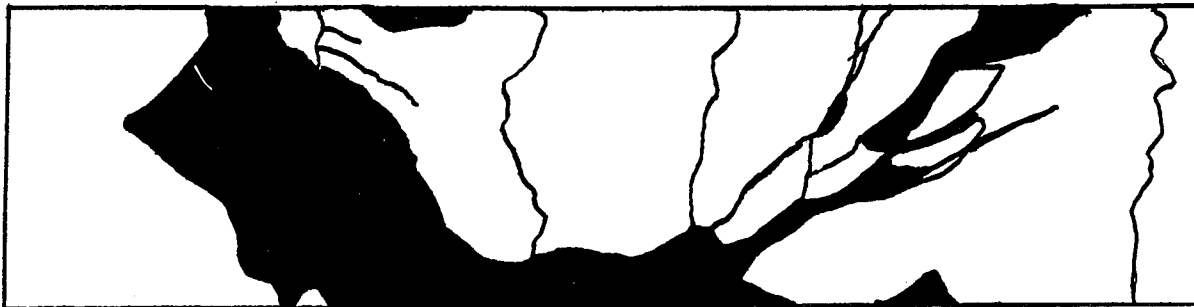


b. Side View

Figure 76. Sketch of Damage for Slab No. 8

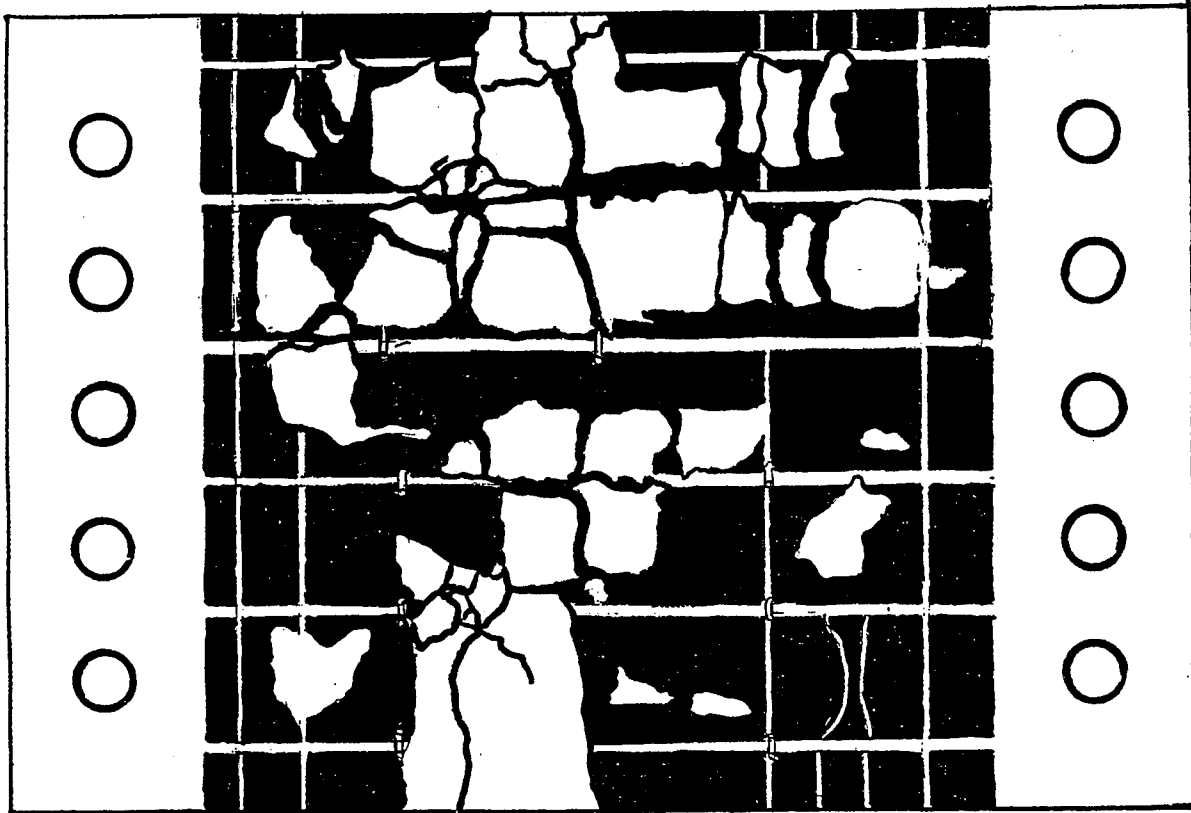


a. Bottom View

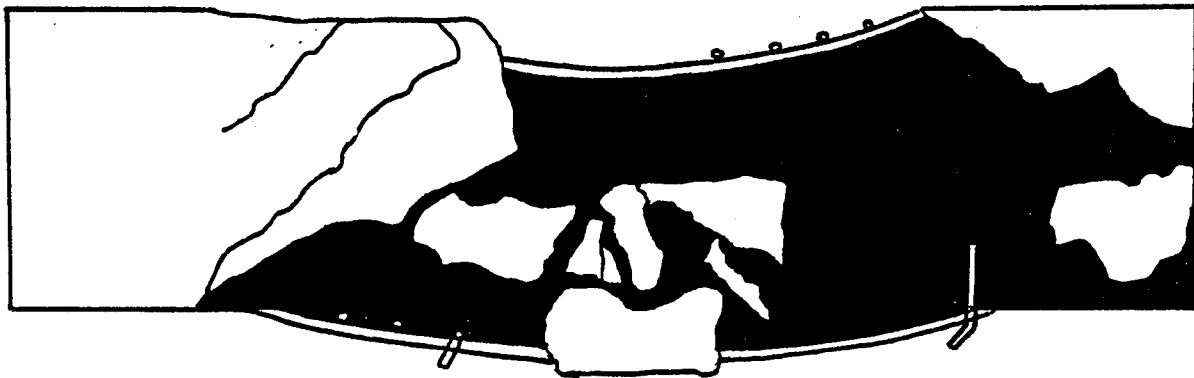


b. Side View

Figure 77. Sketch of Damage for Slab No. 9



a. Bottom View

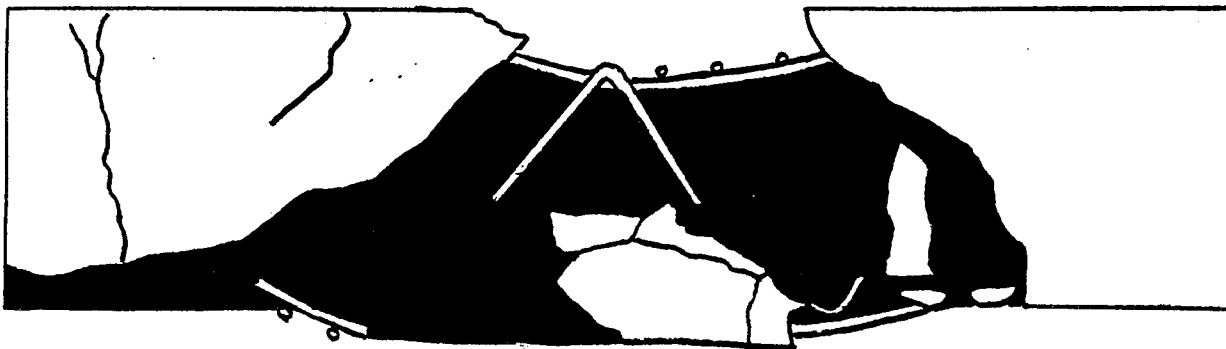


b. Side View

Figure 78. Sketch of Damage for Slab No. 10



a. Bottom View

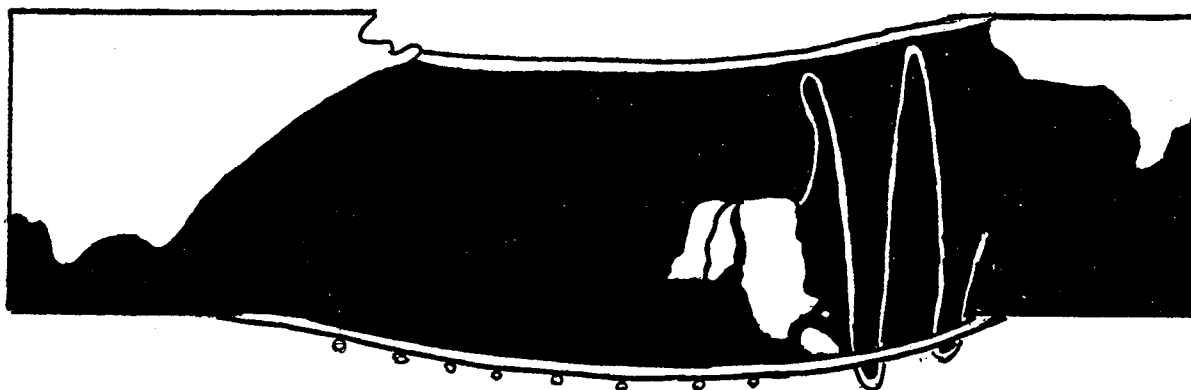


b. Side View

Figure 79. Sketch of Damage for Slab No. 12



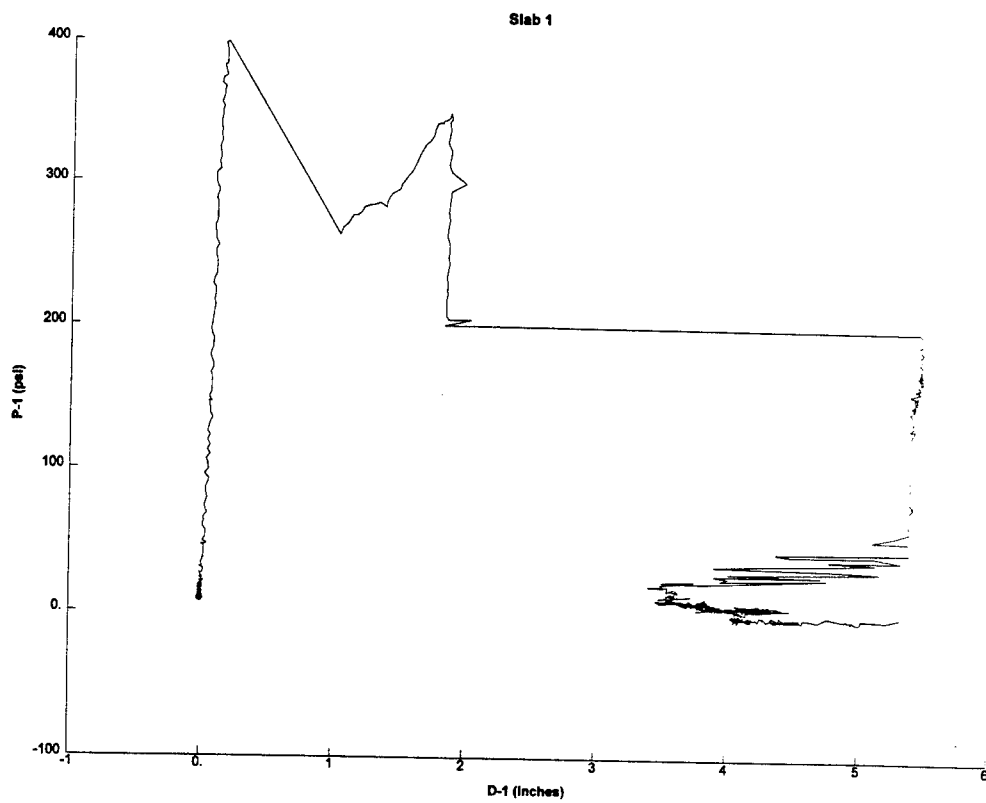
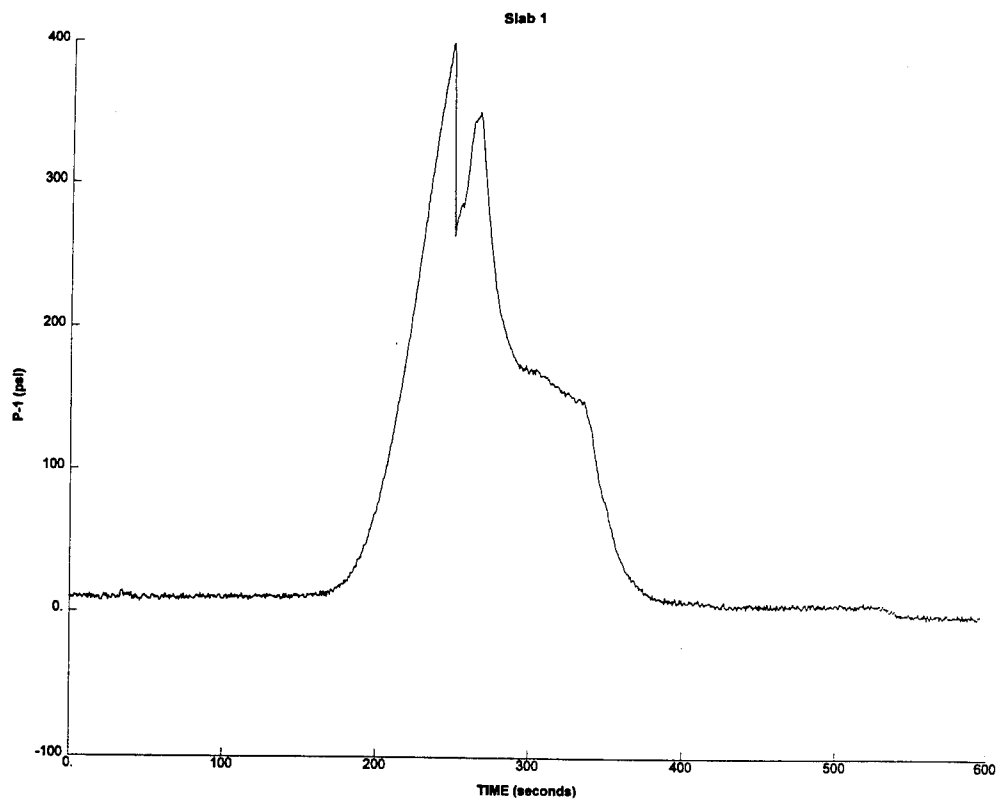
a. Bottom View

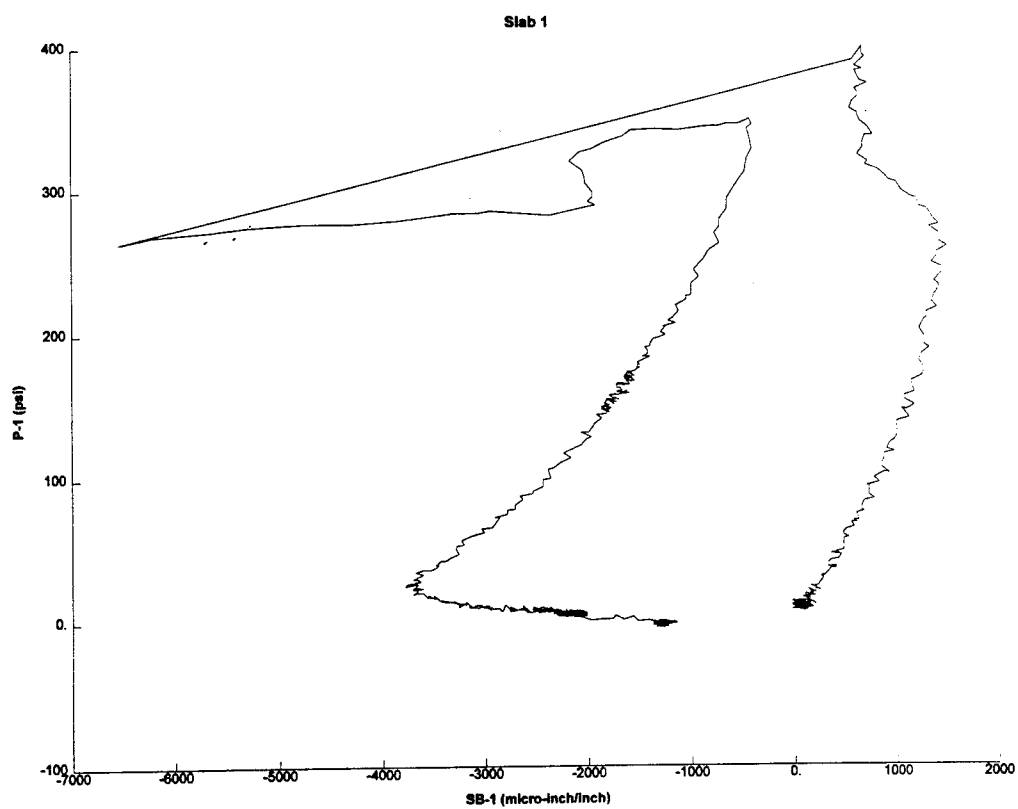
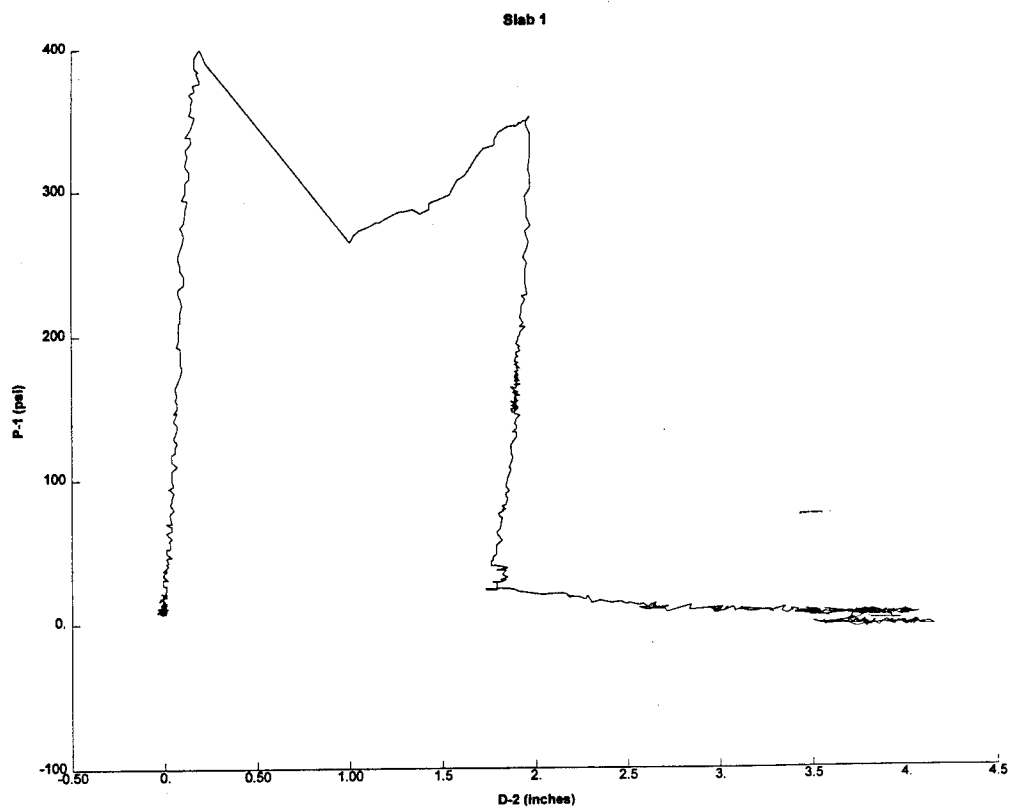


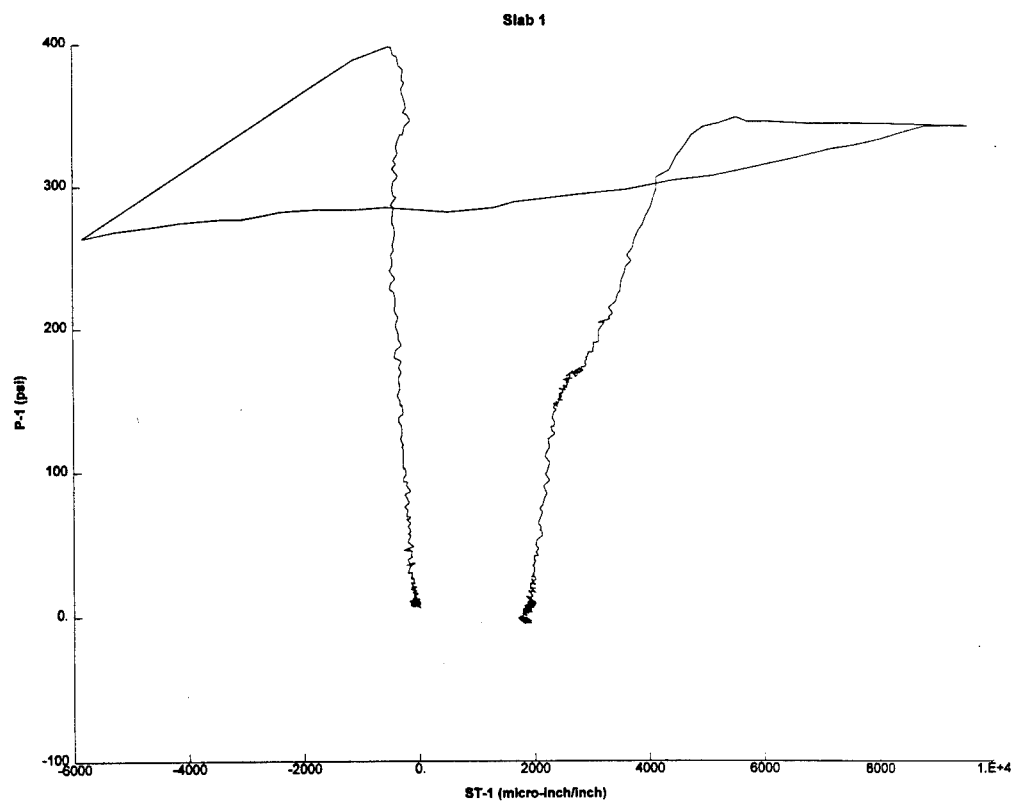
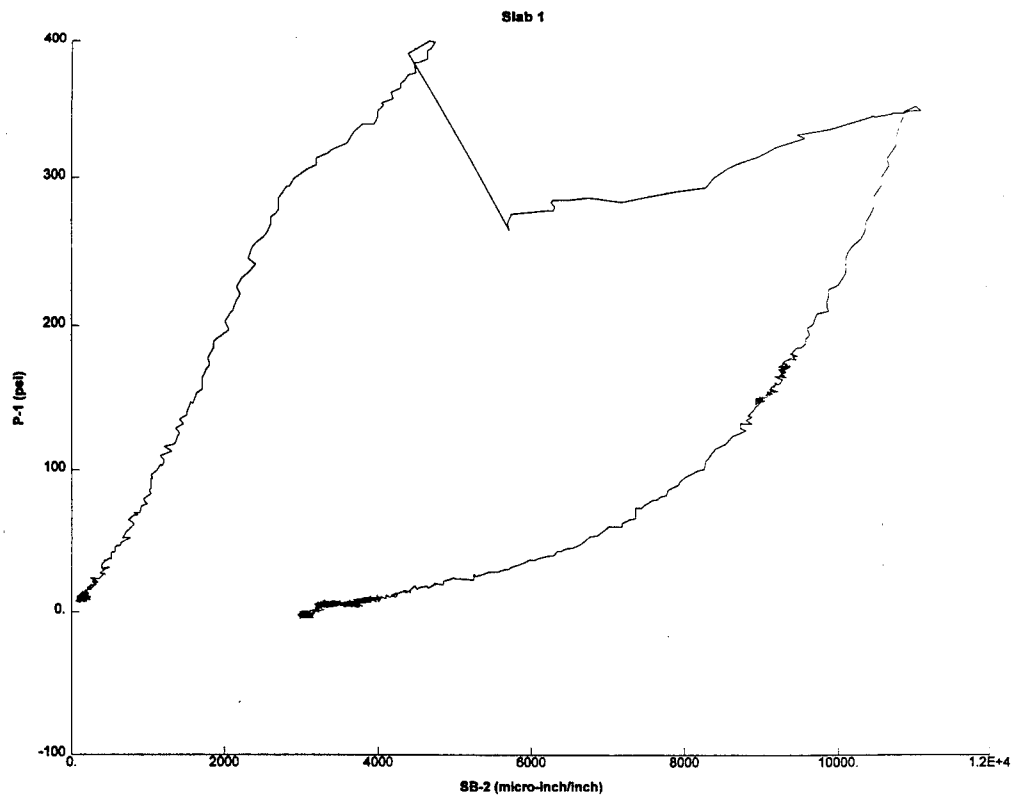
b. Side View

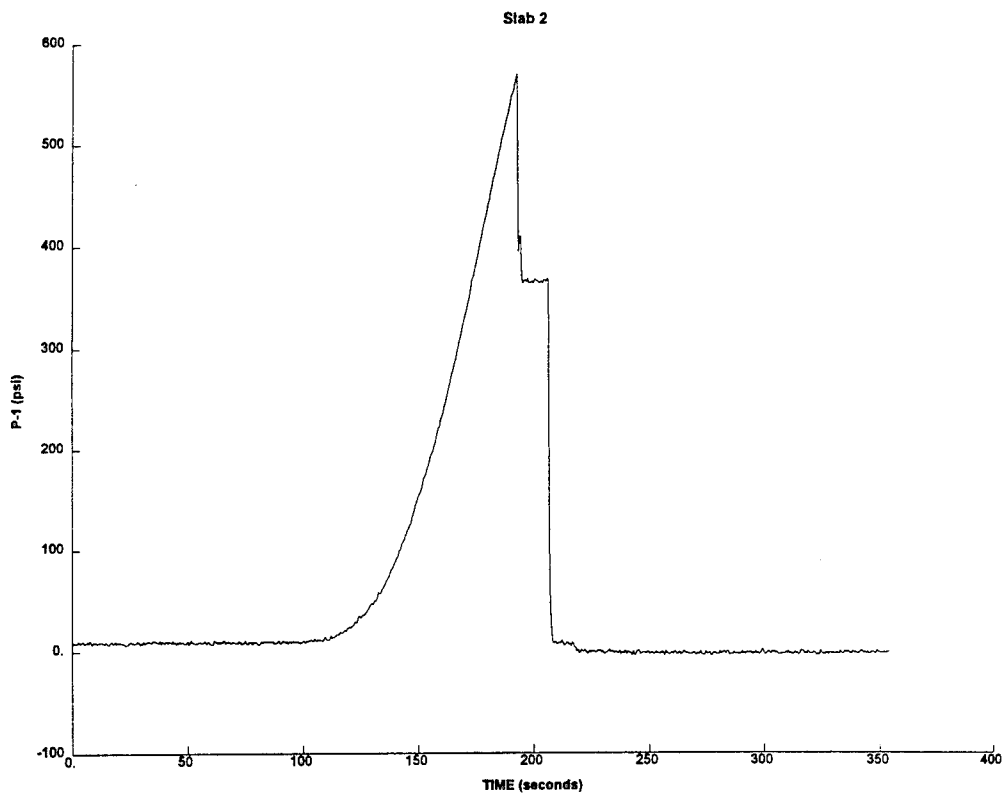
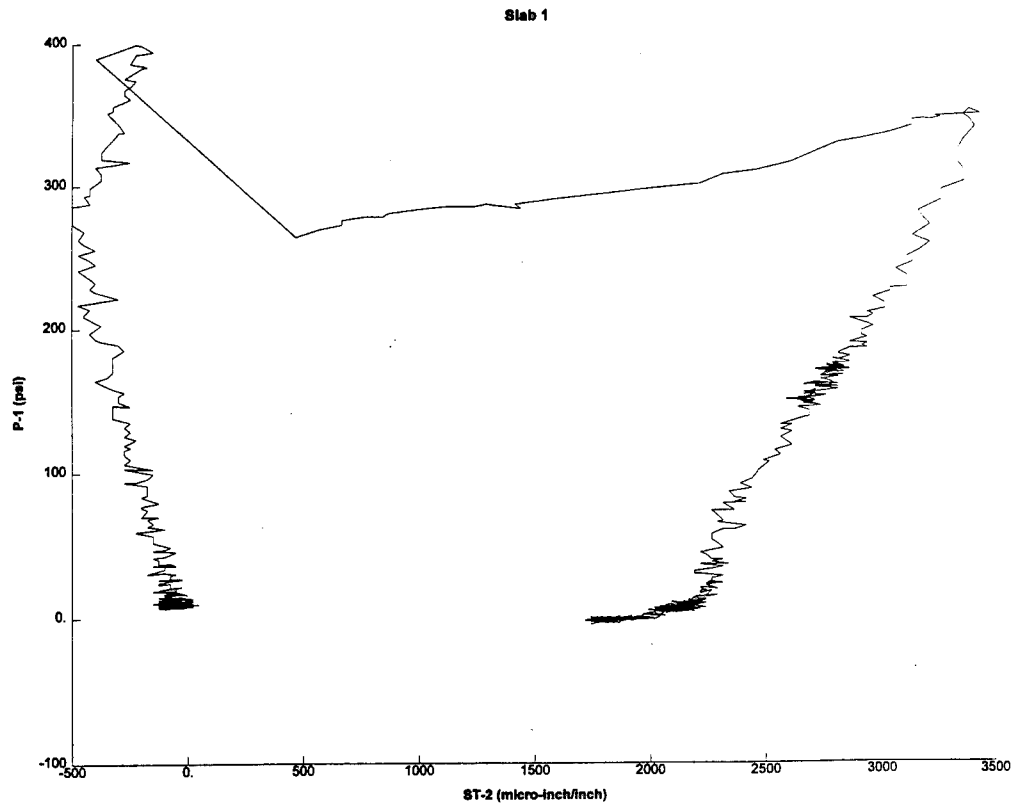
Figure 80. Sketch of Damage for Slab No. 13

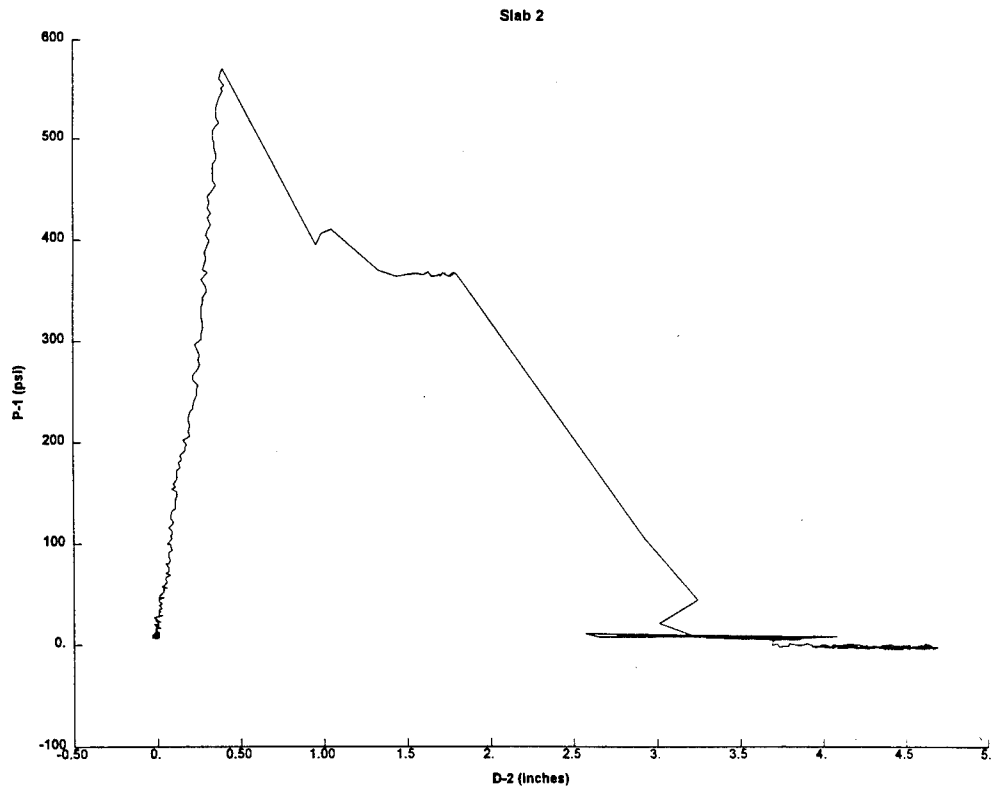
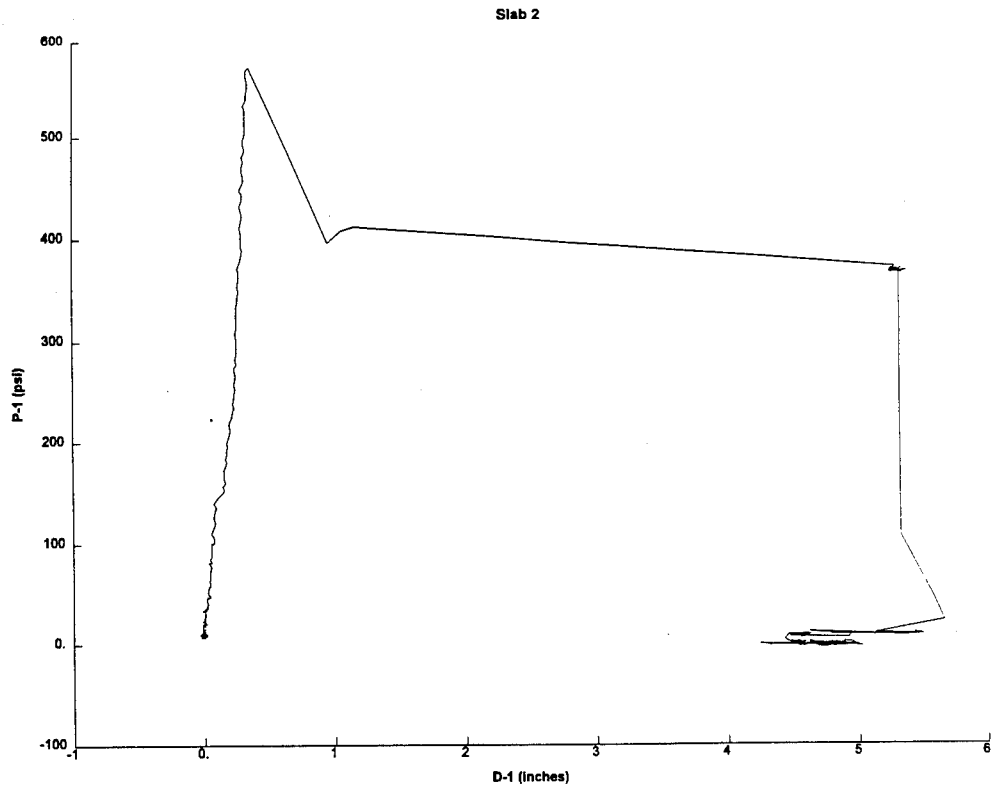
Appendix A: Recorded Data

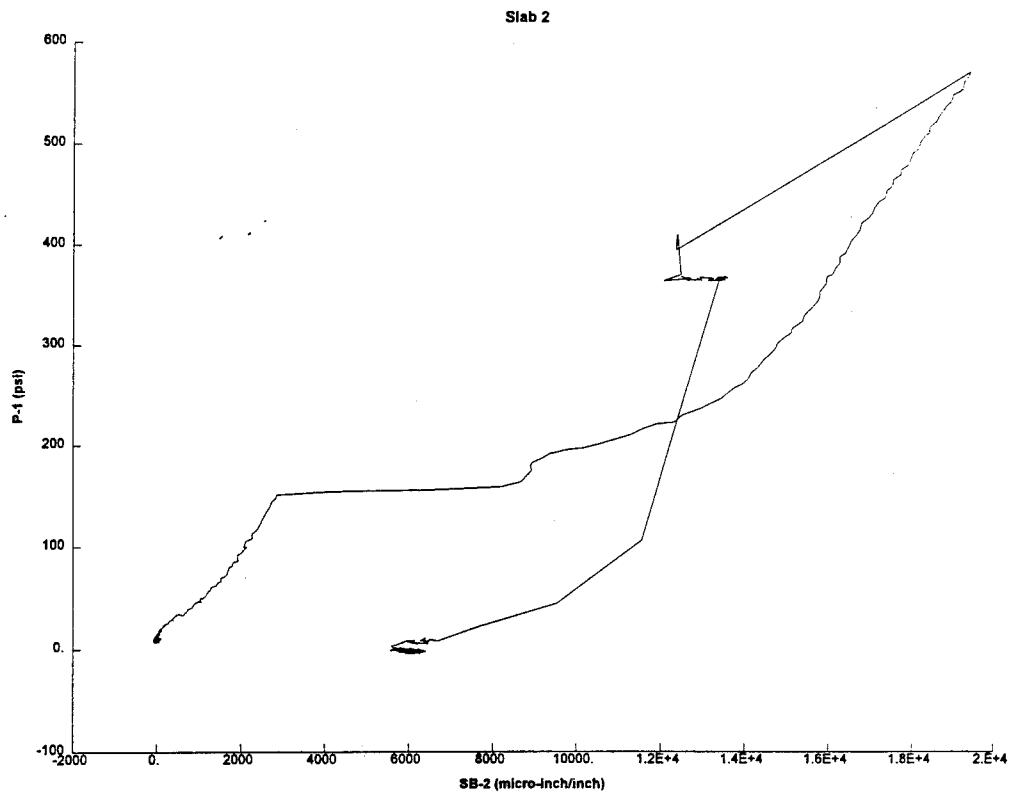
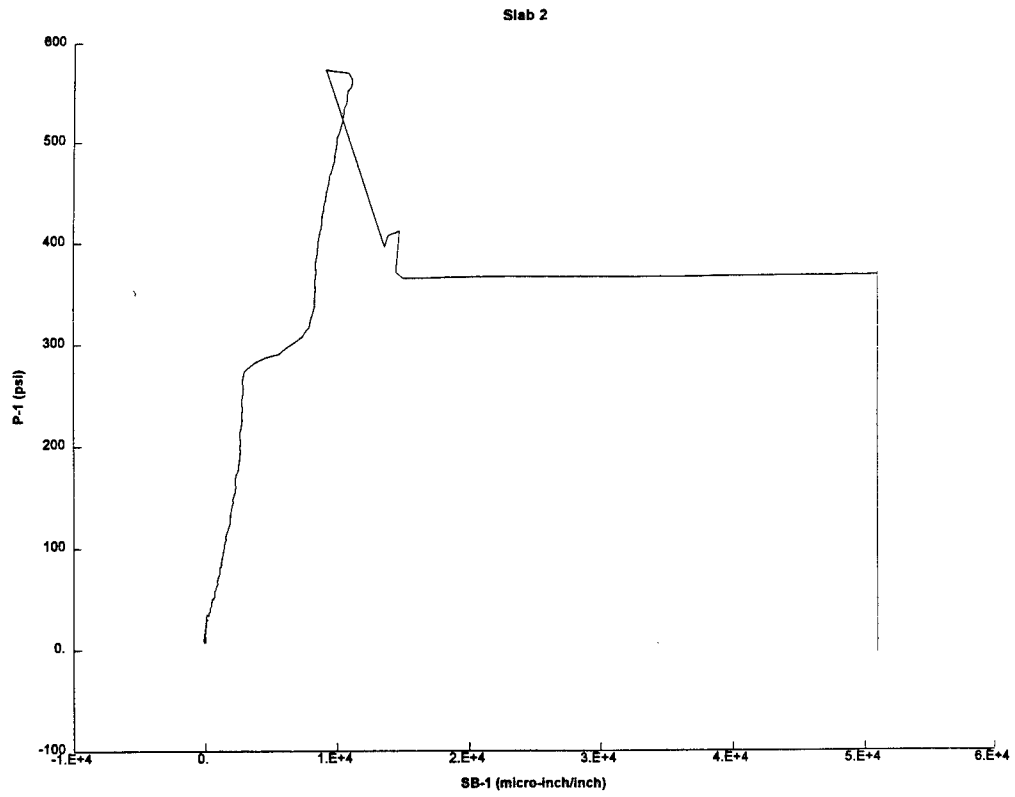


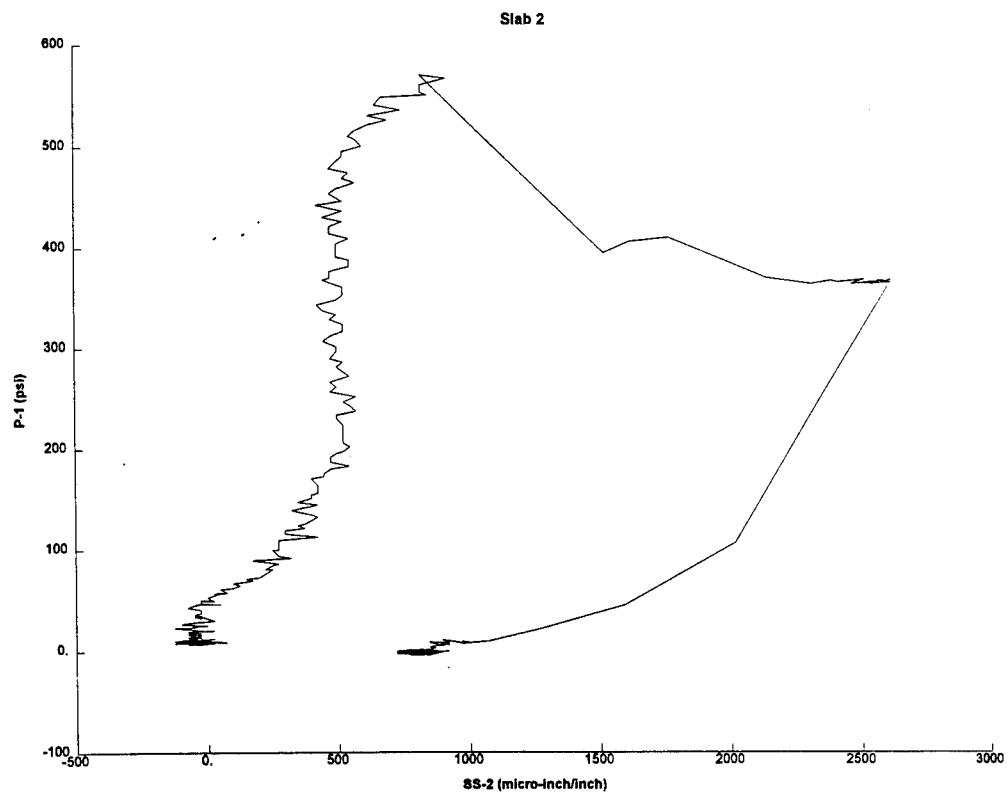
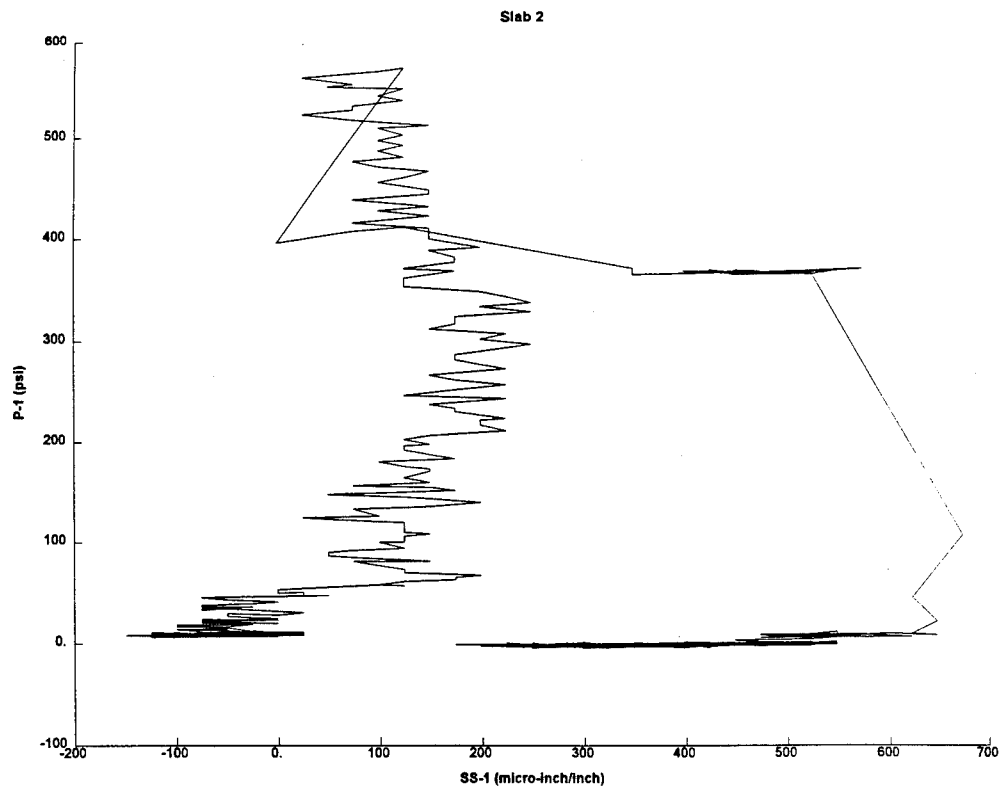


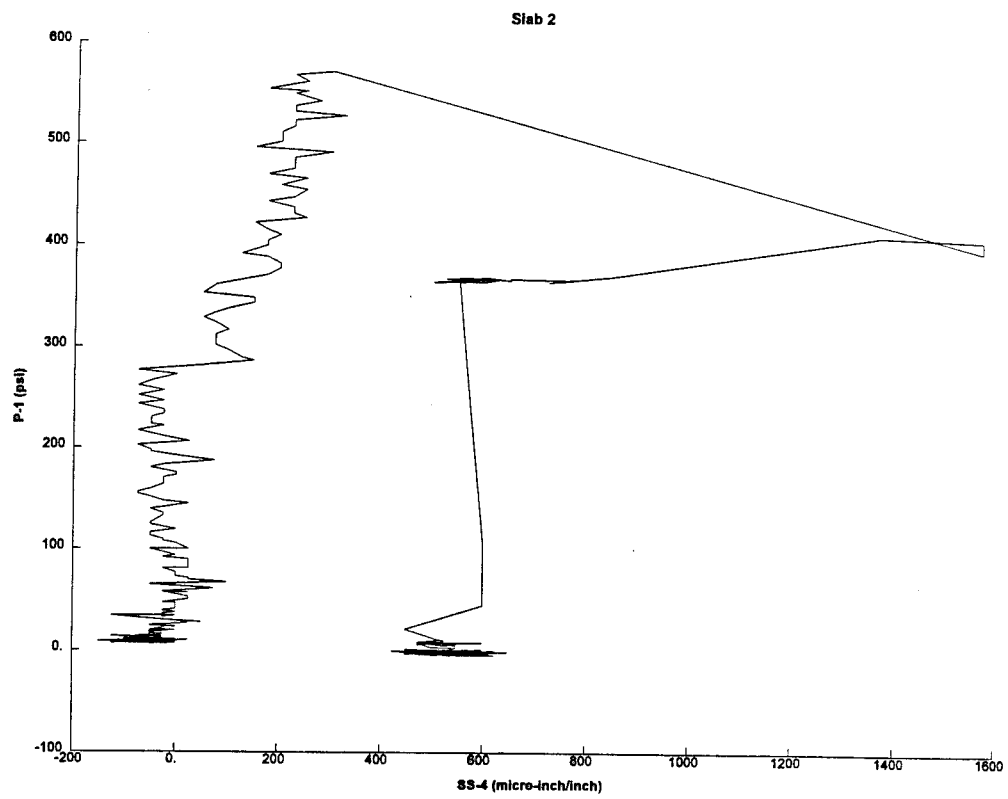
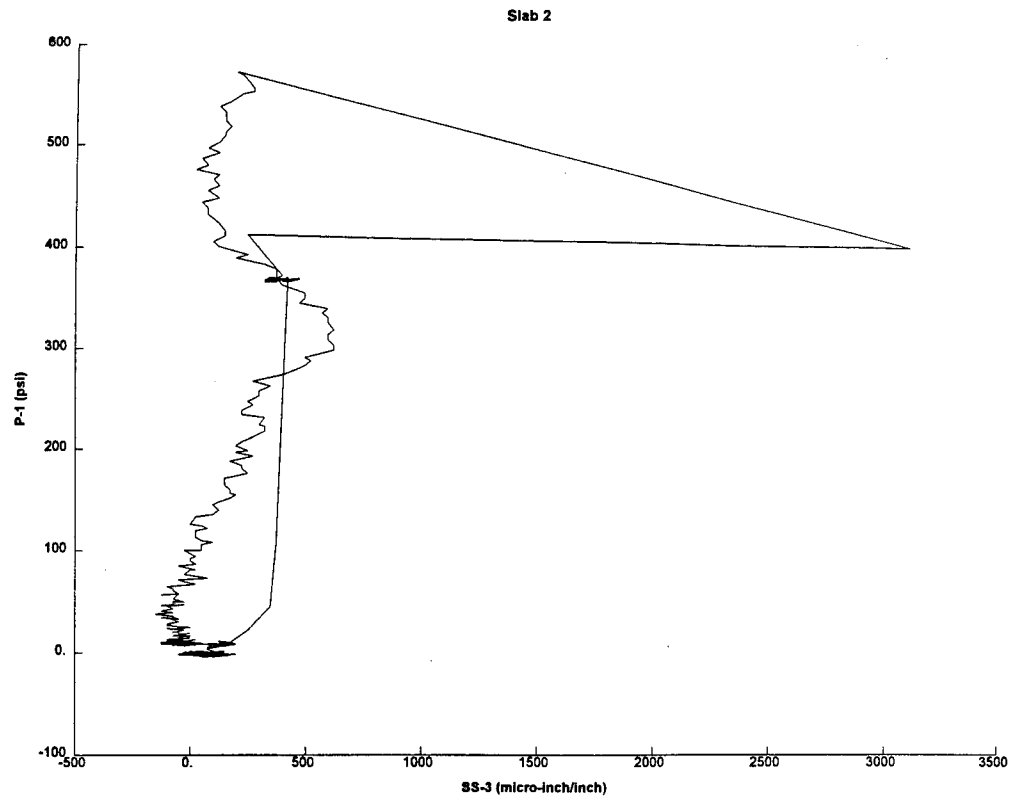


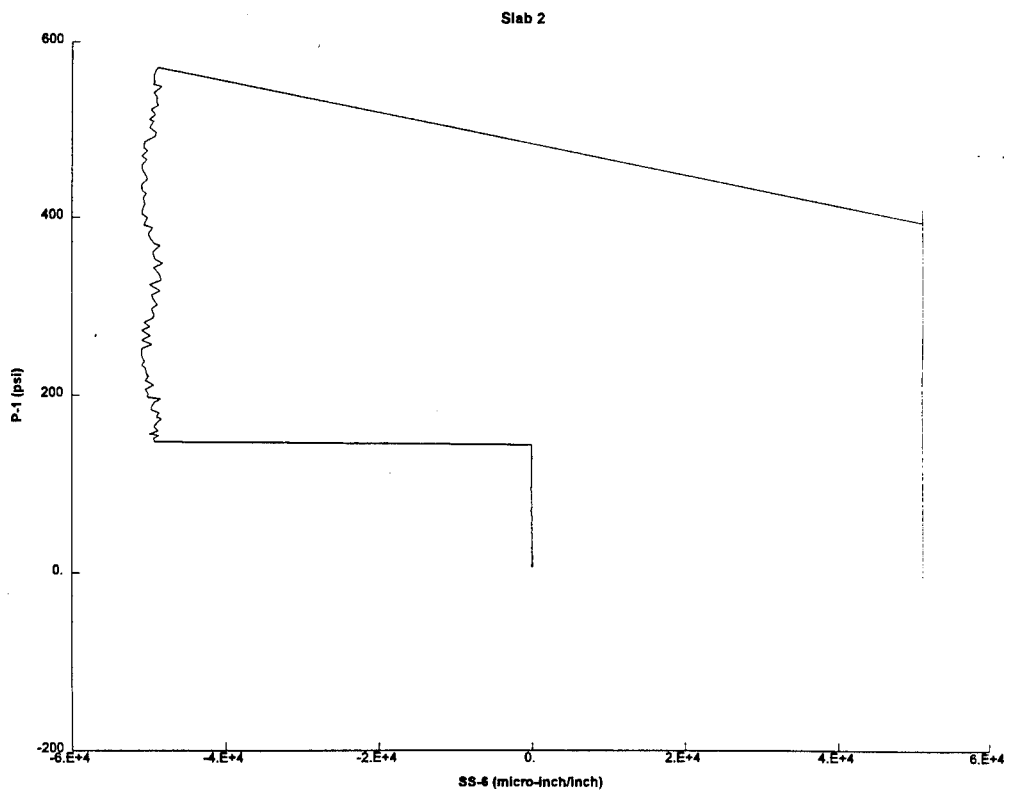
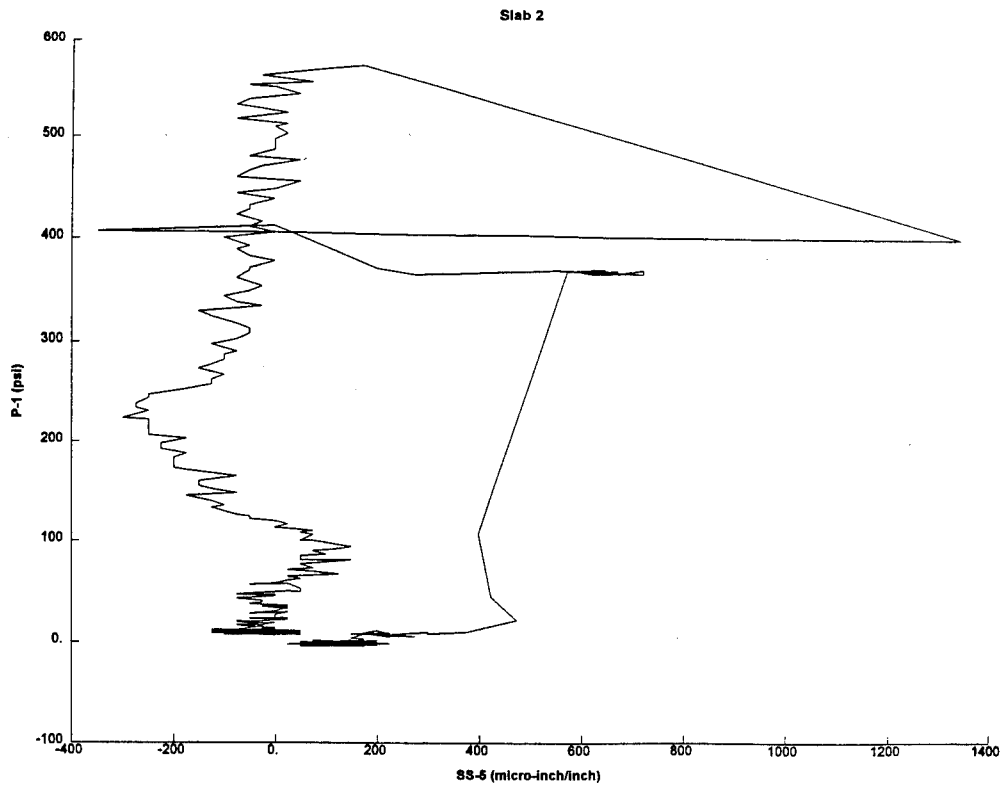


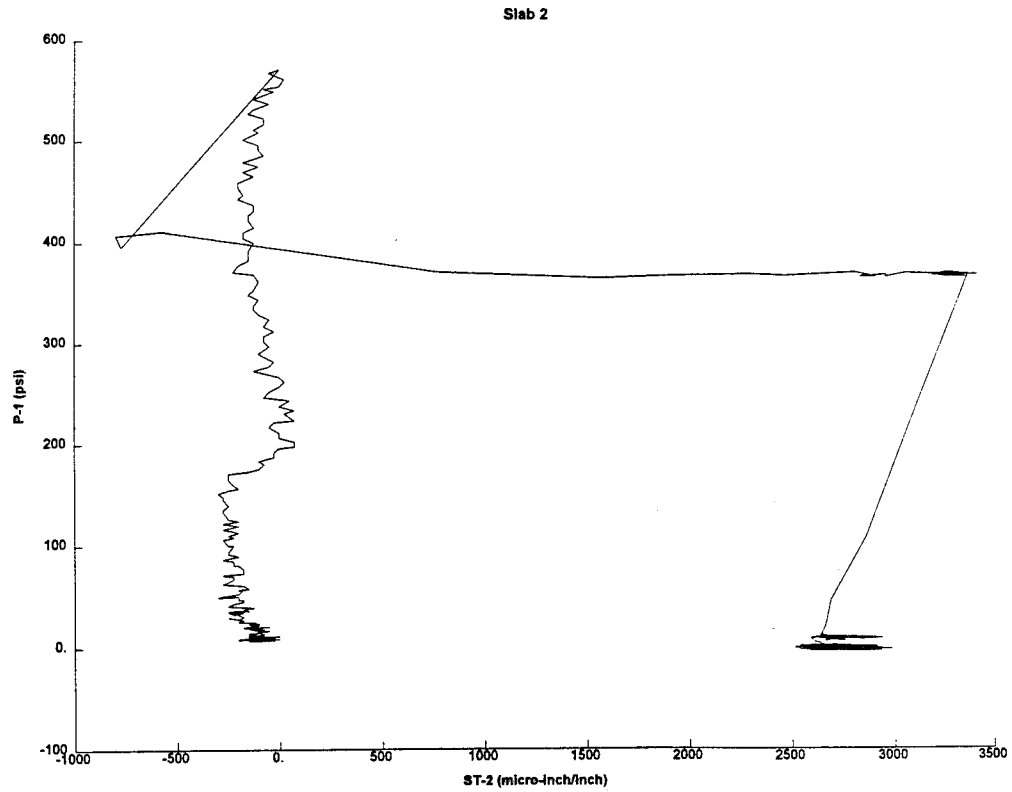
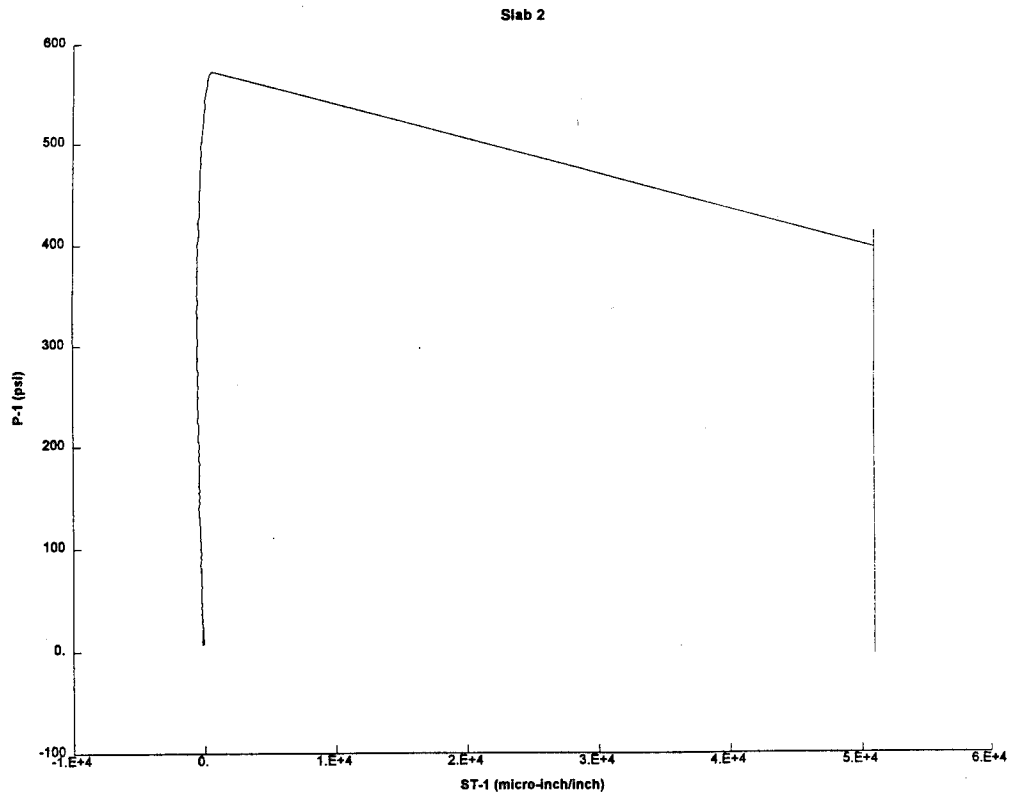


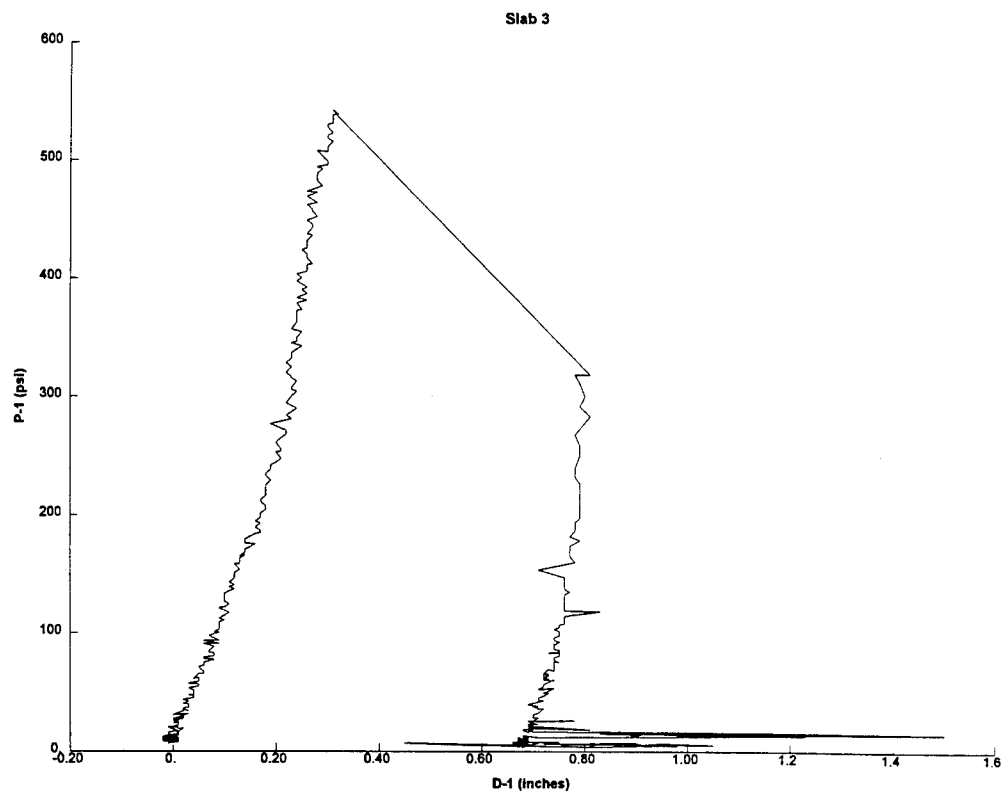
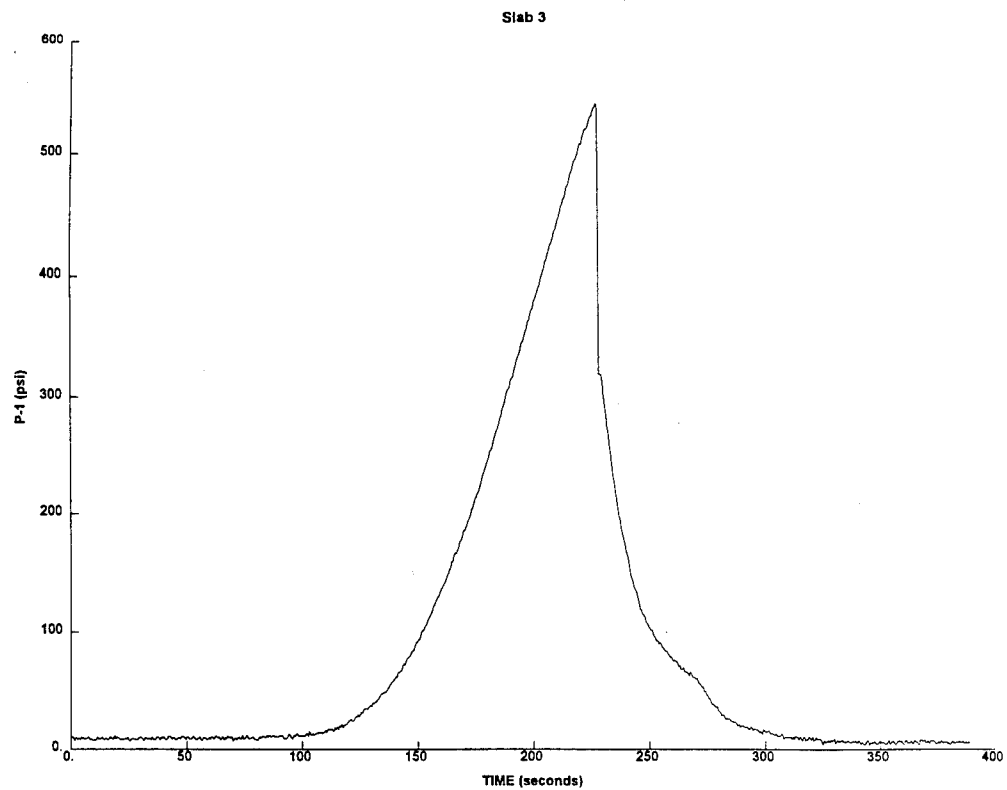


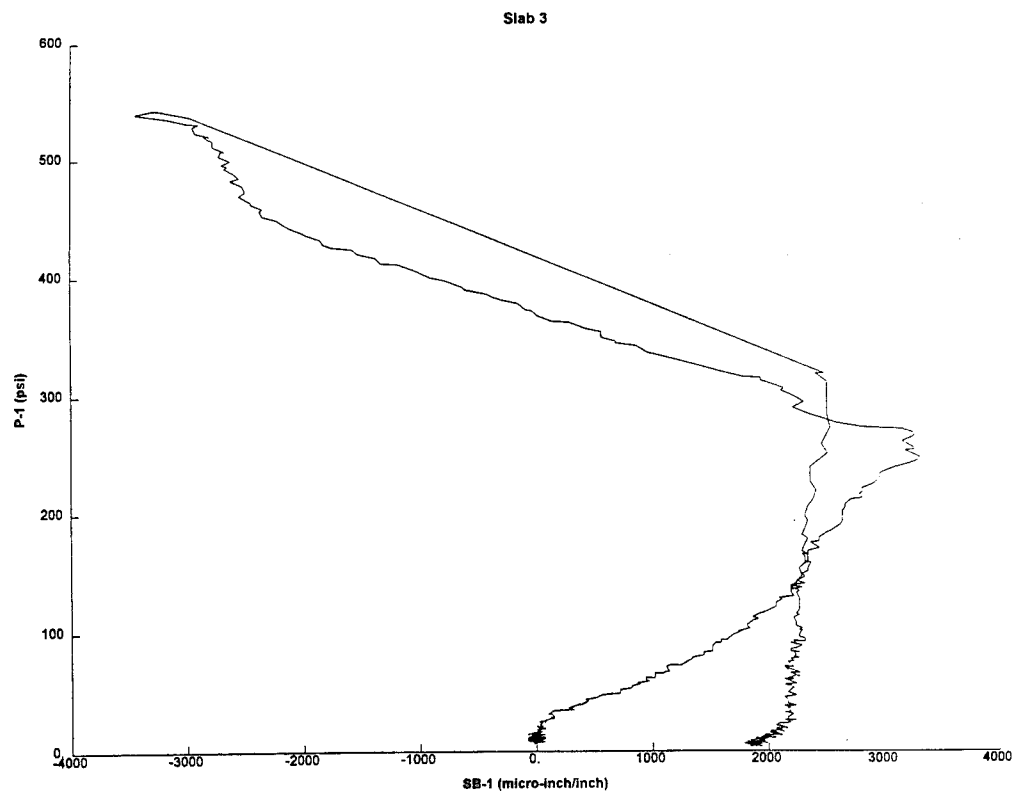
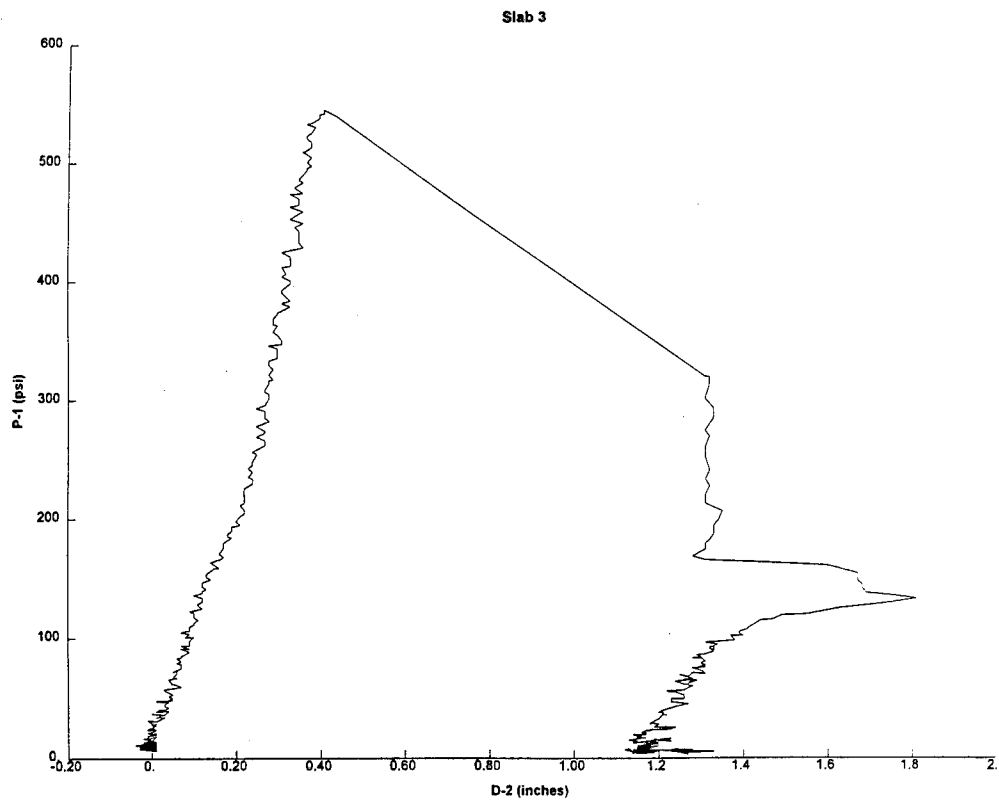


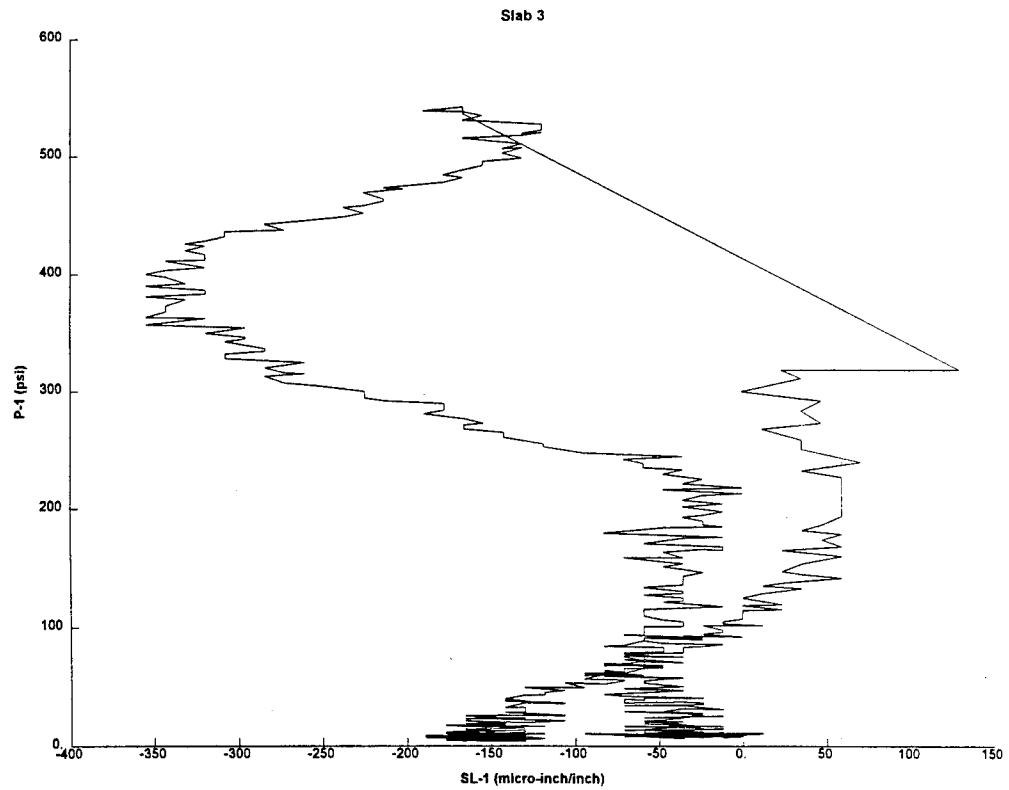
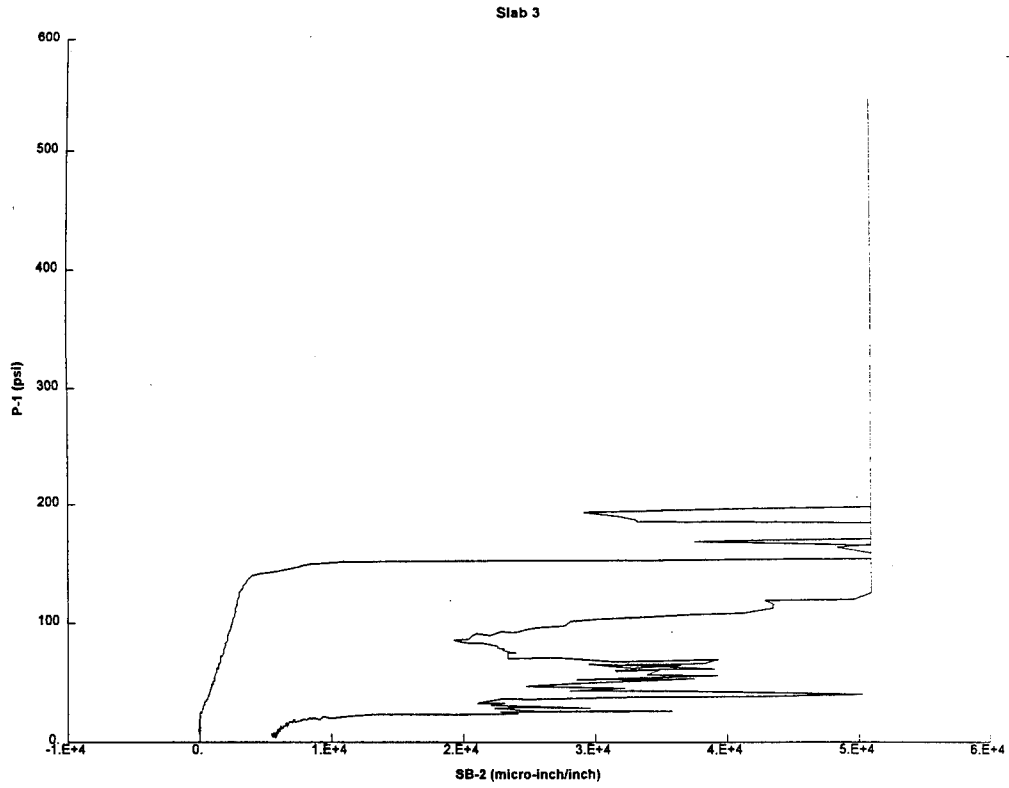


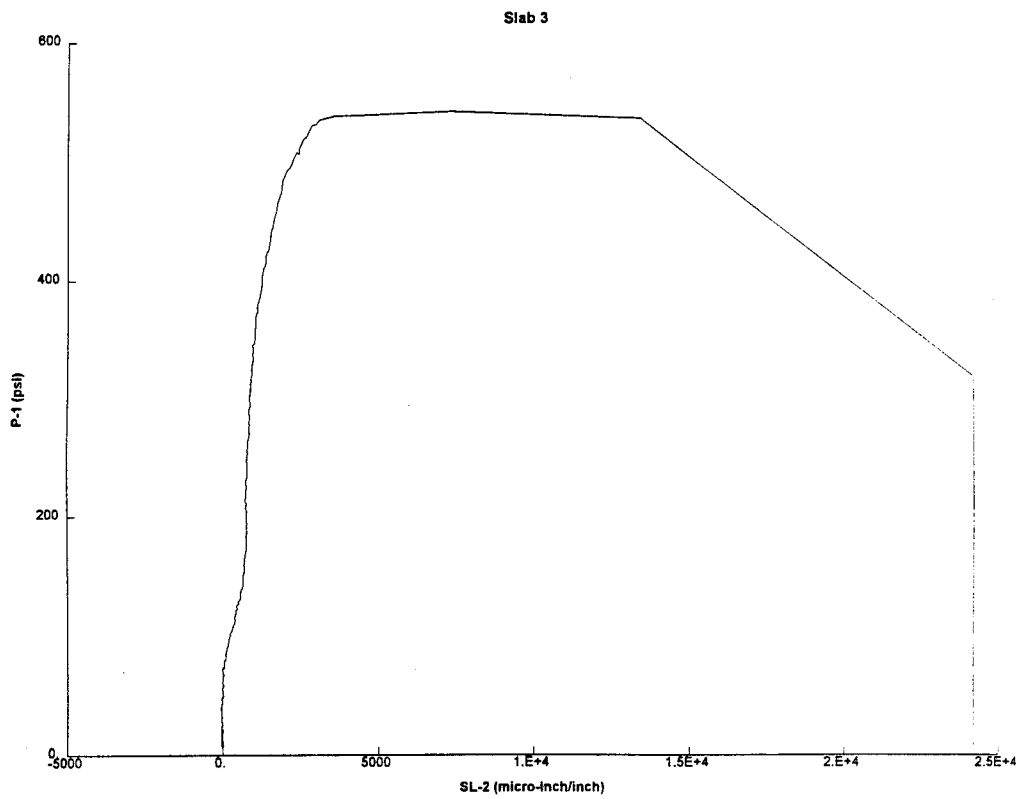
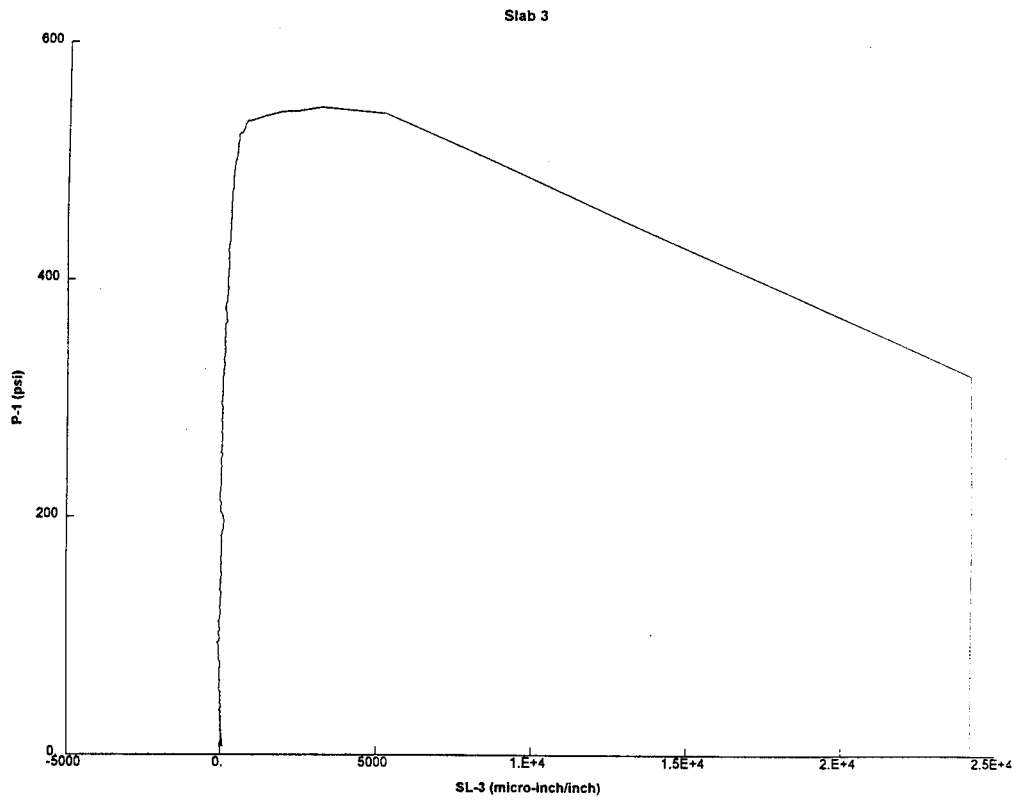


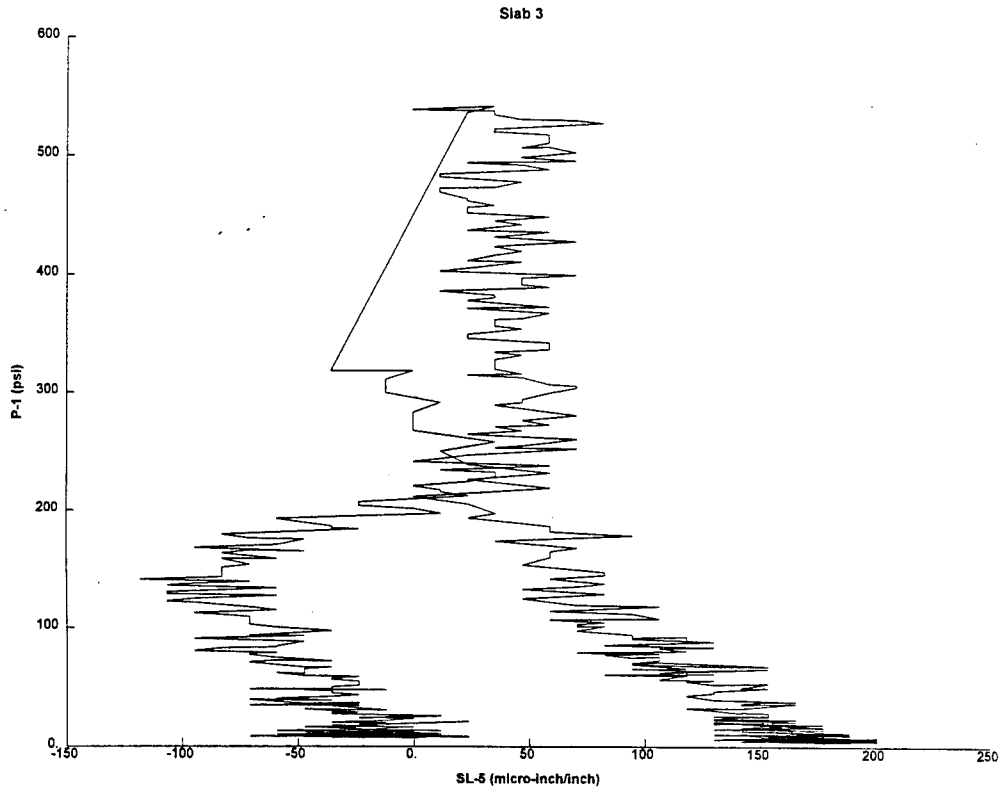
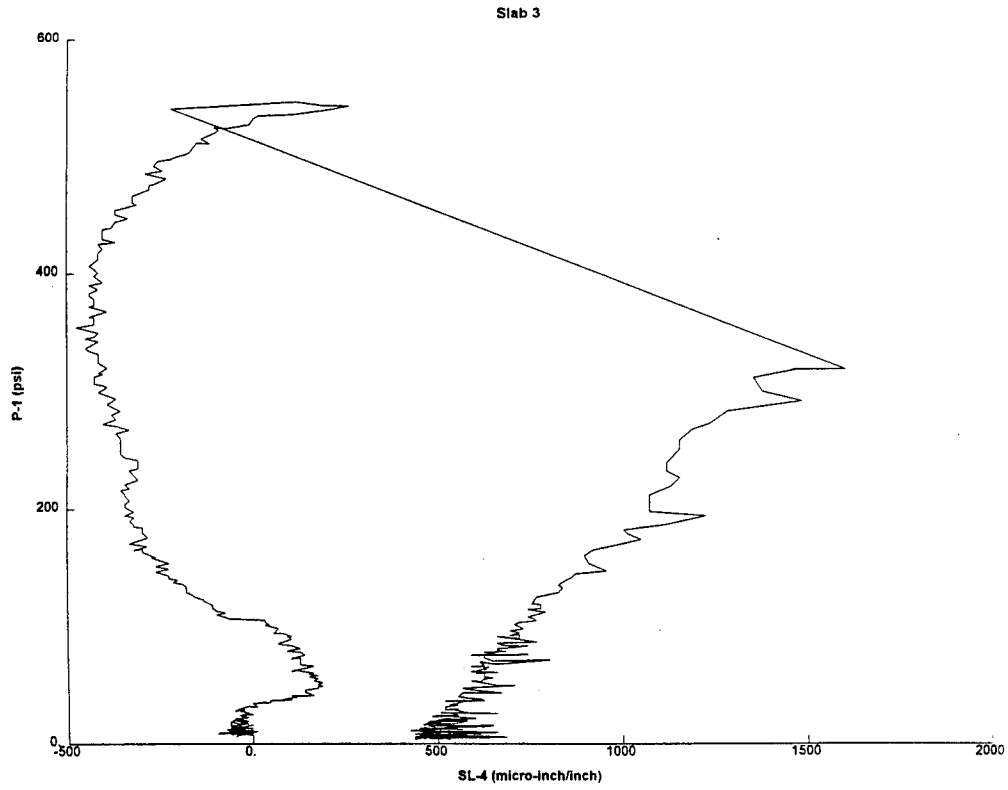


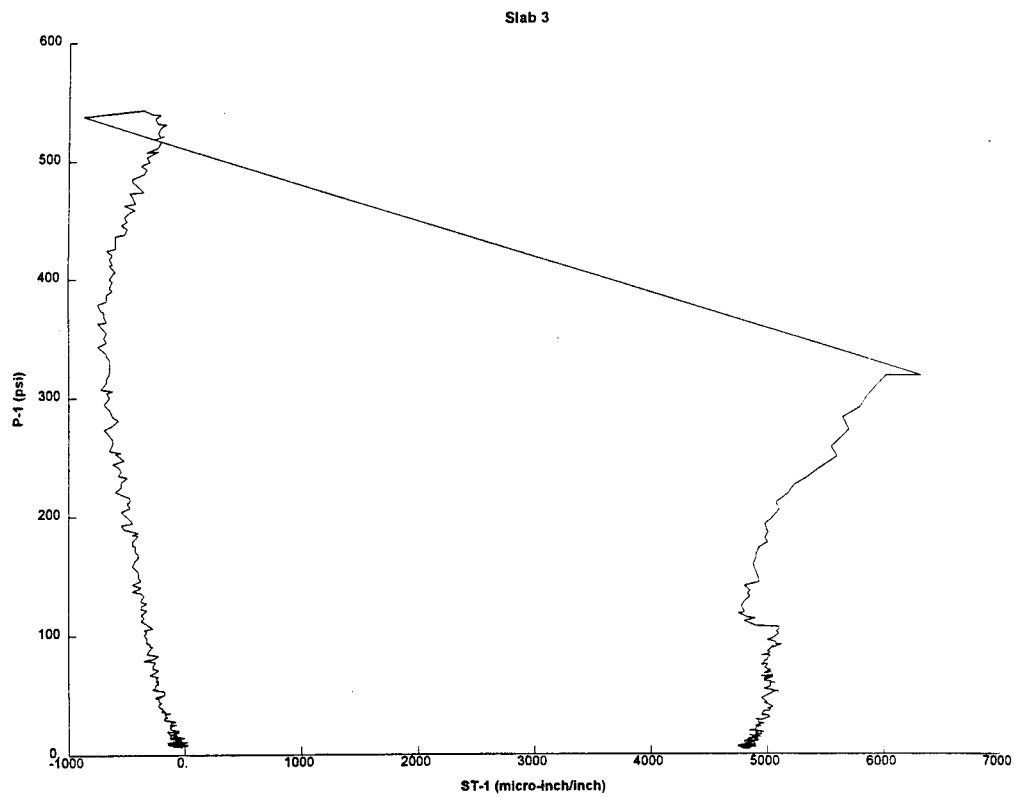
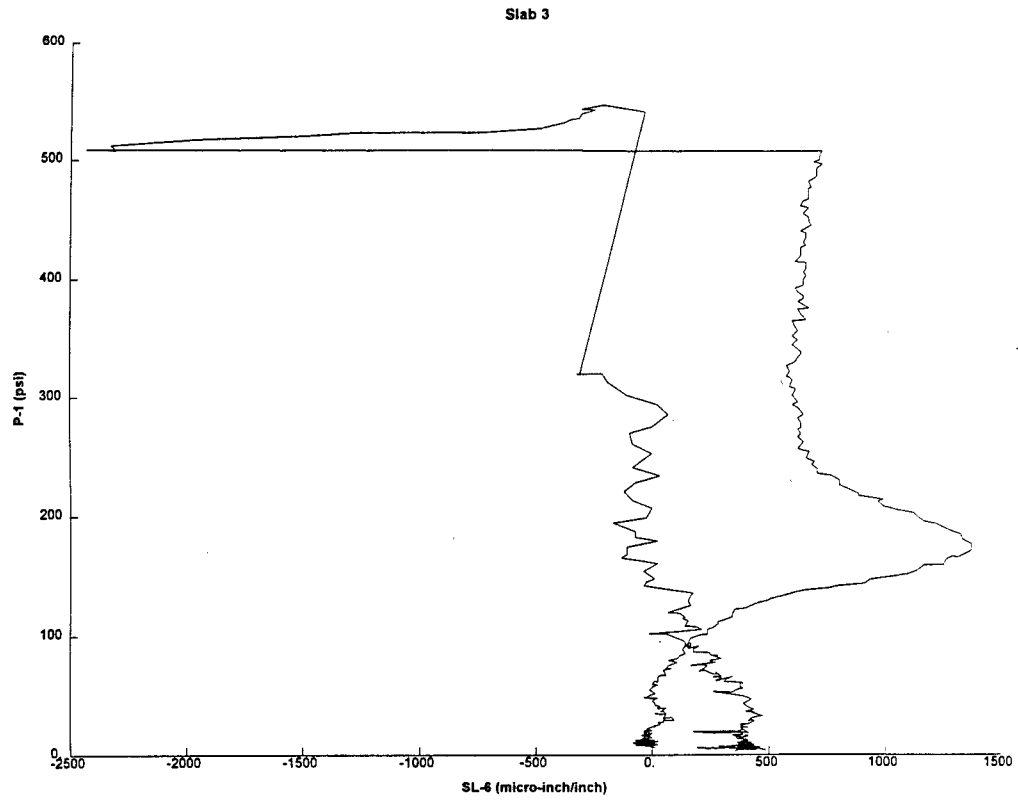


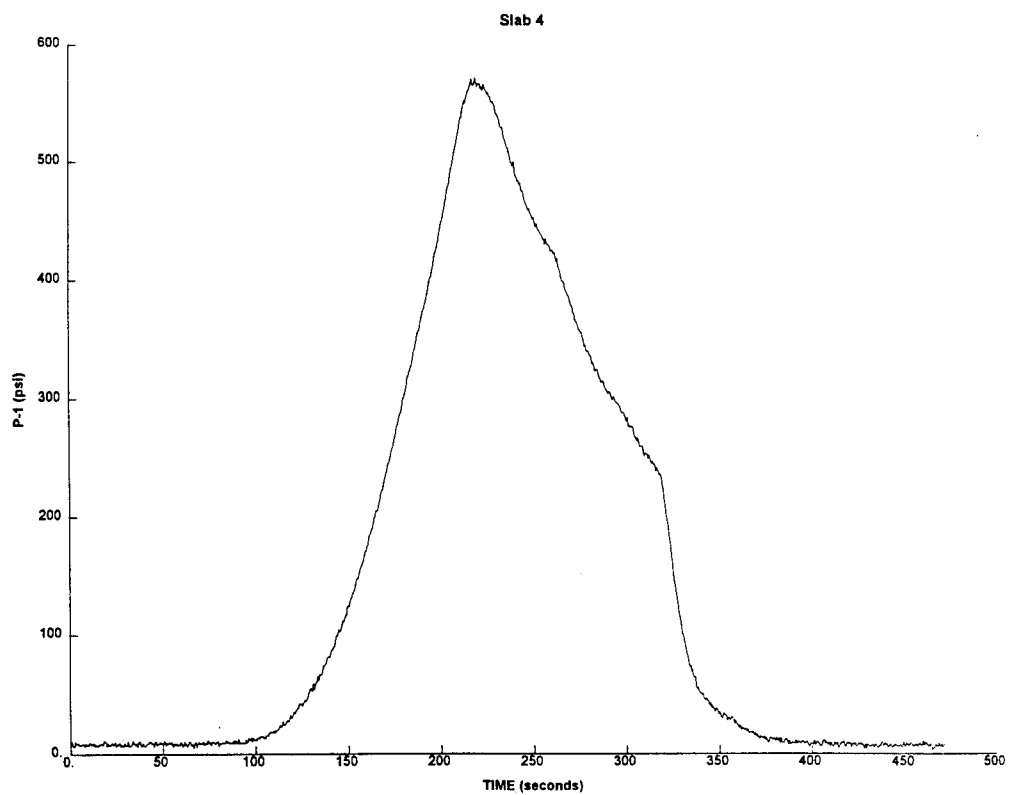
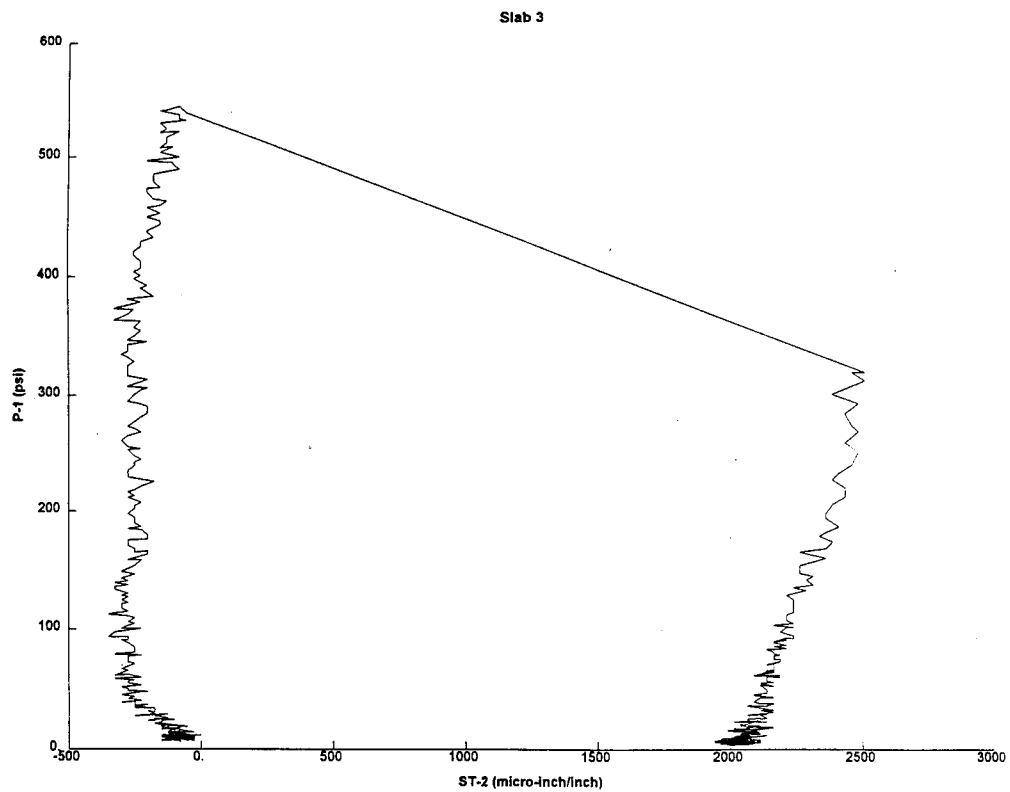


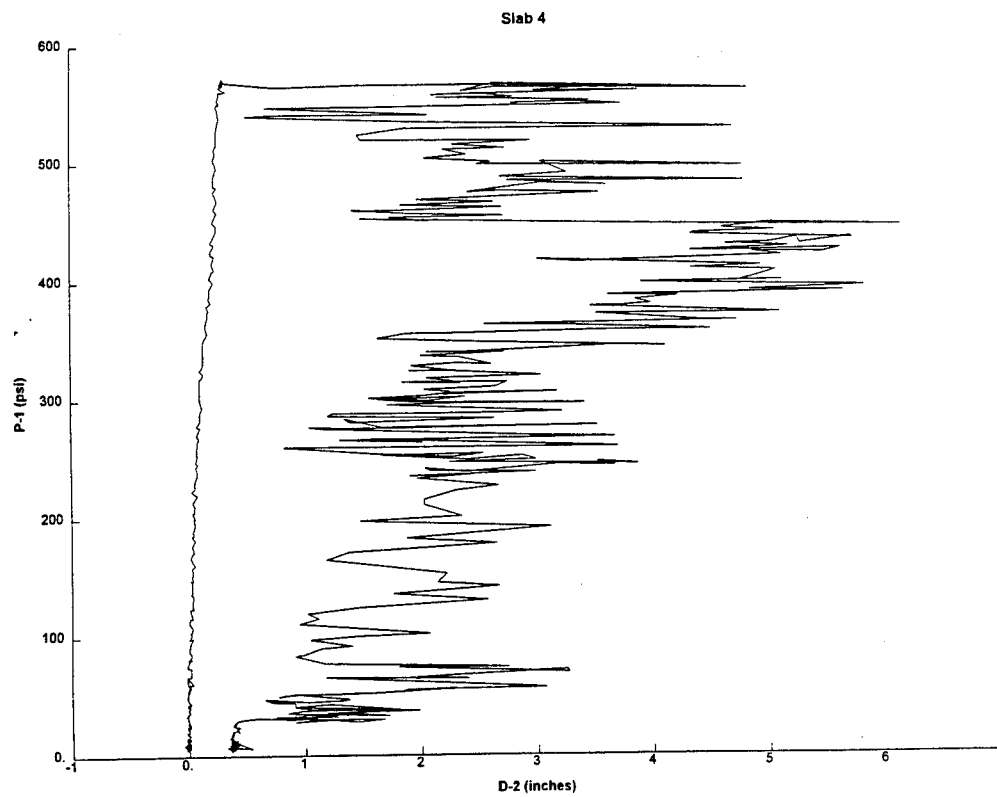
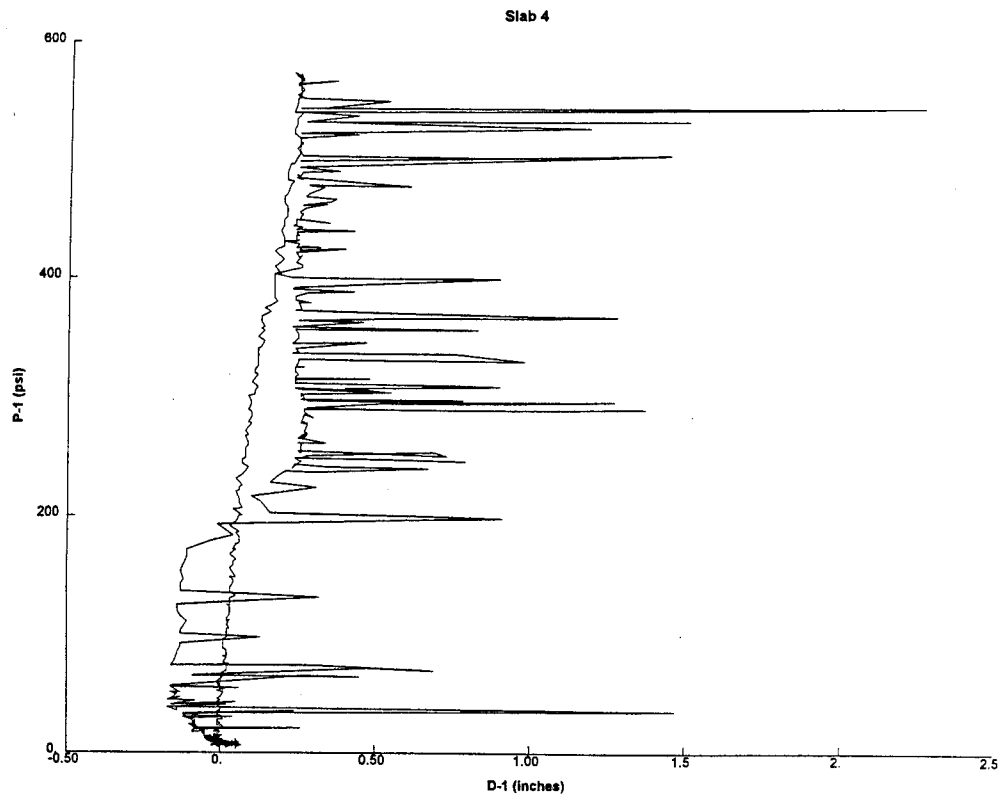


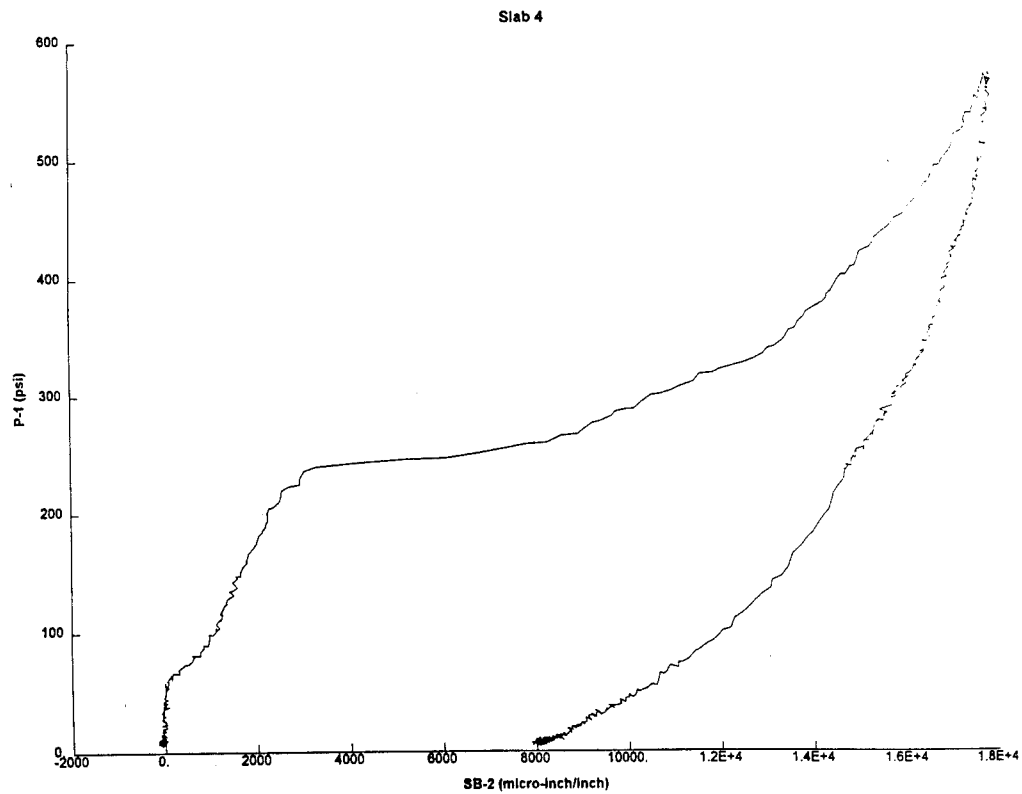
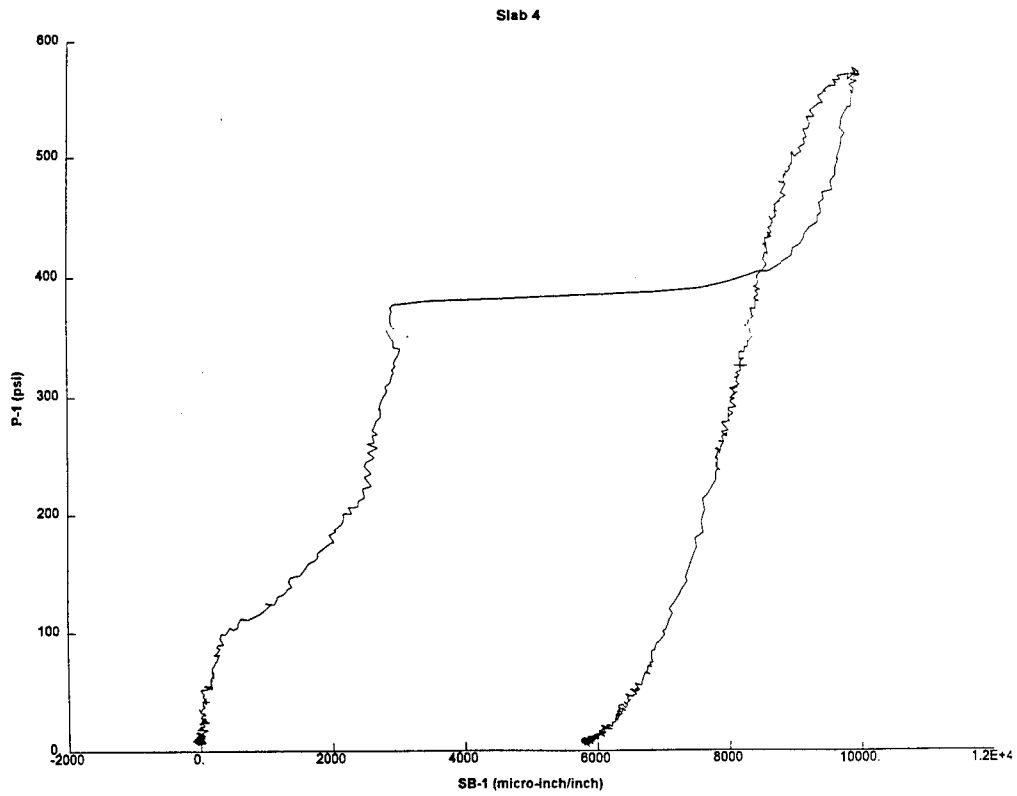


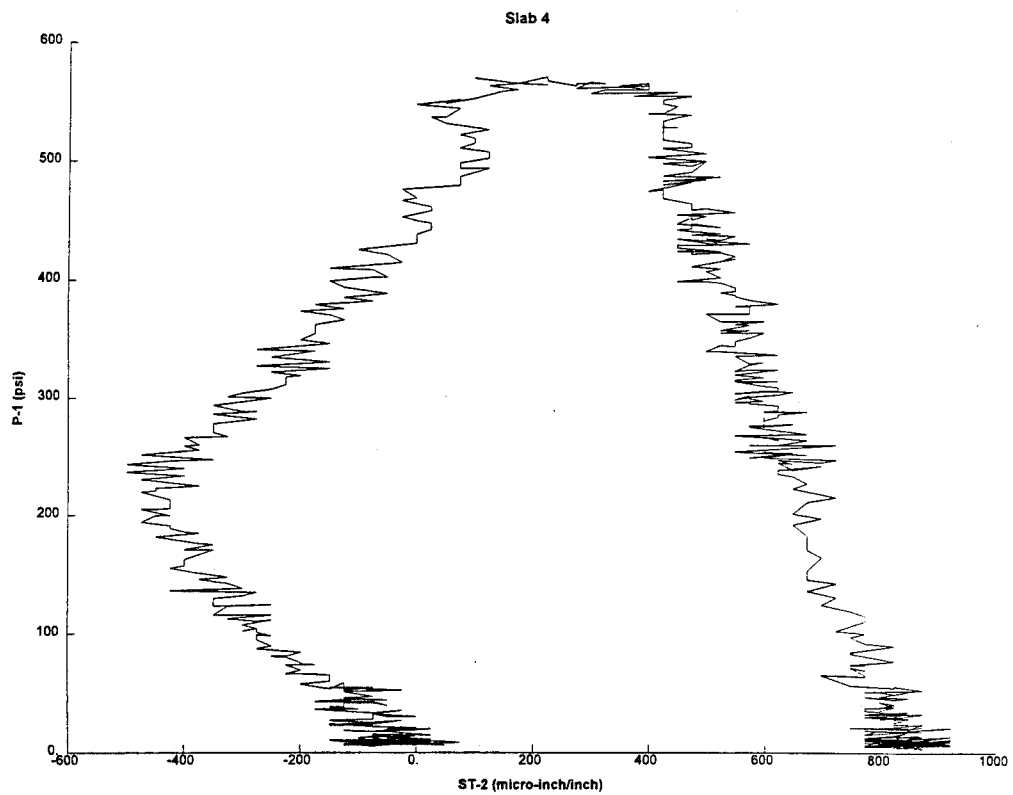
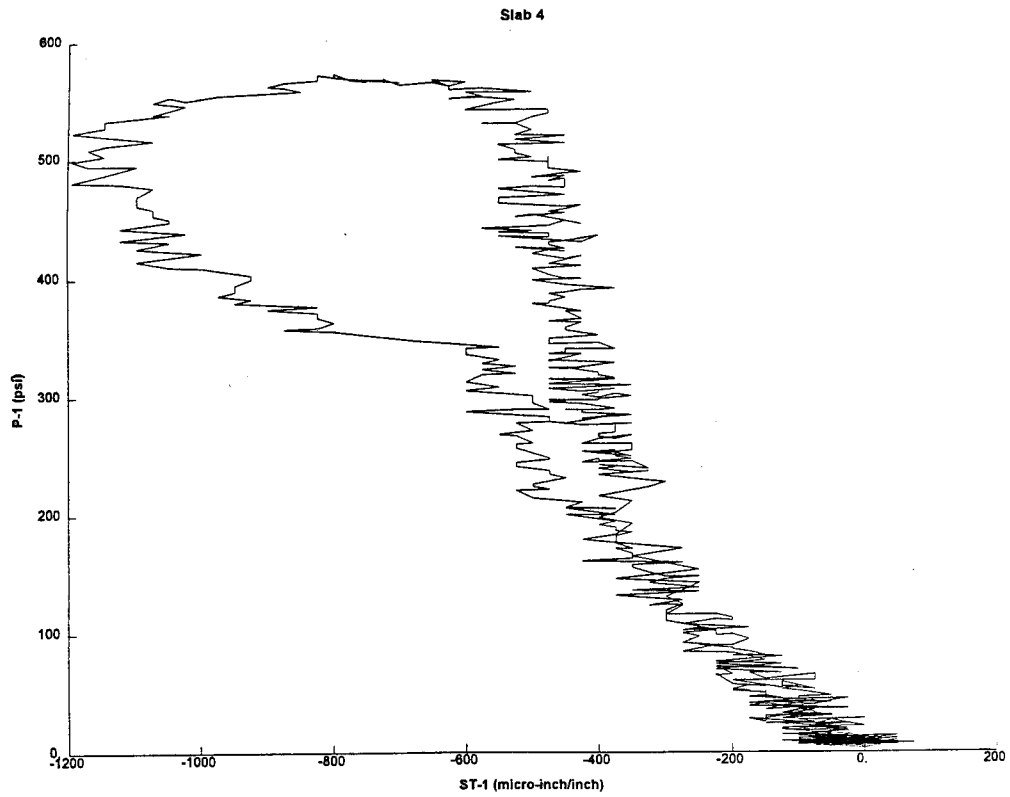


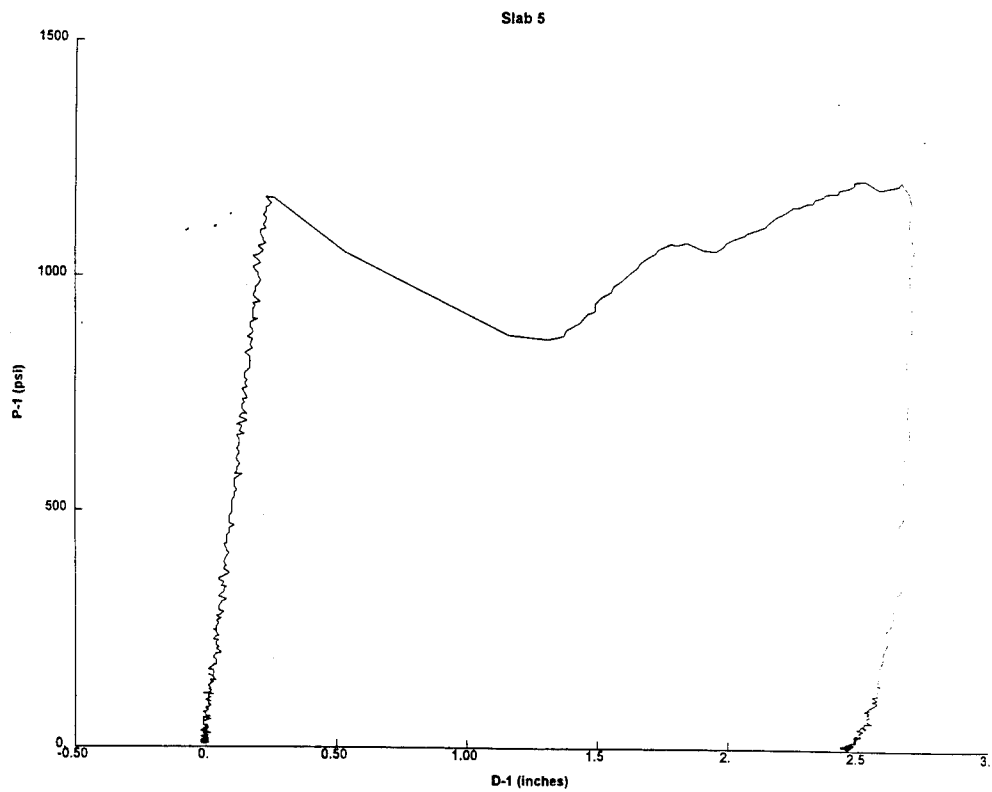
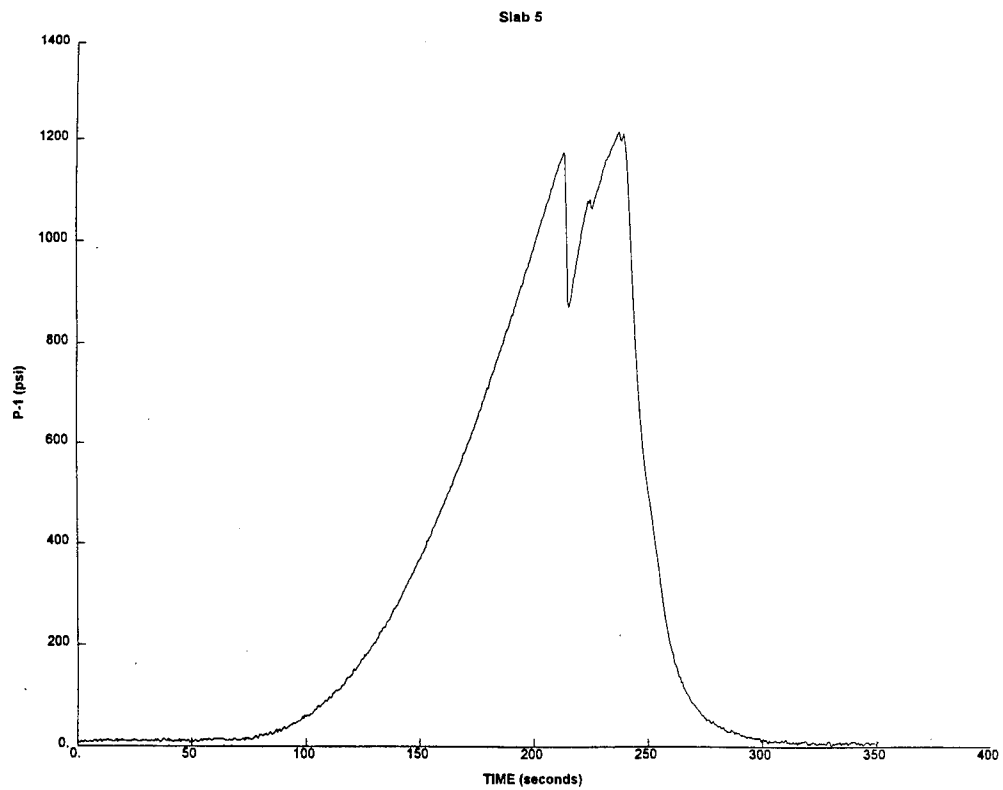




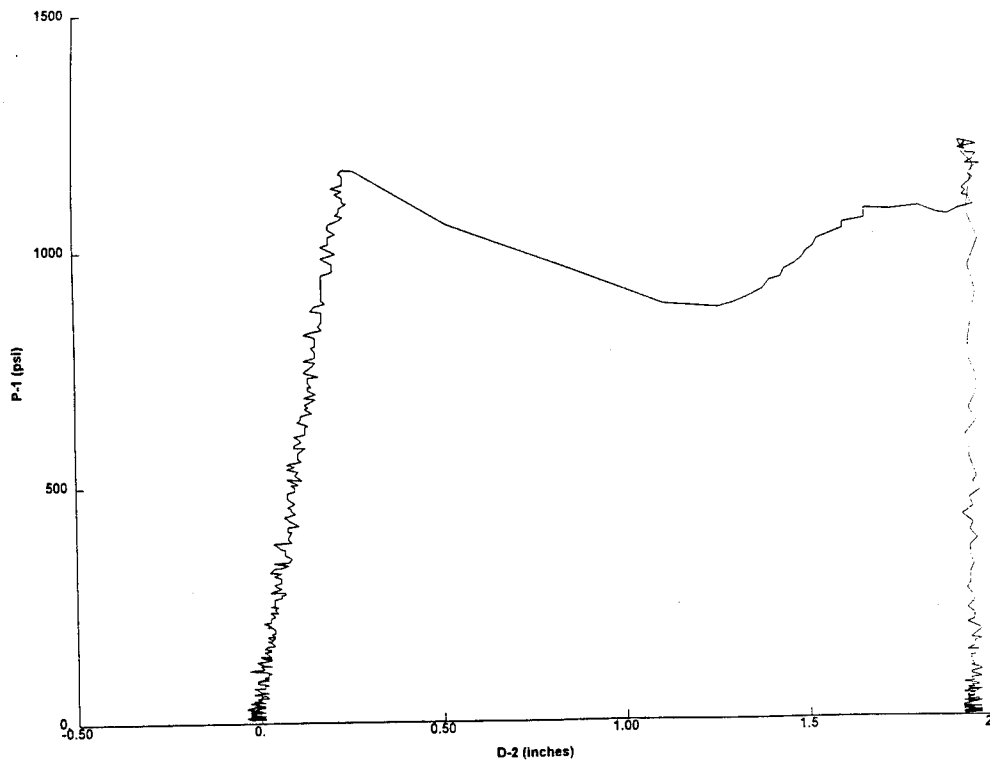




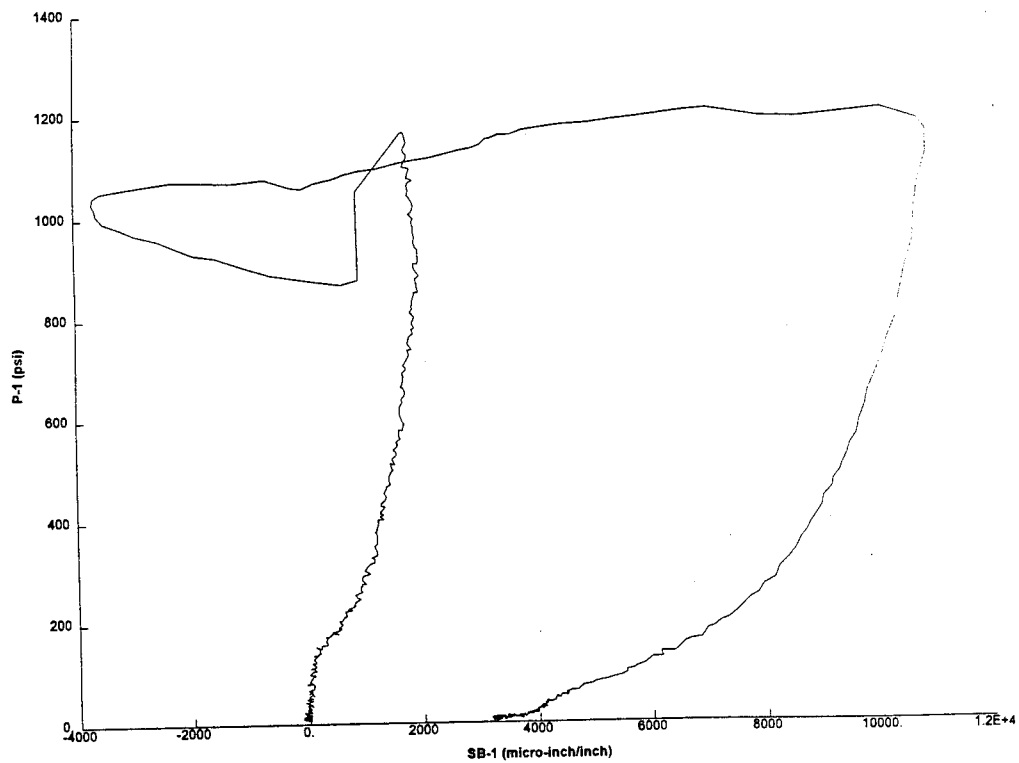


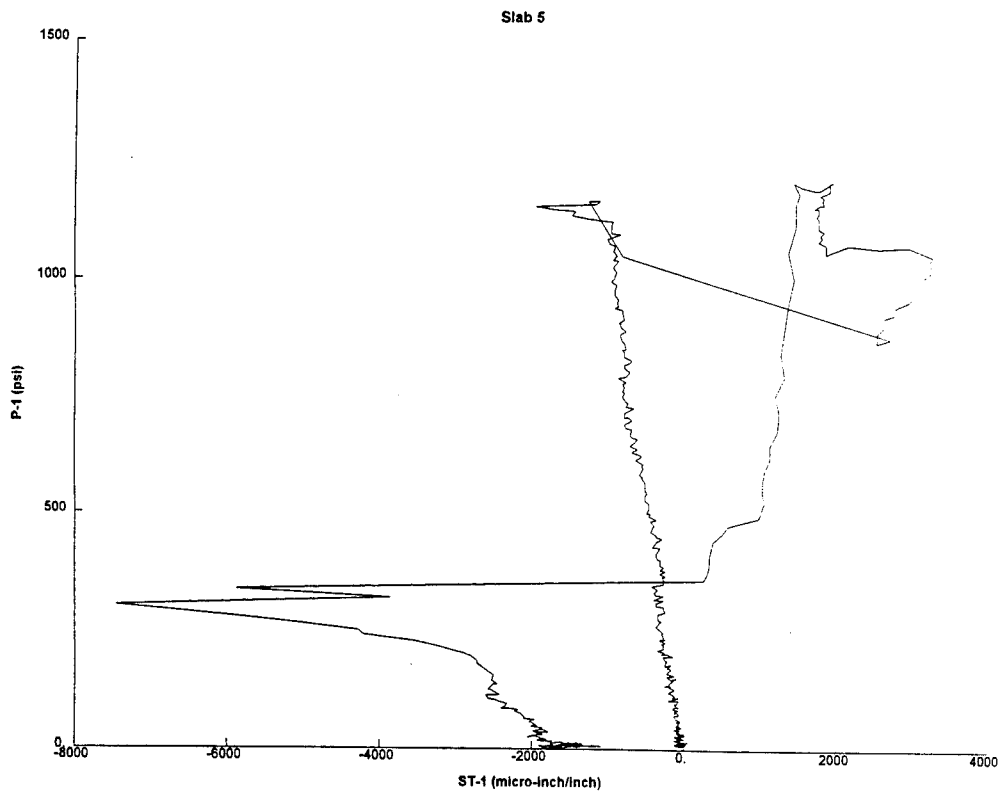
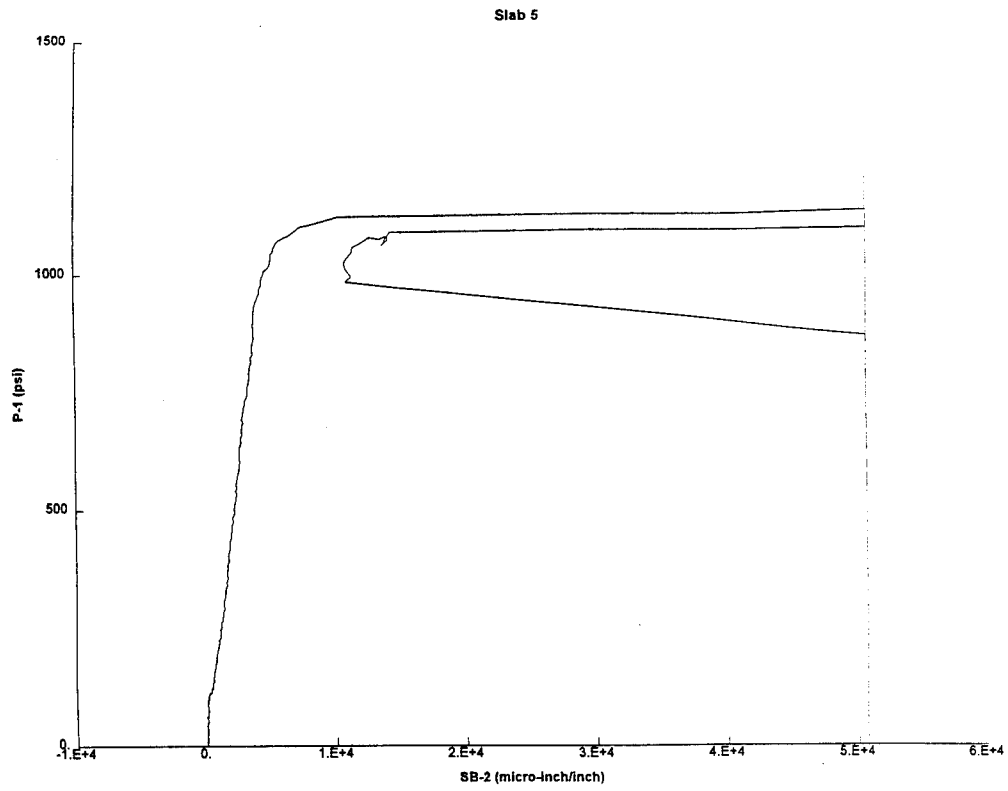


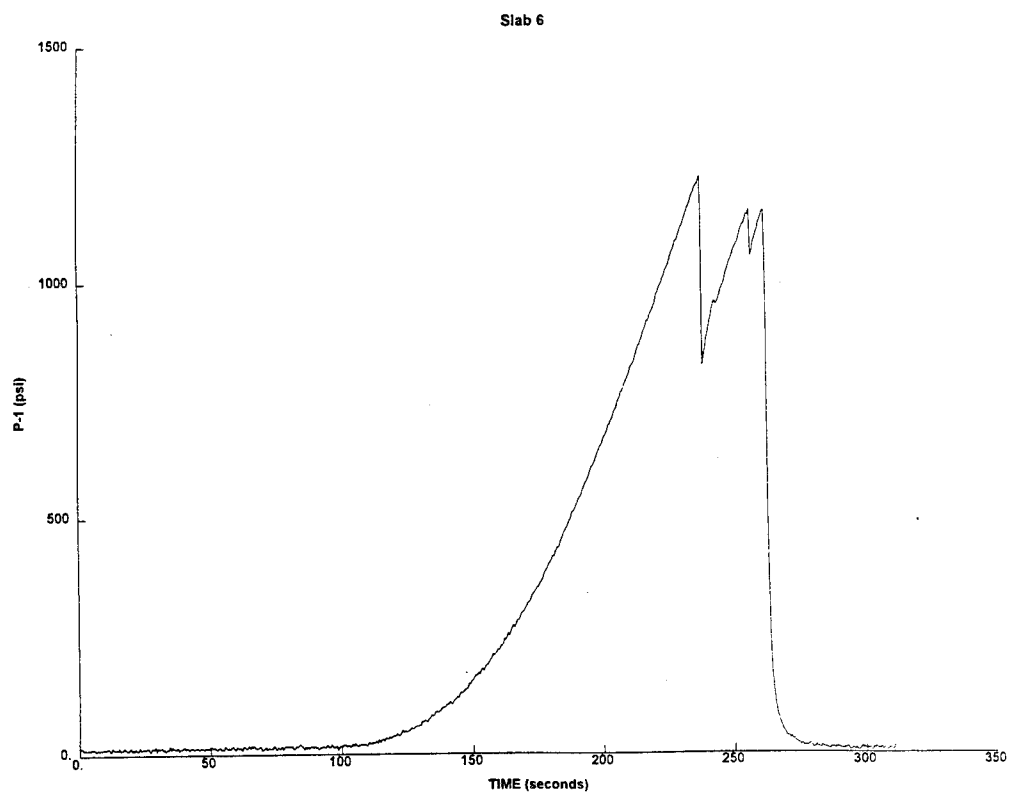
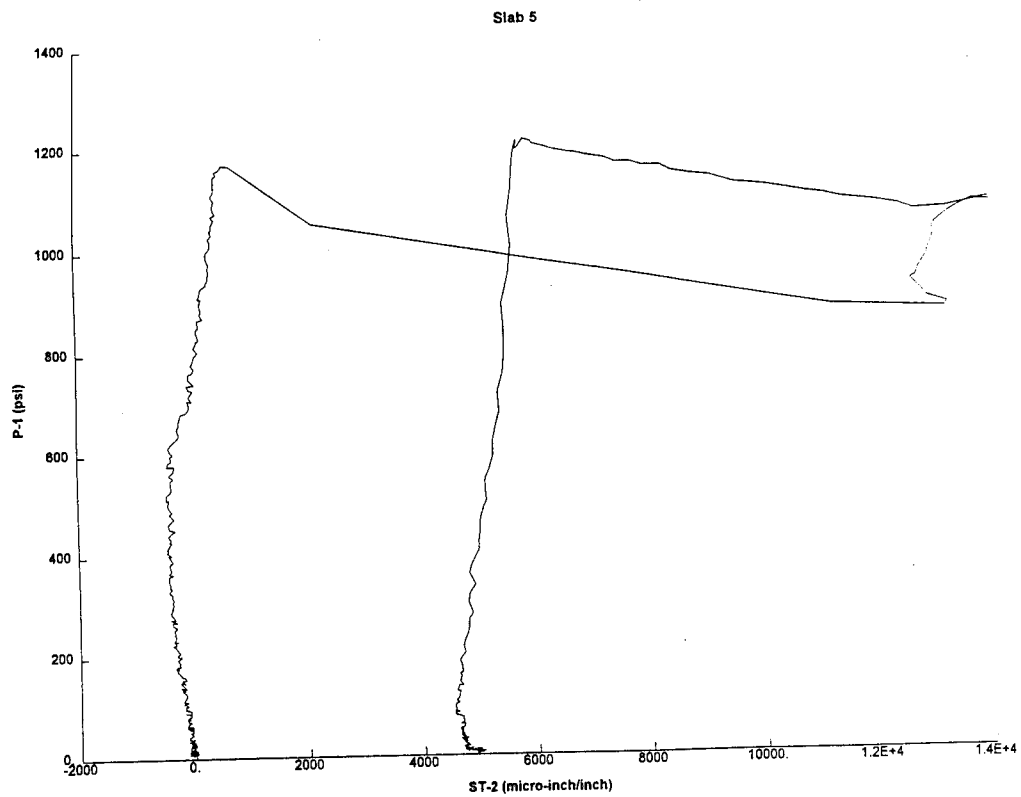
Slab 5

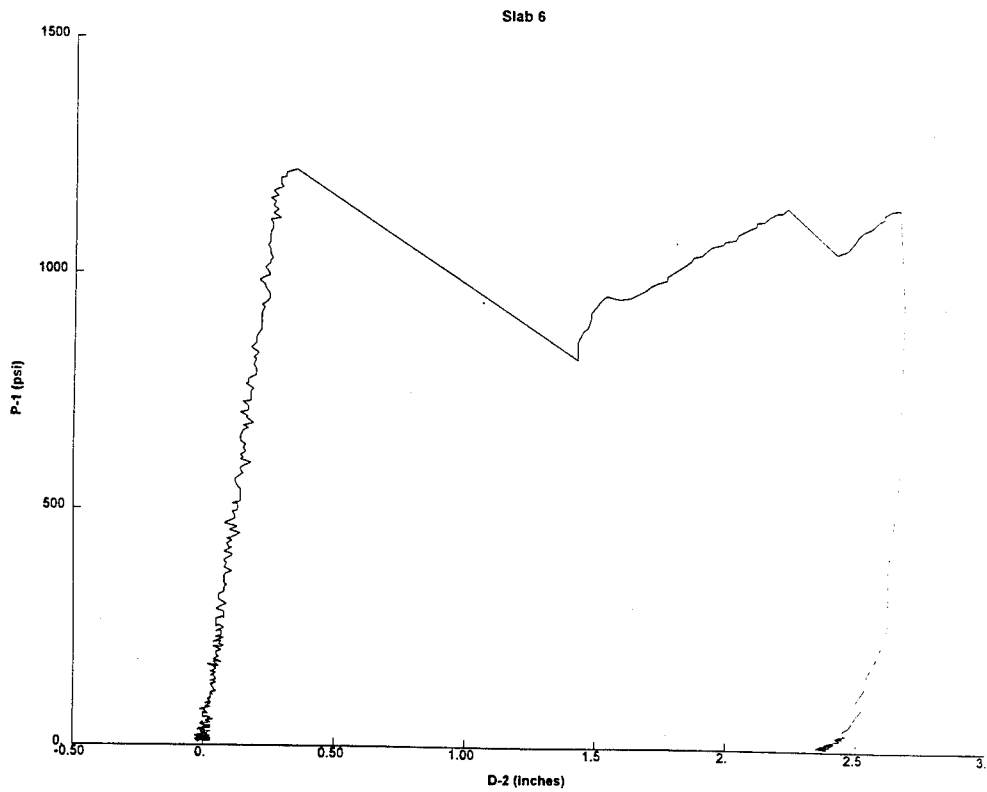
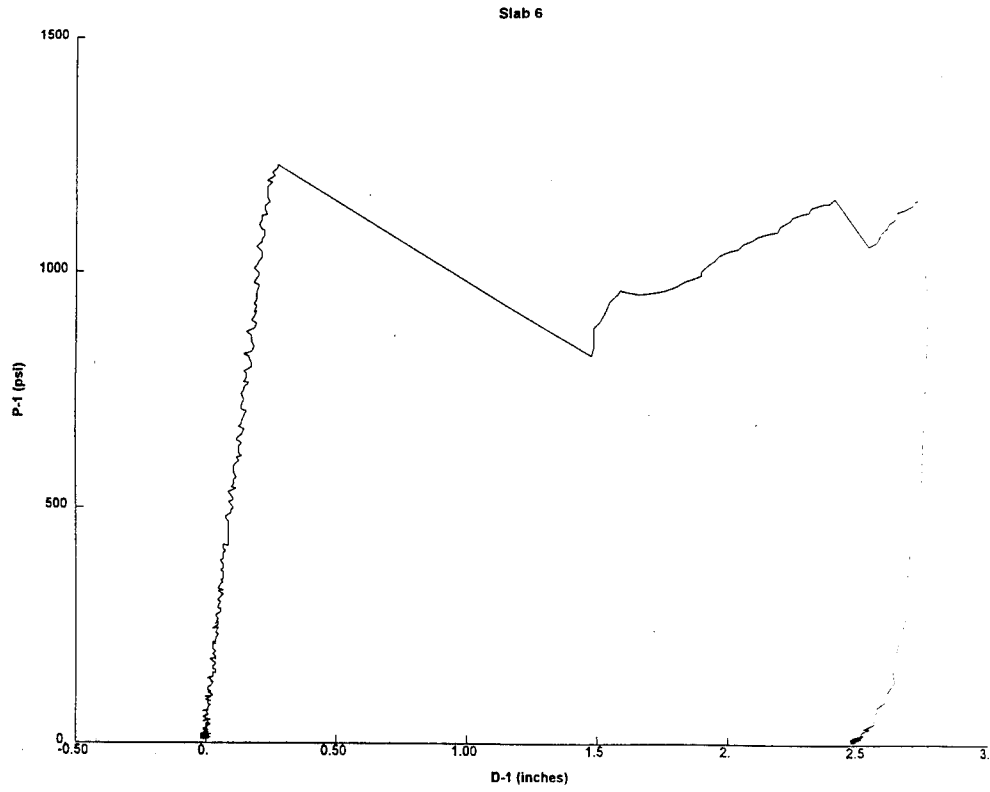


Slab 5

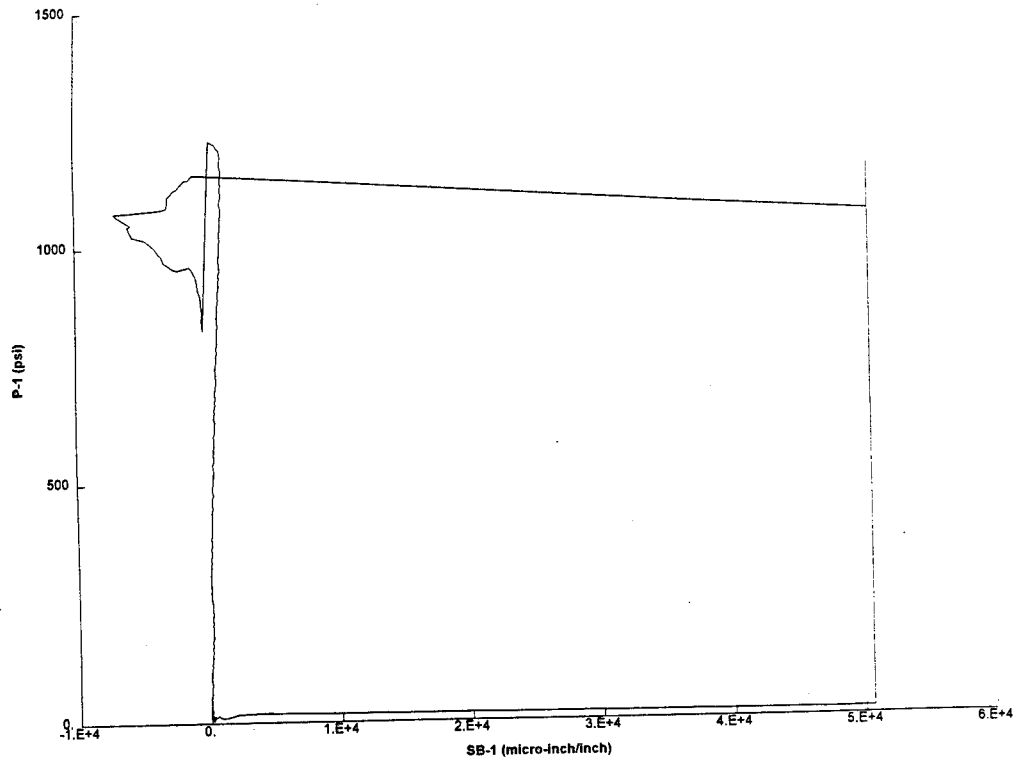






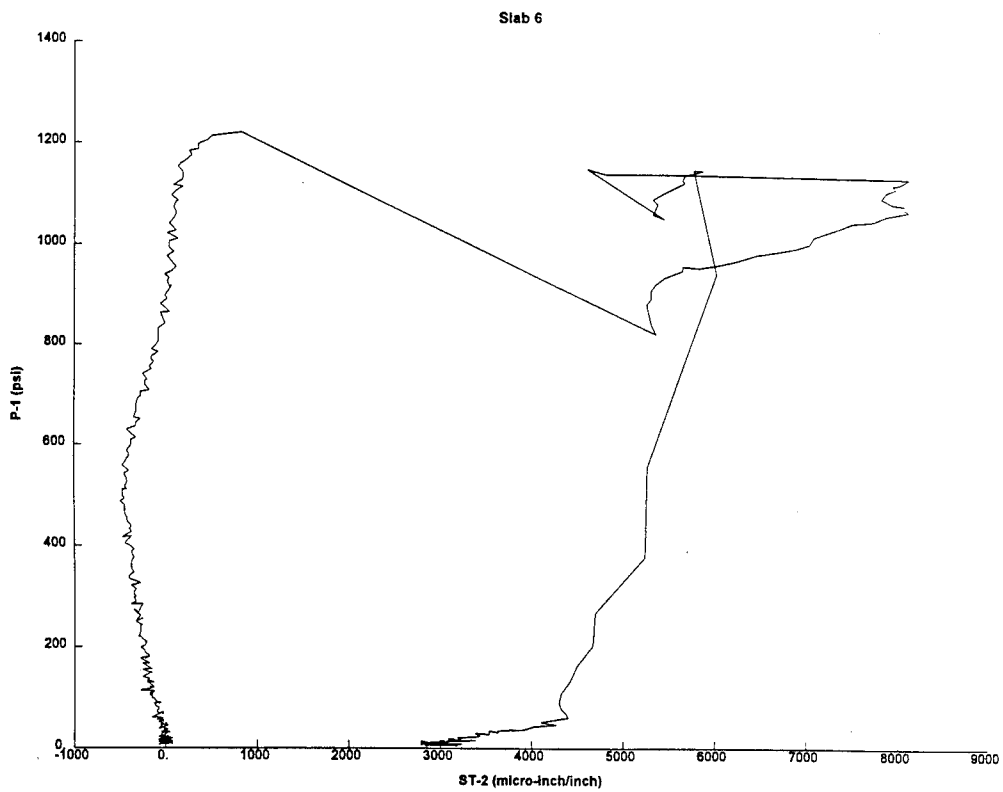
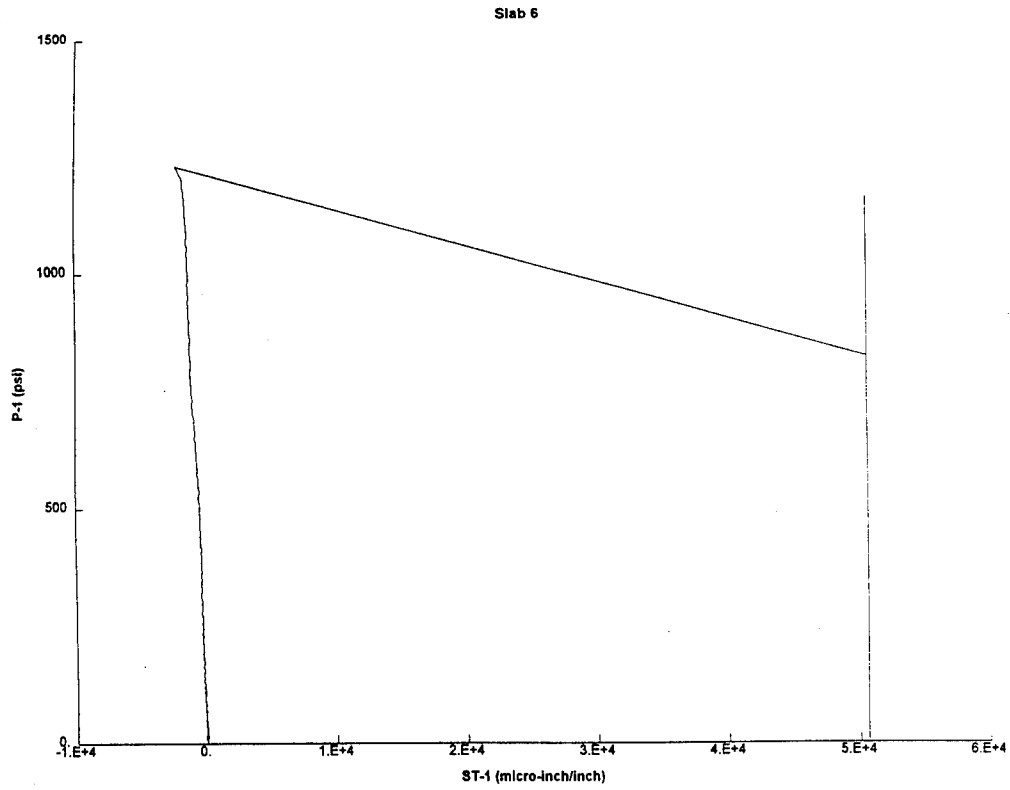


Slab 6

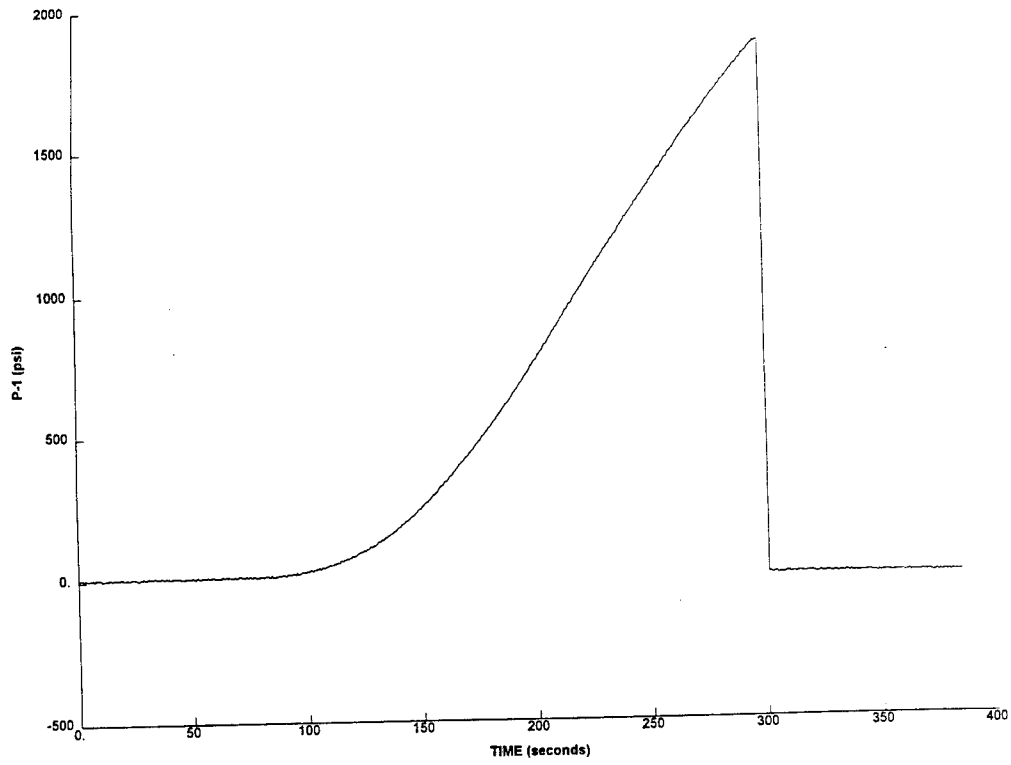


Slab 6

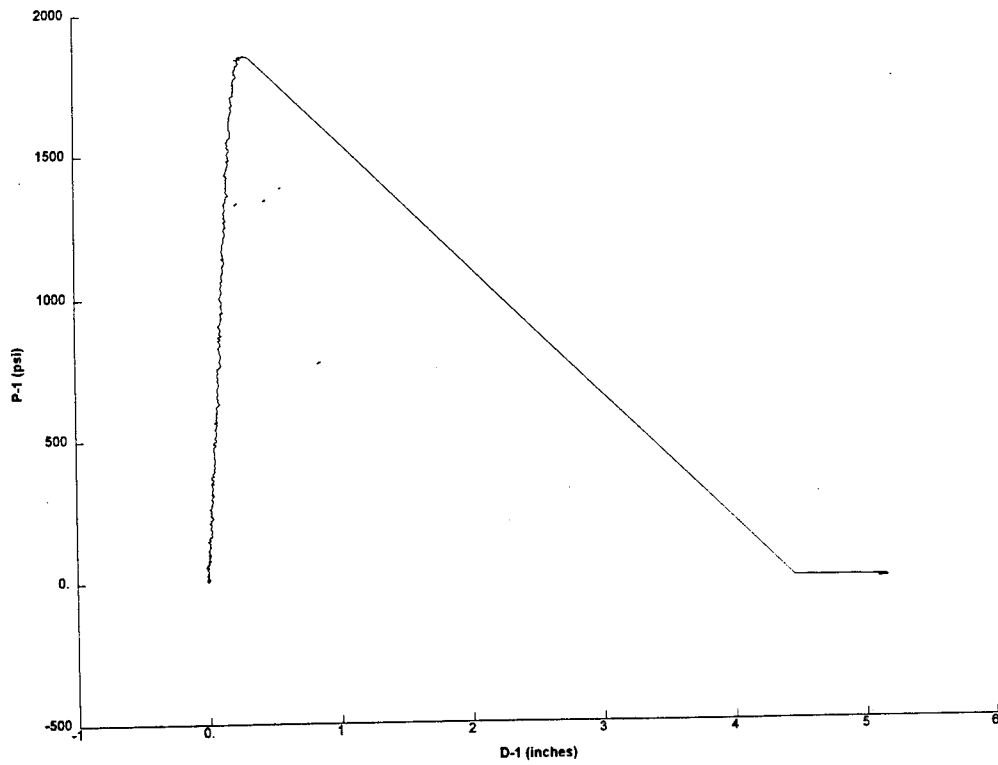


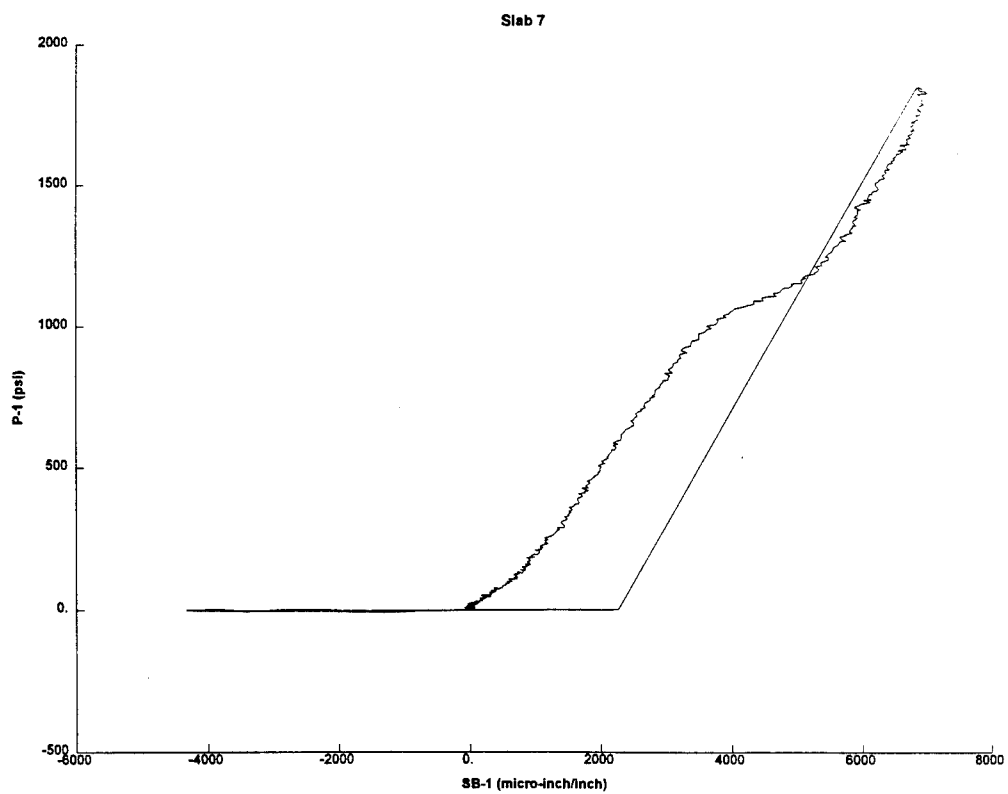
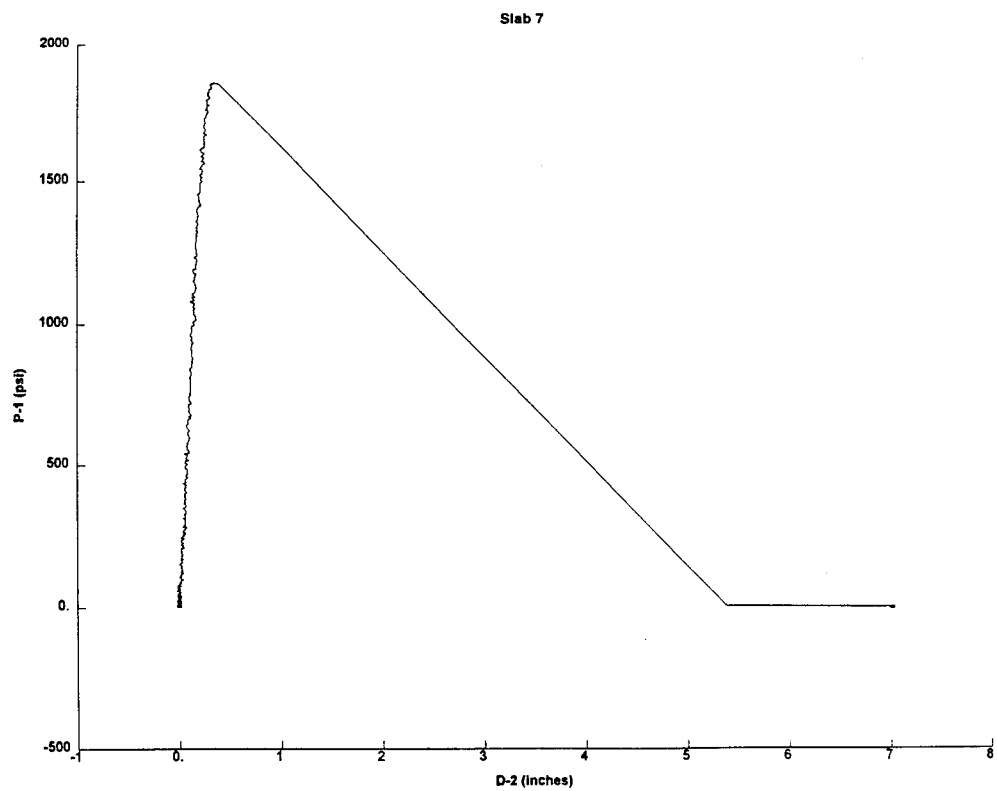


Slab 7

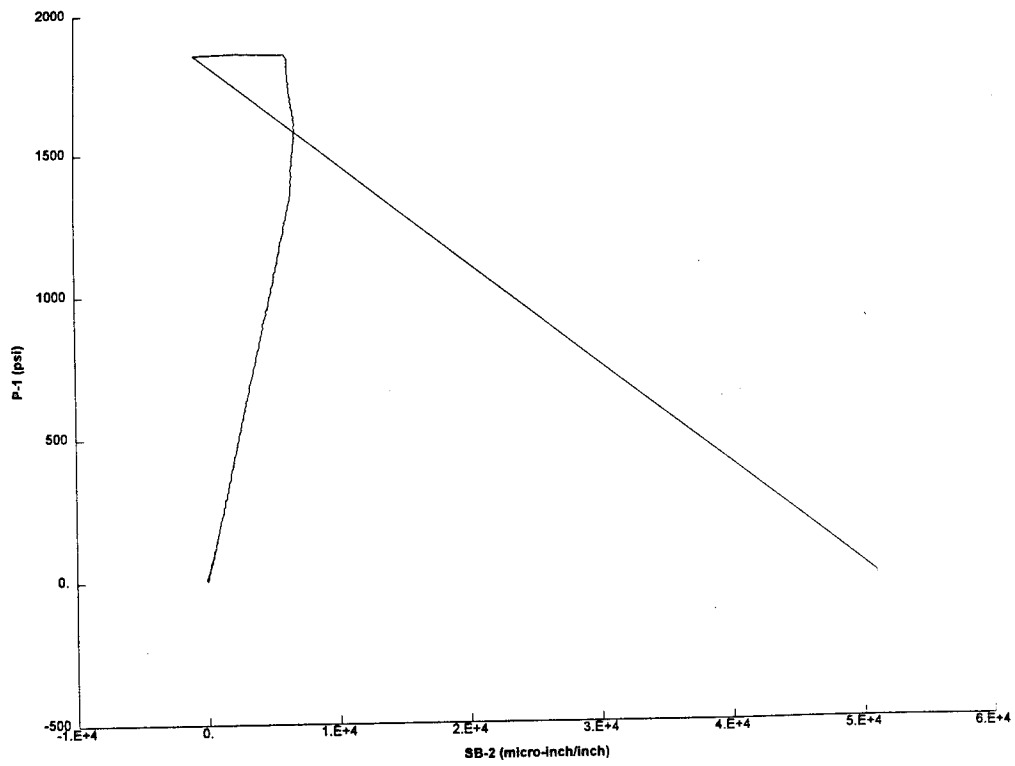


Slab 7

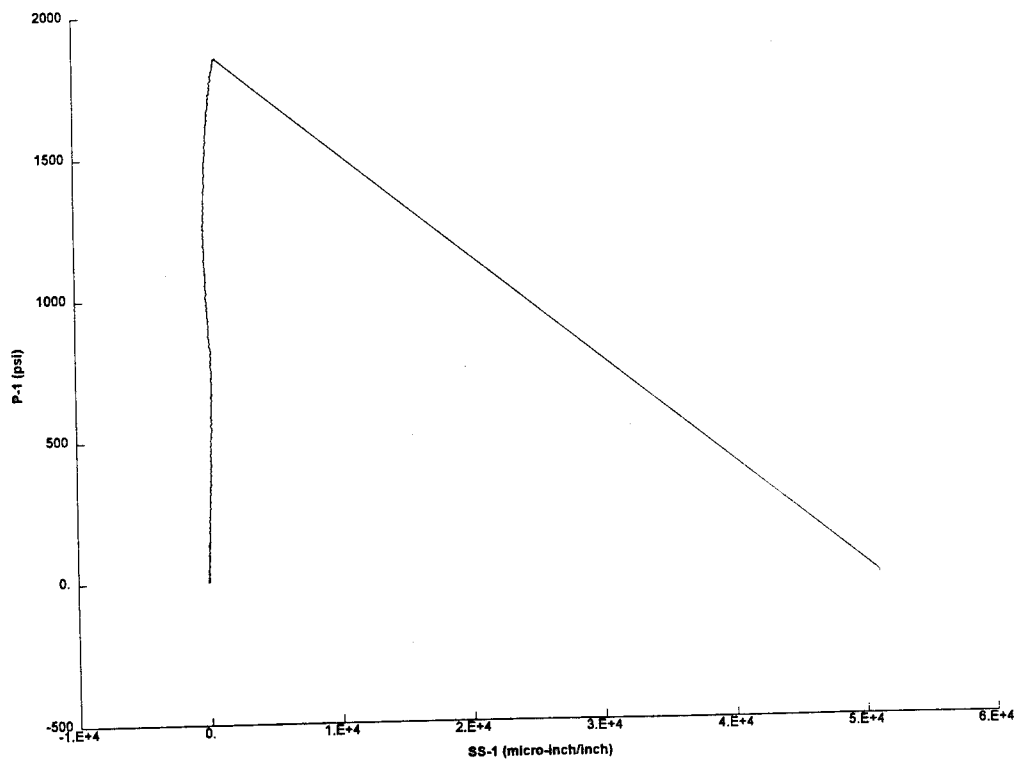


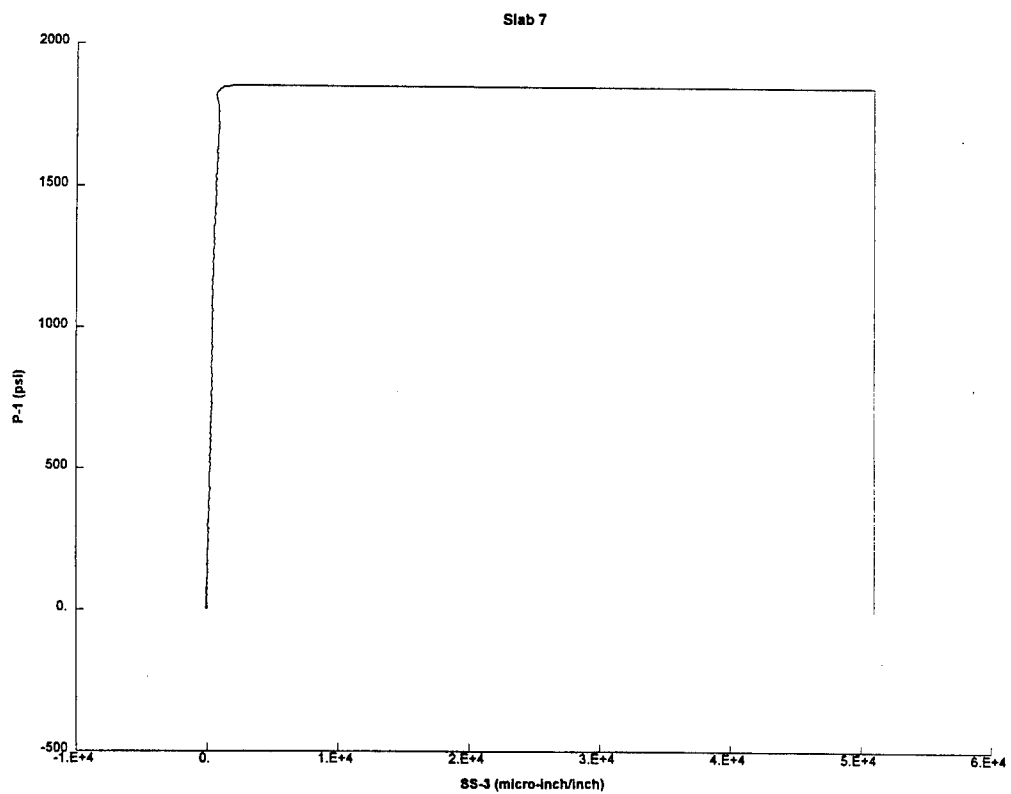
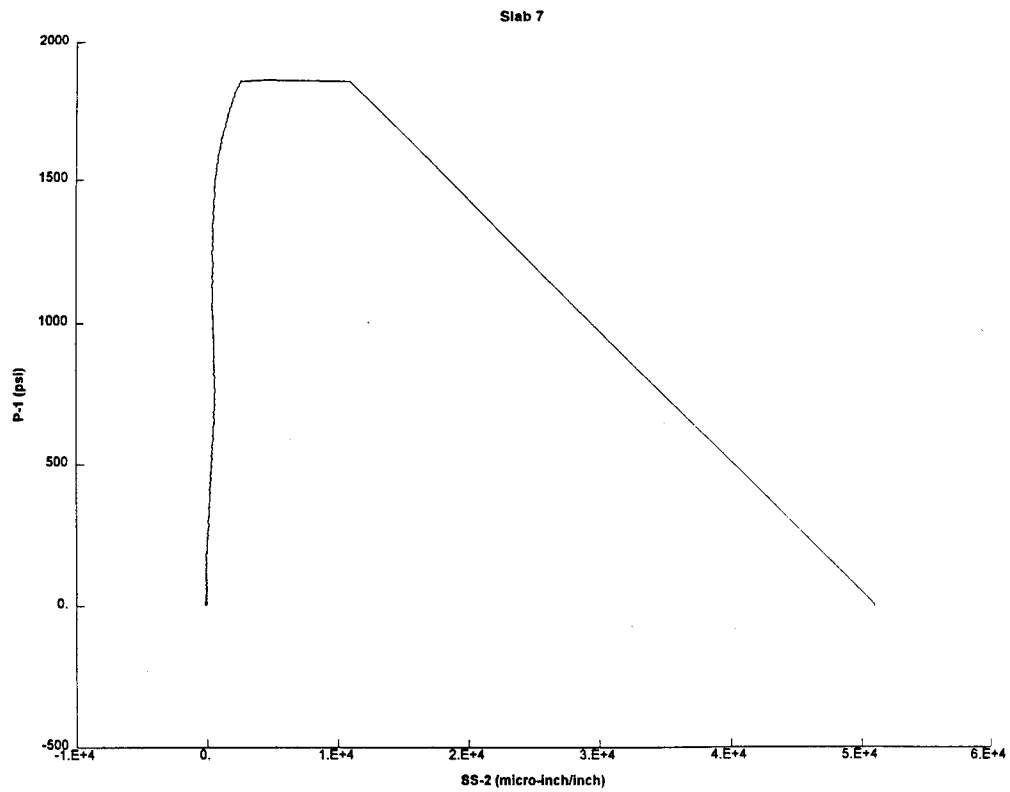


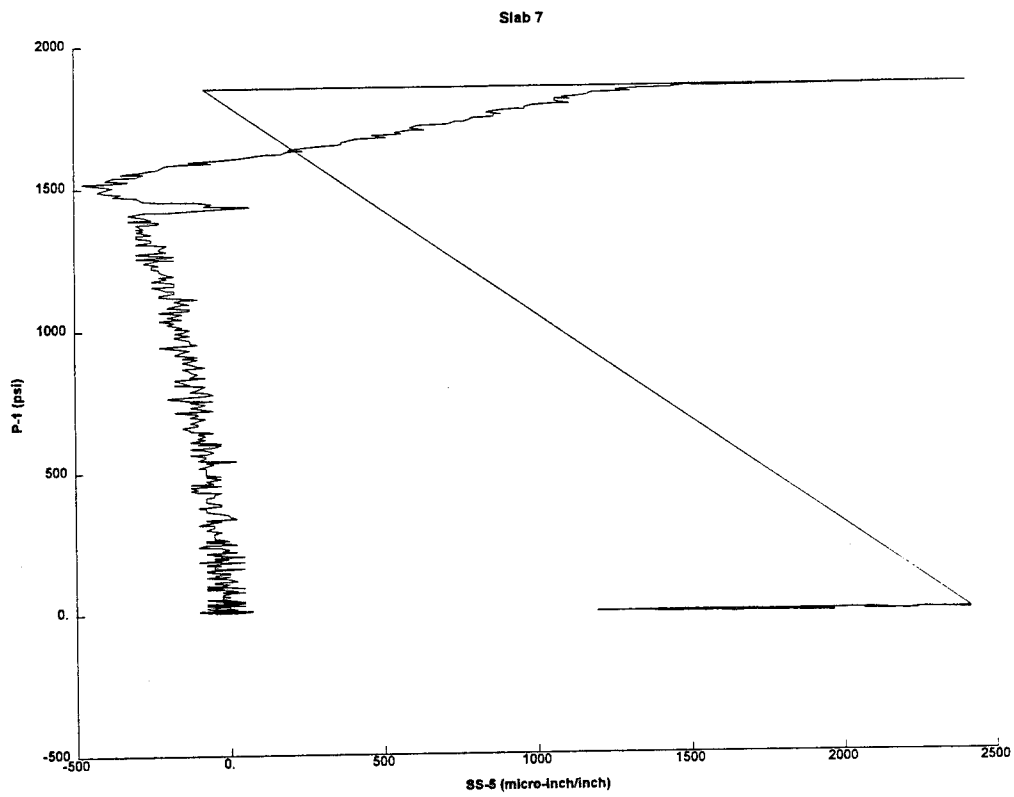
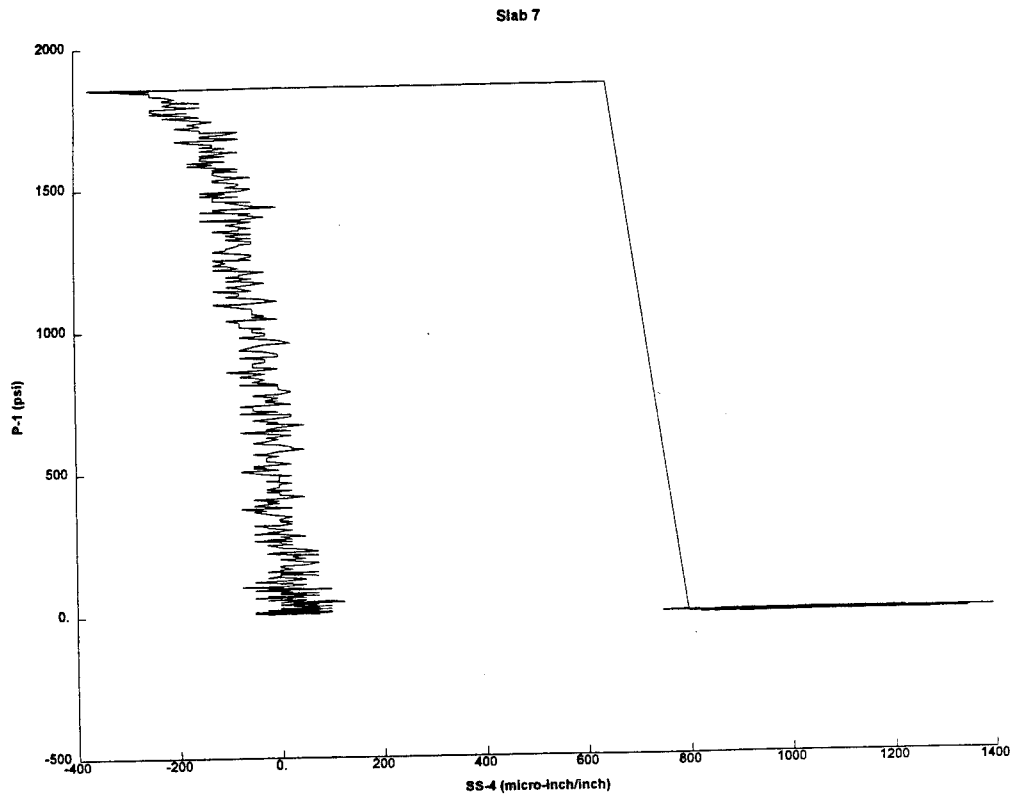
Slab 7

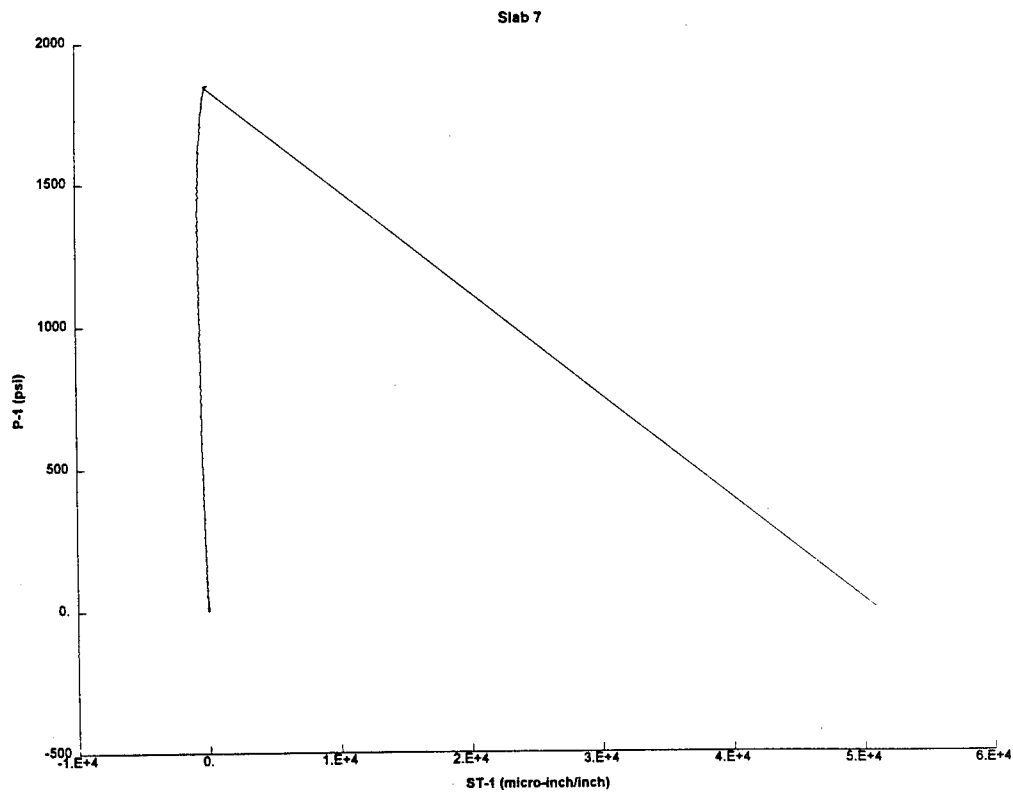
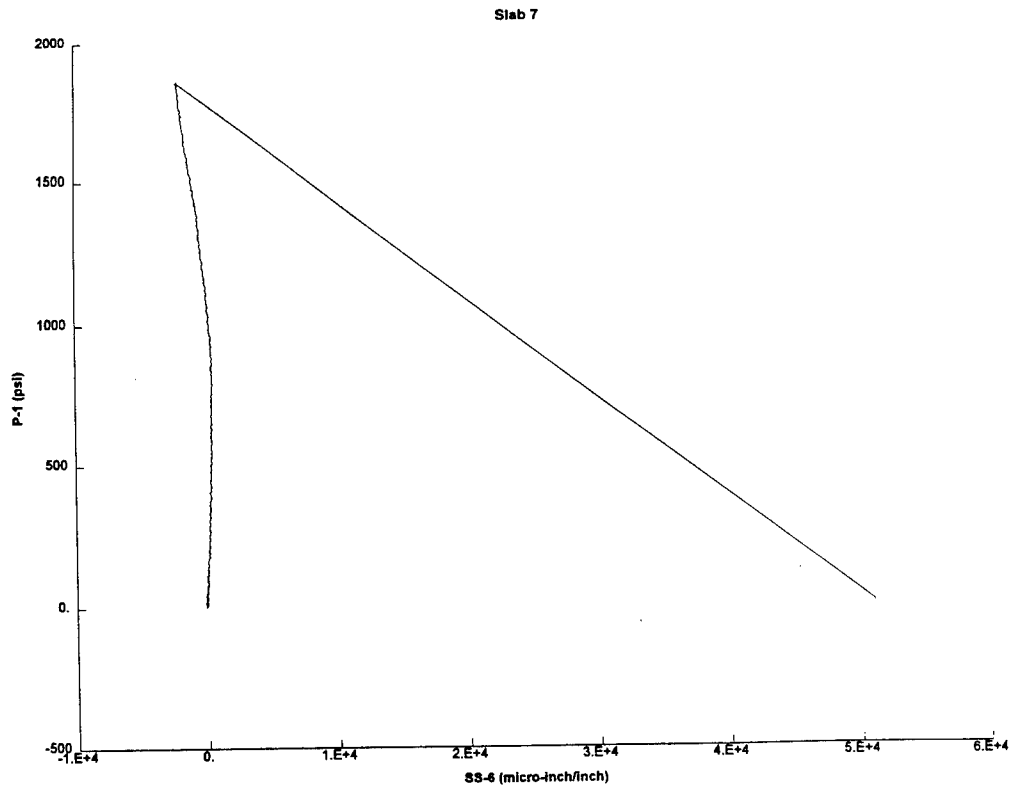


Slab 7

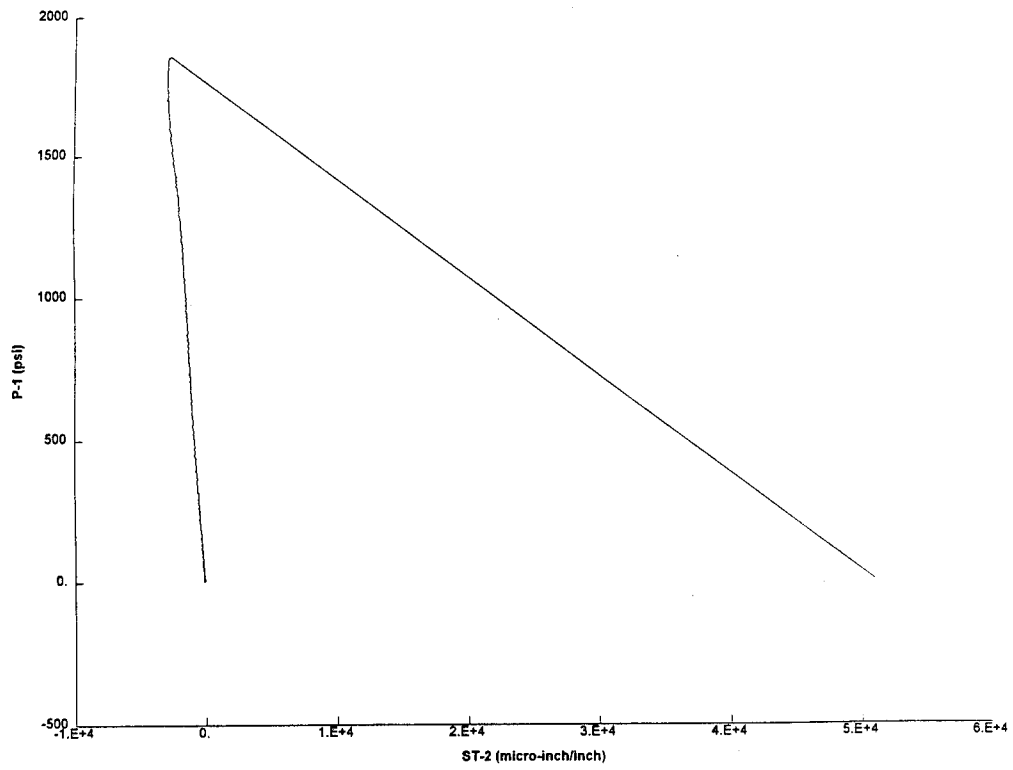




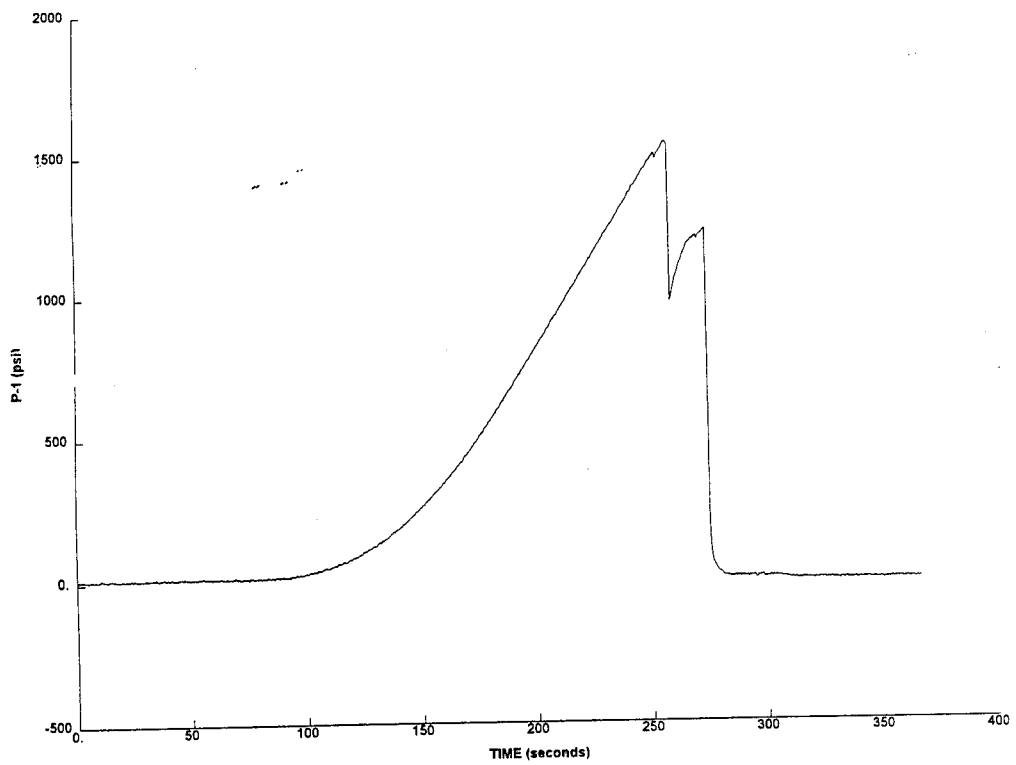




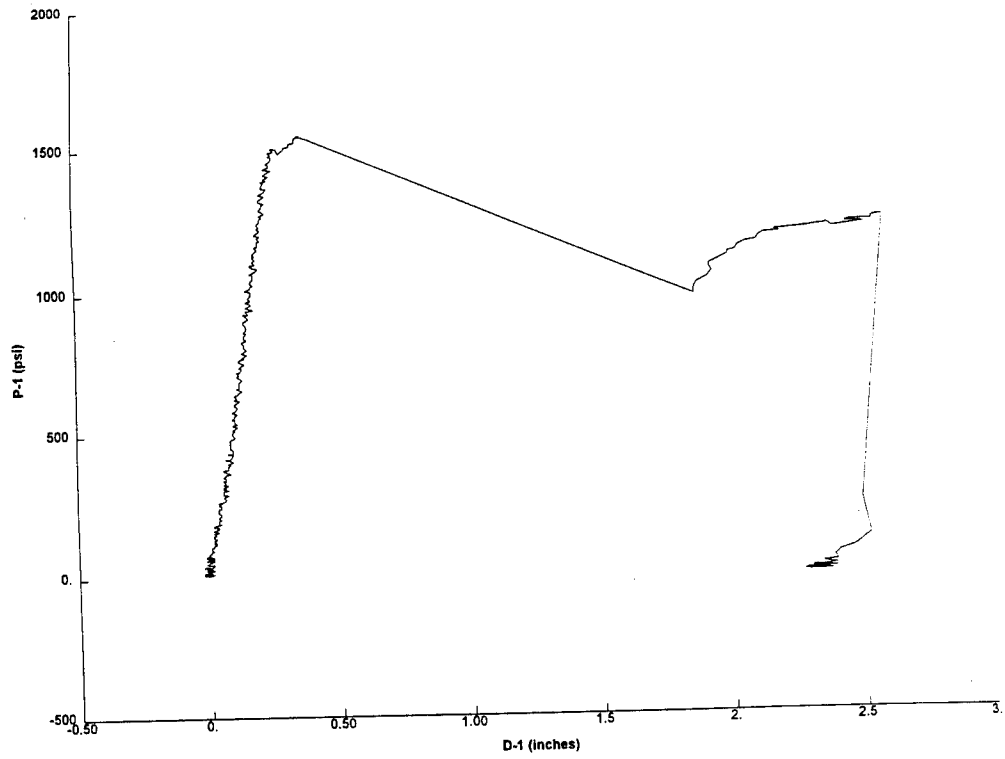
Slab 7



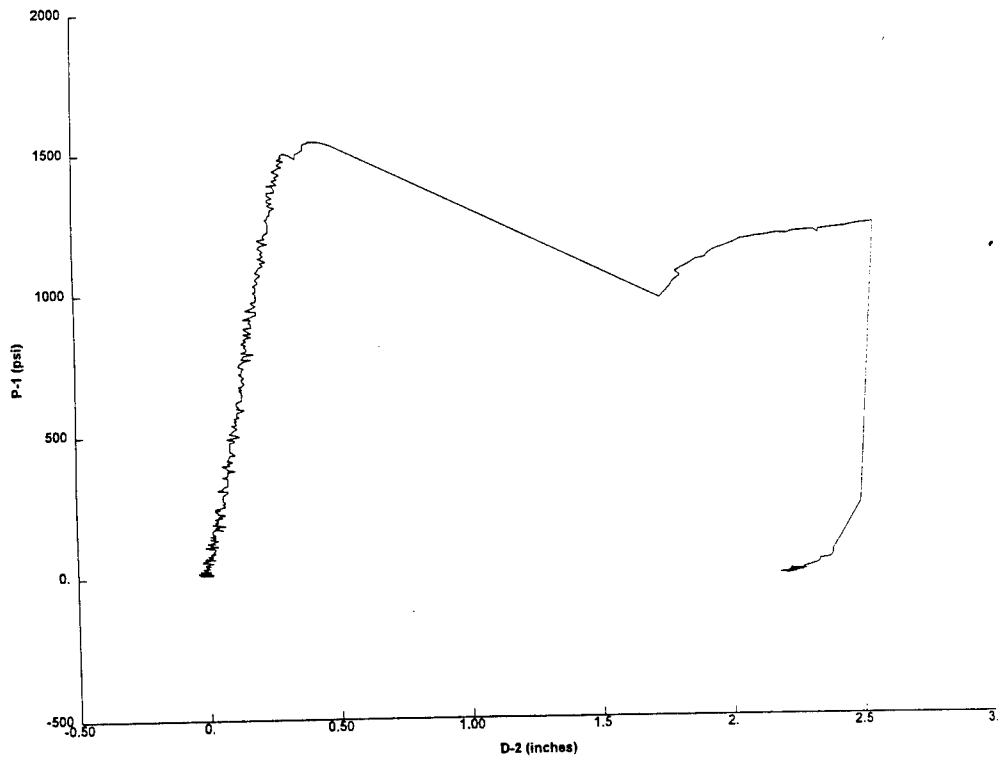
Slab 8

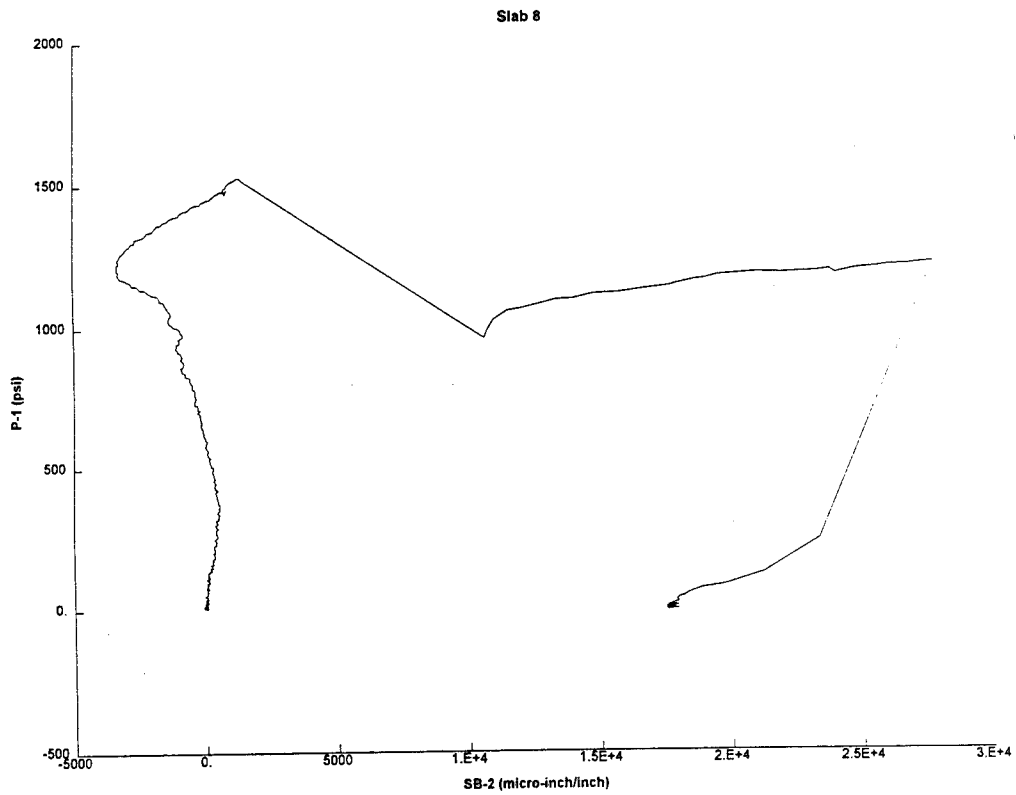
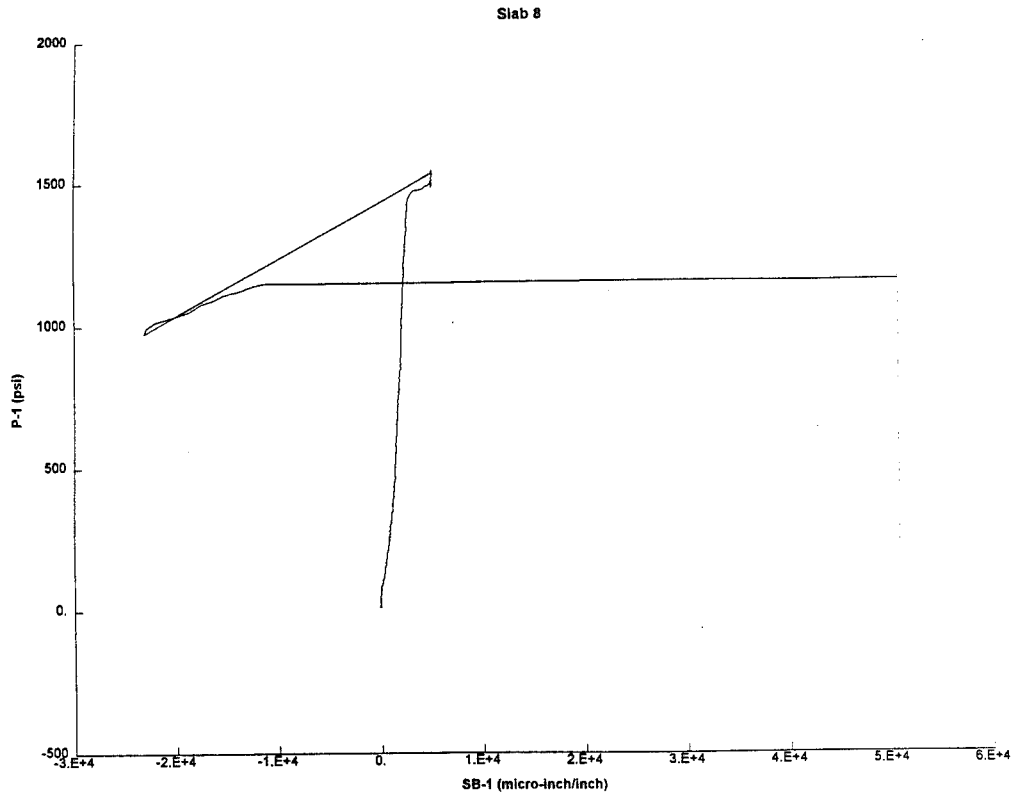


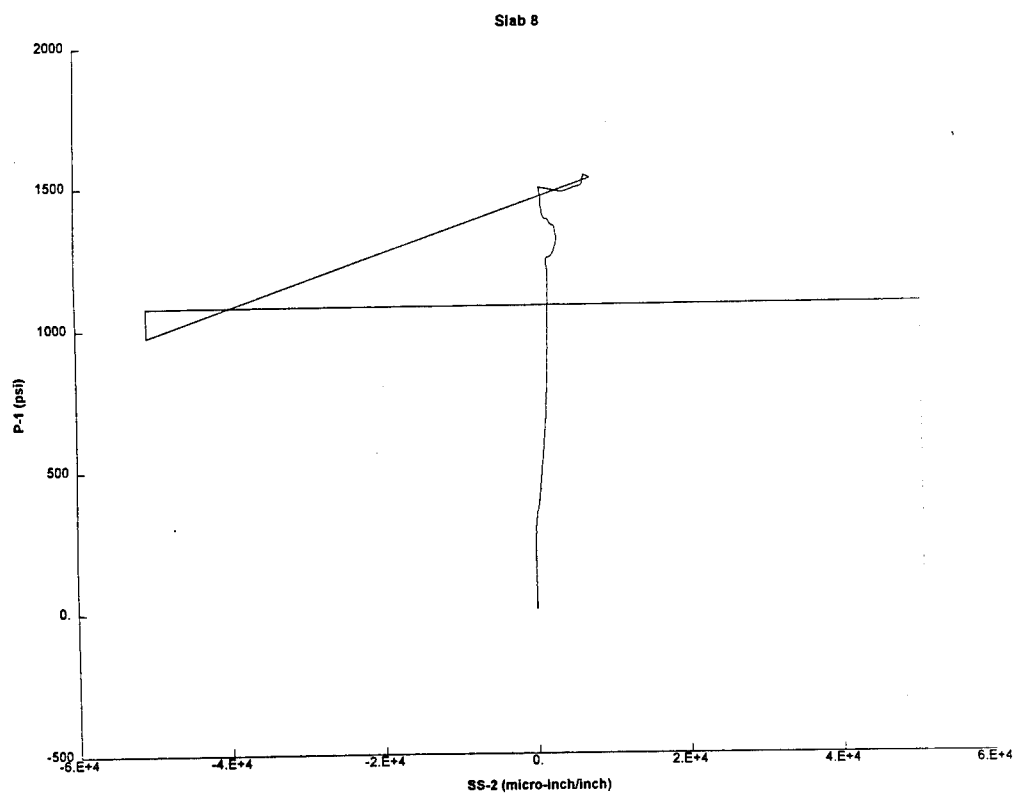
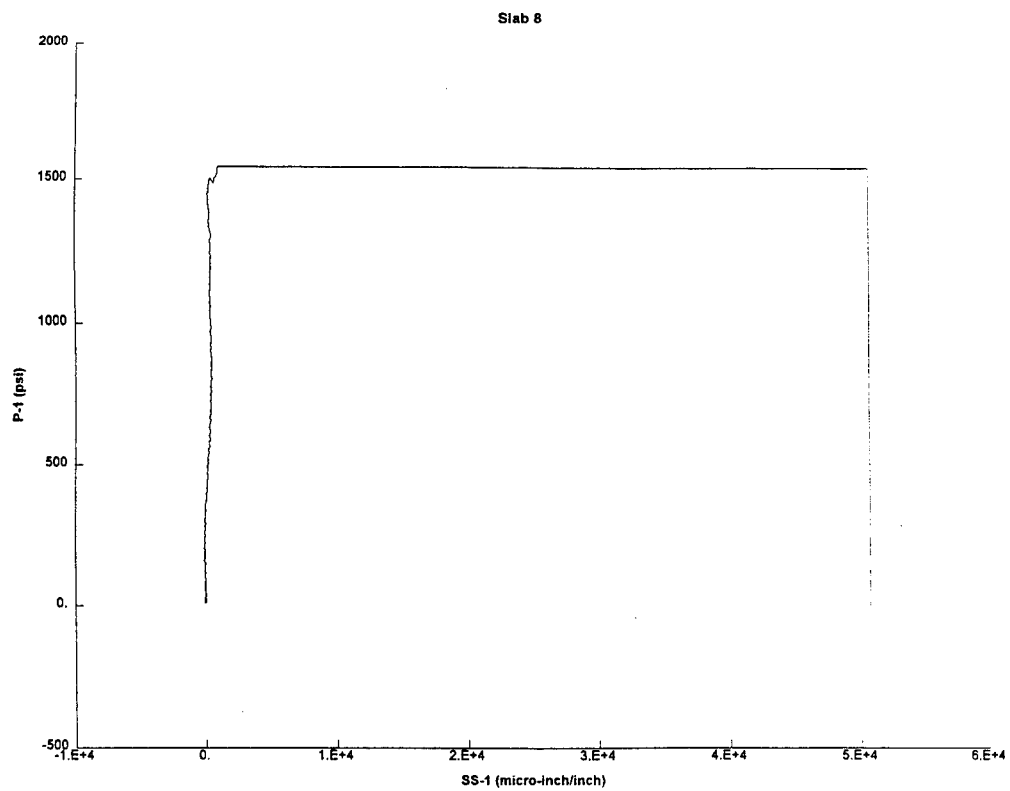
Slab 8



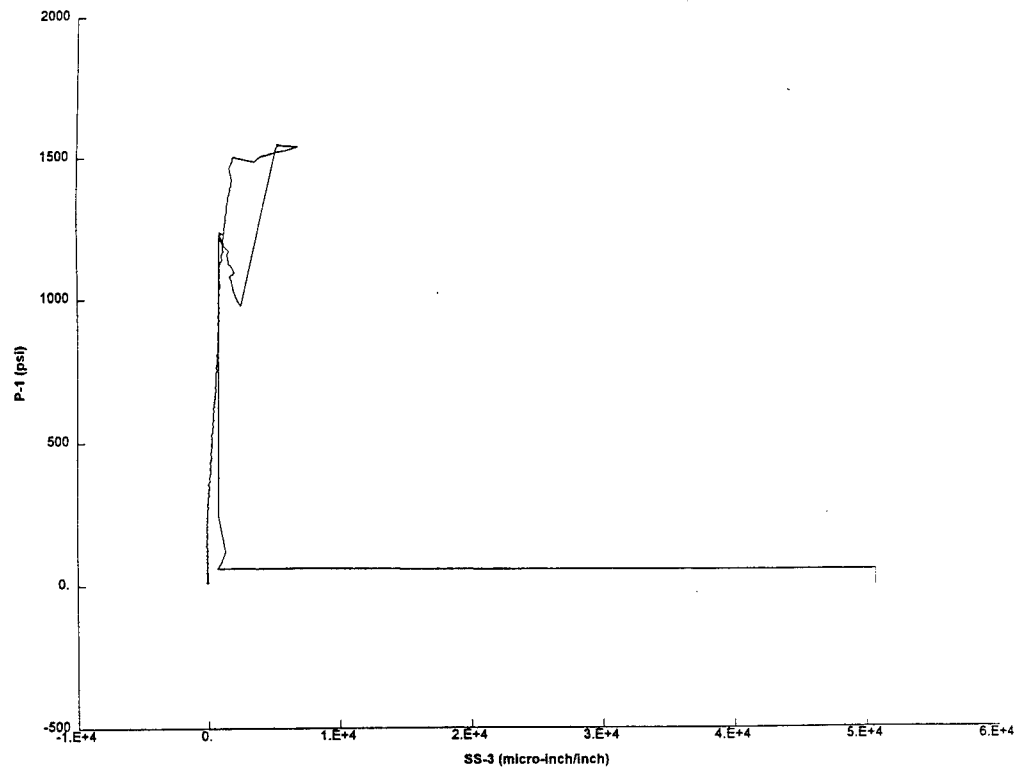
Slab 8



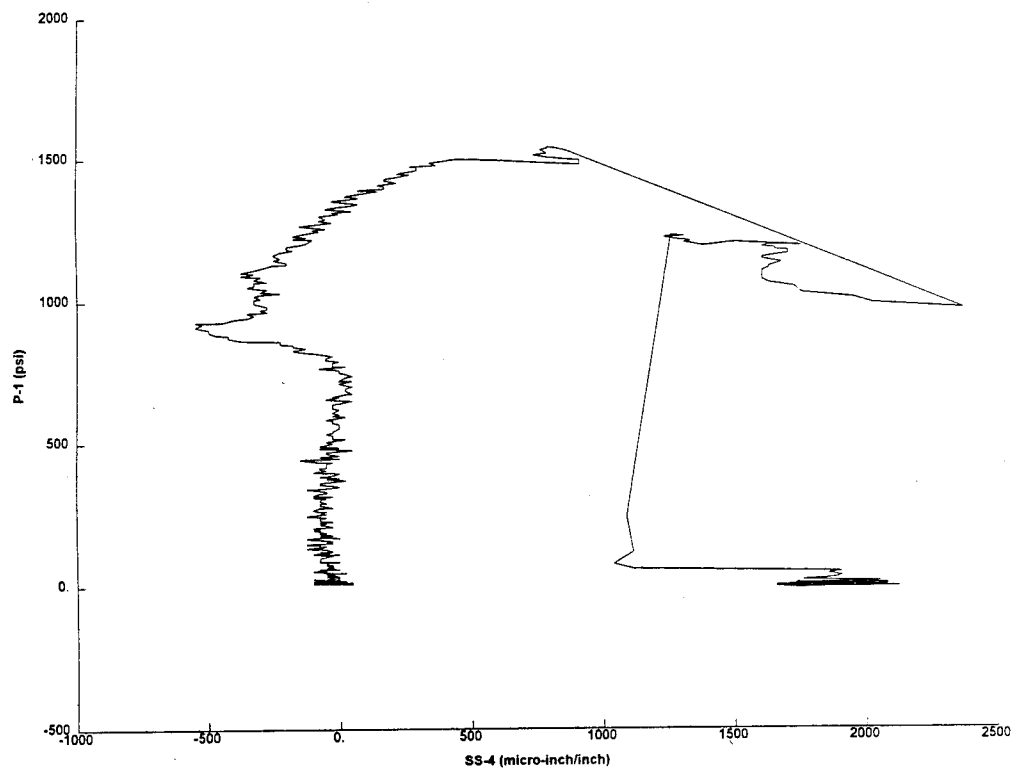


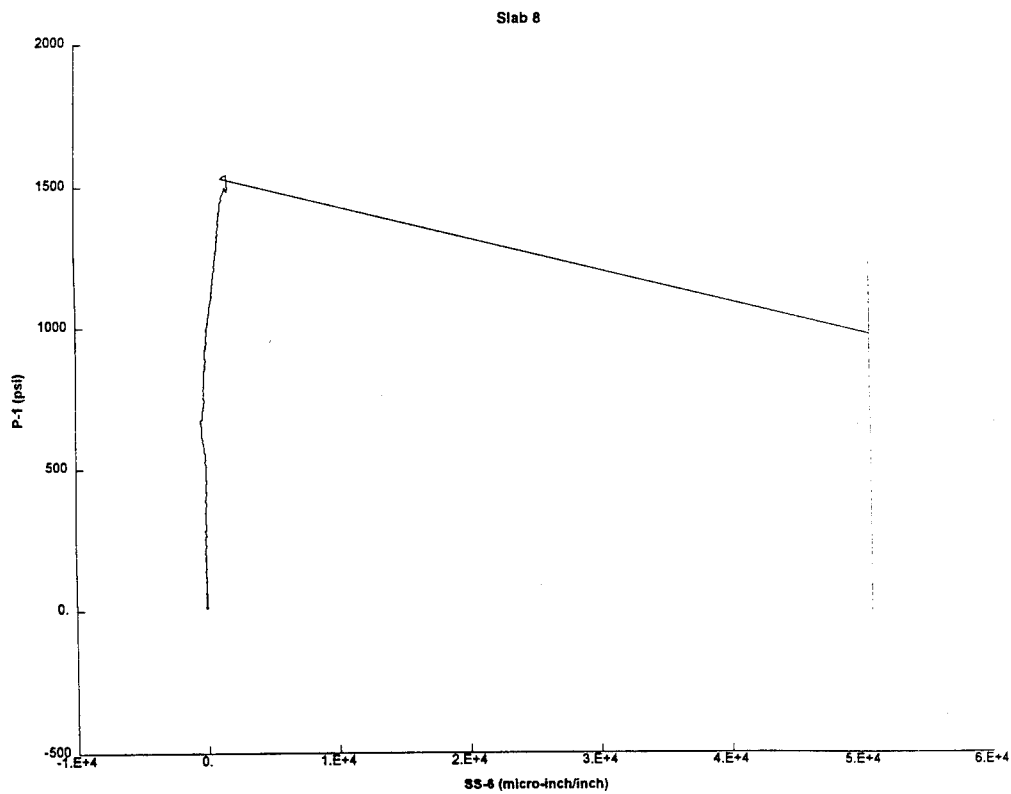
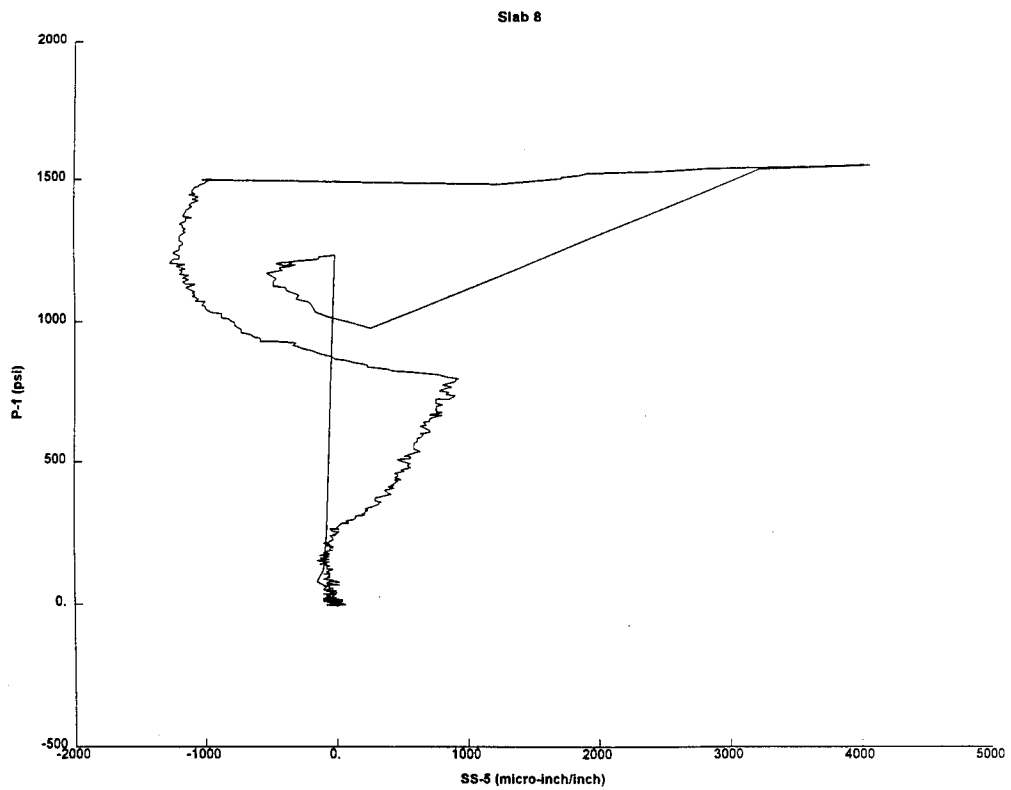


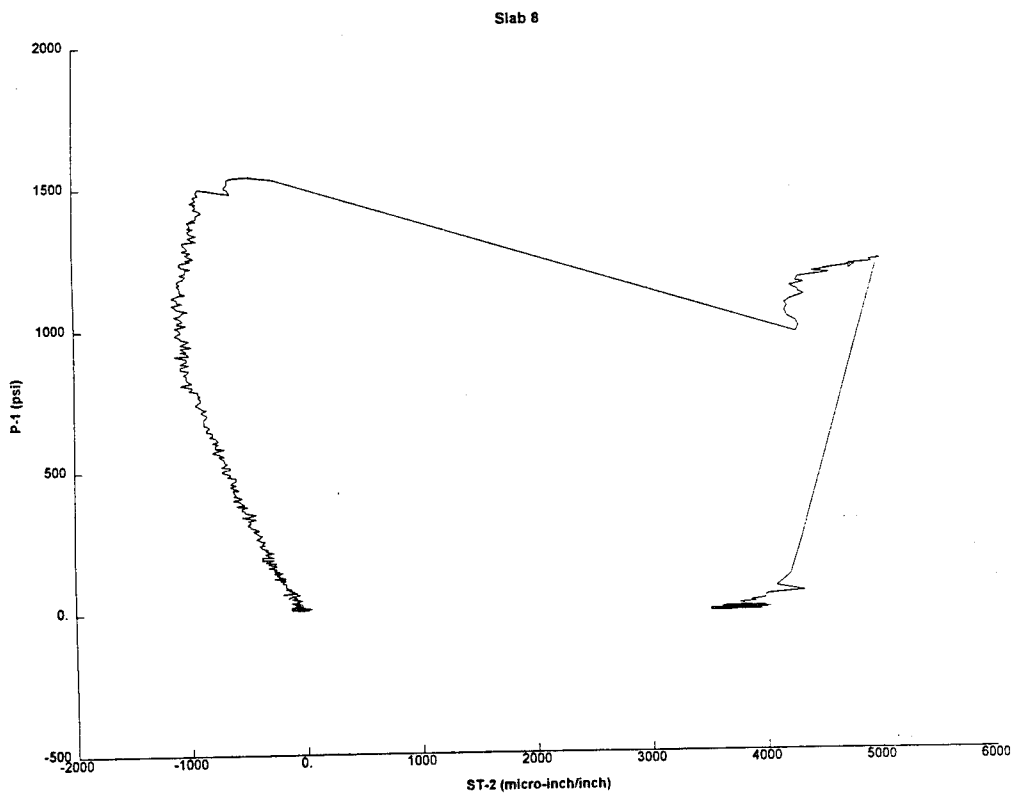
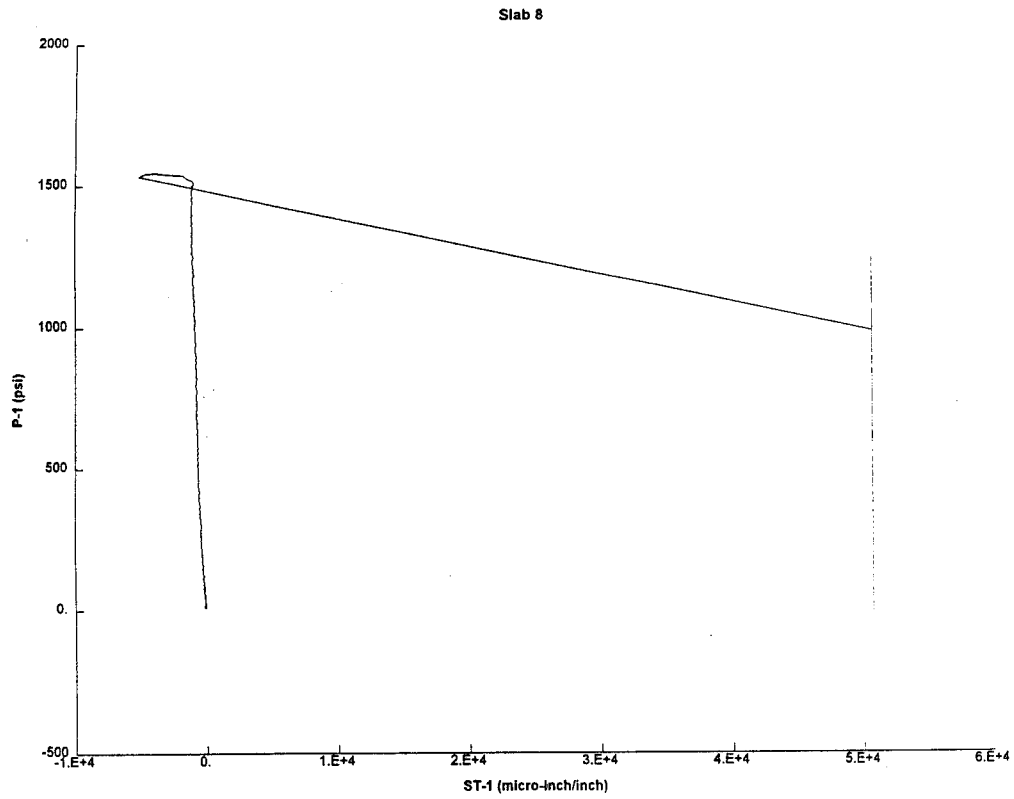
Slab 8

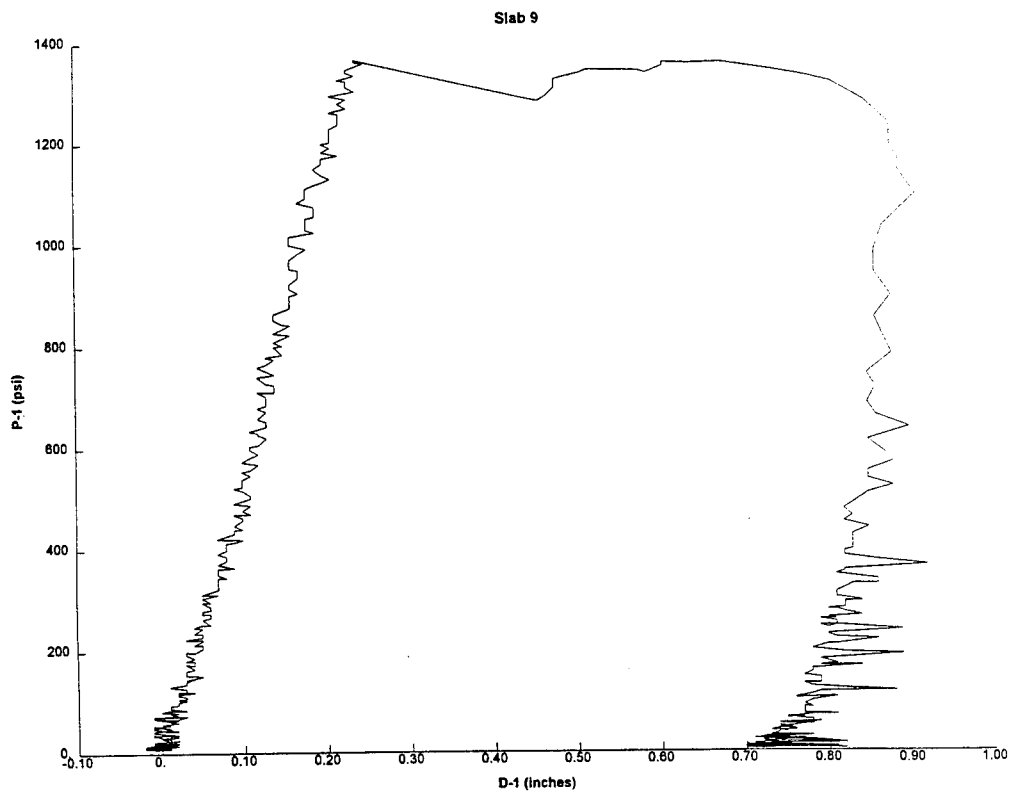
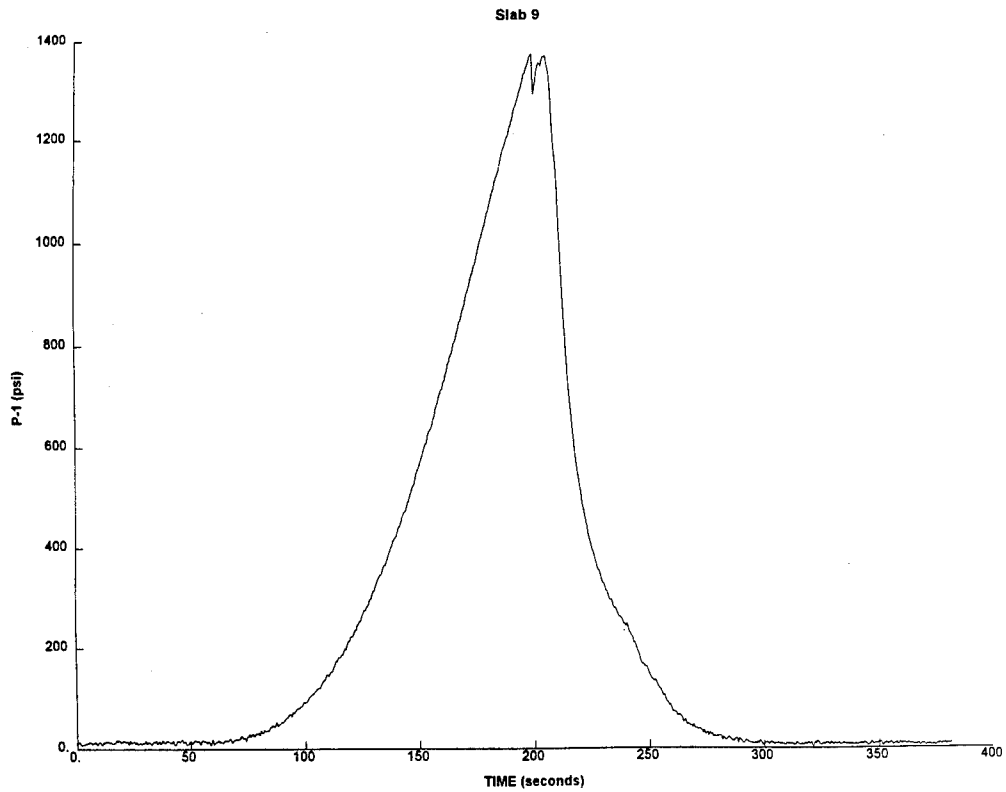


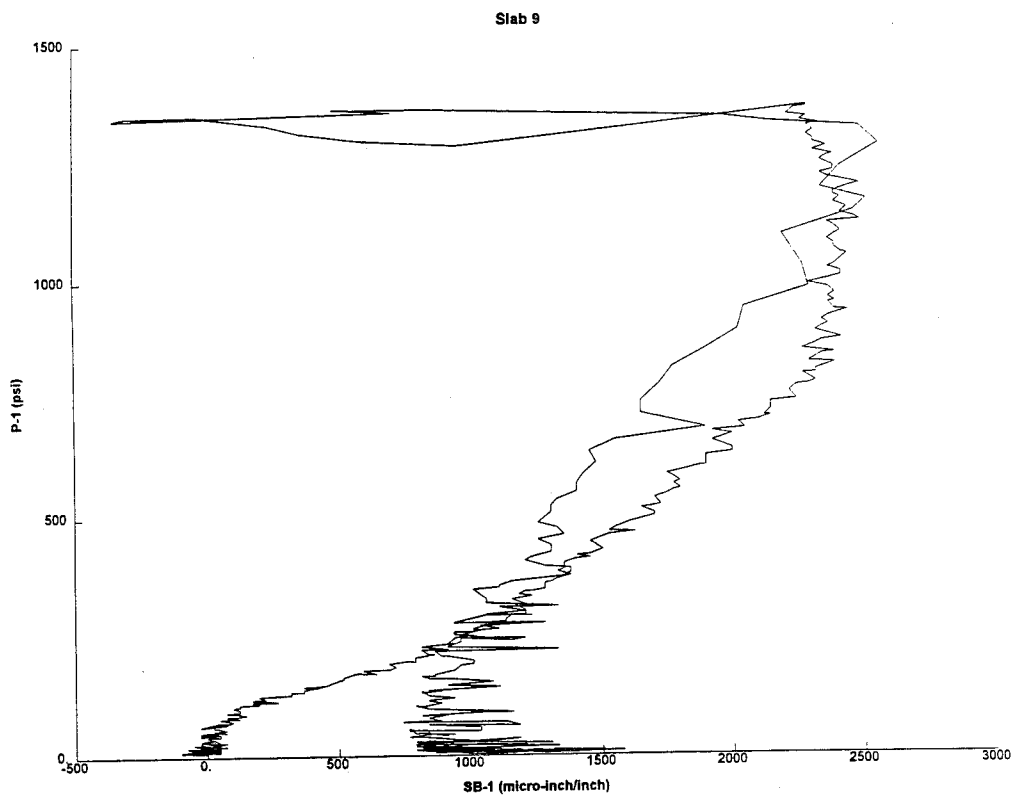
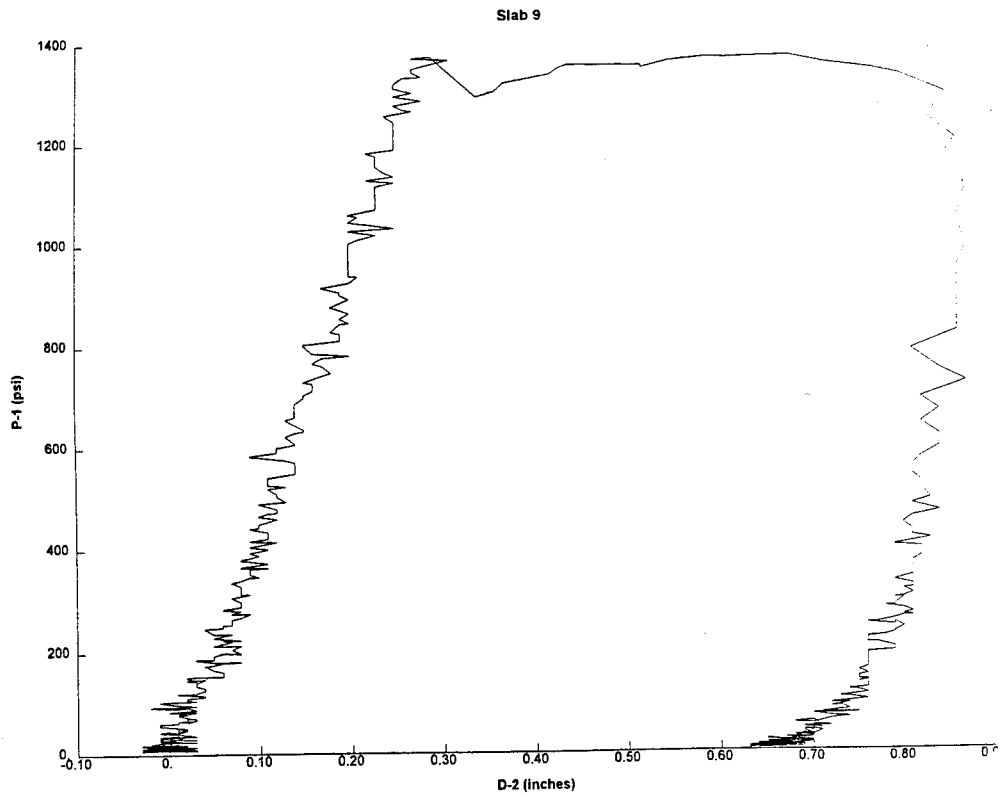
Slab 8

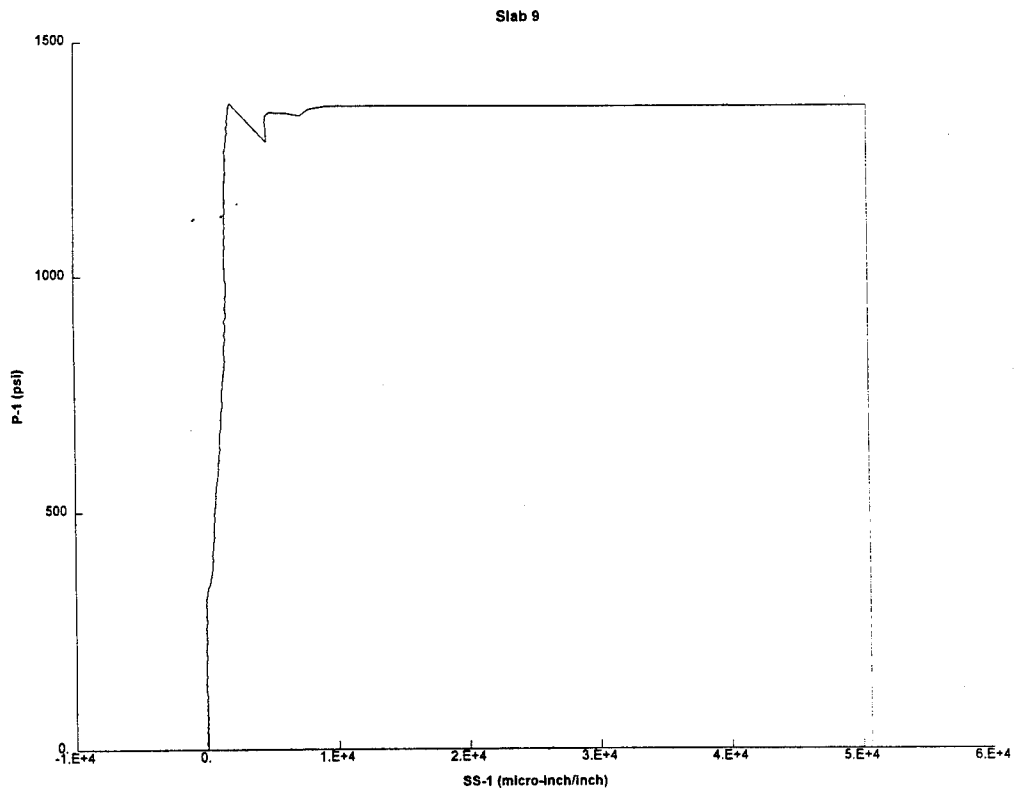
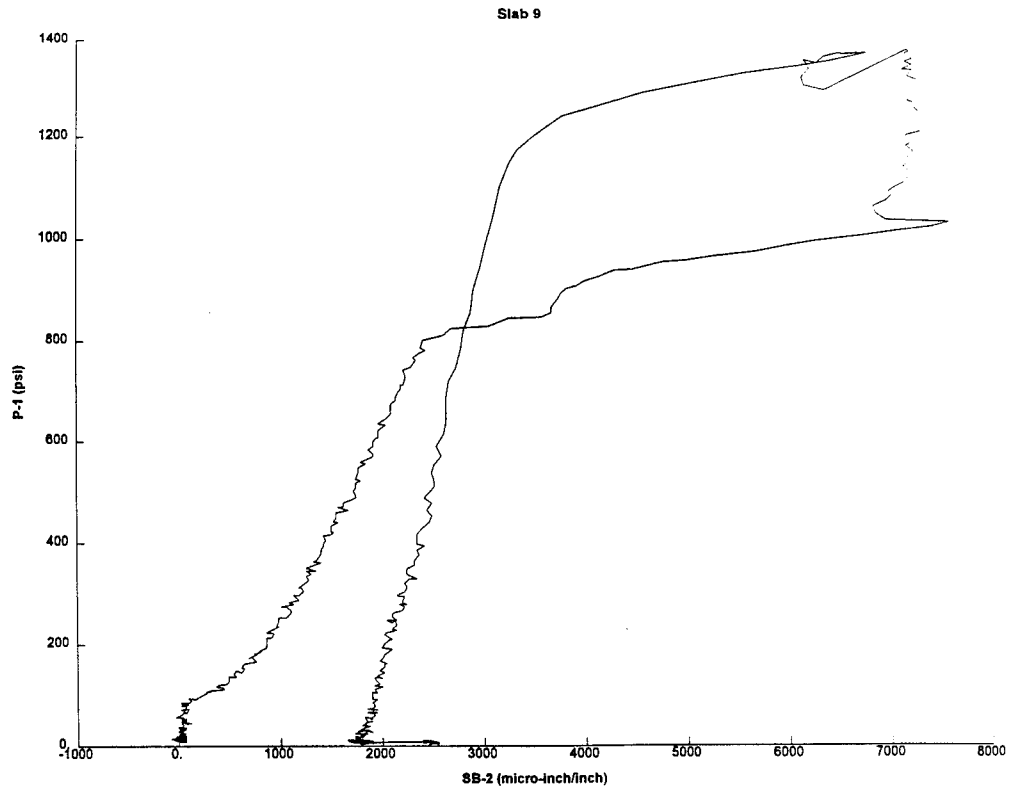


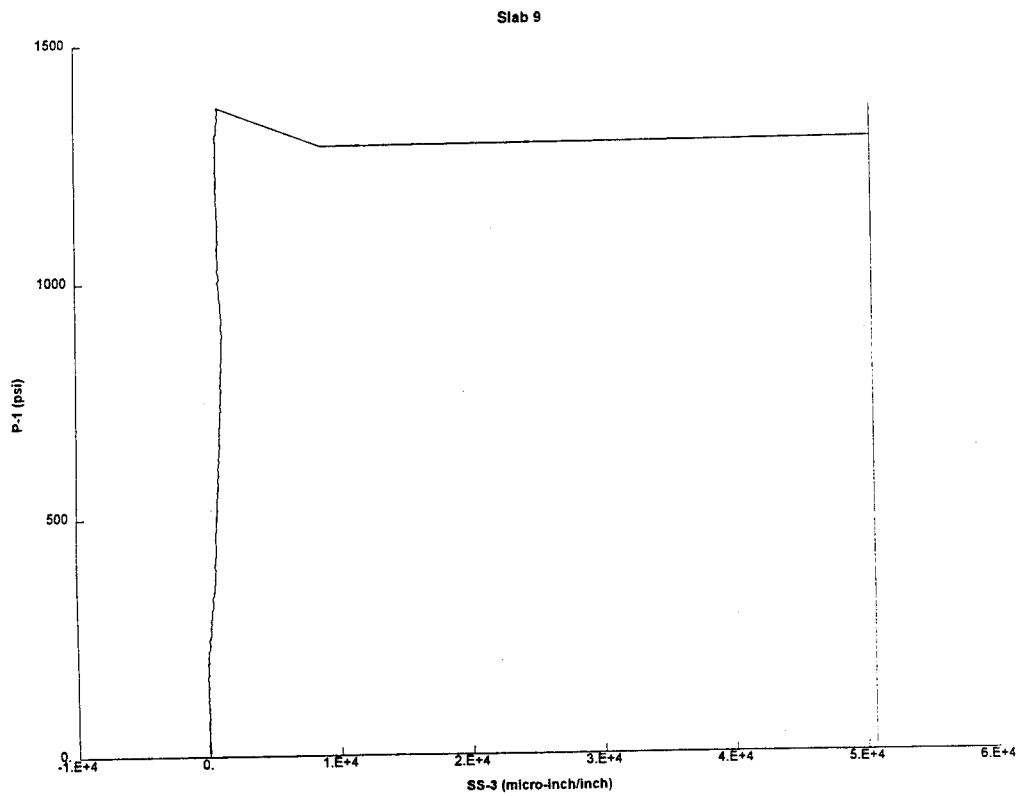
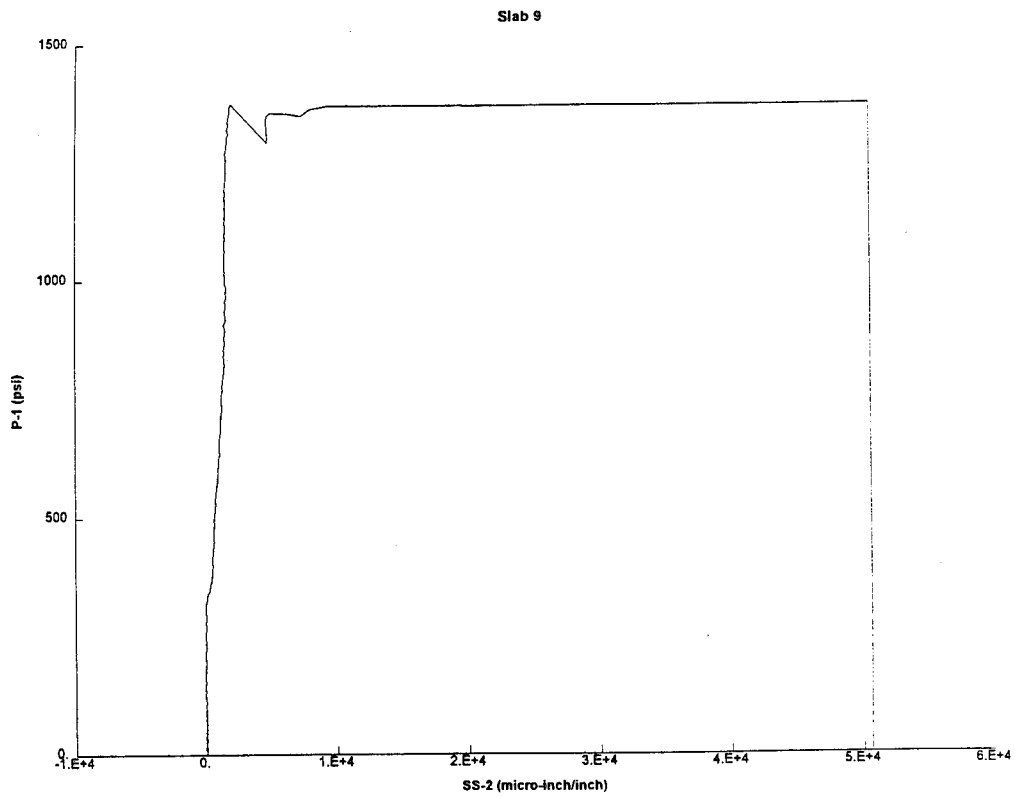


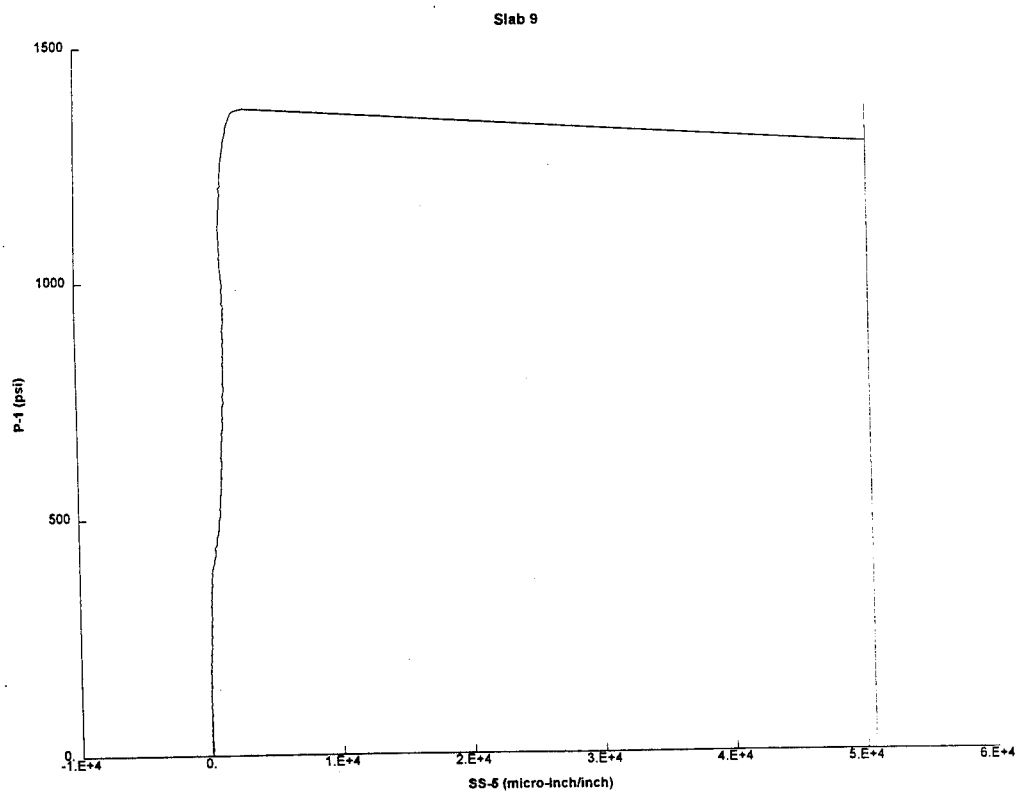
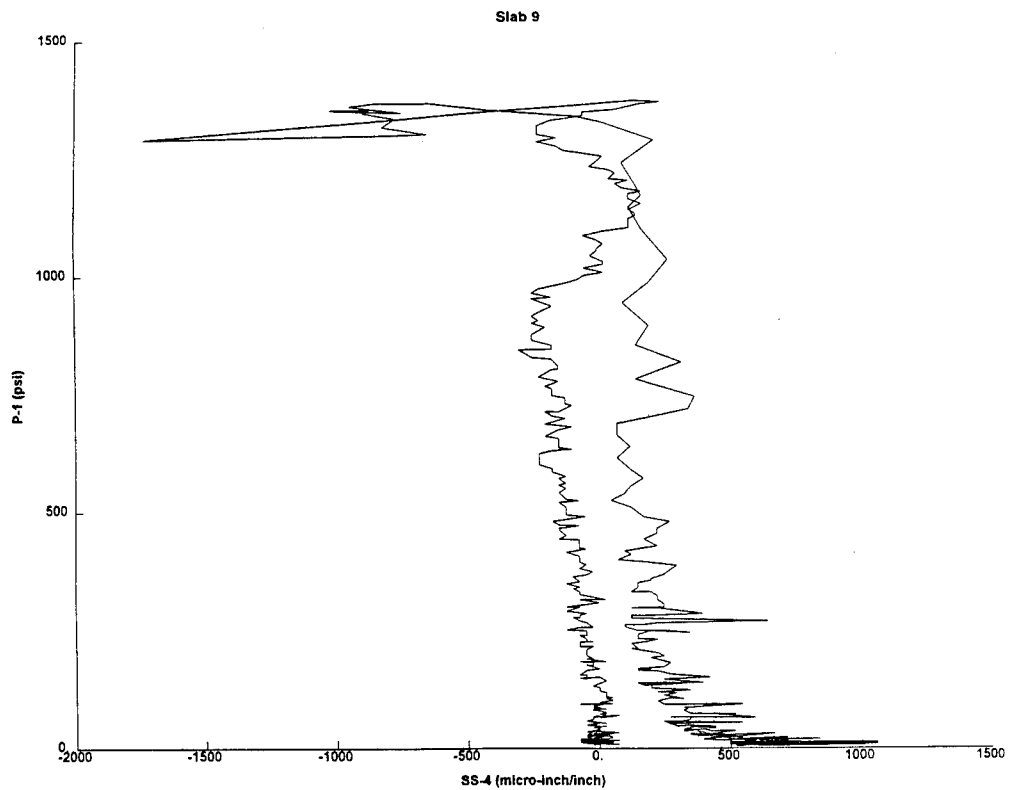


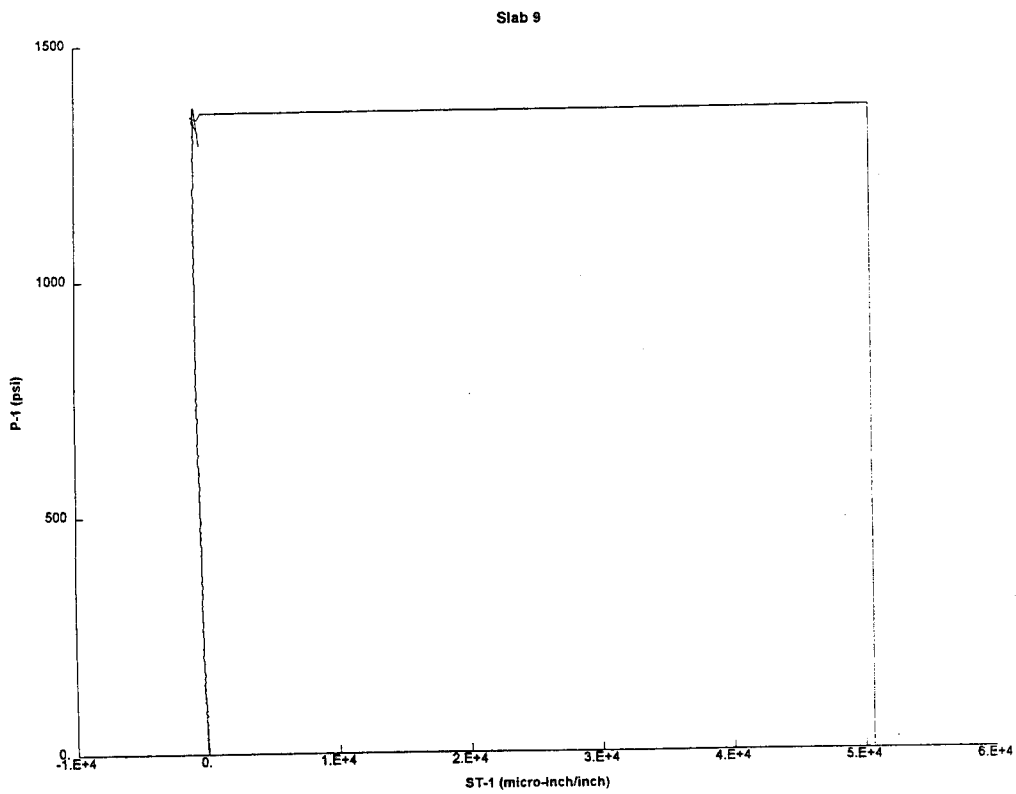
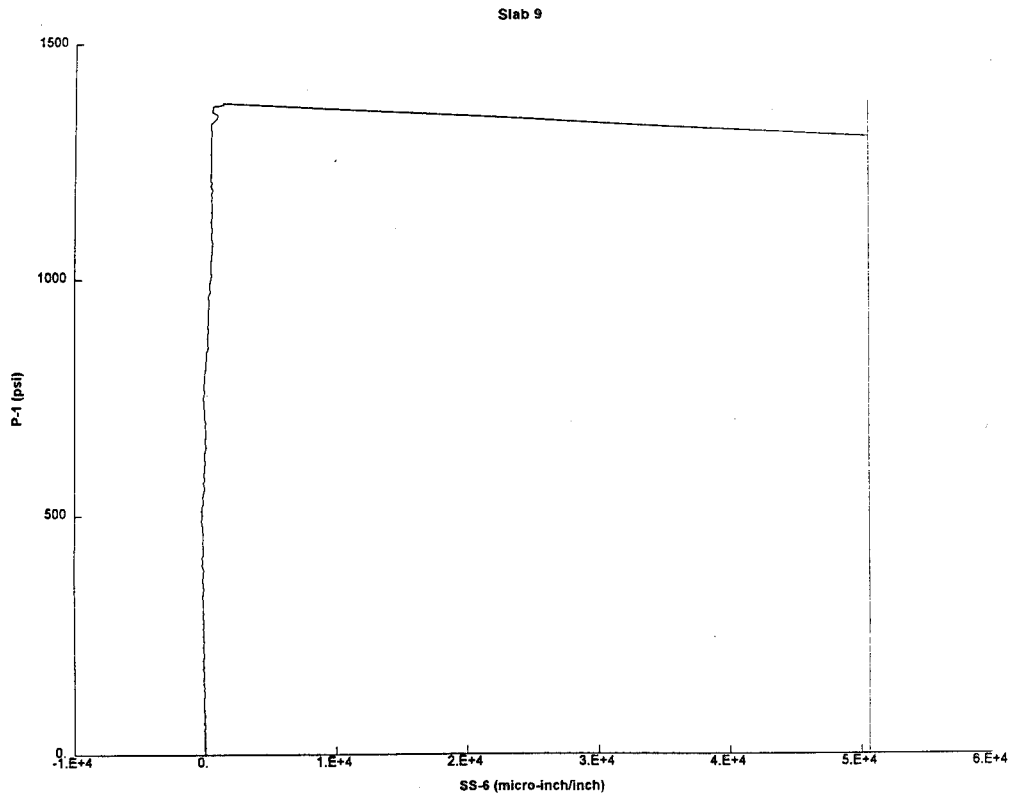


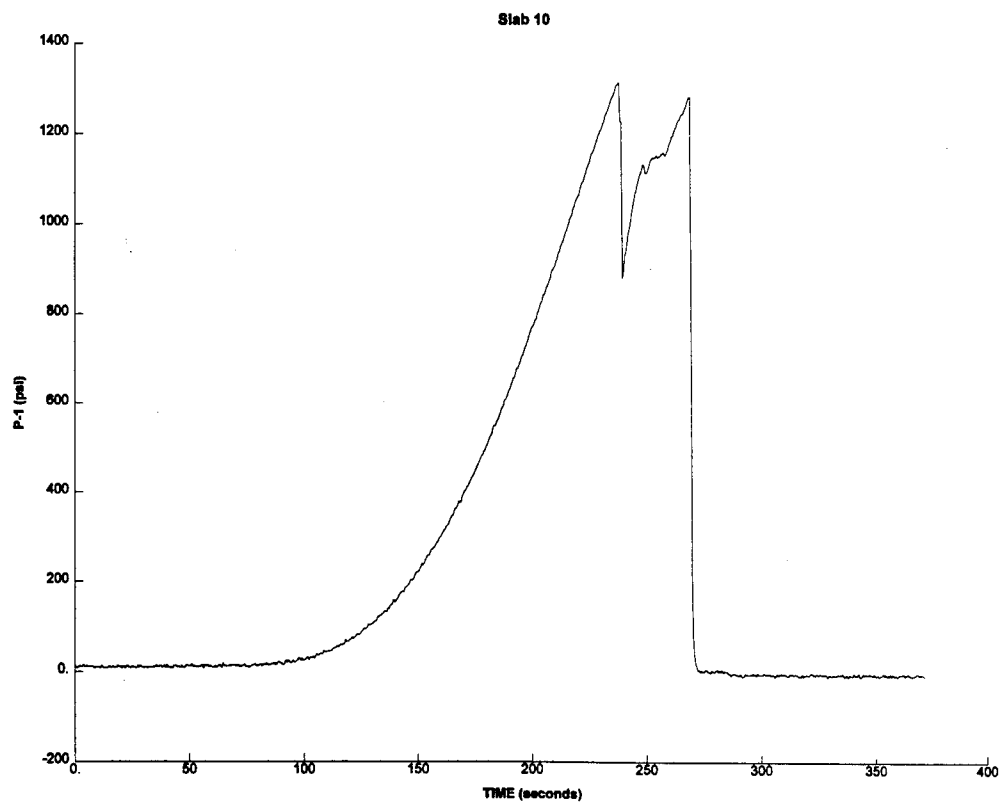
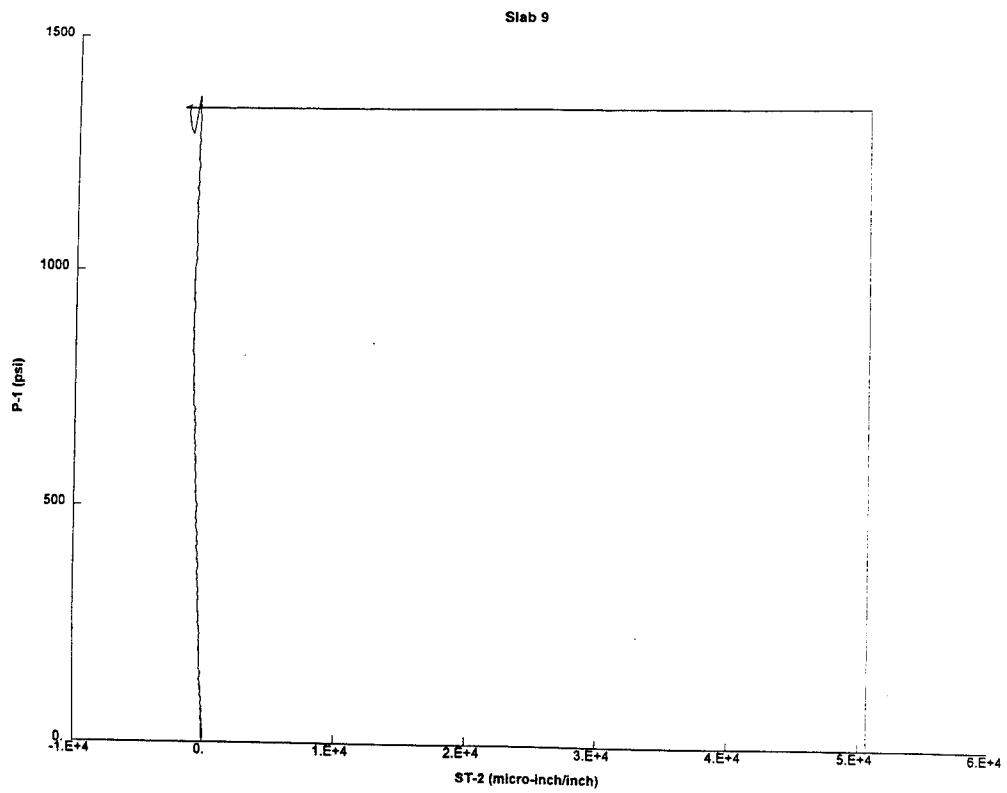




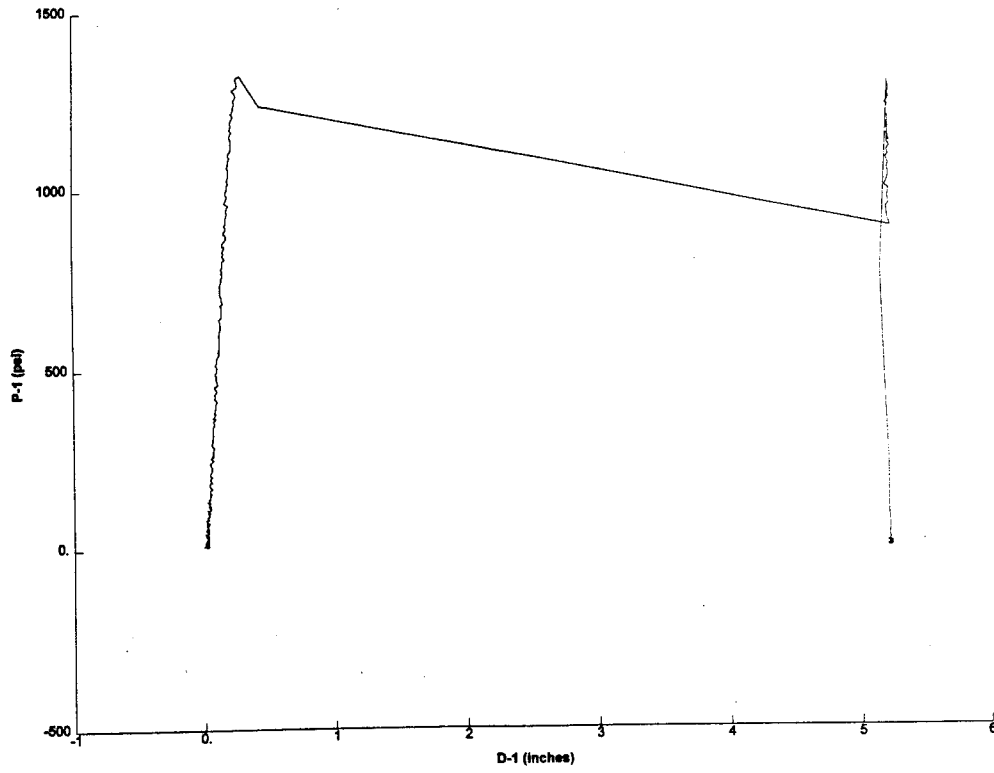




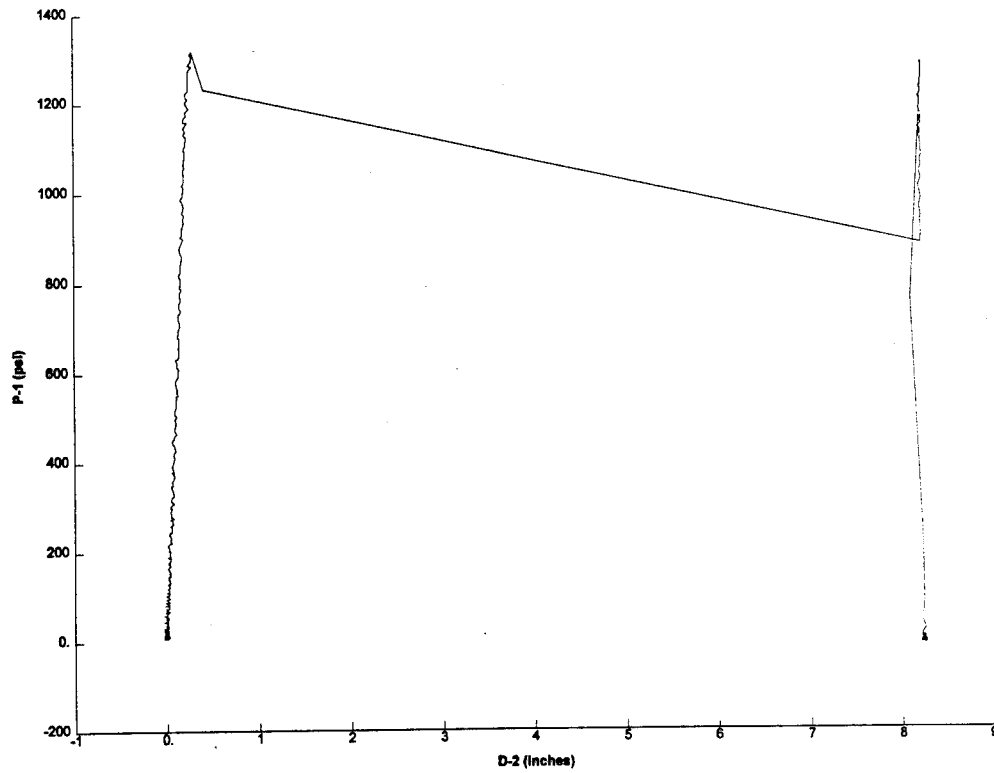


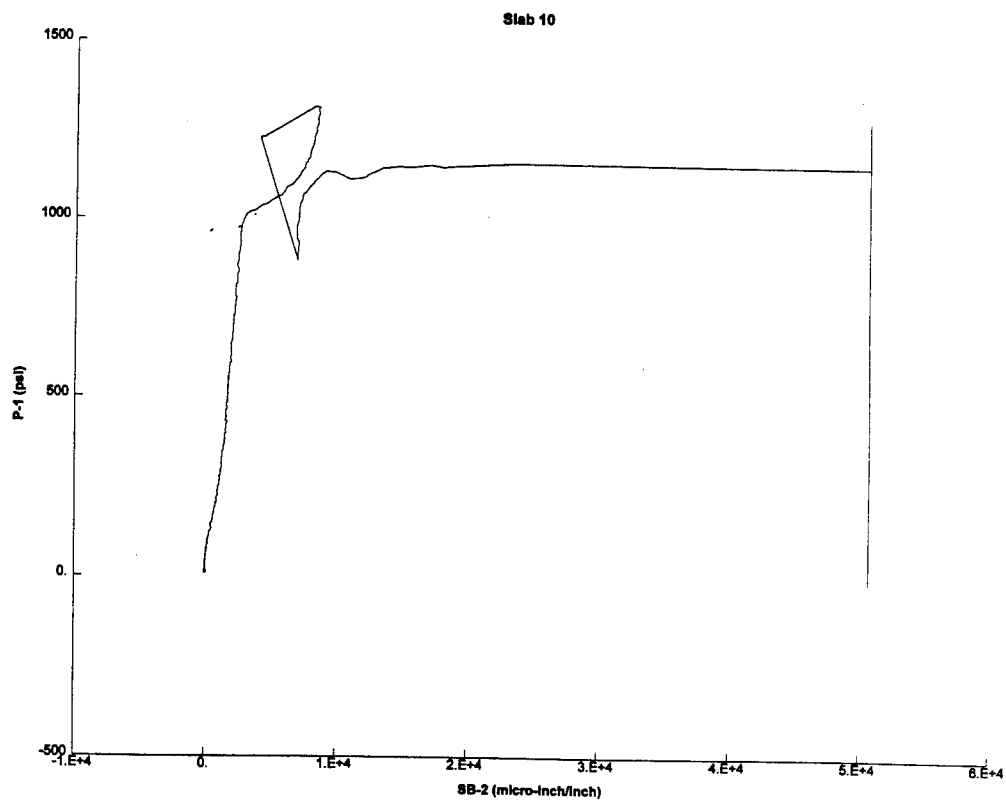
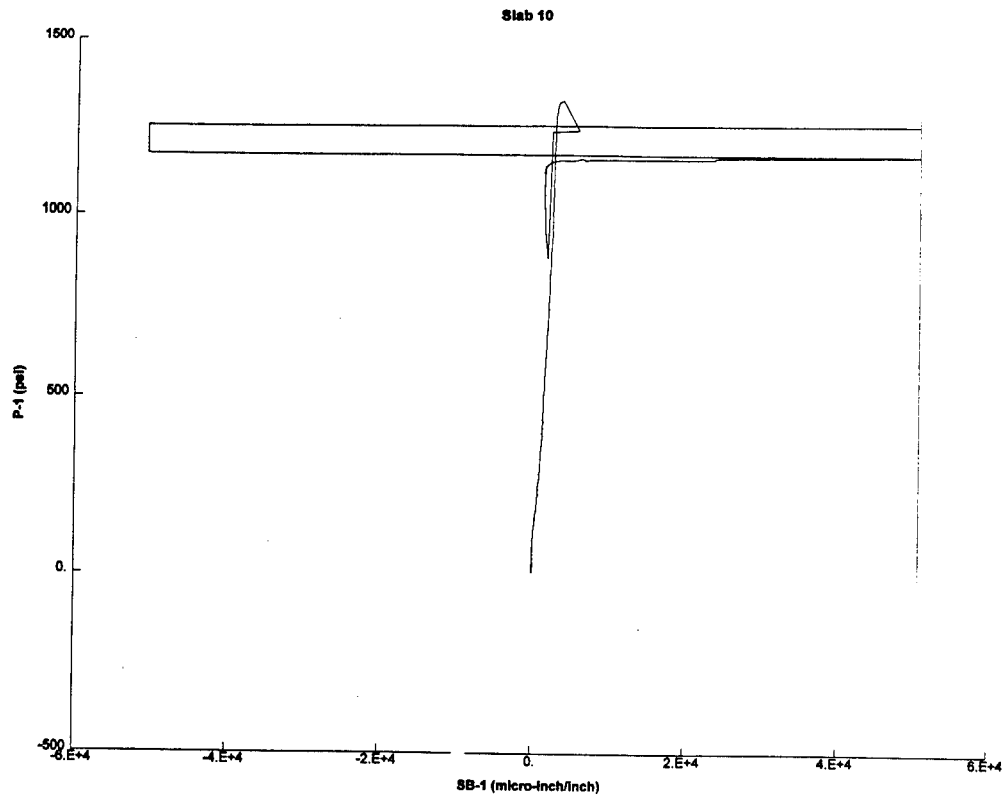


Slab 10

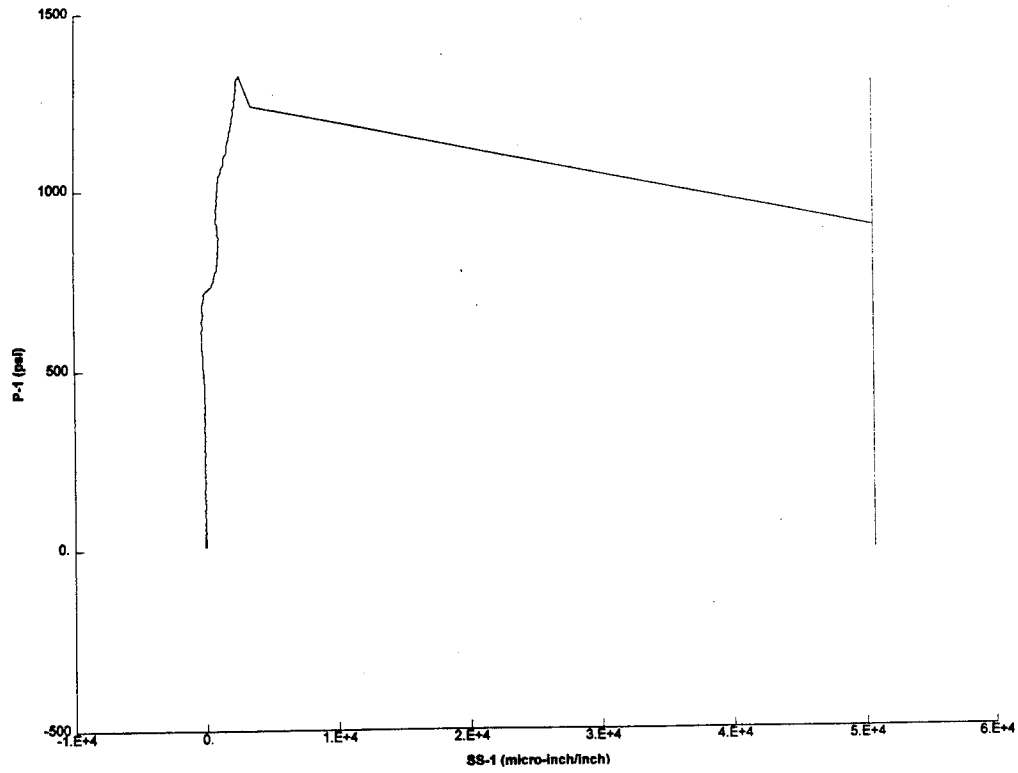


Slab 10

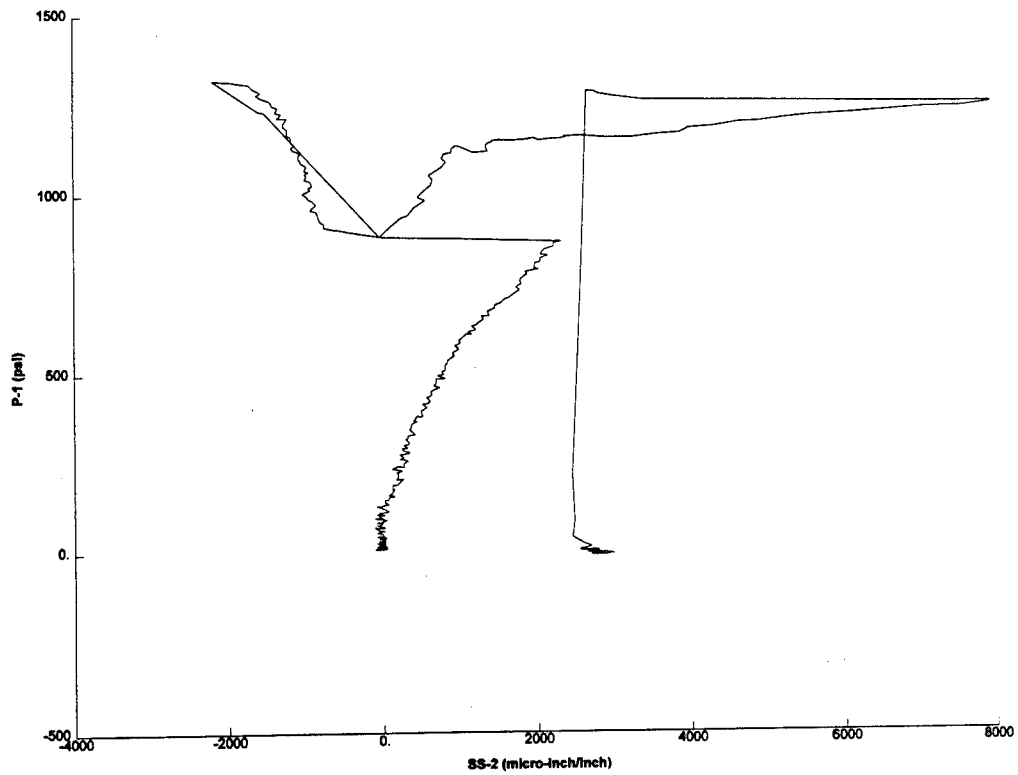


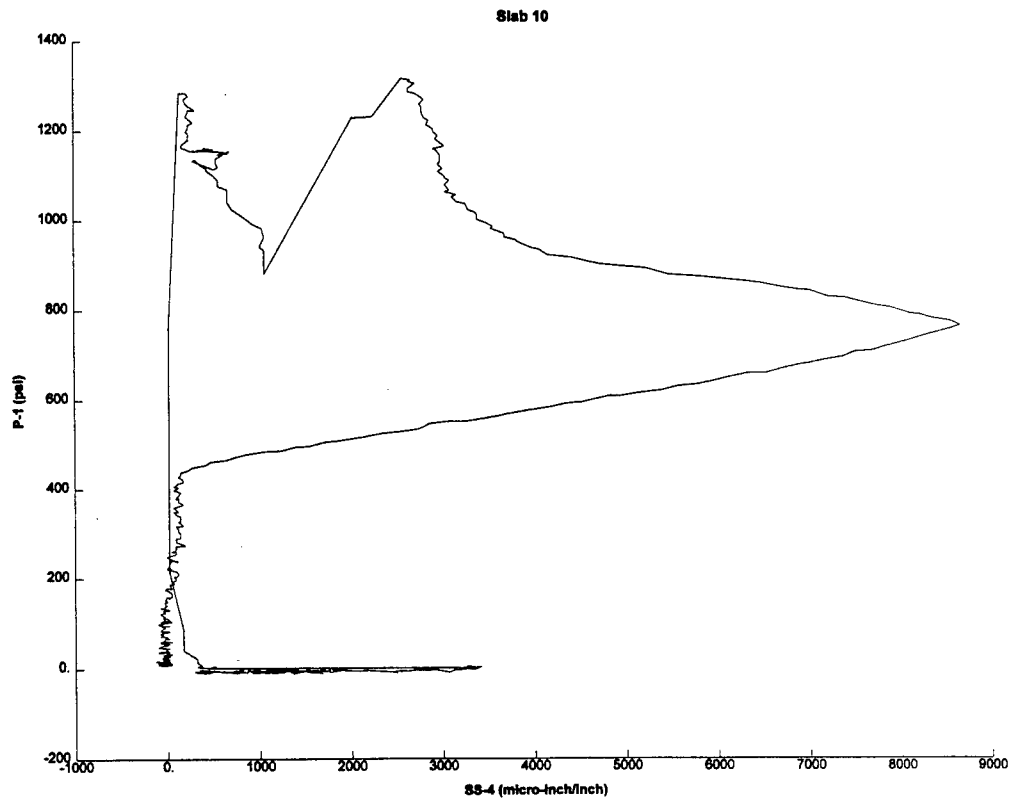
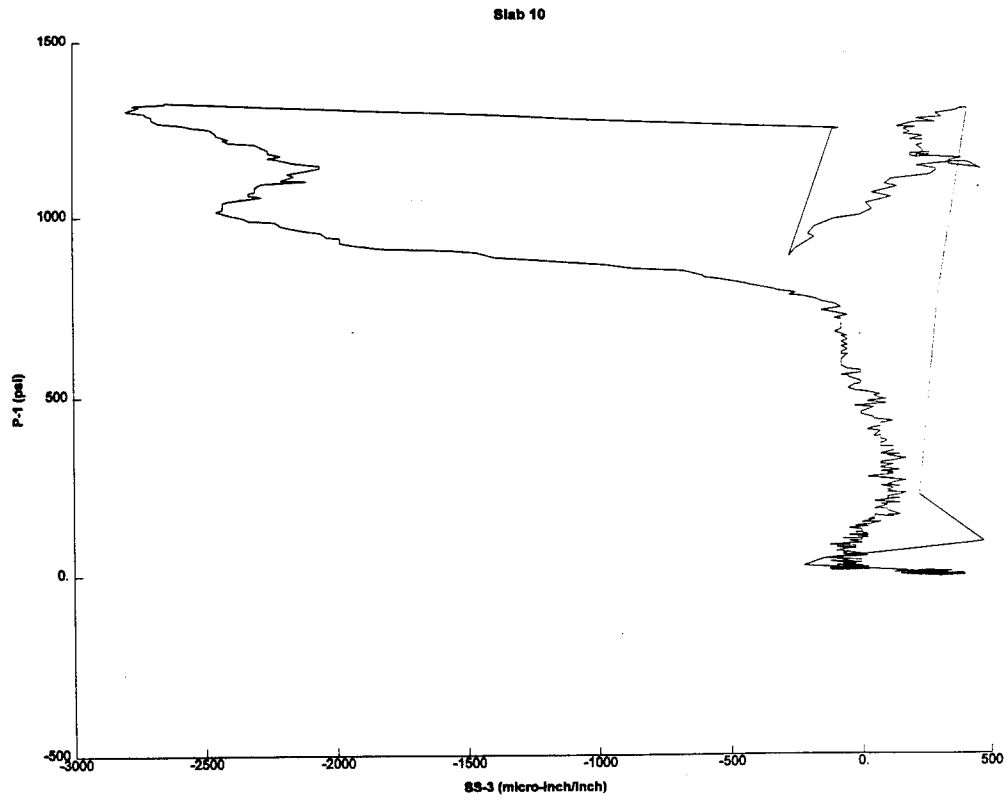


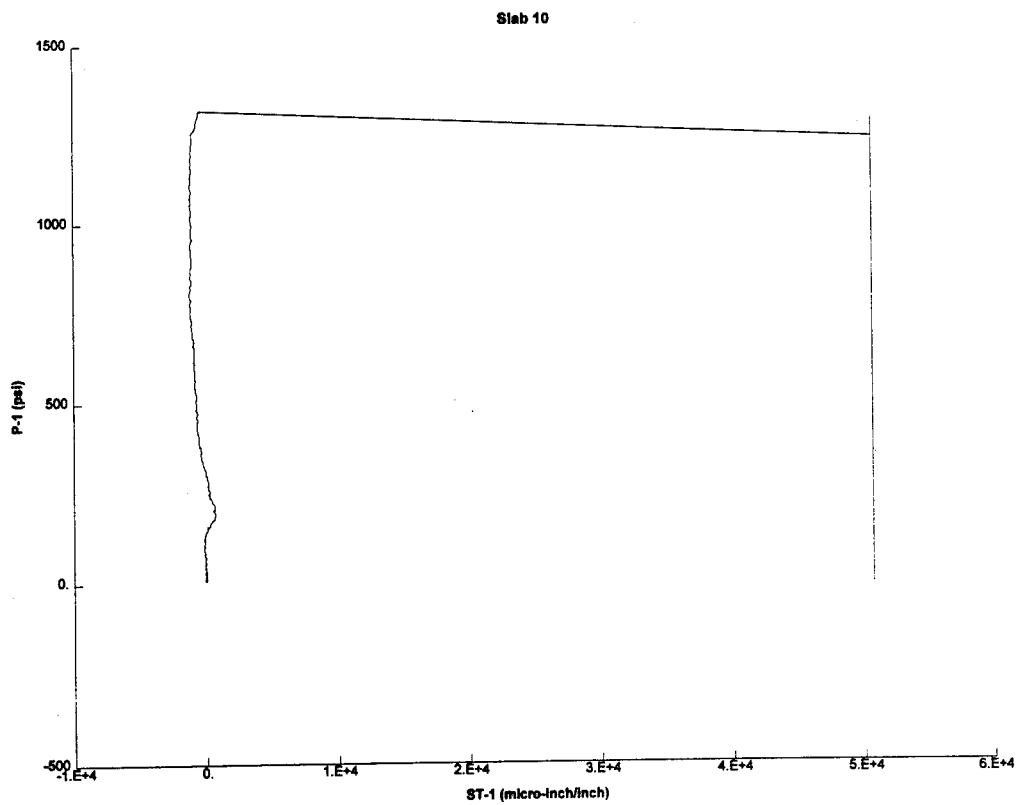
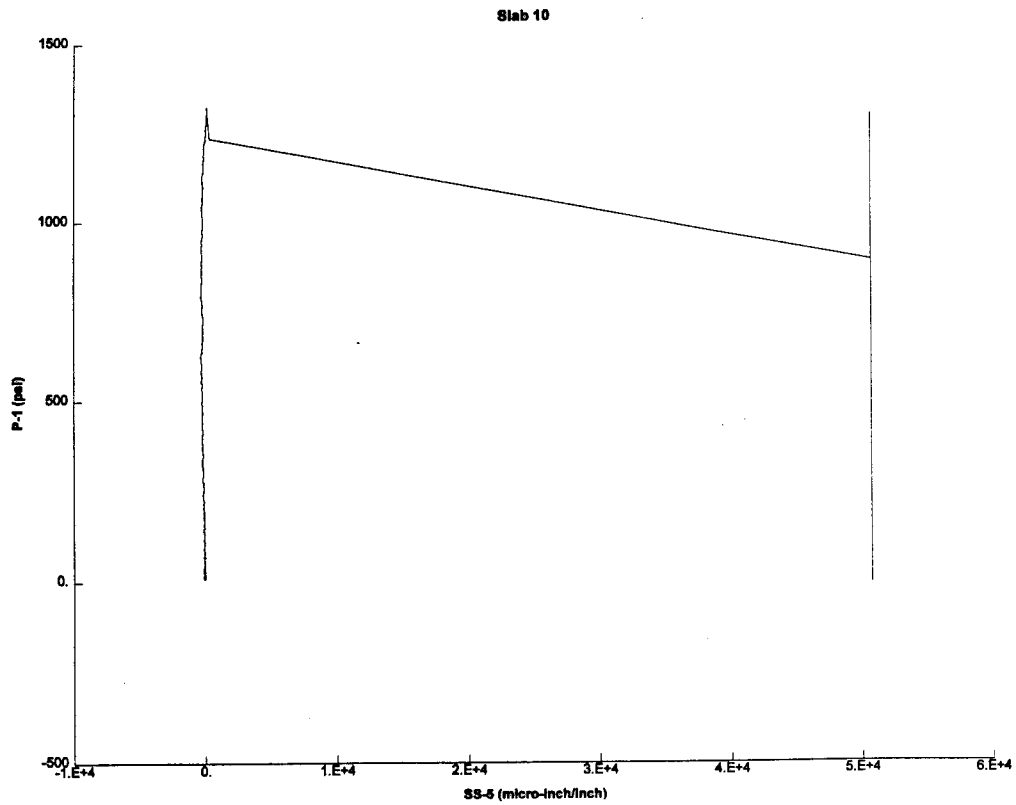
Slab 10

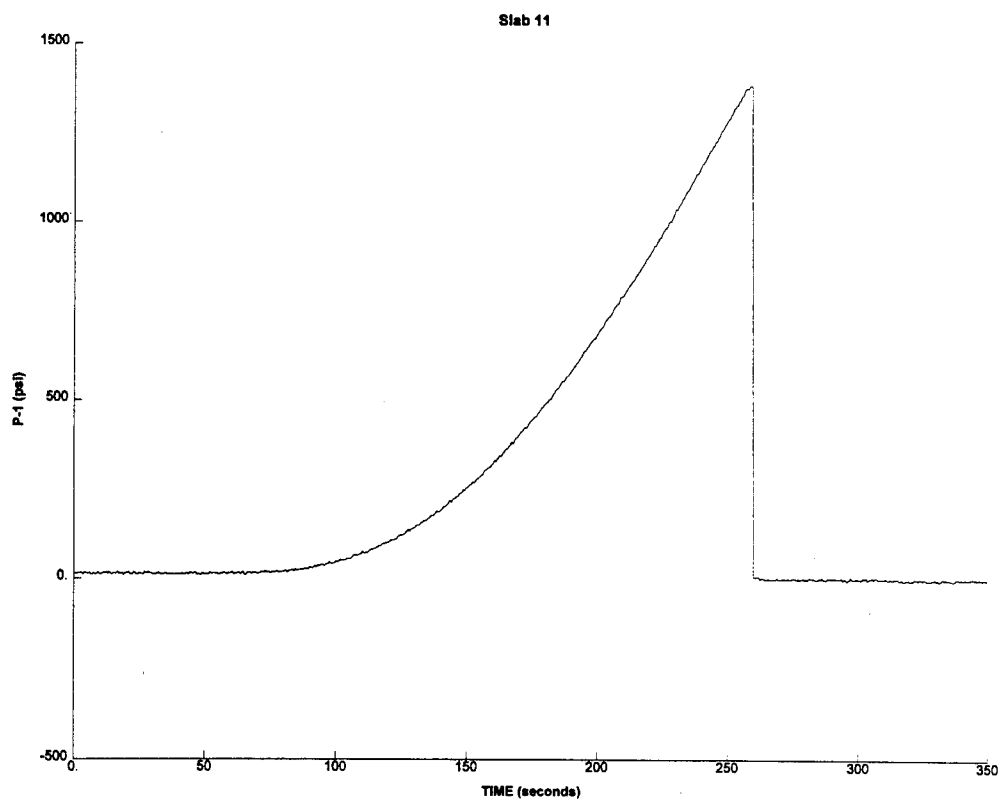
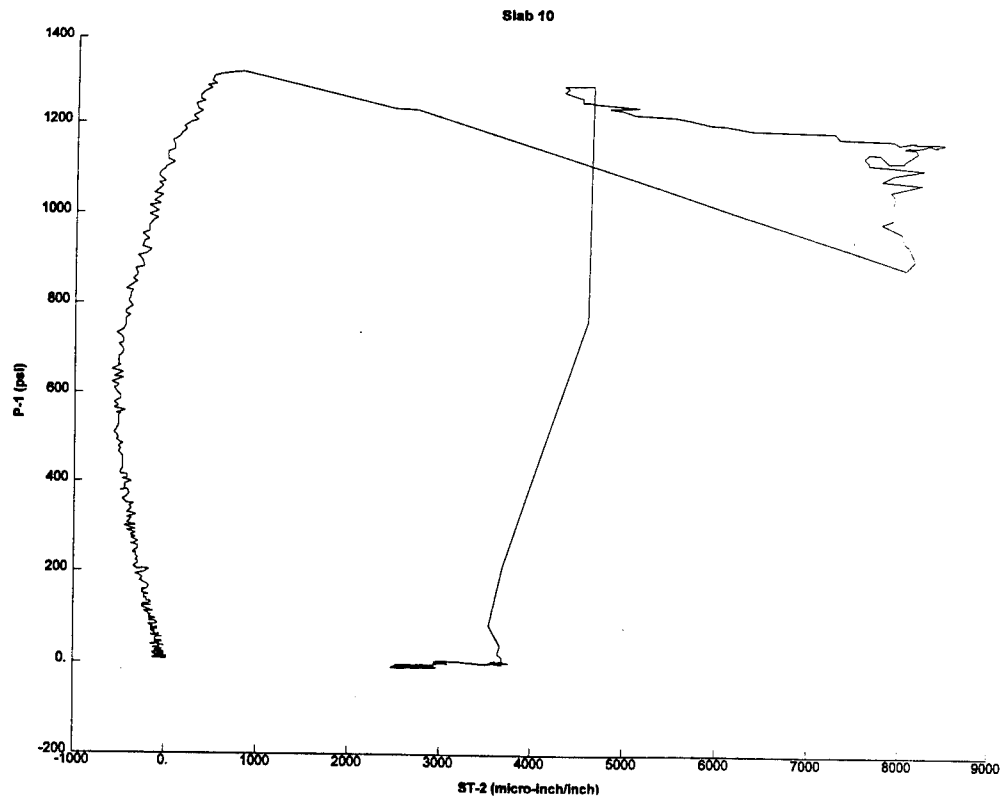


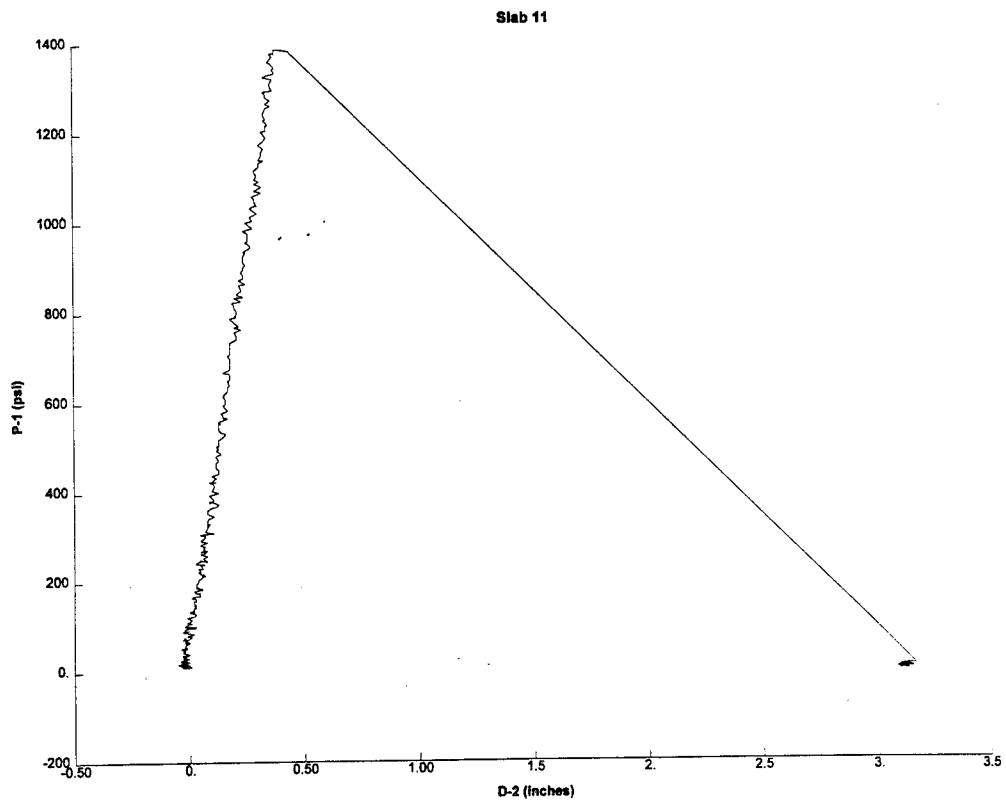
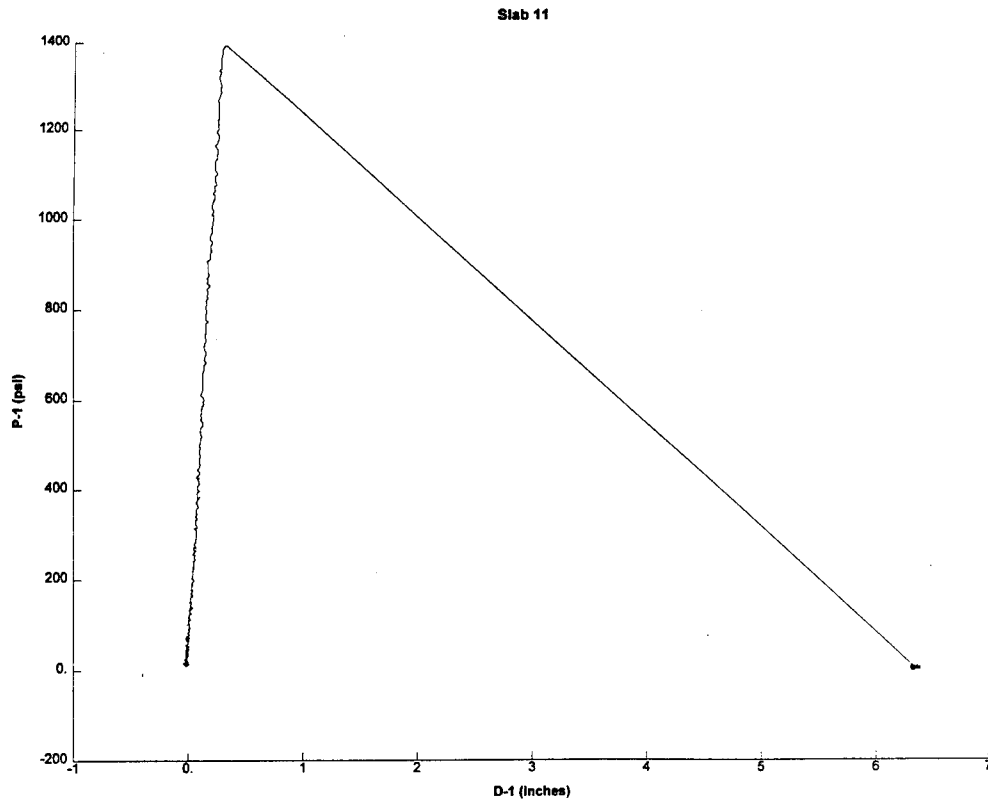
Slab 10

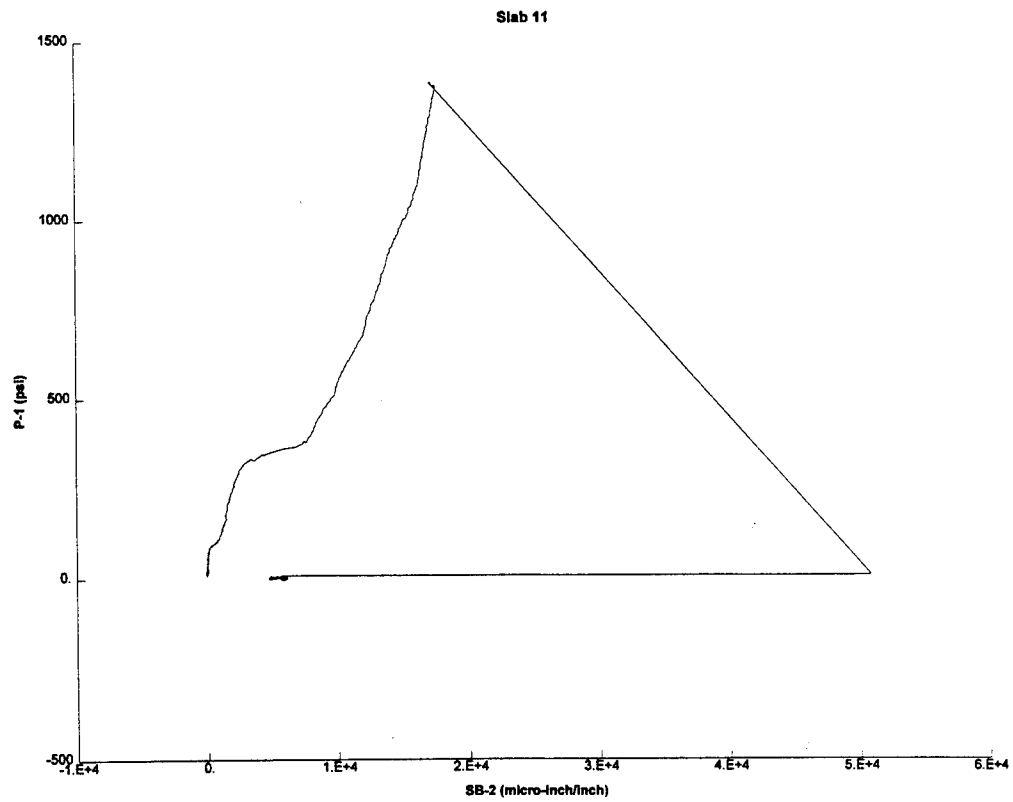
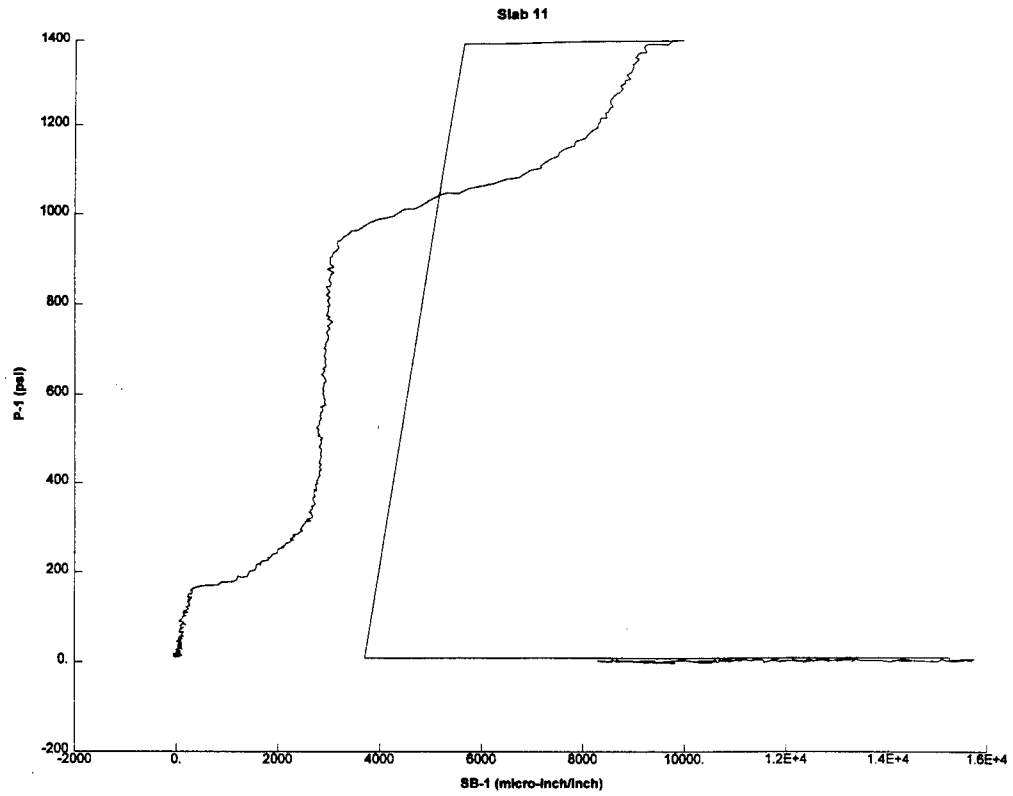




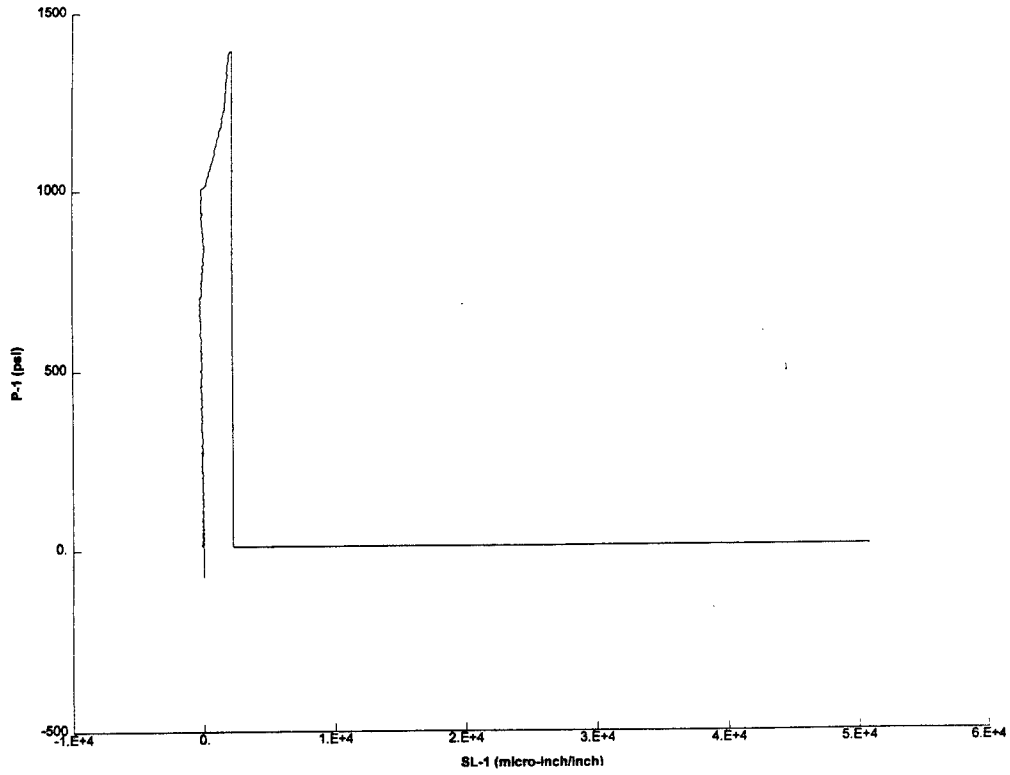




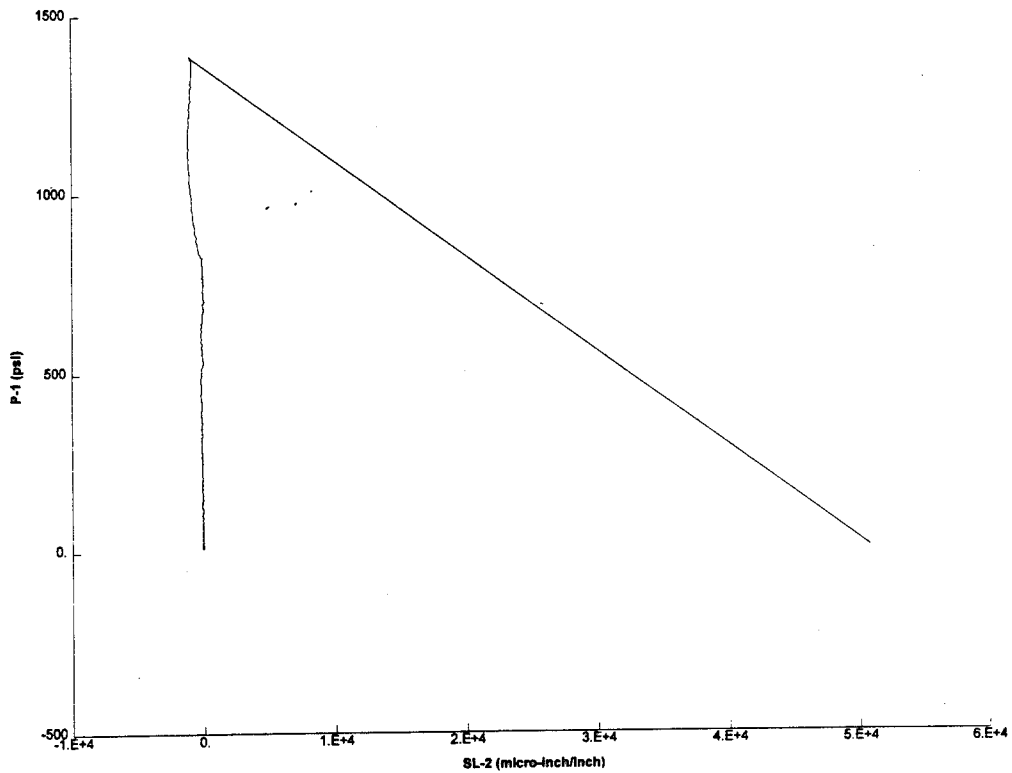


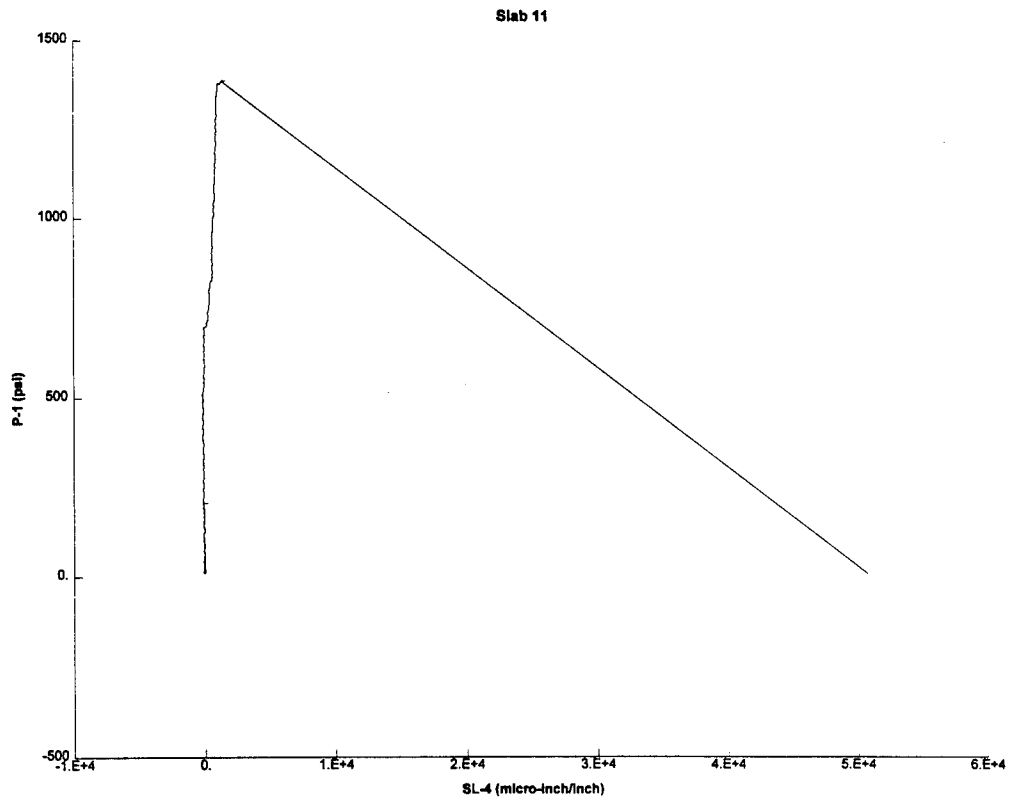
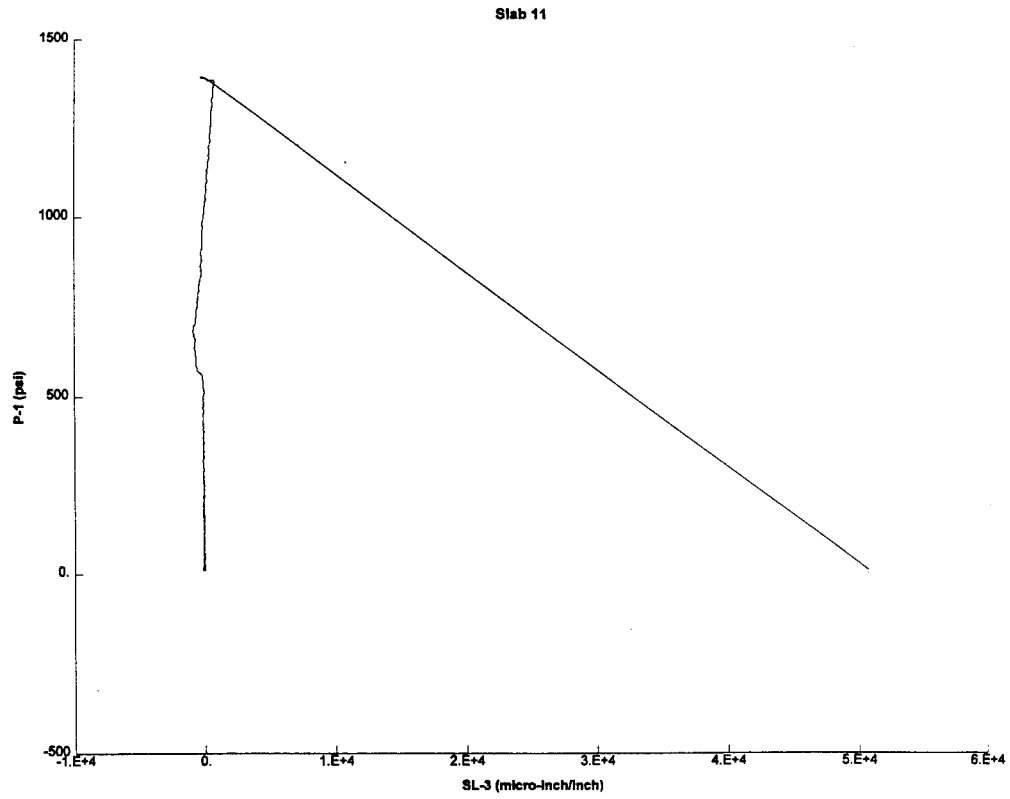


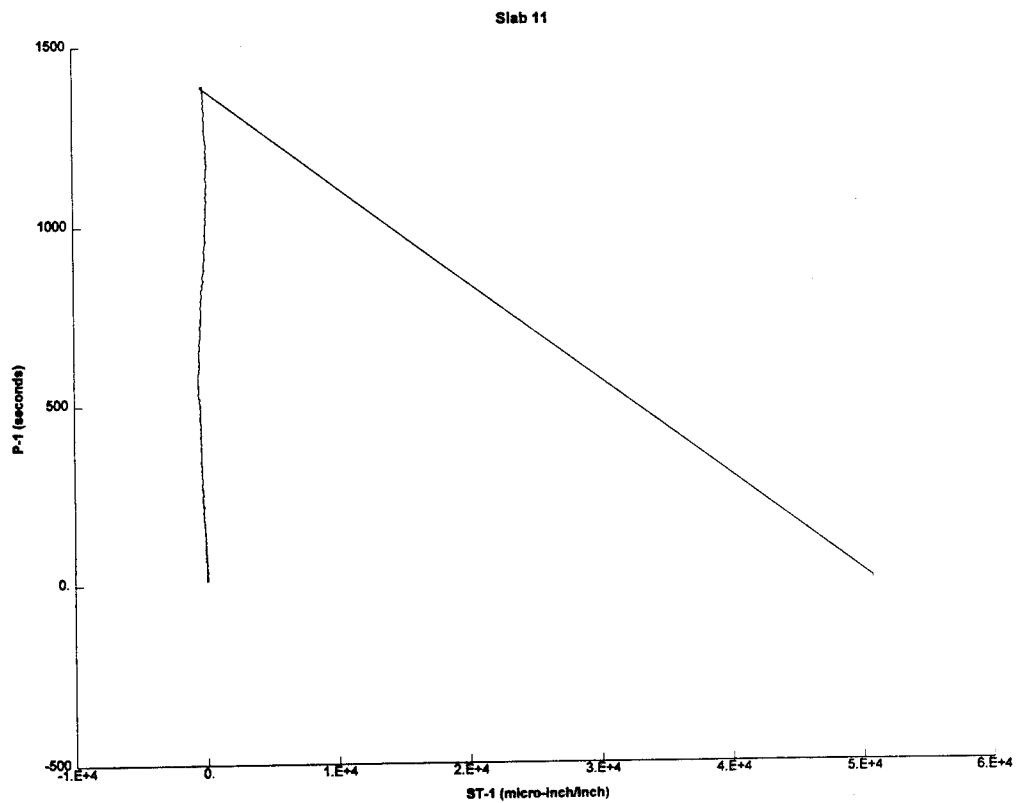
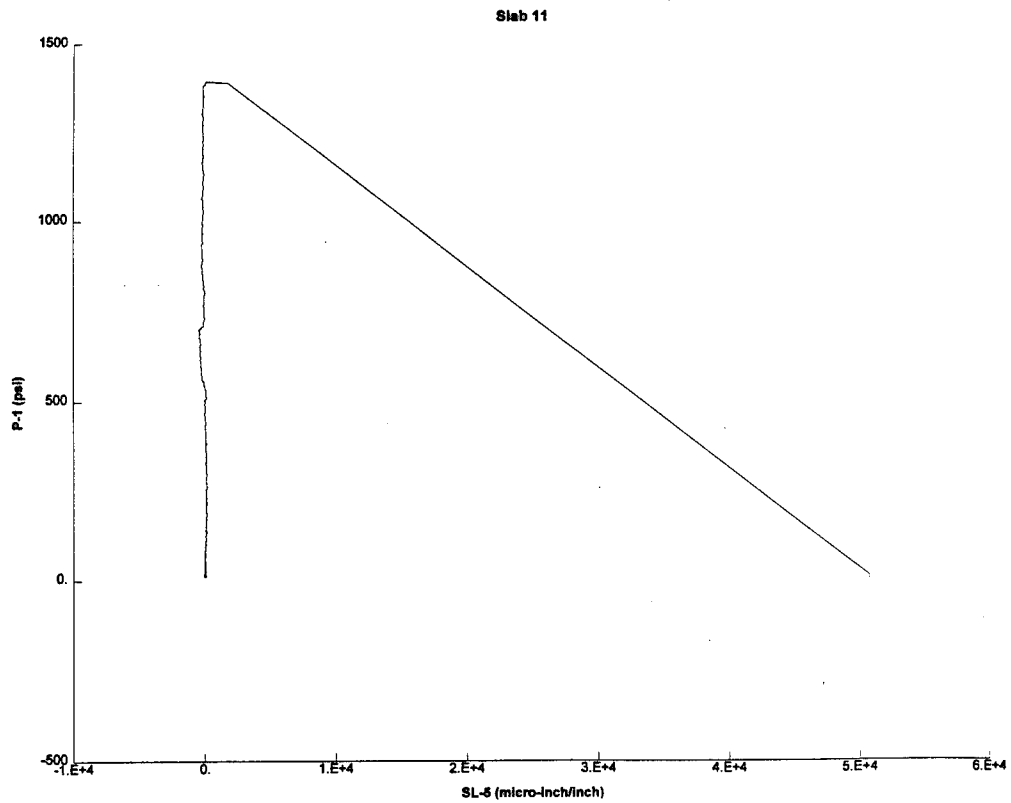
Slab 11



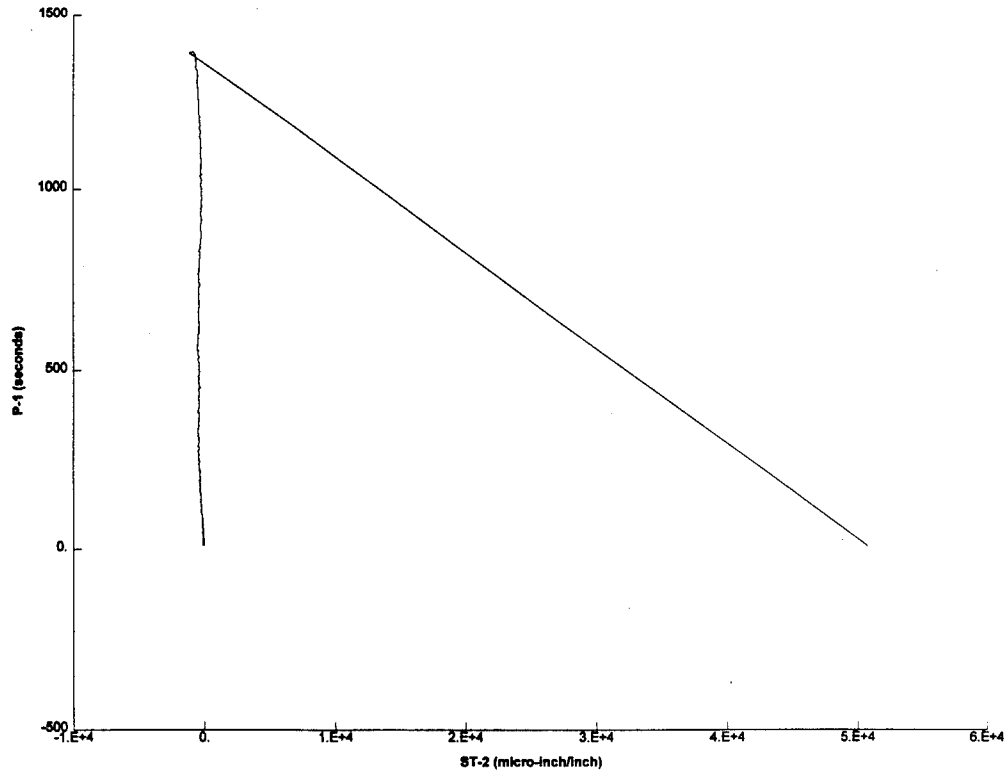
Slab 11



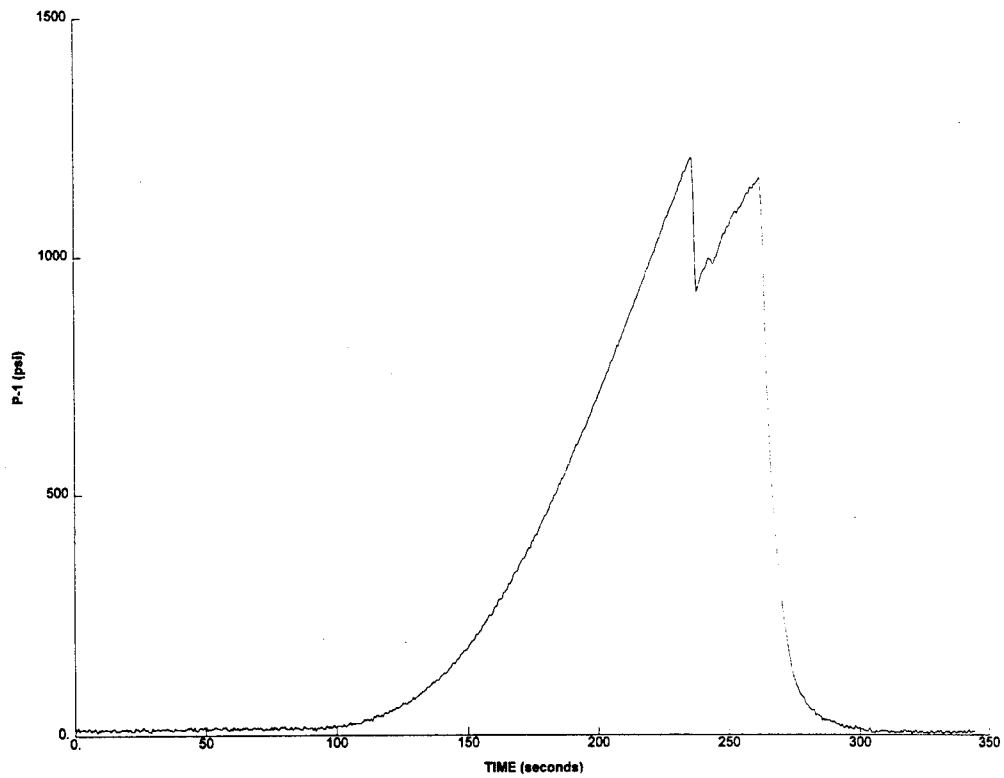


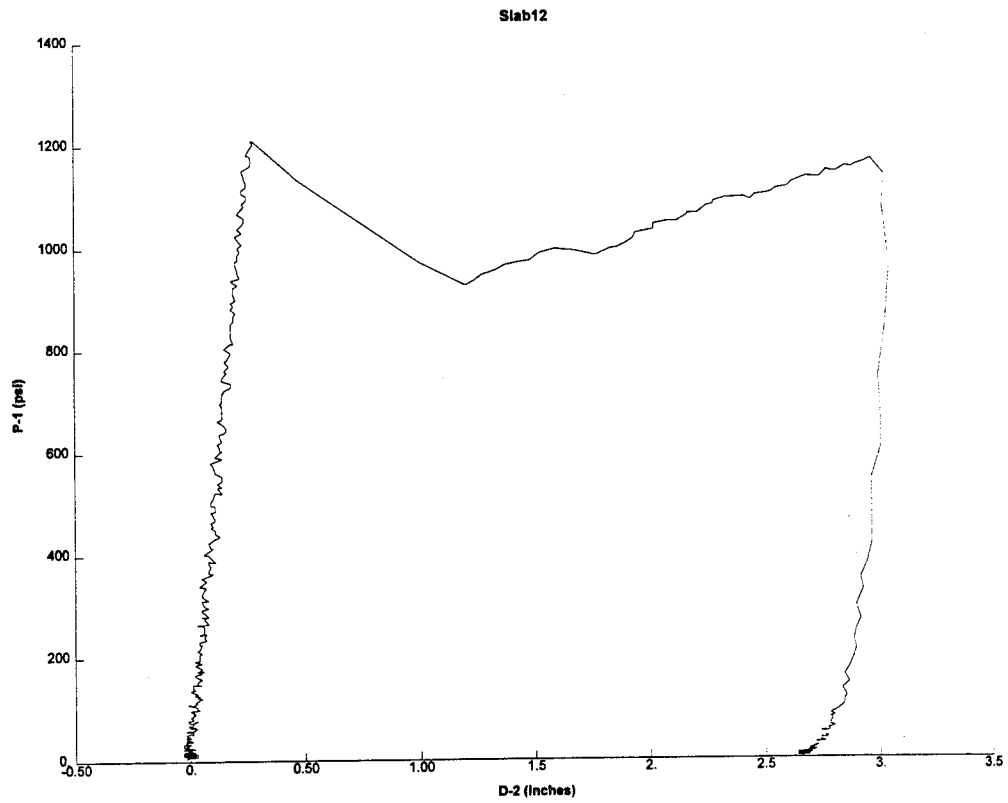
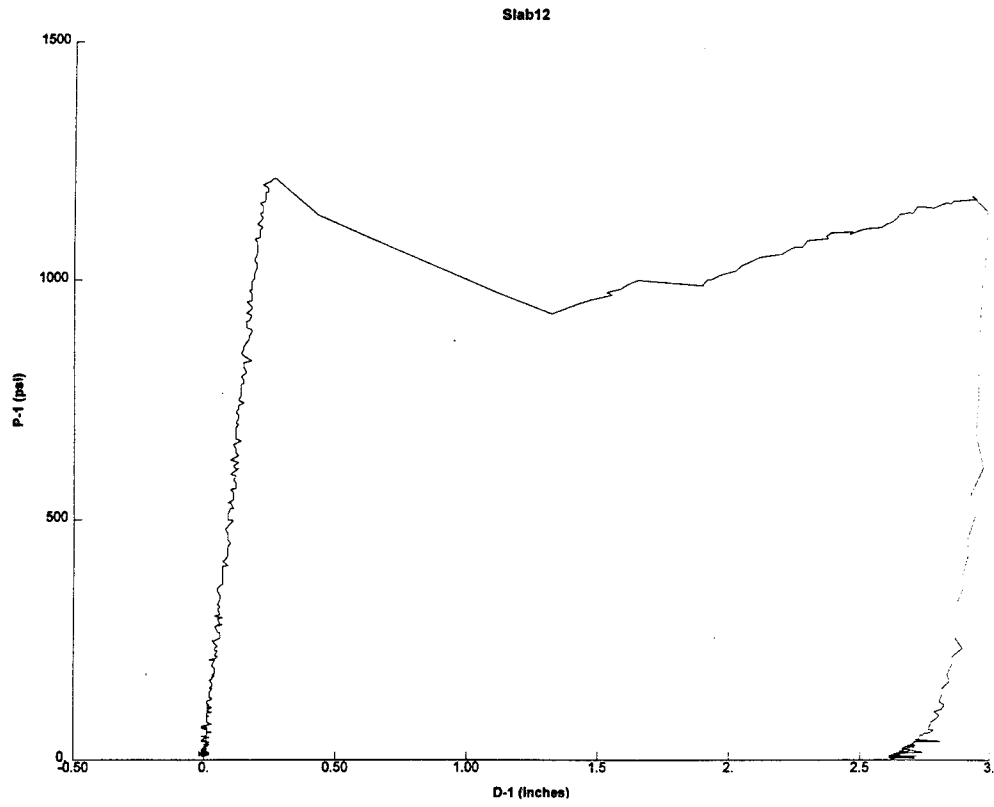


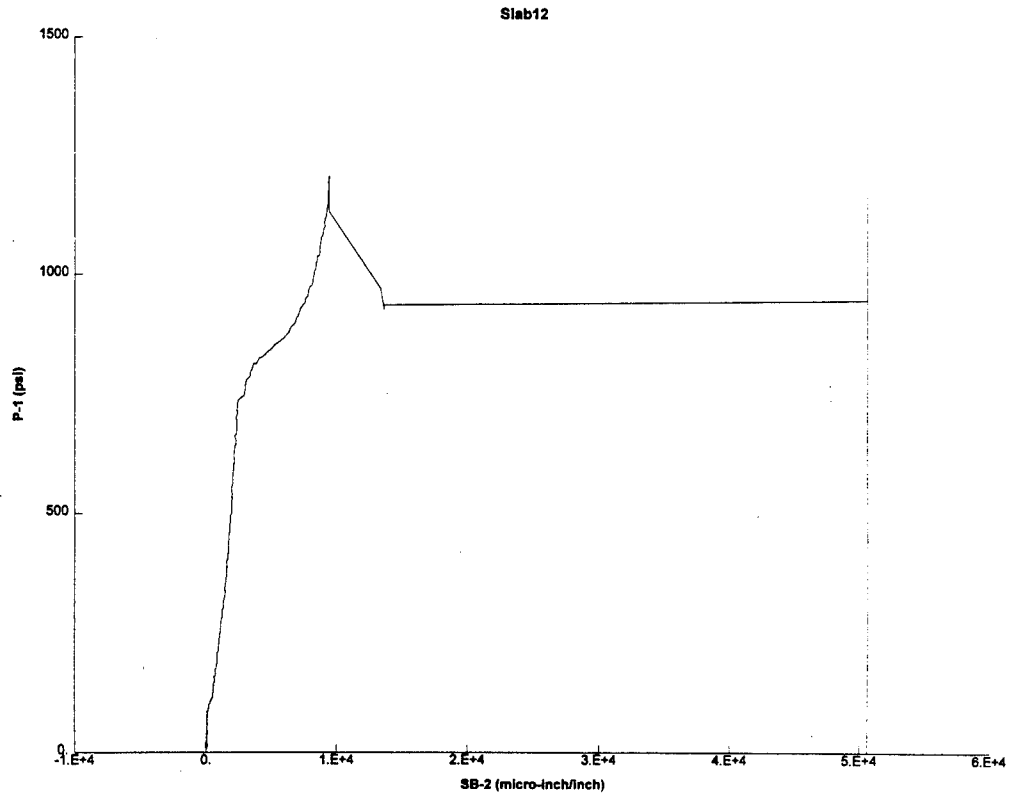
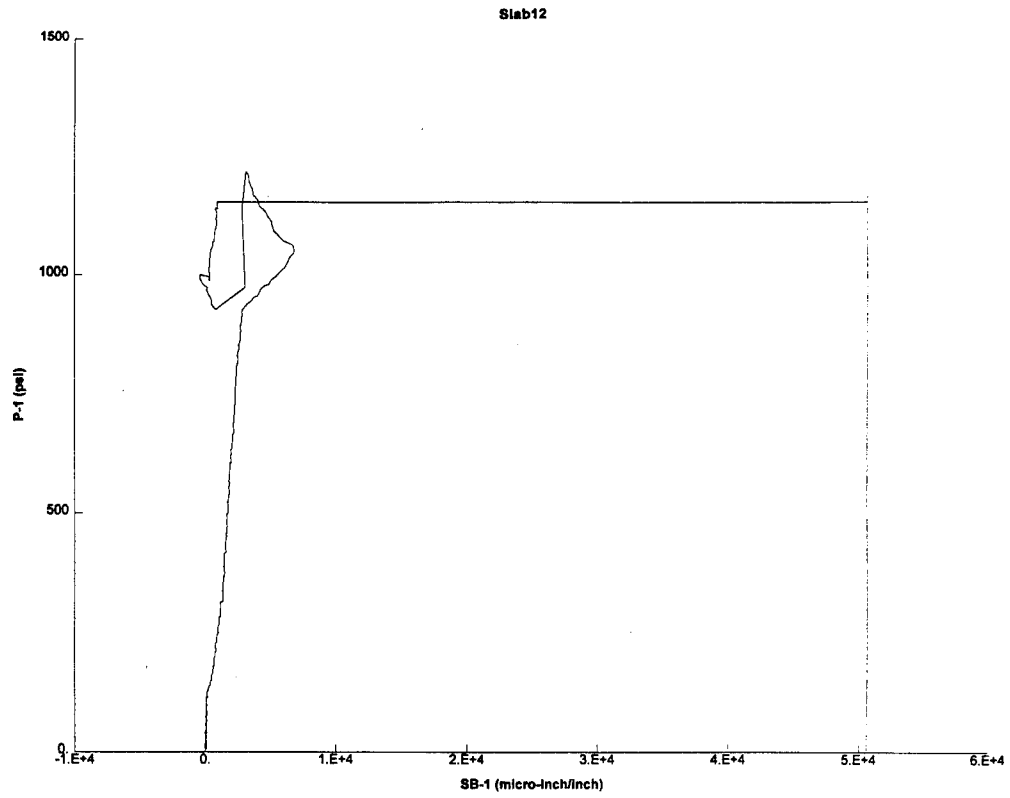
Slab 11

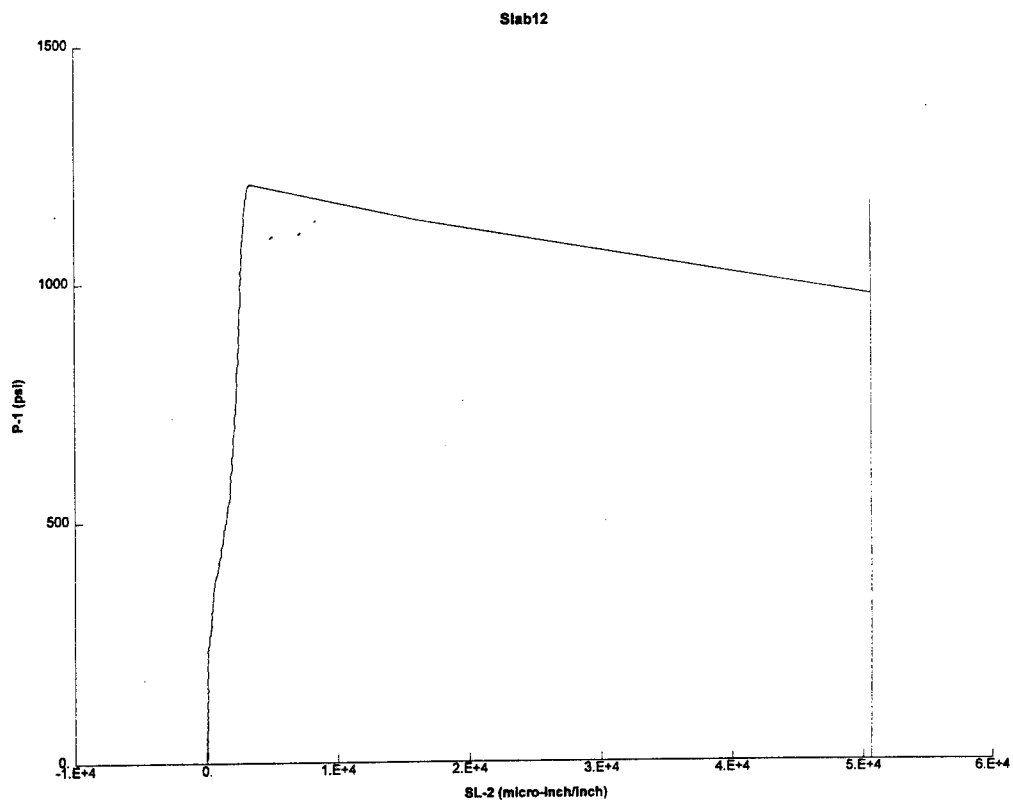
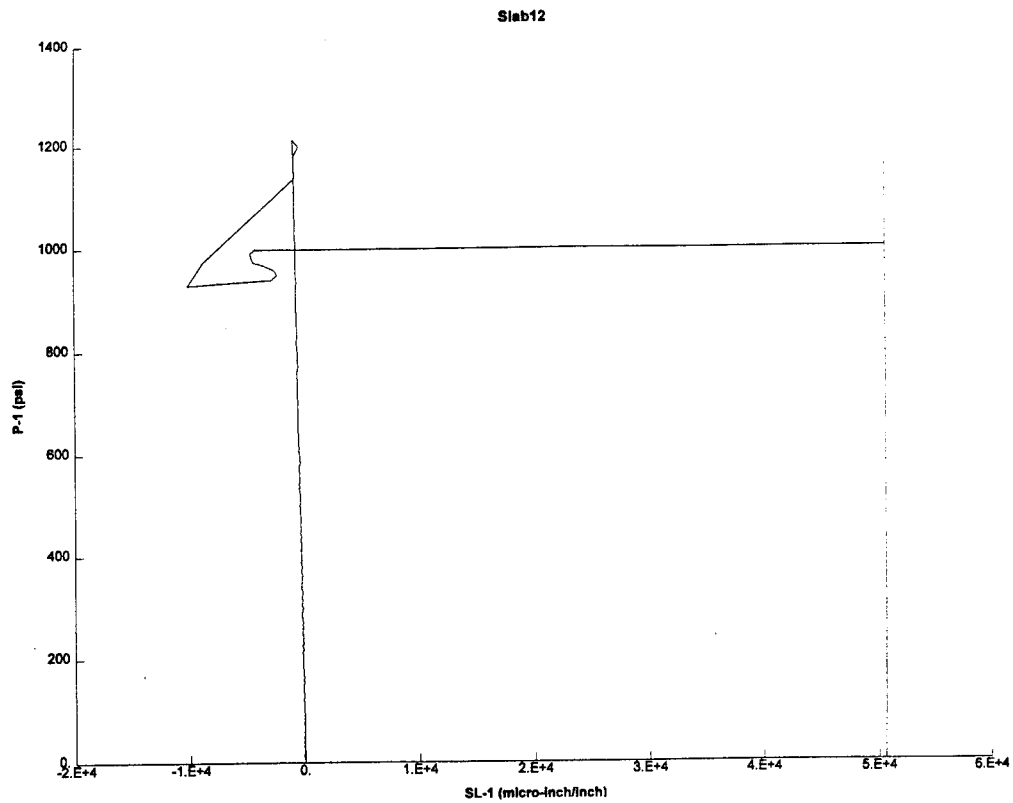


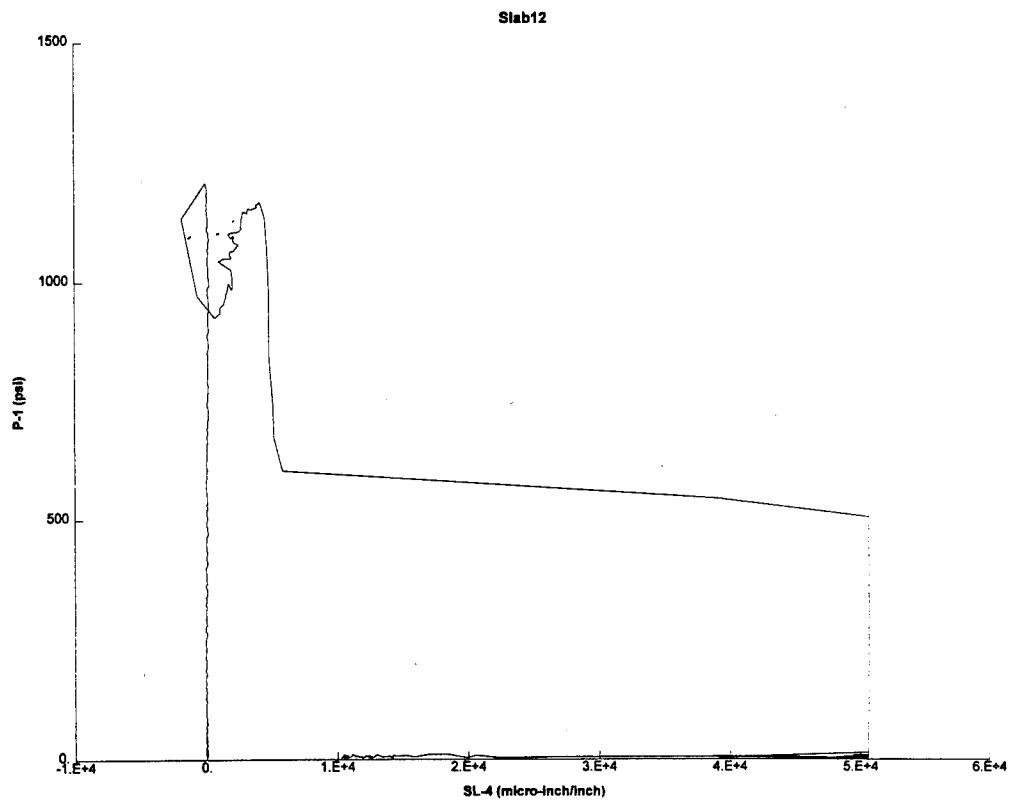
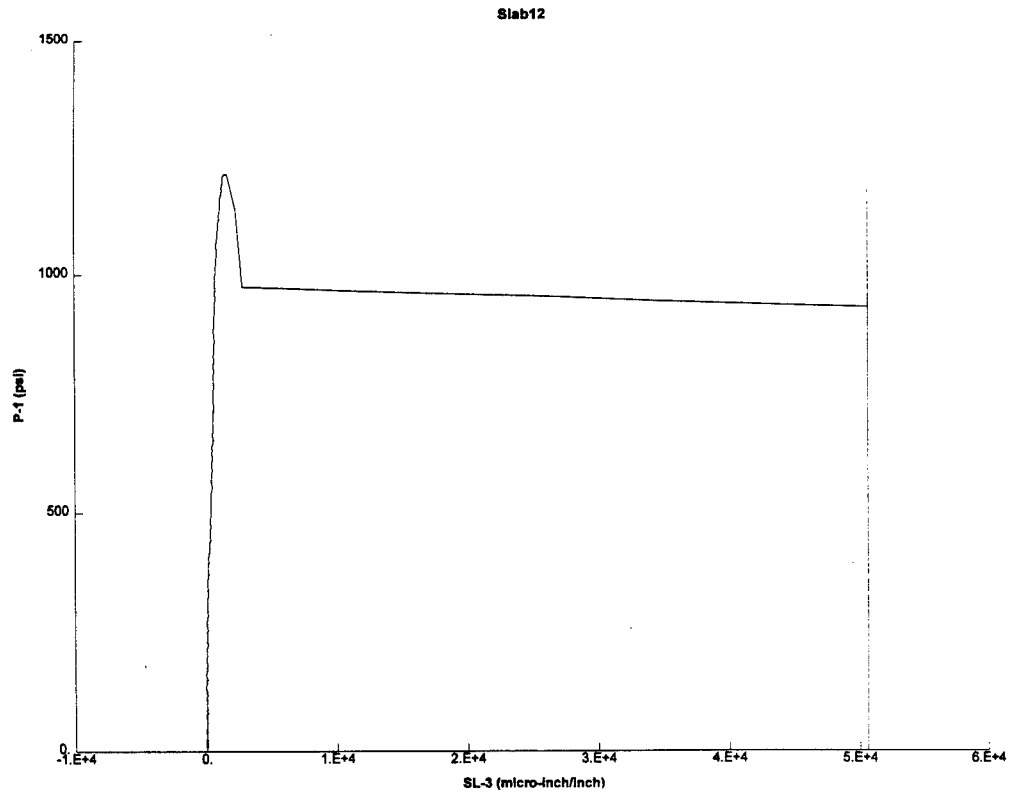
Slab12

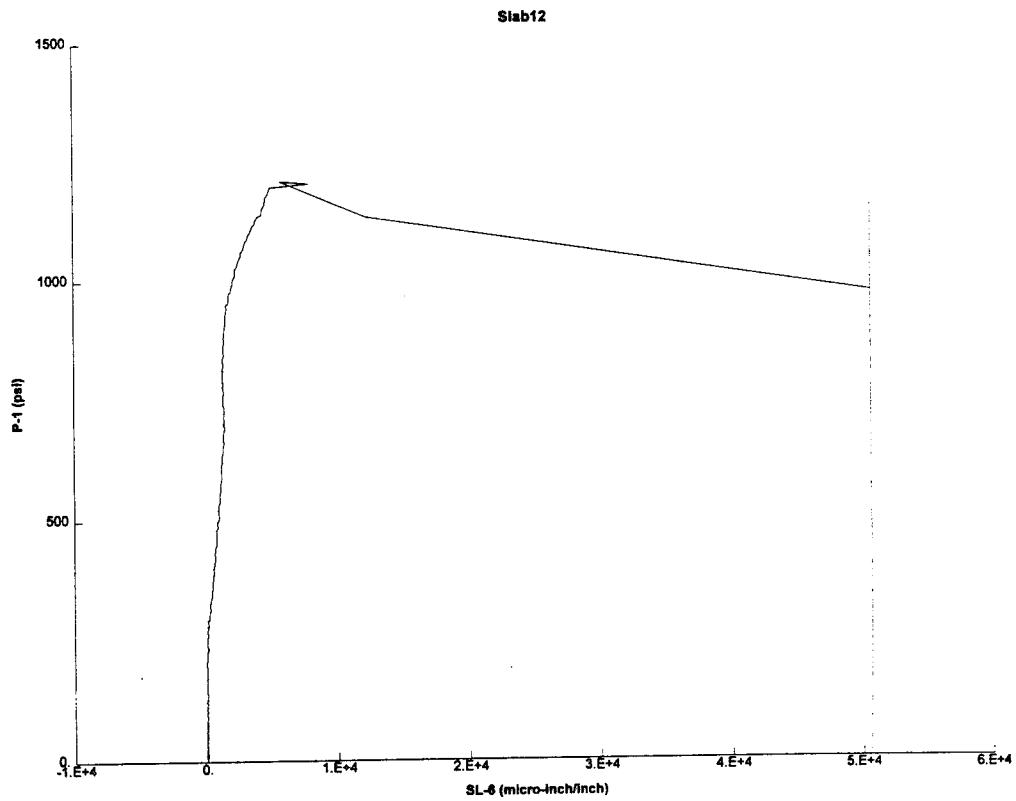
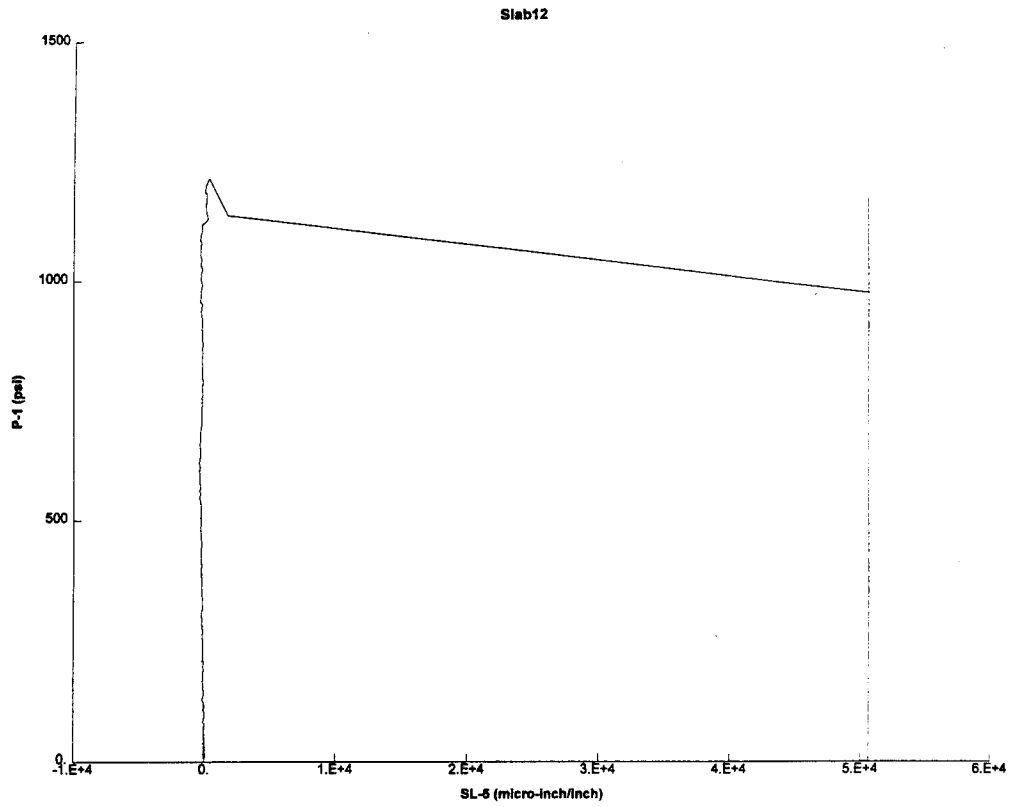


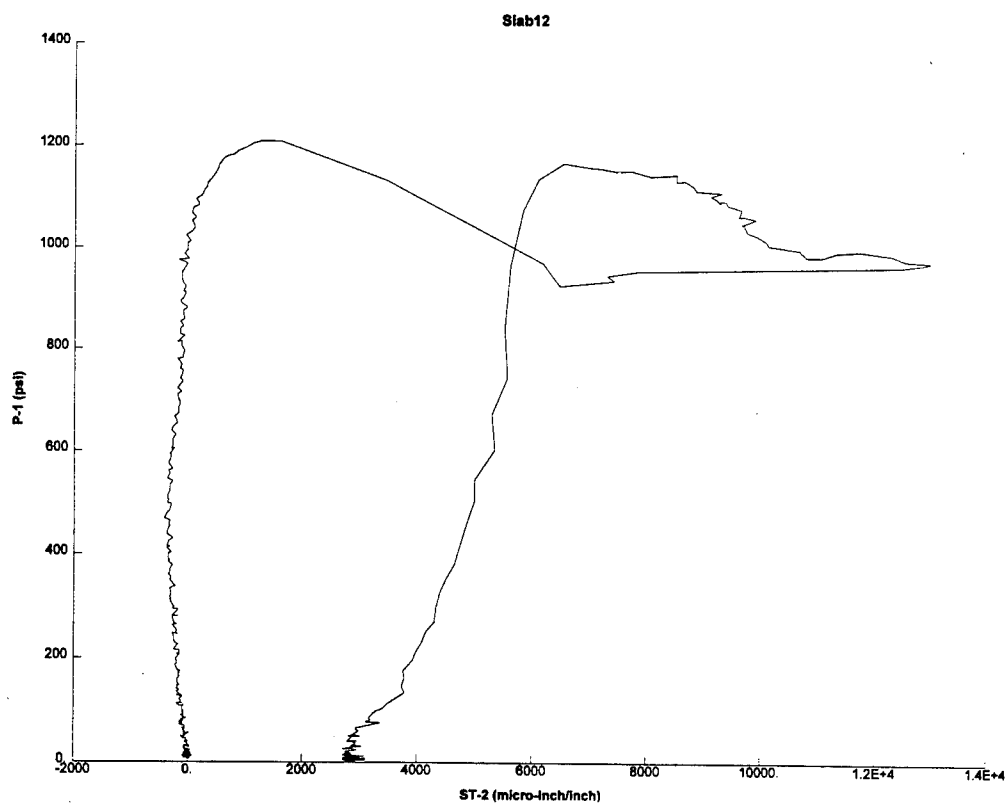
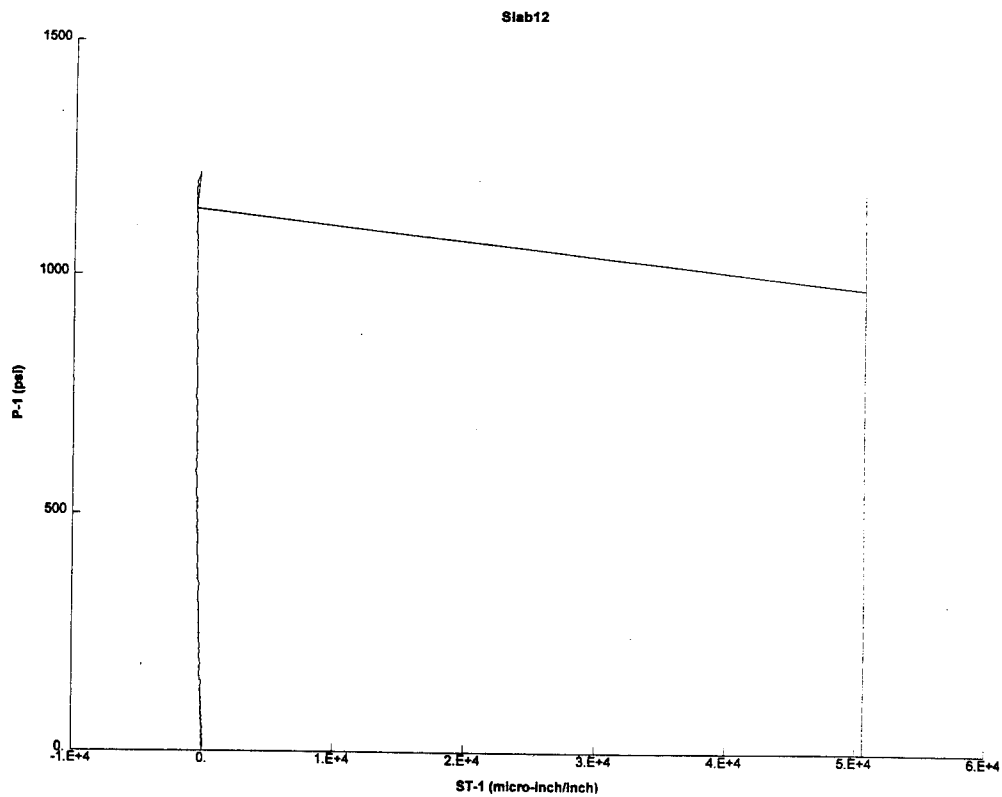




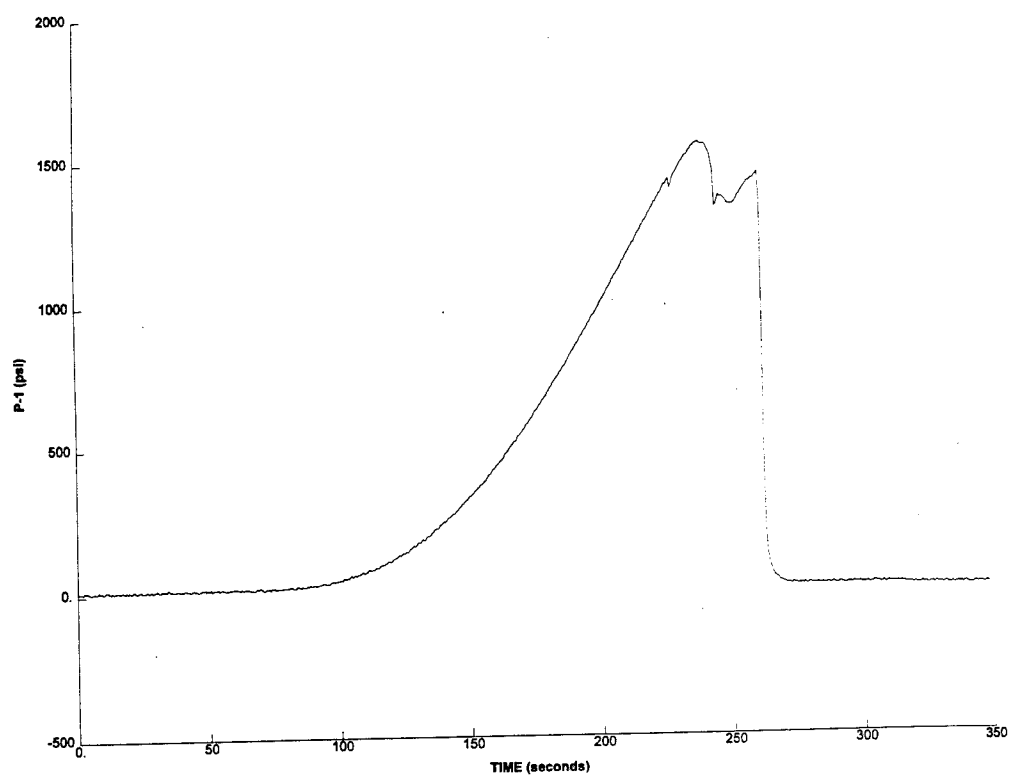




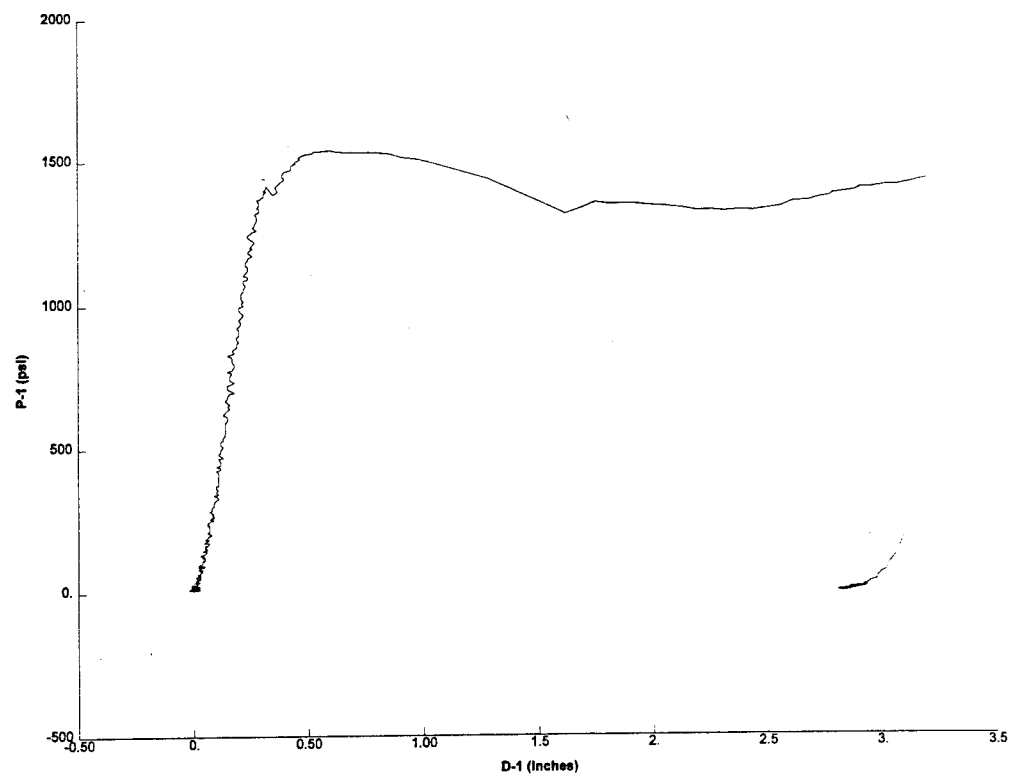


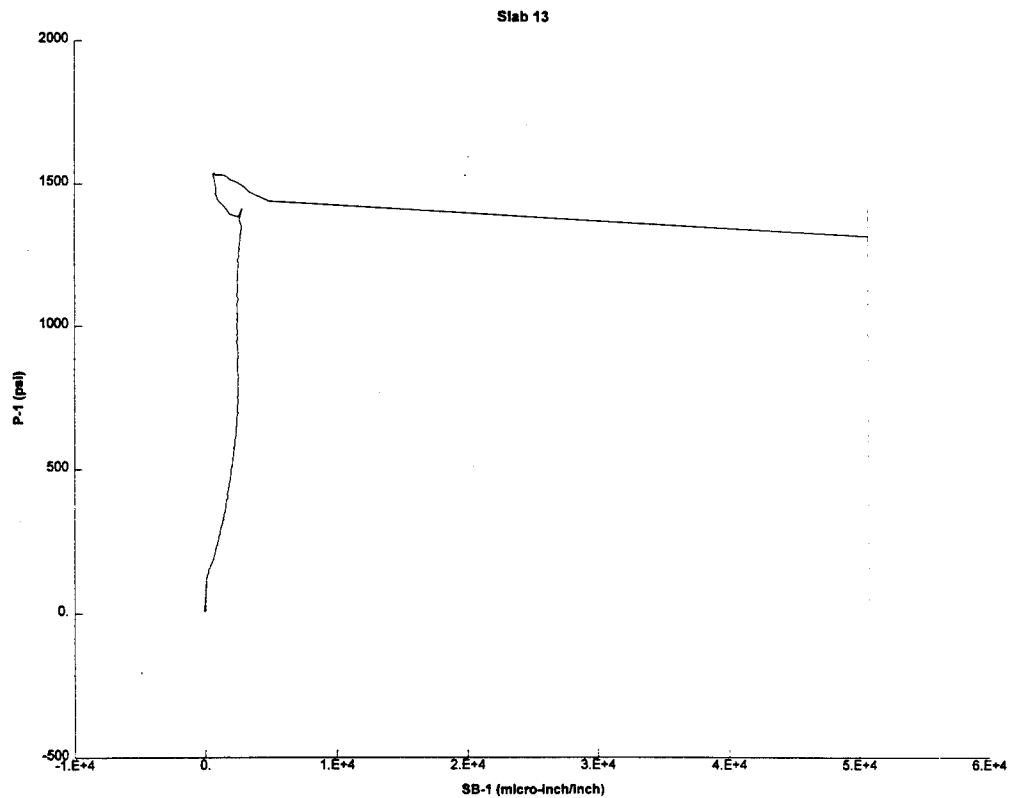
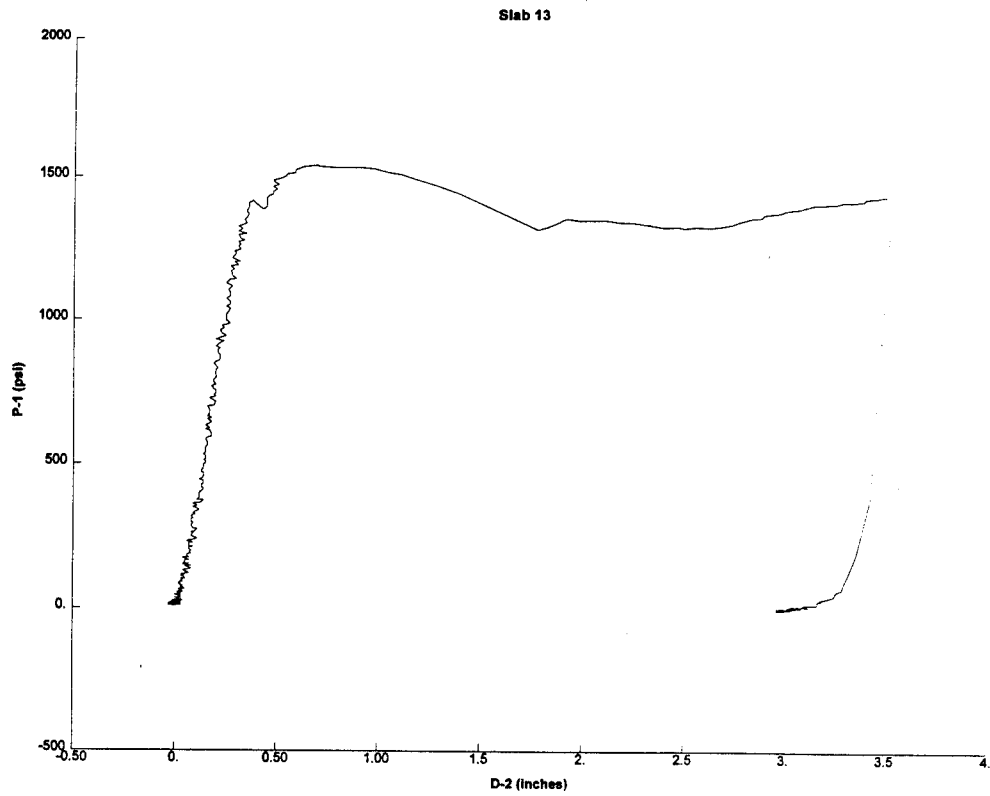


Slab 13

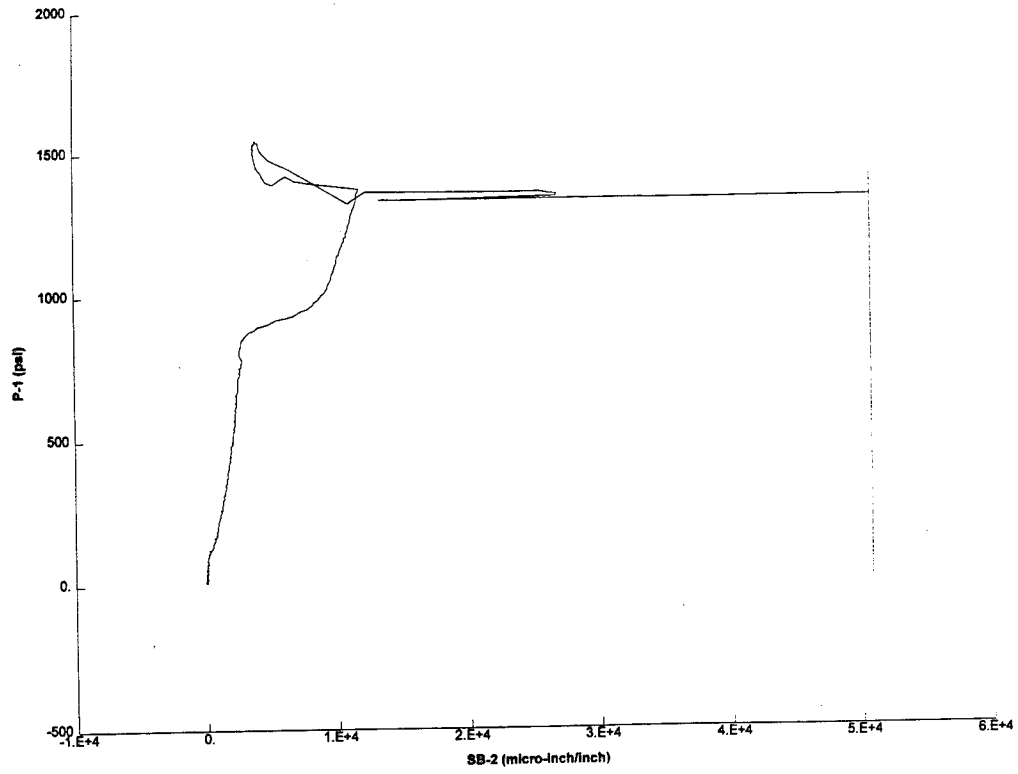


Slab13

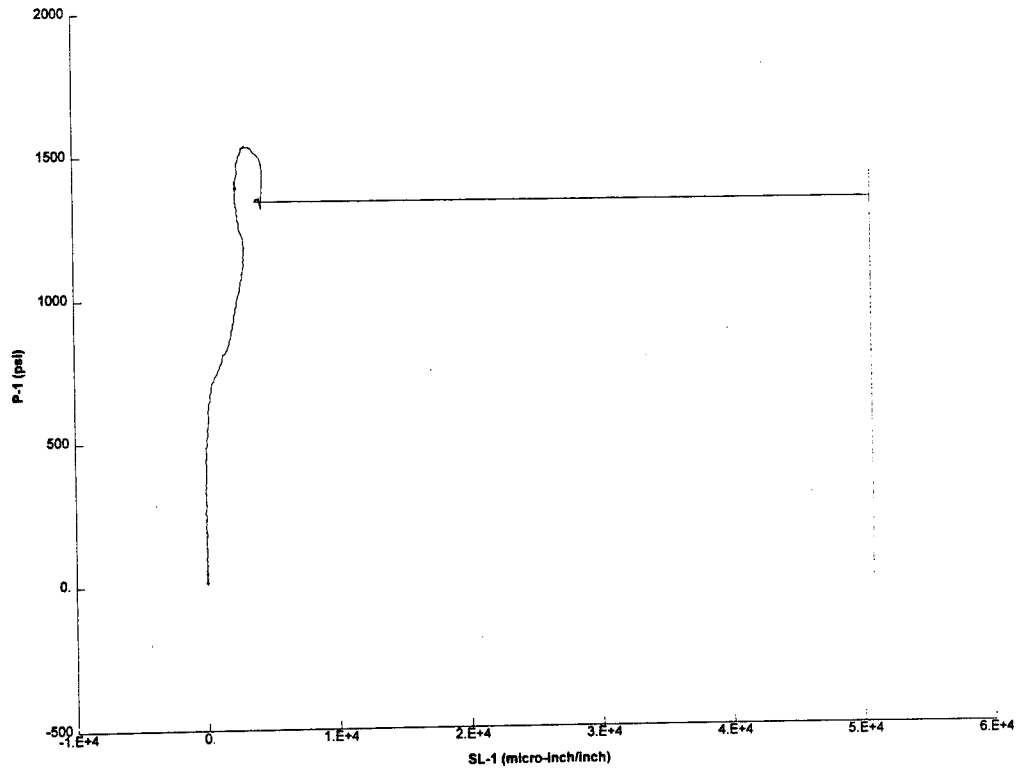




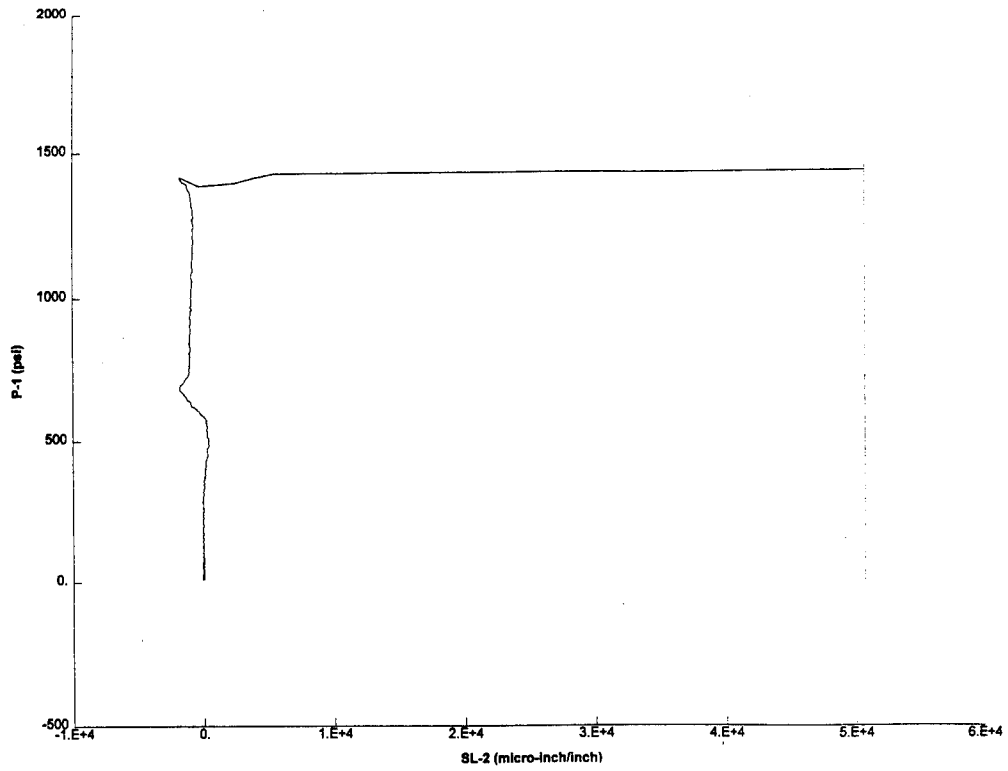
Slab 13



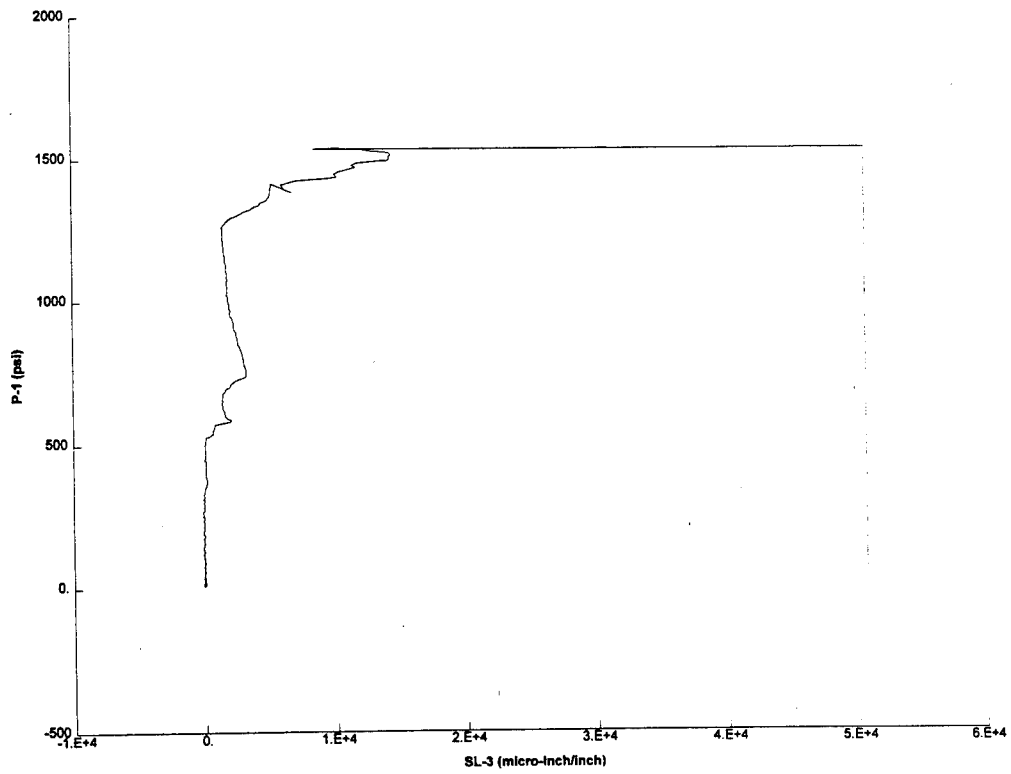
Slab 13

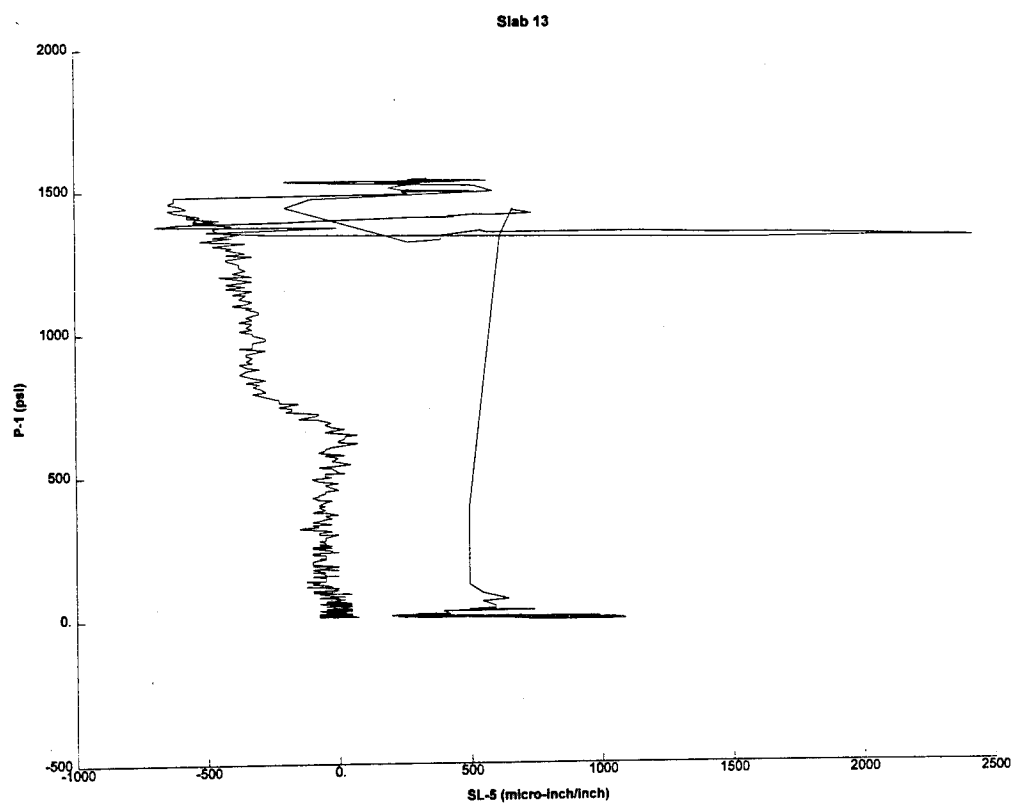
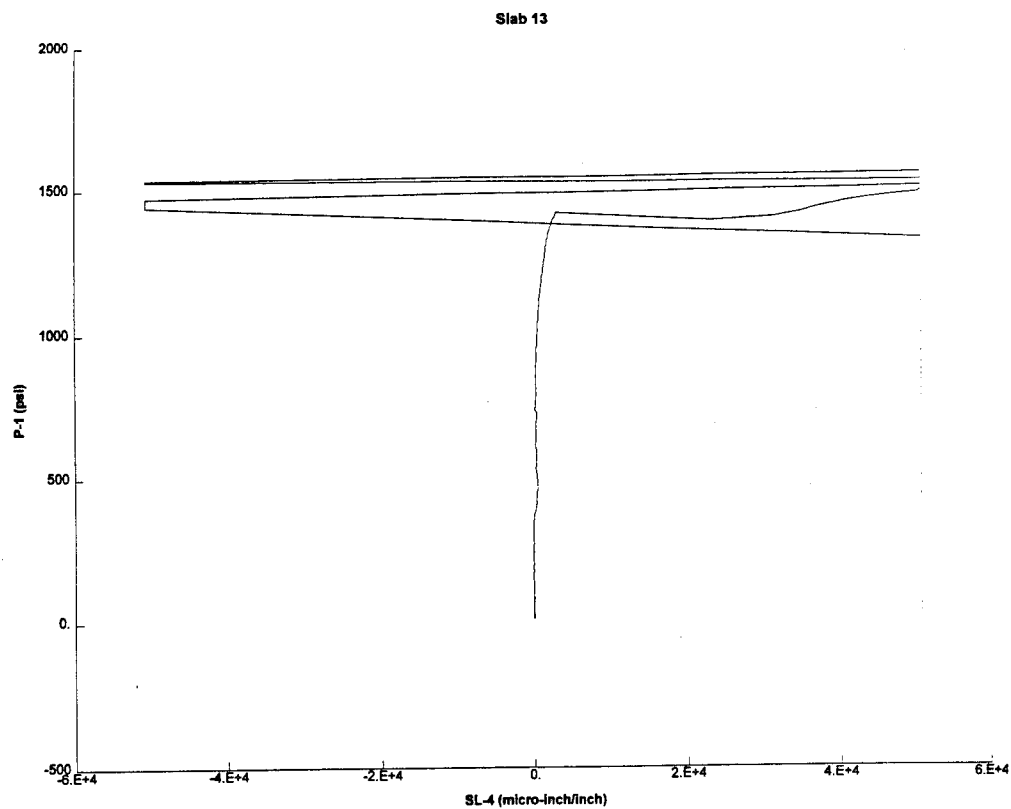


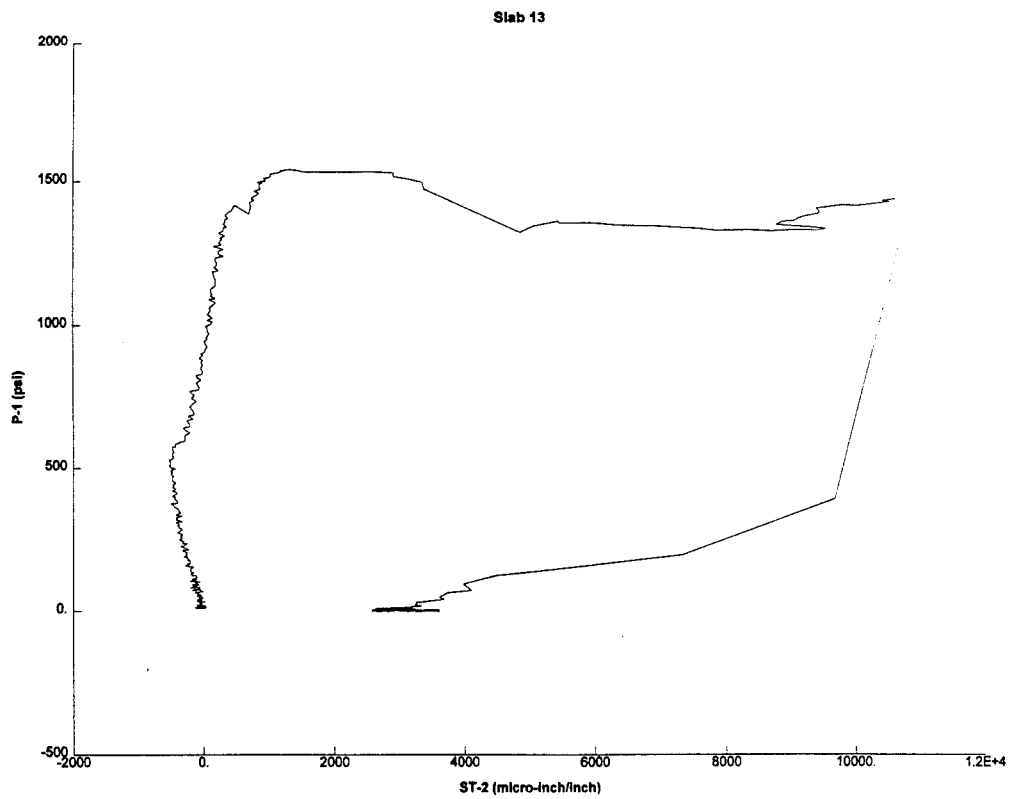
Slab 13



Slab 13







REPORT DOCUMENTATION PAGEForm Approved
OMB No. 0704-0188

Public reporting burden for this collection of information is estimated to average 1 hour per response, including the time for reviewing instructions, searching existing data sources, gathering and maintaining the data needed, and completing and reviewing the collection of information. Send comments regarding this burden estimate or any other aspect of this collection of information, including suggestions for reducing this burden, to Washington Headquarters Services, Directorate for Information Operations and Reports, 1215 Jefferson Davis Highway, Suite 1204, Arlington, VA 22202-4302, and to the Office of Management and Budget, Paperwork Reduction Project (0704-0188), Washington, DC 20503.

1. AGENCY USE ONLY (Leave blank)		2. REPORT DATE November 1994	3. REPORT TYPE AND DATES COVERED Final report	
4. TITLE AND SUBTITLE Shear Reinforcement in Deep Slabs			5. FUNDING NUMBERS	
6. AUTHOR(S) Stanley C. Woodson				
7. PERFORMING ORGANIZATION NAME(S) AND ADDRESS(ES) U.S. Army Engineer Waterways Experiment Station 3909 Halls Ferry Road, Vicksburg, MS 39180-6199			8. PERFORMING ORGANIZATION REPORT NUMBER Technical Report SL-94-24	
9. SPONSORING / MONITORING AGENCY NAME(S) AND ADDRESS(ES) U.S. Army Corps of Engineers Washington, DC 20314-1000			10. SPONSORING / MONITORING AGENCY REPORT NUMBER	
11. SUPPLEMENTARY NOTES Available from National Technical Information Service, 5285 Port Royal Road, Springfield, VA 22161.				
12a. DISTRIBUTION / AVAILABILITY STATEMENT Approved for public release; distribution is unlimited.			12b. DISTRIBUTION CODE	
13. ABSTRACT (Maximum 200 words) A considerable amount of data is available in the literature regarding the behavior of normally proportioned slabs, those with span-to-effective-depth (L/d) ratios greater than approximately 8. However, guidance for shear design and response limits of deep slabs (L/d < 6) used in protective construction is lacking. Thirteen one-way reinforced concrete deep slabs were statically loaded with uniform water pressure to gain a basic understanding of the behavior of deep slabs with reinforcing details typical of protective construction. The post-ultimate behavior of the slabs indicated that a substantial amount of reserve capacity is available in deep slabs with large quantities of principal reinforcement. Based on this series, the recommended response limit for deep slabs having a principal steel ratio near 0.01 and adequate shear reinforcement is approximately 12 deg. For deep slabs with relatively small quantities of principal steel, the response should probably be limited to approximately 8 deg for design purposes.				
14. SUBJECT TERMS Deep slabs Lacing Response limits Shear Stirrups			15. NUMBER OF PAGES 136	
			16. PRICE CODE	
17. SECURITY CLASSIFICATION OF REPORT UNCLASSIFIED	18. SECURITY CLASSIFICATION OF THIS PAGE UNCLASSIFIED	19. SECURITY CLASSIFICATION OF ABSTRACT	20. LIMITATION OF ABSTRACT	